The outer membrane protein assembly machinery of *Neisseria meningitidis*

ISBN: 978-90-393-5145-1

Printed by: Ipskamp Drukkers

Cover illustration: Cindy Dieteren and Elena Volokhina

The studies described in this thesis were performed in the Molecular Microbiology Group, Department of Biology, Faculty of Science, Utrecht University, Padualaan 8, 3584 CH Utrecht, The Netherlands.

The outer membrane protein assembly machinery of *Neisseria meningitidis*

De buitenmembraaneiwit assemblagemachine van *Neisseria meningitidis*

(met een samenvatting in het Nederlands)

Proefschrift

ter verkrijging van de graad van doctor aan de Universiteit Utrecht op gezag van de rector magnificus, prof. dr. J. C. Stoof, ingevolge het besluit van het college voor promoties in het openbaar te verdedigen op dinsdag 22 september 2009 des middags te 4.15 uur

door

Elena Borisovna Volokhina

geboren op 23 februari 1979 te Novosibirsk, Rusland

Promotoren: Prof. dr. J. P. M. Tommassen
Prof. dr. P. Gros

Co-promotor: Dr. M. P. Bos

Терпение и труд все перетрут

Contents

Chapter 1	General introduction	9
Chapter 2	The β-barrel outer membrane protein assembly complex of *Neisseria meningitidis*	31
Chapter 3	Role of the periplasmic chaperones Skp and SurA in outer membrane protein biogenesis in *Neisseria meningitidis*	53
Chapter 4	Species specificity of the Omp85 component of the bacterial outer membrane protein-assembly machinery	75
Chapter 5	Purification and structural characterization of the Omp85 proteins of *N. meningitidis* and *E. coli* and their sub-domains	103
Chapter 6	Functional studies of *N. meningitidis* and *E. coli* Omp85 proteins and their sub-domains	123
Chapter 7	General and summarizing discussion	141
Samenvatting		153
Acknowledgements		157
Curriculum vitae		158

Chapter 1

General introduction

The cell envelope of Gram-negative bacteria

The cell envelope of Gram-negative bacteria consists of an inner membrane (IM) and an outer membrane (OM) with the periplasm in between (Figure 1). The IM is a symmetrical phospholipid bilayer, whereas the OM is asymmetrical, containing phospholipids in the inner and lipopolysaccharides (LPS) in the outer leaflet. LPS is essential in *Escherichia coli* and most other Gram-negative bacteria (32), but, surprisingly, mutants of *Neisseria meningitidis* (103) and of *Moraxella catarrhalis* (78) have been described that are able to survive without LPS in the OM. The periplasm contains a peptidoglycan layer, which is a shape-determining component of the cell envelope. Peptidoglycan is responsible for the cell's resistance to osmotic and mechanical stresses. This structure is formed by highly hydrated oligosaccharides composed of two aminosugars, N-acetylglucosamine and N-acetylmuramic acid, which are cross-linked by short oligopeptides. In many Gram-negative bacteria, the OM is surrounded by a capsular polysaccharide, which offers extra protection for the cell and can play role as a virulence factor in pathogenic bacteria.

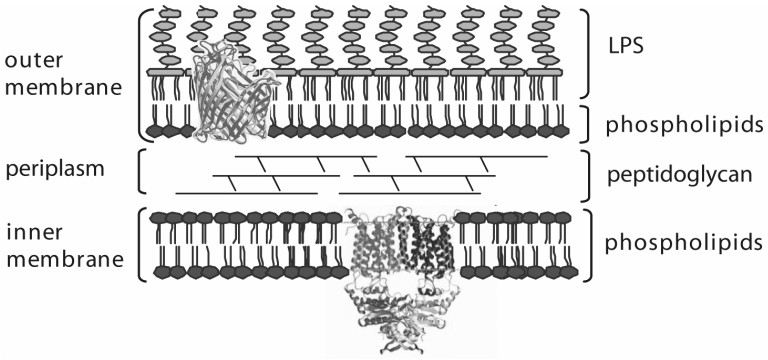

Figure 1

Cell envelope of Gram-negative bacteria. The outer membrane, containing LPS in the outer leaflet and phospholipids in the inner leaflet; the periplasm, containing peptidoglycan, and the inner membrane, containing phospholipids in both leaflets, are indicated. A β-barrel outer membrane protein and an α-helical inner membrane protein are shown.

Structure and function of outer membrane proteins

The protein content of the OM is formed by integral outer membrane proteins (OMPs) and lipoproteins, which are anchored to the membrane via N-terminally attached fatty acyl chains.

Lipoproteins

Proteins containing a so-called lipobox (generally consisting of LXXC, where X is a small amino acid residue) at the end of their signal sequence are lipidated at the Cys in the lipobox by the diacylglyceryl transferase Lgt (93) prior to processing by a dedicated leader peptidase. Next, the cysteine, which is the first residue in the mature protein, is further acylated by the phospholipid:apolipoprotein transacylase Lnt (37). It was shown that amino

acids immediately following the lipidated cysteine determine whether the lipoprotein is sorted to the OM or to the IM. Lipoproteins that have an IM retention signal, in the case of *E. coli* usually an aspartate at the +2 position of the mature protein, remain in the IM (108). Lipoproteins lacking the IM retention signal are bound by the ATP-binding cassette (ABC) transporter LolCDE, which facilitates the release of lipoproteins from the IM and their binding to the periplasmic chaperone LolA (69). LolA shields the lipid moiety of the lipoproteins within its internal hydrophobic cavity and thereby allows for the transport of the lipoprotein substrates as a soluble complex across the aqueous periplasm. At the inner leaflet of the OM, LolA transfers the lipoprotein to the OM receptor LolB, which facilitates its insertion into the OM (69). Some bacteria contain lipoproteins facing the extracellular milieu, which are thus anchored in the outer leaflet of the OM. Examples are LbpB and TbpB of *N. meningitidis* (2, 65, 81). How these lipoproteins are "flipped" over the OM is completely unknown.

Integral outer membrane proteins

Most integral OMPs are characterized by the presence of β-strands, which form a β-barrel embedded in the OM, unlike the IM proteins, which span the membrane by α-helices. The bacterial membrane β-barrels are formed by an even number of next-neighbour antiparallel amphipathic β-strands (Figure 2). Interestingly, the only solved structure of a mitochondrial membrane β-barrel protein revealed an odd number (*i.e.* 19) of β-strands (41, 115). Up until now, 47 structures of various β-barrel OMPs have been solved. They contain 8 to 24 β-strands in a barrel (http://blanco.biomol.uci.edu/Membrane_Proteins_xtal.html). Each strand contains a minimum of six amino acid residues, which is enough to span the membrane, but can contain as many as 25, with an average of 12.3 residues (51). On the periplasmic side, the strands in a β-barrel are usually connected by short turns, and extracellularly by longer, often mobile loops. The external loops of orthologues of the same protein from different isolates of a bacterial species can demonstrate a high degree of sequence variability (96), which may have implications for pathogenic bacteria in escaping host defence mechanisms. In most OMPs, a single protein molecule forms a β-barrel, but in some oligomeric OMPs, several subunits contribute β-strands to the formation of a single β-barrel. For example, in the case of the TolC protein, which is involved in several activities, such as hemolysin secretion, colicin import, and antibiotic efflux, the 12-stranded β-barrel consists of four β-strands from each of three subunits (53). Similarly, the autotransporter Hia of *Haemophilus influenzae* (68) contains a 12-stranded β-barrel formed by oligomerization of three subunits. The Wza protein of *E. coli*, which is involved in the secretion of capsular polysaccharide, is the only integral OMP of known structure that forms a barrel in the OM composed of amphipathic α-helices. Eight monomers each donate one α–helix to the membrane-embedded barrel and form three additional periplasmic domains (Figure 2) (28). Secretins form a group of integral OMPs that is involved in the secretion of a variety of substrates across the OM. According to the EM structure analysis, the walls of the secretin channels are formed by complexes of 12 or 14 monomers (5). Well-known examples are PilQ from *N. meningitidis*, which facilitates the extrusion of the type IV pili (20), and PulD of *Klebsiella oxytoca*, involved in pullulanase secretion (14). A large central cavity formed by association of subunits, which is able to allow for the secretion of large substrates, is a common feature of secretins and Wza (19).

The β-barrel OMPs perform various functions, such as maintaining the structure of the cell, uptake of nutrients, protein secretion and catalysis. The OmpA protein of *E. coli* is functioning in the maintenance of the cell structure by anchoring the OM to the peptidoglycan (50). It contains an N-terminal 8-stranded β-barrel (Figure 2) (77) and a peptidoglycan-associated C-terminal domain (50). The OM contains general porins, which

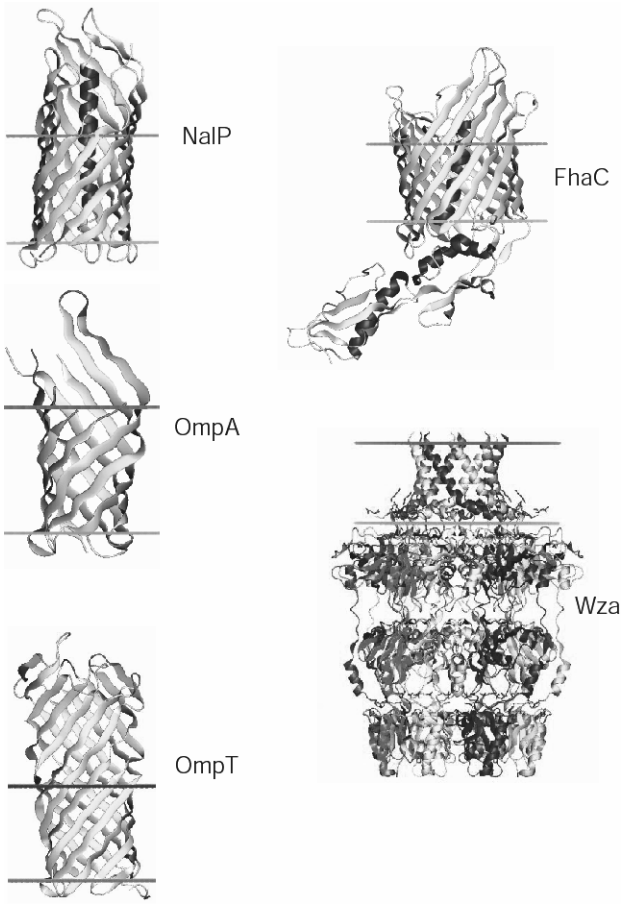

Figure 2

Selected OMPs of known structures. Figures representing structures of the translocator domain of NalP of *N. meningitidis*, FhaC of *B. pertussis*, and the membrane domain of OmpA, OmpT, and Wza of *E. coli*, were obtained from the Orientations of Proteins in Membranes (OPM) database (opm.phar.umich.edu). Dark and light grey horizontal lines indicate the outer and inner borders of the OM, respectively.

allow for the passage of small hydrophilic molecules by passive diffusion and show selectivity for charge only, as opposed to the specific porins, which have a binding site and, therefore, specificity for a certain substrate (70). Structures of several general porins, such as trimeric OmpF and PhoE of *E. coli*, have been solved (21). They show β-barrels composed of 16 β-strands with an internal open channel for each of the monomers. *N. meningitidis* expresses two general diffusion porins: cation-selective PorA (112) and anion-selective PorB (101). Like the *E. coli* porins, they are predicted to be trimeric and to consist of 16 β-strands (25, 116). LamB of *E. coli* is one of the best-characterized substrate-specific porins. Its structure revealed an 18-stranded β-barrel, which, like the general porins, forms trimers (95). LamB facilitates maltose- and maltodextrin uptake. The crystal structure of LamB also revealed a substrate-translocation pathway, consisting of aromatic residues that form a

"greasy slide" lined up with an "ionic track" consisting of polar residues, along which maltose and linear oligosaccharides may be translocated (95). Many bacteria respond to iron limitation by the production and secretion of siderophores, which are small iron-chelating compounds and bind iron in the environment with very high affinity. In addition, these bacteria produce OMPs under these conditions, which function as receptors for the ferric-siderophore complexes. FhuA and FepA are *E. coli* siderophore receptors of known structures, consisting of large 22-stranded β-barrels, with plug domain closing the pore (13, 31, 66). *N. meningitidis* lacks siderophore receptors, instead it produces lactoferrin-binding protein A (LbpA), and transferrin-binding protein A (TbpA) to facilitate iron acquisition. Lactoferrin and transferrin bind free extracellular iron, which most bacteria need to survive. The LbpA and TbpA receptors bind lactoferrin and transferrin and thereby facilitate iron acquisition by *N. meningitidis*. Production of these proteins is down-regulated when iron concentration in the medium is sufficient. No crystal structures of LbpA and TbpA are available, but they are both predicted to consist of 22-stranded β-barrels, with a plug, similar to FhuA and FepA (72, 80). Some of the β-barrel OMPs act as protein translocators. In two-partner secretion (TPS) systems, an OM β-barrel protein, TpsB, recognizes its unfolded substrate protein TpsA and facilitates its translocation across the OM, where the TpsA folds into a β-helix structure and, in many cases, functions as a virulence factor. Examples of TpsBs are ShlB, responsible for the secretion of a *Serratia marcescens* hemolysin (12), and FhaC, the transporter of the *Bordetella pertussis* filamentous hemagglutinin, consisting of a 16-stranded C-terminal β-barrel and a periplasmic part (16, 36) (Figure 2). One of the types of β-barrel translocators are autotransporters. A C-terminal β-barrel part (or translocator domain) of an autotransporter facilitates the passage of its N-terminal passenger domain across the OM. A well-known example of an autotransporter is IgA protease, a virulence factor in *N. meningitidis* and other pathogenic bacteria (83). The solved structure of the translocator domain of another neisserial autotransporter, NalP, shows a β-barrel with an internal α-helix (Figure 2), which would expose a passenger domain, if connected, to the extracellular side of the membrane (73). Only few β-barrel OMPs are enzymes, playing roles in LPS and phospholipid modification and protein degradation (7). In *E. coli*, three β-barrel enzymes are described: outer membrane phospholipase A (OMPLA) (100), lipid A palmitoyltransferase PagP (1), and protease OmpT (Figure 2) (117). Furthermore, other bacteria may express LPS deacylases, such as PagL or LpxR (90, 91).

Transport of OMPs across the periplasm

OM proteins are synthesized in the cytoplasm with an N-terminal signal sequence, which directs their transport over the IM through the Sec machinery (29). The signal sequence is cleaved off by dedicated leader peptidases. There are no integral OM proteins identified to date that use the Tat system (10), which is dedicated to the translocation of folded proteins into the periplasm (63). After passing via the Sec machinery through the IM and release of the signal sequence, unfolded OMPs enter the periplasm where they interact with periplasmic chaperones facilitating their passage to the OM (Figure 3).

The holding chaperone Skp

Skp (seventeen-kilodalton protein) is a periplasmic chaperone. After it was discovered, Skp was suggested to be a histone-like protein and, therefore, the gene was designated *hlpA* (60). Later it was named *ompH*, because the protein fractionated with the OM in *Salmonella typhimurium* (54). These, in retrospect aberrant, subcellular localizations are likely due to the non-specific binding of the highly positively charged protein with negatively charged DNA and LPS after rupturing the cells (109). Then, Skp was postulated to facilitate protein translocation across the IM, because it compensated to some extent the

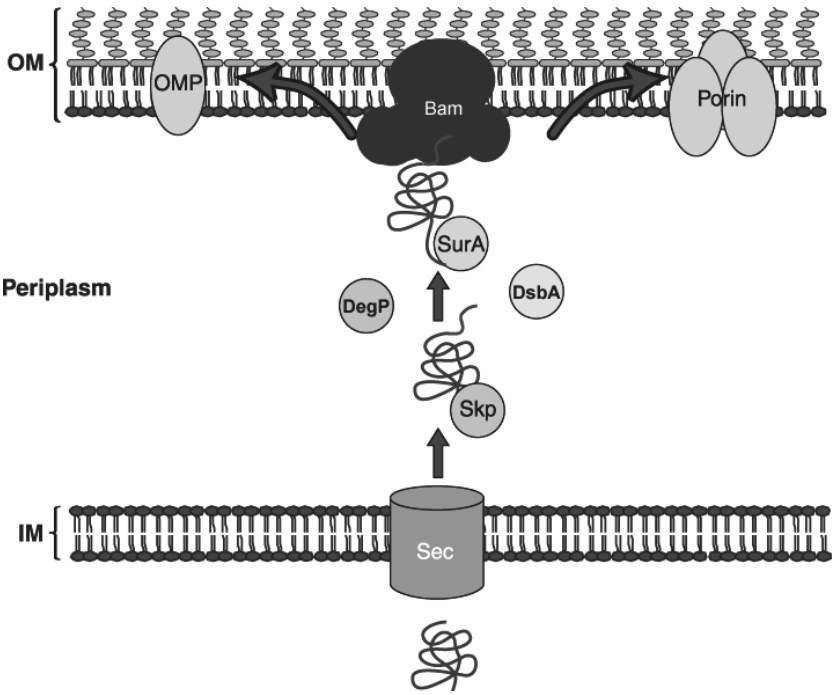

Figure 3

Biogenesis of OMPs in Gram-negative bacteria. OMP precursors are synthesized in the cytosol with an N-terminal signal sequence and transported across the IM via the Sec machinery. The signal sequence is cleaved off by leader peptidase. In the periplasm, nascent OMPs interact with periplasmic chaperones, such as Skp and SurA that prevent their aggregation and facilitate folding. Disulfide bond formation is catalyzed by DsbA. Chaperone protease DegP assists folding and degrades misfolded OMPs. After crossing the periplasm, OMPs are recognized by the Bam complex and inserted into the OM (9).

absence of SecA, the ATPase of the Sec system, in *in vitro* translocation assays (110). Eventually, Skp was described as a periplasmic protein (109) and its apparent function became clearer. Skp binds unfolded β-barrel proteins (15, 23) presumably while they emerge from the Sec machinery (39). The crystal structure of the trimeric protein resembles a jellyfish. Three tentacles protrude from the β-barrel-like association domain and form a cavity containing hydrophobic patches, which might accommodate an unfolded OMP precursor and, possibly, protect it from aggregation in the hydrophilic milieu of the periplasm (52, 121). Thus, Skp acts as a "holding chaperone", rather than as a folding chaperone. Recent NMR and cross-linking data showed indeed that the β-barrel part of the OmpA precursor in an *in vitro*-formed OmpA/Skp complex occupies the Skp cavity in a denatured conformation. The soluble part of OmpA protrudes outside of the cavity and is folded (122). The Skp trimers were shown to associate with unfolded OMPs at 1:1 stoichiometry by means of electrostatic and hydrophobic interactions, irrespective of the size of the OMP (84). The Skp trimer has an unusually large dipole moment with a negatively charged association

domain on one side of the trimer and highly positively charged tentacle tips on the other side. These positive charges might allow the tips to bind anionic phospholipids (23) positioning the Skp protein ideally to receive an OMP as soon as it is released from the Sec machinery. Although Skp is not an essential protein in *E. coli*, *skp* mutants show increased sensitivity to antibiotics, which is indicative of a defective OM barrier function, and show decreased amounts of OMPs, such as OmpA, OmpF, OmpC, and LamB, in the OM (15). The observed decrease in OMP levels is partially caused by degradation of unassembled OMPs by the periplasmic protease DegP. Consistently, unfolded, unassembled OMPs accumulate in the periplasm in an *skp degP* double mutant. These aggregates are apparently detrimental to the cell, since the double mutant only survives under conditions of slow growth, *i.e.*, at 30ºC in minimal medium (94).

The folding chaperone SurA

The SurA protein was initially identified in *E. coli* as a protein essential for the survival of bacteria in the stationary phase (113). Later, it was found that this phenotype only occurs when the cells also lack RpoS, the stationary phase sigma factor (61). It was postulated that the combined absence of SurA and RpoS results in altered production of proteins involved in maintaining the integrity of the cells especially at elevated pH (pH 9), which is a condition normally arising after prolonged growth of *E. coli* in standard LB medium. The chaperone function of SurA became evident when it was found that *surA* mutants were particularly defective in the conversion of unfolded into folded OMPs, whereas the folding of periplasmic proteins was not affected in these mutants (62, 88). Consistently, cells missing SurA were found more sensitive to bacitracin, vancomycin, bile salts, crystal violet, SDS-EDTA, phenethyl alcohol, and rifampicin, indicating that these cells experience an increased OM permeability.

SurA consists of four domains: an N-terminal domain, a C-terminal domain, and two peptidyl-prolyl isomerase (PPIase) domains, P1 and P2, in the central part of the protein. Of the two PPIase domains, only P2 was found to be enzymatically active. Initially, it was suggested that the chaperone function of SurA in *E. coli* is directly linked to its PPIase activity; however, a *surA* mutant lacking both P1 and P2 or with a disturbed P2 could still perform its function (6). SurA was found to have a binding preference for peptides containing aromatic amino acids (Ar) in Ar-Ar or Ar-X-Ar sequence motifs, which are characteristic for OMP β-strands (40), explaining its higher affinity for non-native OMPs above non-OMPs (6). It was suggested that the preference of SurA to bind aromatic residues is determined by the P1 domain (125). Structural studies showed that the N- and C- terminal domains of SurA, together with P1 form a core module with a putative peptide-binding crevice of ~50 Å (8). The SurA protein is able to modify its quaternary structure in order to bind peptides of different conformations (125). It was shown that SurA, unlike Skp, could be cross-linked to the *E. coli* β-barrel assembly machinery (Bam) complex (98, 119), which is located in the OM and is responsible for OMP assembly as will be discussed later. These observations suggest that SurA might act at the OM insertion site. In *E. coli*, depletion of SurA results in a lower density of the OM (98), a phenomenon also observed upon depletion of the essential OMP assembly components (27, 70). The lower density is likely due to severely lower OMP content and was taken as evidence that SurA is the major chaperone required for assembly of the bulk mass of OMPs into the OM (98).

Previously it was shown that a *surA skp* double mutant is viable only when cells are grown in minimal medium (86). The observation that *skp* and *surA* mutations show a synthetic phenotype, *i.e.*, both mutations together have a much more severe effect than the individual mutations, might suggest that these two periplasmic chaperones are acting in parallel complementary pathways. In such situation, the absence of one of the chaperones is

at least partially compensated for by the presence of the remaining one, but the absence of both chaperones is not tolerated. However, in the context of all experimental data, it is more likely that Skp and SurA are acting at different steps in the same pathway, where Skp interacts with OMPs emerging from the Sec machinery and prevents their misfolding and aggregation, whereas SurA is involved in the folding of OMPs (10). In this model, the synthetic phenotype is explained by the increased need for efficient folding when the holding chaperone Skp is lacking, and *vice versa*, by the increased need for the holding chaperone when folding is hampered due to the absence of SurA.

The dual function protein DegP: protease and chaperone

The periplasmic protease DegP acts as a protease and degrades unfolded proteins but also is thought to have a chaperone function and assist in protein folding (102). It belongs to the widely distributed HtrA family of proteases that are characterized by the presence of one or more PDZ domains and a trypsin-like protease domain (17). Structural studies have shown that proteolytically inactive DegP hexamers (58) are transformed into proteolytically active huge cage-like 12- and 24-mers upon binding of denatured proteins (46, 56, 57). Its general chaperone activity was postulated from the finding that addition of proteolytically inactive DegP stimulates folding of several enzymes (102). Furthermore, cryo-electron microscopy revealed a cylindrical density inside the cage of a DegP 12-mer that could accommodate very well the native barrel of OmpC (56). Isolation of a proteolytically inactive DegP from the periplasm resulted in co-purification of at least partially folded monomeric OMPs, but not of trimeric OMPs (56). This might indicate that DegP is involved in OMP folding but is not sufficient for oligomerization. The question remains, though, what exactly makes the DegP multimers decide whether to degrade their cargo or not.

The DegP 24-mer was shown to bind to lipids, which indicates that it might facilitate insertion of OMPs into the OM (56). It has been suggested that, while folded OMPs remain protected inside the DegP cavity, unfolded aggregation-prone structures are degraded by DegP (56) into peptide fragments of 9-20 amino acids long (57). The latter indicates that DegP might carry out a quality control function in the periplasm.

Enzymes involved in disulfide bond formation

While passing through the periplasm, disulfide bonds are being formed and rearranged in the nascent OMPs, implying that OMPs are already partially folded before their insertion into the OM (30). In the periplasm, Dsb (disulfide bond formation) proteins are responsible for the disulfide bond formation and isomerisation (44). Disulfide bond formation is carried out by the DsbA protein, which is kept in an oxidized state by the IM protein DsbB. DsbB transmits electrons from reduced DsbA to either ubiquinone or menaquinone under aerobic or anaerobic conditions, respectively. The disulfide-isomerising pathway consists of the periplasmic DsbC, the integral IM protein DsbD, which keeps DsbC in the reduced state, and cytoplasmic thioredoxin, which acts as an electron donor (44). *N. meningitidis* contains single homologs of the DsbB, DsbC and DsbD proteins. Remarkably, there were three homologs for *dsbA* found in the meningococcal genomes (97, 111), whereas most Gram-negative bacteria contain only one *dsbA*. It has been suggested that the encoded proteins act on different target proteins (97). One of these homologs was found only in meningococci and not in other *Neisseria* species and it was suggested to be involved in the pathogenesis of *N. meningitidis* (79).

Insertion into the outer membrane

Omp85

While much is known about the translocation of OMPs across the IM, their insertion into the OM is poorly understood. Recently, Omp85 was identified in *N. meningitidis* as the key component of the OMP insertion machinery (118). In this organism, Omp85 is essential and its depletion led to the accumulation of unassembled monomers of all OMPs that were analyzed, such as PorA, PorB, PilQ, FrpB, and OMPLA (118). Later, the *E. coli* homolog of Omp85 was shown to have a similar function (27, 123, 124). The *E. coli* Omp85 homolog, formerly known as YaeT, was recently re-named BamA, for β-barrel assembly machinery component A. Like *N. meningitidis* Omp85, the *E. coli* homolog is essential. Pulse-chase experiments showed that only very low amounts of newly synthesized OMPs, such as LamB and OmpA, were inserted into the OM after BamA levels in *E. coli* were depleted (123).

Omp85 superfamily

Omp85 homologs are present in all sequenced Gram-negative bacteria and, interestingly, also in the OM of mitochondria and chloroplasts, probably reflecting the endosymbiont origin of these eukaryotic cell organelles. These proteins share functional and sequential similarities with the bacterial Omp85 and together form the Omp85 superfamily:

- In mitochondria, Tob55, also known as Sam50 or Omp85, was shown to be necessary for the assembly of β-barrel proteins, such as Tom40, a constituent of the translocase of the outer mitochondrial membrane (TOM) complex, and the mitochondrial porin VDAC (34, 55, 75).

- In chloroplasts, there are at least two Omp85 homologs, Toc75 and OEP80. Toc75 is a part of the chloroplast protein import machinery, which serves for protein translocation across the chloroplast outer envelope. The function of OEP80 remains elusive (43, 114), but it has been shown to be essential for the viability of *Arabidopsis thaliana* (76) and it is a strong candidate to be the functional equivalent of Tob55/Sam50, required for the assembly of β-barrel OMPs in the chloroplast OM.

- YtfM, a second Omp85 homolog in *E. coli* is predicted to contain an 8-stranded β-barrel in the C-terminal region (106). Mutants lacking YtfM do not show any OM biogenesis deficiencies, but grow more slowly than wild-type *E. coli* (106). YtfM homologs are present in many Gram-negative bacteria. Its function is still mostly unclear, but it was suggested to have a role in the secretion of YtfN (106).

- The TpsB translocators of Two-partner secretion systems mentioned are transporting their substrates, alike to Toc75, across a membrane, in this case across the OM to the cell surface. Whereas Omp85 is a general insertion factor for OMPs, TpsB proteins appear to recognize only one cognate substrate protein (45).

Structure of Omp85

Members of the Omp85 superfamily of proteins are defined by the presence of two domains (118): an N-terminal domain, comprising a variable number of so-called polypeptide transport-associated (POTRA) repeats, which were found by hidden Markov model searches (92), and a C-terminal β-barrel domain embedded in the membrane (Figure 4A). There is only one complete structure of an Omp85-superfamily member available, *i.e.*, that of the TpsB component FhaC of a two-partner secretion system of *B. pertussis*. This protein consists of two POTRA domains and a 16-stranded β-barrel (16).

The bacterial Omp85 was predicted to contain five POTRA domains extending in the periplasm (92, 118). Such a high number of POTRA domains is remarkable, since all other

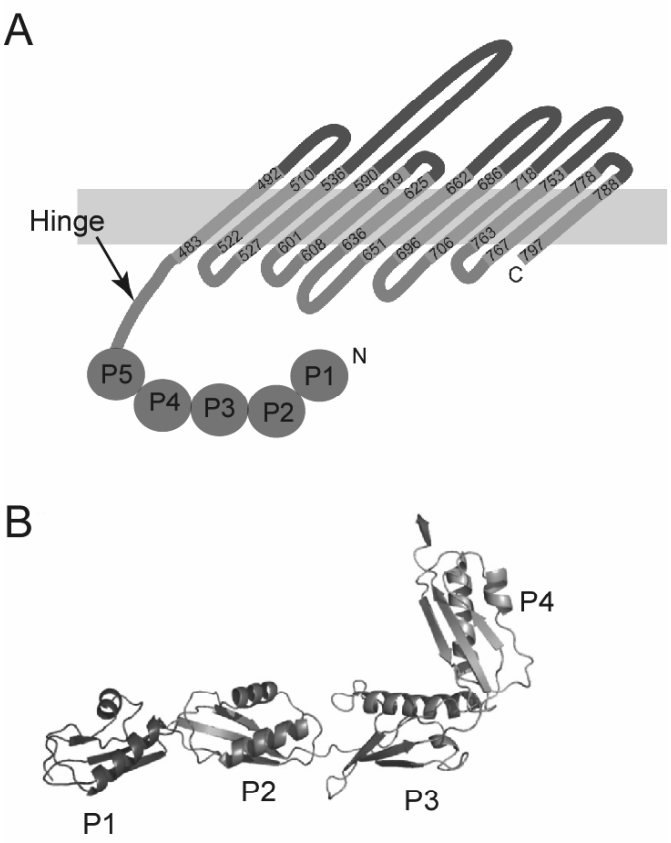

Figure 4

Omp85 structure. (**A**) Topology model of *N. meningitidis* Omp85. The predicted periplasmic part with five POTRA domains (P1-P5) and the membrane-embedded β-barrel domain are shown; numbers indicate the first and the last amino acid in each β-strand (118). The hinge region in between these domains is indicated. (**B**) Structure of an N-terminal fragment of *E. coli* BamA, comprising POTRA1 through POTRA4 and 5 amino acid residues of POTRA5 (33). POTRA domains are indicated by P1 through P4.

members of this superfamily are predicted or known to have fewer, *i.e*., two in FhaC, three in YtfM, Toc75, and OEP80, and one in Tob55 (16, 35). The presence of five POTRA domains in Omp85 was confirmed by crystal structures and small-angle X-ray scattering data obtained for N-terminal fragments of *E. coli* BamA (33, 47, 49). Although the sequence of the POTRA domains is not very well conserved, they all show a similar structure: 3 β-strands and 2 α-helices arranged in an identical fashion (Figure 4B).

The bacterial Omp85 protein was predicted to contain a 12-stranded membrane-embedded β-barrel at the C-terminal end (118). This topology leaves a region between the C terminus of the POTRA5 domain and the first amino acid of the predicted 12-stranded β-barrel of Omp85. In *N. meningitidis* and *E. coli*, this so-called hinge region (Figure 4A) is 61

amino acids long (47, 118). It cannot be excluded at this stage that the hinge region actually contributes four additional β-strands to the barrel, thus generating an Omp85 β-barrel of 16 β-strands, like in the case of FhaC.

Importance of the POTRA domains

Both parts of Omp85, the POTRA-containing region and the β-barrel, are essential for the functioning of Omp85 in OMP assembly. The relevance of having five POTRA for Omp85 function was investigated in deletion analyses. In *N. meningitidis*, mutants producing truncated Omp85 variants lacking up to four POTRA domains were viable and assembled OMPs only somewhat less efficiently than did the wild-type bacteria (11). The severity of the OMP assembly defect was proportional to the number of POTRA domains deleted. Deletion of all five POTRA domains, however, abolished Omp85 function completely, as did the deletion of only POTRA5, showing that POTRA5 is essential (11). In *E. coli*, a somewhat different approach was taken to study the role of the various POTRA domains of BamA. The domains were deleted one at a time. Mutants missing POTRA3, POTRA4, or POTRA5 were not viable, while mutants missing POTRA1 and, to a lesser extent, POTRA2 were severely affected in growth and OMP assembly (47). The discrepancy between these results is, at this stage, difficult to understand. The β-barrel domain of *N. meningitidis* Omp85 was shown to be essential and could not be replaced by another neisserial β-barrel of similar size (11).

The importance for function of the POTRA domains was also investigated for other members of the Omp85 superfamily. Deletion of either one of the two FhaC POTRA domains abolished secretion of FHA in *B. pertussis* (16). The only POTRA domain of Tob55 appeared not to be essential in mitochondria (59), although it was shown to bind OMP substrates (38). The mitochondrial β-barrels were also shown to be recognized by Sam35, a Tob55-associated protein that has no homolog in bacteria. This recognition required a sequence motif, designated the β-signal, which is present in mitochondrial OMPs (59).

Recognition of OMP precursors by Omp85

Many bacterial OMPs carry a C-terminal signature sequence. This sequence is characterized by a phenylalanine or a tryptophan at the C-terminal position, a hydrophobic amino acid residue, preferably a tyrosine, at the position -3 from the C terminus, and hydrophobic residues at the positions -5, -7, and -9 from the C terminus (107). The possibility that this signature sequence is recognized by Omp85 was investigated in planar lipid bilayer experiments (87). Purified BamA of *E. coli* reconstituted in planar lipid bilayers was shown to form pores (87, 105). A specific interaction of BamA with *E. coli* OMPs and their C-terminal peptides was reflected in a change of pore activity upon addition of these proteins or peptides (87). This change most likely represents an increased probability of the open state of the channel (P. Van Gelder, personal communication). Interestingly, a neisserial OMP did not affect the pore activity of BamA, suggesting a species-specific interaction. Although the C termini of the OMPs in both organisms share common features, neisserial OMPs often carry a positively charged residue in the penultimate position, unlike *E. coli* OMPs. Substitution of this residue in the neisserial PorA by a glutamine, which is frequently found at this position in *E. coli* OMPs, improved its assembly in *E. coli* (87). When OMPs are not assembled in *E. coli*, the signature sequence is recognized by the PDZ domain of DegS (120), generating a periplasmic stress response (described below), resulting, amongst others, in an increased protease activity that removes the unassembled OMPs.

Since the POTRA domains extend into the periplasm, they are the prime candidates for initial interactions with the substrate OMPs. The crystal structure of a BamA fragment consisting of the first four POTRA domains and a few amino-acid residues of POTRA5 revealed a dimer with interactions between a β-strand of POTRA3 and the residual N-

terminal fragment of POTRA5 of the other protomer resulting in augmentation of the β-sheet of POTRA3 (47). Although this dimer is probably a crystallization artefact, since the POTRA5 fragment is normally not available for interaction with POTRA3 when it is part of a complete POTRA5 domain, this finding suggested that POTRA domains might interact with substrates via a similar β-augmentation mechanism. This notion was underscored in NMR studies, which revealed significant, albeit weak, interactions of BamA-derived POTRA domains with various peptides from BamA's canonical substrate PhoE (49). Unfortunately, a PhoE C-terminal peptide was not included in this study because of solubility problems. This study revealed that the POTRA domains can act as separate binding units and recruit BamA substrates by association of OMP nascent chains with exposed β-strands of POTRA domains.

Some OMPs do not have the classical C–terminal signature sequences described above, but are still assembled into the OM in an Omp85-dependent manner. One example is OmpA of *E. coli*, in which a signature sequence is located in the last β-strand of N-terminal β-barrel, followed by the C-terminal periplasmic domain and not at the C terminus (48). Another example is TolC, which does not have a recognizable signature sequence at all (123). Similarly, assembly of the secretin PilQ, which also lacks a recognizable signature sequence, is affected by Omp85 depletion in *N. meningitidis* (118). This suggests that the presence of a C-terminal signature sequence is not an absolute requirement for OMP assembly. Consistently, a PhoE variant missing the C-terminal phenylalanine is assembled into the OM when expression levels are low (18).

Omp85 complex

Omp85 appears to function in a complex. In *N. meningitidis*, a high molecular weight complex containing Omp85 was detected when cell envelopes were analyzed by non-denaturing SDS-PAGE, but the components of this complex have not been analyzed so far (118). In *E. coli*, BamA was shown to be associated with at least four different lipoproteins, YfgL, NlpB, YfiO, and SmpA (99, 124). This *E. coli* Omp85 complex was recently re-named Bam (β-barrel assembly machinery) and its constituents were called BamA (Omp85), BamB (YfgL), BamC (NlpB), BamD (YfiO), and BamE (SmpA) (Figure 5). Like BamA, BamD is an essential protein in *E. coli*, which is also required for OMP assembly (67). BamB, BamC, and BamE are not essential, but the phenotypes of knockout mutants suggest that they are important for the maintenance of OM integrity in *E. coli* (99, 124). The *bamB*, and *bamC E. coli* mutants were shown to have increased OM permeability (124), while *bamB* and *bamE* mutant showed somewhat decreased levels of LamB and OmpA (99, 124). When double mutants were constructed, strong OMP assembly defects and, in some combinations, even synthetic lethality were observed (99).

Pull-down assays using His-tagged versions of the Bam components expressed in different mutants provided some insight into the organization of the Bam complex. The results indicated that BamB and BamD interact directly, but independently, with BamA. Interaction of BamC and BamE with the Bam complex requires the C terminus of BamD. BamE is associated with BamD and BamC independent of BamB (67, 99). The results obtained from pull-down experiments also indicated that the association between BamA and BamD is weakened in the *bamE* mutant but not in *bamC* mutant, indicating that BamE might play a role in the stabilization of the Bam complex in *E. coli* (99). Furthermore, BamA of *E. coli* was shown to form oligomers, probably tetramers *in vitro* (87). A His-tagged, truncated version of BamA did not pull-down full-length BamA produced in the same cells, indicating that multimers may not exist *in vivo* (47). However the dissociation of oligomers might have occurred during membrane extraction in this assay.

The role of the POTRA domains for Bam complex formation was investigated in *E. coli* (47). Mutants producing His-tagged BamA variants each lacking one POTRA domain

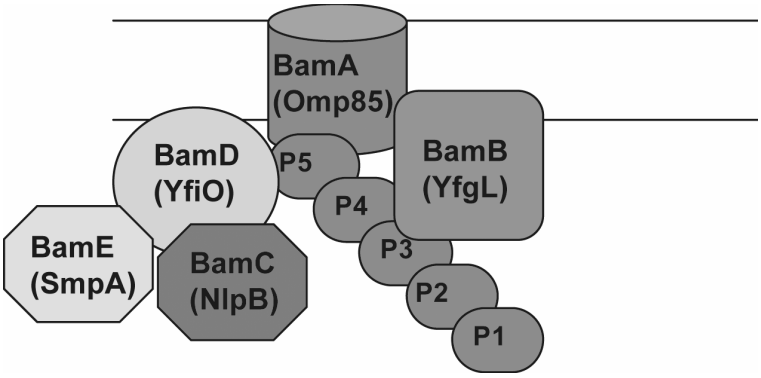

Figure 5

Putative organization of the Bam complex of *E. coli*. BamB interacts with BamA independent of BamC, BamD, or BamE. POTRA domains are indicated by P1 through P5. BamC and BamE require the C-terminal part of BamD for association with the complex (47, 67, 99). Former names of the proteins are indicated.

were constructed. Subsequent pull-down assays showed that deletion of any POTRA domain except for POTRA1 abolished the interaction of BamA with BamB. BamC, BamD and BamE were pulled-down with all BamA variants except when POTRA5 was lacking. These results suggested that BamB association with the Bam complex is more sensitive to the changes in the POTRA domains than association of other lipoproteins. Thus, POTRA domains are not only important for the interaction of BamA with substrates, but also for the formation of the Bam complex.

Periplasmic stress response

In *E. coli* there are three signaling pathways described: Cpx, σ^E, and Bae (89). Cpx stress-sensing system is activated by accumulation of pilus subunits in the periplasm, high pH, abnormalities in the IM, the presence of heavy metals or interaction of the cells with hydrophobic surfaces. The Cpx system consists of an IM-spanning histidine kinase CpxA, which transmits a signal from the periplasm to its cytoplasmic response regulator CpxR through phosphorylation. Phosphorylated CpxR activates transcription of the structural genes for cell envelope biogenesis factors, such as DsbA, DegP, and the peptidyl-prolyl isomerase PpiA (82). In the absence of periplasmic stress Cpx pathway is down-regulated. The periplasmic negative regulator CpxP is thought to interact with CpxA, this interaction might be disrupted in the presence of stress by proteolysis or through titration by unfolded proteins (89). The Cpx-mediated response may affect more than 100 genes (26). The exact signals activating the Cpx system are not clear. The best-understood signal so far is that provided by misfolded PapE, a tip fibrillar subunit of the P pilus, where the N-terminal extension of the protein is necessary for induction of a Cpx response (64).

The σ^E–dependent cell envelope stress response can be triggered by several abnormalities in the periplasm, such as unfolded OMPs and high temperatures. This stress response system is essential in *E. coli* (24), whereas inactivation of the other two described systems can be tolerated (42, 85). Activation of the σ^E–dependent response by unfolded OMPs accumulating in the periplasm is well understood (Figure 6). The DegS protease is

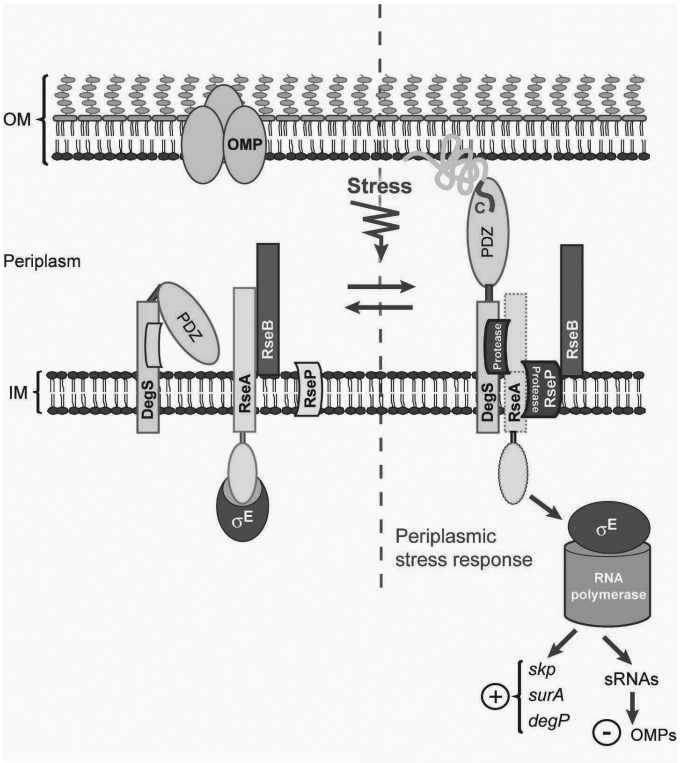

Figure 6

The σ^E–dependent cell envelope stress response. C termini of unfolded OMPs, accumulating in the periplasm under stress conditions, interact with the PDZ domain of DegS thereby activating this protease. DegS cleaves the anti-σ factor RseA, and this initial cleavage is followed by a series of proteolytic reactions, eventually resulting in the release of the cytoplasmic σ factor σ^E. The σ^E factor binds the RNA polymerase core enzyme, which enhances the transcription of the genes for periplasmic chaperones, such as SurA and Skp and the protease DegP. In addition, σ^E-containing RNA polymerase stimulates the production of small regulatory RNAs (sRNAs), which down-regulate OMP expression (10).

activated by the C termini of unfolded OMPs, which bind to its PDZ domain (120). A proteolytic cascade, involving DegS and RseP, amongst others, then follows leading to the release of the sigma factor σ^E from the anti-σ factor RseA, a cytoplasmic membrane protein. After binding of σ^E to the RNA-polymerase core enzyme, transcription of genes encoding SurA, Skp, Bam components, which could help to rescue unfolded OMPs, and protease DegP, involved in the degradation of unfolded OMPs, is enhanced. In *E. coli*, 20 σ^E-dependent promoters were identified by analyzing reporter gene expression (22). Moreover, σ^E triggers the production of small regulatory RNAs that down-regulate OMP production (74) (Figure 6). All together, the σ^E response helps the cells to cope with deficiencies in OMP assembly by removing unassembled OMPs and by down regulating their production. However, this system may not be generally present in Gram-negative bacteria, since, for instance, unassembled OMPs accumulate as aggregates in the periplasm of *N. meningitidis*

when their assembly is inhibited by Omp85 depletion (118). This is consistent with the lack of several essential components of the σ^E stress response pathway in this bacterial species (10).

The most recently discovered and not yet well-understood pathway is the two-component system Bae (85) consisting of the sensor kinase BaeS and the response regulator BaeR. This system is known to influence expression of the *spy* gene in response to cell envelope stress, whose product has an unknown function, but which is also upregulated by the better-described Cpx system. Further, the Bae system was reported to be involved in regulation of drugs efflux pumps, maltose transport, chemotactic responses, and flagellar biosynthesis (4, 71).

Scope of this thesis

So far, most of the research concerning OMP assembly in Gram-negative bacteria has been performed in *E. coli*. However, with the release of more and more genome sequences of Gram-negative bacteria, it becomes clear that the OMP assembly process may not be entirely similar in all Gram-negatives, since some of the components implicated in the assembly process cannot always be found in each genome. Furthermore, Gram-negatives other than *E. coli* may demonstrate different phenotypes when genes for OM assembly components are inactivated, and their analysis may yield novel insights into the biogenesis of the OM. The Gram-negative bacterium *N. meningitidis* has been especially useful in this respect. It was the first Gram-negative shown to be able to survive without the major OM component LPS and to still assemble OMPs correctly in those conditions (103, 104). Furthermore, a mutational analysis of neisserial Omp85, which was not possible in *E. coli*, resulted in the definition of the crucial POTRA5 domain (11). Also, *E. coli* BamA cannot deal properly with neisserial OMPs (87) and the way *E. coli* and *N. meningitidis* deal with OMPs that fall off from the folding and insertion route appears to be different (118).

The goal of this work was to characterize the OMP assembly process in *N. meningitidis* to further our understanding of OMP assembly in Gram-negative bacteria in general. To that end, in Chapter 2, we characterized the Omp85-containing β-barrel assembly complex in *N. meningitidis*. Several components were found to be similar to those found in *E. coli*, but one was lacking and a new component was also identified.

In Chapter 3, we addressed the roles of the major periplasmic chaperones that are generally implicated in OMP assembly, i.e. SurA and Skp, in *N. meningitidis* and found considerable differences compared to *E. coli*, particularly with respect to the role of SurA.

Emanating from the observation that *E. coli* BamA did not interact with a neisserial OMP *in vitro* (87), we addressed in Chapter 4 the species specificity of Omp85 by analyzing the functionality of Omp85 homologs from other proteobacteria in *E. coli* and in *N. meningitidis*.

In Chapters 5 and 6, we purified *E. coli* and *N. meningitidis* Omp85 proteins and some of their subdomains and studied properties, such as secondary structure, pore formation and substrate recognition *in vitro*.

Finally, the results are summarized and discussed in Chapter 7.

References

1. **Ahn, V. E., E. I. Lo, C. K. Engel, L. Chen, P. M. Hwang, L. E. Kay, R. E. Bishop, and G. G. Privé.** 2004. A hydrocarbon ruler measures palmitate in the enzymatic acylation of endotoxin. EMBO J. **23:**2931-2941.
2. **Ala'Aldeen, D. A. A., and S. P. Borriello.** 1996. The meningococcal transferrin-binding proteins 1 and 2 are both surface exposed and generate bactericidal antibodies capable of killing homologous and heterologous strains. Vaccine **14:**49-53.
3. **Aasland, R., J. Coleman, A. L. Holck, C. L. Smith, C. R. H. Raetz, and K. Kleppe.** 1988. Identity of the 17-kilodalton protein, a DNA-binding protein from *Escherichia coli*, and the *firA* gene product. J. Bacteriol. **170:**5916-5918.
4. **Baranova, N., and H. Nikaido.** 2002. The *baeSR* two-component regulatory system activates transcription of the *yegMNOB* (*mdtABCD*) transporter gene cluster in *Escherichia coli* and increases its resistance to novobiocin and deoxycholate. J. Bacteriol. **184:**4168-4176.
5. **Bayan, N., I. Guilvout, and A. P. Pugsley.** 2006. Secretins take shape. Mol. Microbiol. **60:**1-4.
6. **Behrens, S., R. Maier, H. de Cock, F. X. Schmid, and C. A. Gross.** 2001. The SurA periplasmic PPIase lacking its parvulin domains functions *in vivo* and has chaperone activity. EMBO J. **20:**285-294.
7. **Bishop, R. E.** 2008. Structural biology of membrane-intrinsic beta-barrel enzymes: sentinels of the bacterial outer membrane. Biochim. Biophys. Acta **1778:**1881-1896.
8. **Bitto, E., and D. B. McKay.** 2002. Crystallographic structure of SurA, a molecular chaperone that facilitates folding of outer membrane porins. Structure **10:**1489-1498.
9. **Bos, M. P., and J. Tommassen.** 2004. Biogenesis of the Gram-negative bacterial outer membrane. Curr. Opin. Microbiol. **7:**610-616.
10. **Bos, M. P., V. Robert, and J. Tommassen.** 2007. Biogenesis of the gram-negative bacterial outer membrane. Annu. Rev. Microbiol. **61:**191-214.
11. **Bos, M. P., V. Robert, and J. Tommassen.** 2007. Functioning of outer membrane protein assembly factor Omp85 requires a single POTRA domain. EMBO Rep. **8:**1149-1154.
12. **Braun, V., R. Ondraczek, and S. Hobbie.** 1993. Activation and secretion of *Serratia* hemolysin. Zentralbl. Bakteriol. **278:**306-315.
13. **Buchanan, S. K., B. S. Smith, L. Venkatramani, D. Xia, L. Esser, M. Palnitkar, R. Chakraborty, D. van der Helm, and J. Deisenhofer.** 1999. Crystal structure of the outer membrane active transporter FepA from *Escherichia coli*. Nat. Struct. Biol. **6:**56-63.
14. **Chami, M., I. Guilvout, M. Gregorini, H. W. Rémigy, S. A. Müller, M. Valerio, A. Engel, A. P. Pugsley, and N. Bayan.** 2005. Structural insights into the secretin PulD and its trypsin-resistant core. J. Biol. Chem. **280:**37732-37741.
15. **Chen, R., and U. Henning.** 1996. A periplasmic protein (Skp) of *Escherichia coli* selectively binds a class of outer membrane proteins. Mol. Microbiol. **19:**1287-1294.
16. **Clantin, B., A. S. Delattre, P. Rucktooa, N. Saint, A. C. Méli, C. Locht, F. Jacob-Dubuisson, and V. Villeret.** 2007. Structure of the membrane protein FhaC: a member of the Omp85-TpsB transporter superfamily. Science **317:**957-961.
17. **Clausen, T., C. Southan, and M. Ehrmann.** 2002. The HtrA family of proteases: implications for protein composition and cell fate. Mol. Cell **10:**443-455.
18. **de Cock H, M. Struyvé, M. Kleerebezem, T. van der Krift, and J Tommassen J.** 1997. Role of the carboxy-terminal phenylalanine in the biogenesis of outer membrane protein PhoE of *Escherichia coli* K-12. J. Mol. Biol. **269:**473-478.
19. **Collins, R. F., and J. P. Derrick.** 2007. Wza: a new structural paradigm for outer membrane secretory proteins? Trends Microbiol. **15:**96-100.
20. **Collins, R. F., S. A. Frye, A. Kitmitto, R. C. Ford, T. Tønjum, and J. P. Derrick.** 2004. Structure of the *Neisseria meningitidis* outer membrane PilQ secretin complex at 12 Å resolution. J. Biol. Chem. **279:**39750-39756.

21. **Cowan, S. W., T. Schirmer, G. Rummel, M. Steiert, R. Ghosh, R. A. Pauptit, J. N. Jansonius, and J. P. Rosenbusch.** 1992. Crystal structures explain functional properties of two *E. coli* porins. Nature **358:**727-733.
22. **Dartigalongue, C., D. Missiakas, and S. Raina.** 2001. Characterization of the *Escherichia coli* σ^E regulon. J. Biol. Chem. **276:**20866-20875.
23. **de Cock, H., U. Schäfer, M. Potgeter, R. Demel, M. Müller, and J. Tommassen.** 1999. Affinity of the periplasmic chaperone Skp of *Escherichia coli* for phospholipids, lipopolysaccharides and non-native outer membrane proteins. Role of Skp in the biogenesis of outer membrane protein. Eur. J. Biochem. **259:**96-103.
24. **De Las Peñas, A., L. Connolly, and C. A. Gross.** 1997. σ^E is an essential sigma factor in *Escherichia coli*. J. Bacteriol. **179:**6862-6864.
25. **Derrick, J.P., R. Urwin, J. Suker, I. M. Feavers, and M. C. J. Maiden.** 1999. Structural and evolutionary inference from molecular variation in *Neisseria* porins. Infect. Immun. **67:**2406-2413.
26. **De Wulf, P., A. M. McGuire, X. Liu, and E. C. C. Lin.** 2002. Genome-wide profiling of promoter recognition by the two-component response regulator CpxR-P in *Escherichia coli*. J. Biol. Chem. **277:**26652–26661.
27. **Doerrler**, **W. T., and C. R. H. Raetz.** 2005. Loss of outer membrane proteins without inhibition of lipid export in an *Escherichia coli* YaeT mutant. J. Biol. Chem. **280:**27679-27687.
28. **Dong, C., K. Beis, J. Nesper, A. L. Brunkan-Lamontagne, B. R. Clarke, C. Whitfield, and J. H. Naismith.** 2006. Wza the translocon for *E. coli* capsular polysaccharides defines a new class of membrane protein. Nature **444:**226-229.
29. **Driessen, A. J. M., and N. Nouwen.** 2008. Protein translocation across the bacterial cytoplasmic membrane. Annu. Rev. Biochem. **77:**643-667.
30. **Eppens, E. F., N. Nouwen, and J. Tommassen.** 1997. Folding of a bacterial outer membrane protein during passage through the periplasm. EMBO J. **16:**4295-4301.
31. **Ferguson, A. D., E. Hofmann, J. W. Coulton, K. Diederichs, and W. Welte.** 1998. Siderophore-mediated iron transport: crystal structure of FhuA with bound lipopolysaccharide. Science **282:**2215-2220.
32. **Galloway, S. M., and C. R. H. Raetz.** 1990. A mutant of *Escherichia coli* defective in the first step of endotoxin biosynthesis. J. Biol. Chem. **265:**6394-6402.
33. **Gatzeva-Topalova, P. Z., T. A. Walton, and M. C. Sousa.** 2008. Crystal structure of YaeT: conformational flexibility and substrate recognition. Structure **16:**1873–1881.
34. **Gentle, I., K. Gabriel, P. Beech, R. Waller, and T. Lithgow.** 2004. The Omp85 family of proteins is essential for outer membrane biogenesis in mitochondria and bacteria. J. Cell. Biol. **164:**19-24.
35. **Gentle, I. E., L. Burri, and T. Lithgow.** 2005. Molecular architecture and function of the Omp85 family of proteins. Mol. Microbiol. **58:**1216-1225.
36. **Guédin, S., E. Willery, J. Tommassen, E. Fort, H. Drobecq, C. Locht, and F. Jacob-Dubuisson.** 2000. Novel topological features of FhaC, the outer membrane transporter involved in the secretion of the *Bordetella pertussis* filamentous hemagglutinin. J. Biol. Chem. **275:**30202-30210.
37. **Gupta, S. D., K. Gan, M. B. Schmid, and H. C. Wu.** 1993. Characterization of a temperature-sensitive mutant of *Salmonella typhimurium* defective in apolipoprotein N-acyltransferase. J. Biol. Chem. **268:**16551-16556.
38. **Habib, S. J., T. Waizenegger, A. Niewienda, S. A. Paschen, W. Neupert, and D. Rapaport.** 2007. The N-terminal domain of Tob55 has a receptor-like function in the biogenesis of mitochondrial beta-barrel proteins. J. Cell. Biol. **176:**77-88.
39. **Harms, N., G. Koningstein, W. Dontje, M. Müller, B. Oudega, J. Luirink, and H. de Cock.** 2001. The early interaction of the outer membrane protein PhoE with the periplasmic chaperone Skp occurs at the cytoplasmic membrane. J. Biol. Chem. **276:**18804-18811.
40. **Hennecke, G., J. Nolte, R. Volkmer-Engert, J. Schneider-Mergener, and S. Behrens.** 2005. The periplasmic chaperone SurA exploits two features characteristic of integral outer membrane proteins for selective substrate recognition. J. Biol. Chem. **280:**23540-23548.

41. **Hiller, S., R. G. Garces, T. J. Malia, V. Y. Orekhov, M. Colombini, and G. Wagner.** 2008. Solution structure of the integral human membrane protein VDAC-1 in detergent micelles. Science **321:**1206-1210.
42. **Hung, D. L., T. L. Raivio, C. H. Jones, T. J. Silhavy, and S. J. Hultgren.** 2001. Cpx signaling pathway monitors biogenesis and affects assembly and expression of P pili. EMBO J. **20:**1508-1518.
43. **Inoue, K., and D. Potter.** 2004. The chloroplastic protein translocation channel Toc75 and its paralog OEP80 represent two distinct protein families and are targeted to the chloroplastic outer envelope by different mechanisms. Plant J. **39:**354-365.
44. **Ito, K., and K. Inaba.** 2008. The disulfide bond formation (Dsb) system. Curr. Opin. Struct. Biol. **18:**450-458.
45. **Jacob-Dubuisson, F., C. Locht, and R. Antoine.** 2001. Two-partner secretion in Gram-negative bacteria: a thrifty, specific pathway for large virulence proteins. Mol. Microbiol. **40:**306-313.
46. **Jiang, J., X. Zhang, Y. Chen, Y. Wu, Z. H. Zhou, Z. Chang, and S. F. Sui.** 2008. Activation of DegP chaperone-protease via formation of large cage-like oligomers upon binding to substrate proteins. Proc. Natl. Acad. Sci. U S A **105:**11939-11944.
47. **Kim, S., J. C. Malinverni, P. Sliz, T. J. Silhavy, S. C. Harrison, and D. Kahne.** 2007. Structure and function of an essential component of the outer membrane protein assembly machine. Science **317:**961-964.
48. **Klose, M., H. Schwarz, S. MacIntyre, R. Freudl, M. L. Eschbach, and U. Henning.** 1988. Internal deletions in the gene for an *Escherichia coli* outer membrane protein define an area possibly important for recognition of the outer membrane by this polypeptide. J. Biol. Chem. **263:**13291-13296.
49. **Knowles, T. J., M. Jeeves, S. Bobat, F. Dancea, D. McClelland, T. Palmer, M. Overduin, and I. R. Henderson.** 2008. Fold and function of polypeptide transport-associated domains responsible for delivering unfolded proteins to membranes. Mol. Microbiol. **68:**1216-1227.
50. **Koebnik, R**. 1995. Proposal for a peptidoglycan-associating alpha-helical motif in the C-terminal regions of some bacterial cell-surface proteins. Mol. Microbiol. **16:**1269-1270.
51. **Koebnik, R., K. P. Locher, and P. Van Gelder.** 2000. Structure and function of bacterial outer membrane proteins: barrels in a nutshell. Mol. Microbiol. **37:**239-253.
52. **Korndörfer, I. P., M. K. Dommel, and A. Skerra.** 2004. Structure of the periplasmic chaperone Skp suggests functional similarity with cytosolic chaperones despite differing architecture. Nat. Struct. Mol. Biol. **11:**1015-1020.
53. **Koronakis, V., A. Sharff, E. Koronakis, B. Luisi, and C. Hughes.** 2000. Crystal structure of the bacterial membrane protein TolC central to multidrug efflux and protein export. Nature **405:**914-919.
54. **Koski, P., M. Rhen, J. Kantele, and M. Vaara.** 1989. Isolation, cloning, and primary structure of a cationic 16-kDa outer membrane protein of *Salmonella typhimurium*. J. Biol. Chem. **264:**18973-18980.
55. **Kozjak, V., N. Wiedemann, D. Milenkovic, C. Lohaus, H. E. Meyer, B. Guiard, C. Meisinger, and N. Pfanner.** 2003. An essential role of Sam50 in the protein sorting and assembly machinery of the mitochondrial outer membrane. J. Biol. Chem. **278:**48520-48523.
56. **Krojer, T., J. Sawa, E. Schäfer, H. R. Saibil, M. Ehrmann, and T. Clausen.** 2008. Structural basis for the regulated protease and chaperone function of DegP. Nature **453:**885-890.
57. **Krojer, T., K. Pangerl, J. Kurt, J. Sawa, C. Stingl, K. Mechtler, R. Huber, M. Ehrmann, and T. Clausen**. 2008. Interplay of PDZ and protease domain of DegP ensures efficient elimination of misfolded proteins. Proc. Natl. Acad. Sci. U S A **105:**7702-7707.
58. **Krojer, T., M. Garrido-Franco, R. Huber, M. Ehrmann, and T. Clausen.** 2002. Crystal structure of DegP (HtrA) reveals a new protease-chaperone machine. Nature **416:**455-459.
59. **Kutik, S., D. Stojanovski, L. Becker, T. Becker, M. Meinecke, V. Krüger, C. Prinz, C. Meisinger, B. Guiard, R. Wagner, N. Pfanner, and N. Wiedemann.** 2008. Dissecting membrane insertion of mitochondrial β-barrel proteins. Cell **132:**1011-1024.

60. **Lathe, R., H. Buc, J. P. Lecocq, and E. K. Bautz.** 1980. Prokaryotic histone-like protein interacting with RNA polymerase. Proc. Natl. Acad. Sci. U S A **77:**3548-3552.
61. **Lazar, S. W., M. Almirón, A. Tormo, and R. Kolter.** 1998. Role of the *Escherichia coli* SurA protein in stationary-phase survival. J. Bacteriol. **180:**5704-5711.
62. **Lazar, S. W., and R. Kolter.** 1996. SurA assists the folding of *Escherichia coli* outer membrane proteins. J. Bacteriol. **178:**1770-1773.
63. **Lee, P. A., D. Tullman-Ercek, and G. Georgiou.** 2006. The bacterial twin-arginine translocation pathway. Annu. Rev. Microbiol. **60:**373-395.
64. **Lee, Y. M., P. A. DiGiuseppe, T. J. Silhavy, and S. J. Hultgren.** 2004. P pilus assembly motif necessary for activation of the CpxRA pathway by PapE in *Escherichia coli*. J. Bacteriol. **186:**4326-4337.
65. **Lewis, L. A., K. Rohde, M. Gipson, B. Behrens, E. Gray, S. I. Toth, B. A. Roe, and D. W. Dyer.** 1998. Identification and molecular analysis of *lbpBA*, which encodes the two-component meningococcal lactoferrin receptor. Infect. Immun. **66:**3017-3023.
66. **Locher, K. P., B. Rees, R. Koebnik, A. Mitschler, L. Moulinier, J. P. Rosenbusch, and D. Moras.** 1998. Transmembrane signaling across the ligand-gated FhuA receptor: crystal structures of free and ferrichrome-bound states reveal allosteric changes. Cell **95:**771-778.
67. **Malinverni, J. C., J. Werner, S. Kim, J. G. Sklar, D. Kahne, R. Misra, and T. J. Silhavy.** 2006. YfiO stabilizes the YaeT complex and is essential for outer membrane protein assembly in *Escherichia coli*. Mol. Microbiol. **61:**151-164.
68. **Meng, G., N. K. Surana, J. W. St Geme III, and G. Waksman.** 2006. Structure of the outer membrane translocator domain of the *Haemophilus influenzae* Hia trimeric autotransporter. EMBO J. **25:**2297–2304.
69. **Narita, S., S. Matsuyama, and H. Tokuda.** 2004. Lipoprotein trafficking in *Escherichia coli*. Arch. Microbiol. **182:**1-6.
70. **Nikaido, H.** 1992. Porins and specific channels of bacterial outer membranes. Mol. Microbiol. **6:**435-442.
71. **Nishino, K., T. Honda, and A. Yamaguchi**. 2005. Genome-wide analyses of *Escherichia coli* gene expression responsive to the BaeSR two-component regulatory system. J. Bacteriol. **187:**1763-1772.
72. **Oakhill, J. S., B. J. Sutton, A. R. Gorringe, and R. W. Evans.** 2005. Homology modelling of transferrin-binding protein A from *Neisseria meningitidis*. Protein Eng. Des. Sel. **18:**221-228.
73. **Oomen, C. J., P. van Ulsen, P. van Gelder, M. Feijen, J. Tommassen, and P. Gros.** 2004. Structure of the translocator domain of a bacterial autotransporter. EMBO J. **23:**1257-1266.
74. **Papenfort, K., V. Pfeiffer, F. Mika, S. Lucchini, J. C. D. Hinton, and J. Vogel.** 2006. σ^E-dependent small RNAs of *Salmonella* respond to membrane stress by accelerating global *omp* mRNA decay. Mol. Microbiol. **62:**1674–1688.
75. **Paschen, S. A., T. Waizenegger, T. Stan, M. Preuss, M. Cyrklaff, K. Hell, D. Rapaport, and W. Neupert.** 2003. Evolutionary conservation of biogenesis of beta-barrel membrane proteins. Nature **426:**862-866.
76. **Patel, R, S. C. Hsu, J. Bédard, K. Inoue, P. Jarvis.** 2008. The Omp85-related chloroplast outer envelope protein OEP80 is essential for viability in *Arabidopsis*. Plant. Physiol. **148:**235-245.
77. **Pautsch, A., and G. E. Schulz.** 1998. Structure of the outer membrane protein A transmembrane domain. Nat. Struct. Biol. **5:**1013-1017.
78. **Peng, D., W. Hong, B. P. Choudhury, R. W. Carlson, and X. X. Gu.** 2005. *Moraxella catarrhalis* bacterium without endotoxin, a potential vaccine candidate. Infect. Immun. **73:**7569-7577.
79. **Perrin, A., S. Bonacorsi, E. Carbonnelle, D. Talibi, P. Dessen, X. Nassif, C. Tinsley.** 2002. Comparative genomics identifies the genetic islands that distinguish *Neisseria meningitidis*, the agent of cerebrospinal meningitis, from other *Neisseria* species. Infect. Immun. **70:**7063-7072.

80. **Pettersson, A., J. Kortekaas, V. E. Weynants, P. Voet, J. T. Poolman, M. P. Bos, and J. Tommassen.** 2006. Vaccine potential of the *Neisseria meningitidis* lactoferrin-binding proteins LbpA and LbpB. Vaccine **24:**3545-3557.
81. **Pettersson, A, T. Prinz, A. Umar, J. van der Biezen, and J. Tommassen.** 1998. Molecular characterization of LbpB, the second lactoferrin-binding protein of *Neisseria meningitidis*. Mol. Microbiol. **27:**599-610.
82. **Pogliano, J., A. S. Lynch, D. Belin, E. C. C. Lin, and J. Beckwith.** 1997. Regulation of *Escherichia coli* cell envelope proteins involved in protein folding and degradation by the Cpx two-component system. Genes Dev. **11:**1169-1182.
83. **Pohlner, J., R. Halter, K. Beyreuther, and T. F. Meyer.** 1987. Gene structure and extracellular secretion of *Neisseria gonorrhoeae* IgA protease. Nature **325:**458–462.
84. **Qu, J., C. Mayer, S. Behrens, O. Holst, and J. H. Kleinschmidt.** 2007. The trimeric periplasmic chaperone Skp of *Escherichia coli* forms 1:1 complexes with outer membrane proteins via hydrophobic and electrostatic interactions. J. Mol. Biol. **374:**91-105.
85. **Raffa, R. G., and T. L. Raivio.** 2002. A third envelope stress signal transduction pathway in *Escherichia coli*. Mol. Microbiol. **45:**1599–1611.
86. **Rizzitello, A. E., J. R. Harper, and T. J. Silhavy.** 2001. Genetic evidence for parallel pathways of chaperone activity in the periplasm of *Escherichia coli*. J. Bacteriol. **183:**6794-6800.
87. **Robert, V., E. B. Volokhina, F. Senf, M. P. Bos, P. Van Gelder, and J. Tommassen.** 2006. Assembly factor Omp85 recognizes its outer membrane protein substrates by a species-specific C-terminal motif. PLoS Biol. **4:**e377.
88. **Rouvière, P. E., and C. A. Gross.** 1996. SurA, a periplasmic protein with peptidyl-prolyl isomerase activity, participates in the assembly of outer membrane porins. Genes Dev. **10:**3170-3182.
89. **Ruiz, N., and T. J. Silhavy.** 2005. Sensing external stress: watchdogs of the *Escherichia coli* cell envelope. Curr. Opin. Microbiol. **8:**122-126.
90. **Rutten, L., J. Geurtsen, W. Lambert, J. J. Smolenaers, A. M. Bonvin, A. de Haan, P. van der Ley, M. R. Egmond, P. Gros, and J. Tommassen.** 2006. Crystal structure and catalytic mechanism of the LPS 3-O-deacylase PagL from *Pseudomonas aeruginosa*. Proc. Natl. Acad. Sci. U S A **103:**7071-7076.
91. **Rutten, L., J. P. Mannie, C. M. Stead, C. R. Raetz, C. M. Reynolds, A. M. Bonvin, J. P. Tommassen, M. R. Egmond, M. S. Trent, and P. Gros.** 2009. Active-site architecture and catalytic mechanism of the lipid A deacylase LpxR of *Salmonella typhimurium*. Proc. Natl. Acad. Sci. USA **106:**1960-1964.
92. **Sánchez-Pulido, L., D. Devos, S. Genevrois, M. Vicente, and A. Valencia.** 2003. POTRA: a conserved domain in the FtsQ family and a class of β-barrel outer membrane proteins. Trends Biochem. Sci. **28:**523-526.
93. **Sankaran, K., and H. C. Wu.** 1994. Lipid modification of bacterial prolipoprotein. Transfer of diacylglyceryl moiety from phosphatidylglycerol. J. Biol. Chem. **269:**19701-19706.
94. **Schäfer, U., K. Beck, and M. Müller.** 1999. Skp, a molecular chaperone of gram-negative bacteria, is required for the formation of soluble periplasmic intermediates of outer membrane proteins. J. Biol. Chem. **274:**24567-24574.
95. **Schirmer, T., T. A. Keller, Y. F. Wang, and J. P. Rosenbusch.** 1995. Structural basis for sugar translocation through maltoporin channels at 3.1 Å resolution. Science. **267:**512-514.
96. **Schulz, G. E.** 2000. β-Barrel membrane proteins. Curr. Opin. Struct. Biol. **10:**443-447.
97. **Sinha, S., P. R. Langford, J. S. Kroll.** 2004. Functional diversity of three different DsbA proteins from *Neisseria meningitidis*. Microbiology **150:**2993-3000.
98. **Sklar, J. G., T. Wu, D. Kahne, and T. J. Silhavy.** 2007. Defining the roles of the periplasmic chaperones SurA, Skp, and DegP in *Escherichia coli*. Genes Dev. **21:**2473-2484.
99. **Sklar, J. G., T. Wu, L. S. Gronenberg, J. C. Malinverni, D. Kahne, and T. J. Silhavy.** 2007. Lipoprotein SmpA is a component of the YaeT complex that assembles outer membrane proteins in *Escherichia coli*. Proc. Natl. Acad. Sci. U S A **104:**6400-6405.

100. **Snijder, H. J., I. Ubarretxena-Belandia, M. Blaauw, K. H. Kalk, H. M. Verheij, M. R. Egmond, N. Dekker, and B. W. Dijkstra.** 1999. Structural evidence for dimerization-regulated activation of an integral membrane phospholipase. Nature **401:**717-721.
101. **Song, J., C. A. Minetti, M. S. Blake, and M. Colombini.** 1998. Successful recovery of the normal electrophysiological properties of PorB (class 3) porin from *Neisseria meningitidis* after expression in *Escherichia coli* and renaturation. Biochim. Biophys. Acta **1370:**289-298.
102. **Spiess, C., A. Beil, and M. Ehrmann.** 1999. A temperature-dependent switch from chaperone to protease in a widely conserved heat shock protein. Cell **97:**339-347.
103. **Steeghs, L., R. den Hartog, A. den Boer, B. Zomer, P. Roholl, and P. van der Ley.** 1998. Meningitis bacterium is viable without endotoxin. Nature **392:**449-450.
104. **Steeghs, L., H. de Cock, E. Evers, B. Zomer, J. Tommassen, and P. van der Ley.** 2001. Outer membrane composition of a lipopolysaccharide-deficient *Neisseria meningitidis* mutant. EMBO J. **20:**6937-6945.
105. **Stegmeier, J. F., and C. Andersen.** 2006. Characterization of pores formed by YaeT (Omp85) from *Escherichia coli*. J. Biochem. (Tokyo) **140:**275-283.
106. **Stegmeier, J. F., A. Glück, S. Sukumaran, W. Mäntele, and C. Andersen.** 2007. Characterisation of YtfM, a second member of the Omp85 family in *Escherichia coli*. Biol. Chem. **388:**37-46.
107. **Struyvé, M., M. Moons, and J. Tommassen.** 1991. Carboxy-terminal phenylalanine is essential for the correct assembly of a bacterial outer membrane protein. J. Mol. Biol. **218:**141-148.
108. **Terada, M., T. Kuroda, S. I. Matsuyama, and H. Tokuda.** 2001. Lipoprotein sorting signals evaluated as the LolA-dependent release of lipoproteins from the cytoplasmic membrane of *Escherichia coli*. J. Biol. Chem. **276:**47690-47694.
109. **Thome, B. M., and M. Müller.** 1991. Skp is a periplasmic *Escherichia coli* protein requiring SecA and SecY for export. Mol. Microbiol. **5:**2815-2821.
110. **Thome, B. M., H. K. Hoffschulte, E. Schiltz, and M. Müller.** 1990. A protein with sequence identity to Skp (FirA) supports protein translocation into plasma membrane vesicles of *Escherichia coli*. FEBS Lett. **269:**113-116.
111. **Tinsley, C. R., R. Voulhoux, J. L. Beretti, J. Tommassen, and X. Nassif.** 2004. Three homologues, including two membrane-bound proteins, of the disulfide oxidoreductase DsbA in *Neisseria meningitidis*: effects on bacterial growth and biogenesis of functional type IV pili. J. Biol. Chem. **279:**27078-27087.
112. **Tommassen, J., P. Vermeij, M. Struyvé, R. Benz, and J. T. Poolman.** 1990. Isolation of *Neisseria meningitidis* mutants deficient in class 1 (PorA) and class 3 (PorB) outer membrane proteins. Infect. Immun. **58:**1355-1359.
113. **Tormo, A.**, **M. Almirón, and R. Kolter.** 1990. *surA*, an *Escherichia coli* gene essential for survival in stationary phase. J. Bacteriol. **172:**4339-4347.
114. **Tu, S. L., L. J. Chen, M. D. Smith, Y. S. Su, D. J. Schnell, and H. M. Li.** 2004. Import pathways of chloroplast interior proteins and the outer-membrane protein OEP14 converge at Toc75. Plant Cell **16:**2078-2088.
115. **Ujwal, R., D. Cascio, J. P. Colletier, S. Faham, J. Zhang, L. Toro, P. Ping, and J. Abramson.** 2008. The crystal structure of mouse VDAC1 at 2.3 Åresolution reveals mechanistic insights into metabolite gating. Proc. Natl. Acad. Sci. U S A **105:**17742-17747.
116. **van der Ley, P., J. E. Heckels, M. Virji, P. Hoogerhout, and J. T. Poolman.** 1991. Topology of outer membrane porins in pathogenic *Neisseria* spp. Infect. Immun. **59:**2963-2971.
117. **Vandeputte-Rutten, L., R. A. Kramer, J. Kroon, N. Dekker, M. R. Egmond, and P. Gros.** 2001. Crystal structure of the outer membrane protease OmpT from *Escherichia coli* suggests a novel catalytic site. EMBO J. **20:**5033-5039.
118. **Voulhoux, R., M. P. Bos, J. Geurtsen, M. Mols, and J. Tommassen.** 2003. Role of a highly conserved bacterial protein in outer membrane protein assembly. Science **299:**262-265.
119. **Vuong, P., D. Bennion, J. Mantei, D. Frost, and R. Misra.** 2008. Analysis of YfgL and YaeT interactions through bioinformatics, mutagenesis, and biochemistry. J. Bacteriol. **190:**1507-1517.

120. **Walsh, N. P., B. M. Alba, B. Bose, C. A. Gross, and R. T. Sauer.** 2003. OMP peptide signals initiate the envelope-stress response by activating DegS protease via relief of inhibition mediated by its PDZ domain. Cell **113:**61-71.
121. **Walton, T. A., and M. C. Sousa.** 2004. Crystal structure of Skp, a prefoldin-like chaperone that protects soluble and membrane proteins from aggregation. Mol. Cell **15:**367-374.
122. **Walton, T. A., C. M. Sandoval, C. A. Fowler, A. Pardi, and M. C. Sousa.** 2009. The cavity-chaperone Skp protects its substrate from aggregation but allows independent folding of substrate domains. Proc. Natl. Acad. Sci. U S A **106:**1772-1777.
123. **Werner, J., and R. Misra.** 2005. YaeT (Omp85) affects the assembly of lipid-dependent and lipid-independent outer membrane proteins of *Escherichia coli*. Mol. Microbiol. **57:**1450-1459.
124. **Wu, T., J. Malinverni, N. Ruiz, S. Kim, T. J. Silhavy, and D. Kahne.** 2005. Identification of a multicomponent complex required for outer membrane biogenesis in *Escherichia coli*. Cell **121:**235-245.
125. **Xu, X., S. Wang, Y. X. Hu, and D. B. McKay.** 2007. The periplasmic bacterial molecular chaperone SurA adapts its structure to bind peptides in different conformations to assert a sequence preference for aromatic residues. J. Mol. Biol. **373:**367-381.

Chapter 2

The β-barrel outer membrane protein assembly complex of *Neisseria meningitidis*

Elena B. Volokhina, Frank Beckers, Jan Tommassen and Martine P. Bos

Department of Molecular Microbiology and Institute of Biomembranes, Utrecht University, Padualaan 8, 3584 CH Utrecht, The Netherlands

Submitted for publication

Abstract

The evolutionary conserved protein Omp85 is required for outer membrane protein (OMP) assembly in Gram-negative bacteria and in mitochondria. In *E. coli*, it functions with four accessory lipoproteins: BamB, BamC, BamD, and BamE, which together with Omp85 form the β-barrel assembly machinery (Bam). In this work, we addressed the composition of this machinery and the function of the identified components in *Neisseria meningitidis*, a model organism for the study of outer membrane biogenesis. Analysis of the available genome sequences revealed homologs of BamC, BamD (previously described as ComL), BamE, and a second homolog of BamE, Mlp. No homolog of BamB was found. Like in *E. coli*, ComL/BamD appeared essential for viability and for OMP assembly, and it could not be substituted by its *E. coli* homolog. BamE was not essential but was found to contribute to the efficiency of OMP assembly and to the maintenance of outer membrane integrity. No obvious OMP assembly defects were observed in *bamC* or *mlp* mutants. Co-purification assays demonstrated the association of BamC, ComL, and BamE with Omp85. Semi-native gel electrophoresis identified the RmpM protein as an additional component of the Omp85 complex. RmpM was not required for OMP folding but stabilized OMP complexes. Thus, the Bam complex in *N. meningitidis* consists, besides of Omp85, of RmpM, BamC, ComL, and BamE as accessory components of which ComL and BamE appear to be the most important for OMP assembly.

Introduction

Membrane-embedded β-barrel proteins are found in the outer membranes (OMs) of Gram-negative bacteria, mitochondria and chloroplasts. Only in recent years, cellular components required for assembly and insertion of these outer membrane proteins (OMPs) into the OM have been identified. Omp85, which was first characterized in *Neisseria meningitidis*, is the key protein of the OMP assembly machinery (41). The function of Omp85 has been preserved during evolution, not only in Gram-negative bacteria (8, 37, 44, 46) but also in mitochondria, where an Omp85 homolog, also known as Tob55 or Sam50, was shown to mediate assembly of β-barrel proteins into the OM (15, 23, 27). Accordingly, bacterial OMPs are still recognized by the eukaryotic assembly machinery: when expressed in yeast, bacterial OMPs were found to be assembled into the mitochondrial OM in a Tob55-dependent manner (43). Omp85 in *E. coli*, which was recently re-named BamA for β-barrel assembly machinery (Bam) component A, is associated with at least four lipoproteins: BamB (formerly known as YfgL), BamC (NlpB), BamD (YfiO), and BamE (SmpA) (32, 46). In *E. coli*, BamB, BamC, and BamE are not essential, but the phenotypes of deletion mutants suggest that these proteins contribute to the efficiency of OMP assembly. Like Omp85, BamD is an essential protein in *E. coli*, involved in OMP assembly (24). These lipoproteins are evolutionarily less well conserved: the mitochondrial Tob55 protein is associated with two accessory proteins, but they do not show any sequence similarity with the lipoproteins of the *E. coli* Bam complex (14).

Besides *E. coli*, *N. meningitidis* is one of the major bacterial model organisms in studies on OM assembly. As mentioned above, it was the first organism in which the function of Omp85 was identified (41), and also the role of an integral OMP, designated Imp/OstA/LptD, in the transport of lipopolysaccharide (LPS) to the cell surface was first established in this *N. meningitidis* (3). With regard to OM biogenesis, *N. meningitidis* has several distinguishing features as compared to *E. coli*. For example, in contrast to *E. coli* (13), *N. meningitidis* mutants defective in LPS synthesis or transport are viable (3, 34), and OMPs are perfectly well assembled in such mutants (33). Furthermore, in OMP-assembly mutants of *E. coli*, the periplasmic accumulation of unassembled OMPs is prevented due to the induction of the σ^E extracytoplasmic stress response, which results in the degradation of unfolded OMPs (30) and the inhibition of their synthesis by small regulatory RNAs (20). In contrast, in *N. meningitidis* most of the components involved in this response are absent (4), and unassembled OMPs accumulate as periplasmic aggregates when OMP assembly is halted (41). However, the composition of the Bam complex and the role of accessory components in OMP assembly have, so far, not been studied in this organism. Therefore, to further understand the OMP assembly process in *N. meningitidis*, we have now analyzed the composition of the Bam complex and addressed the roles of the different components.

Materials and Methods

Bacterial strains and growth conditions

The bacterial strains used in this study are listed in Table 1. *E. coli* strains were grown on LB agar plates at 37˚C. When necessary, an appropriate antibiotic (25 μg/ml chloramphenicol or 50 μg/ml kanamycin) was added for plasmid maintenance. *N. meningitidis* strains were grown at 37°C in candle jars on GC agar plates (Oxoid), supplemented with Vitox (Oxoid) and, when necessary, with an antibiotic (10 μg/ml chloramphenicol or 80 μg/ml kanamycin). Liquid cultures were grown in tryptic soy broth (TSB) (Becton Dickinson). To achieve depletion of

Table 1. Strains and plasmids used in this study

Strain or plasmid	Relevant characteristics	Reference
Strains		
E. coli		
TOP10F'	Cloning strain	Invitrogen
DH5α	Cloning strain	Laboratory collection
N. meningitidis		
H44/76	Wild-type serogroup B strain	18
HB-1	H44/76 with the capsule locus replaced by an erythromycin resistance gene cassette	2
HB-1Δ*bamE*	HB-1 with *bamE* replaced by a *kan*^{R} cassette	This study
HB-1Δ*mlp*	HB-1 with *mlp* replaced by a *cat*^{R} cassette	This study
HB-1Δ*bamC*	HB-1 with *bamC* replaced by a *kan*^{R} cassette	This study
HB-1Δ*comL*(pComL)	HB-1 containing pEN11-ComL with the chromosomal *comL* copy replaced by a *kan*^{R} cassette	This study
HB-1Δ*bamE(*pBamE)	HB-1Δ*bamE* transformed with pEN11-BamE	This study
HB-1Δ*mlp*Δ*bamE*	HB-1Δ*mlp* with *bamE* replaced by a *kan*^{R} cassette	This study
HB-1Δ*omp85*(pHisOmp85)	HB-1 containing pEN11-HisOmp85 with the chromosomal copy of omp85 replaced by a *kan*^{R} cassette	This study
H44/76-Δcl4	H44/76 containing *rmpM::kan*	39
HB-1-Δcl4	HB-1 containing *rmpM::kan*	This study
HB-1Δ*rmpM*	HB-1 with *rmpM* replaced by a *kan*^{R} cassette	This study
Plasmids		
pCRII-TOPO	TA-cloning vector for PCR products	Invitrogen
pCRII-Δ*comL*	*comL* deletion plasmid.	This study
pCRII-Δ*bamE*	*bamE* deletion plasmid	This study
pCRII-Δ*bamC*	*bamC* deletion plasmid.	This study
pCRII-Δ*rmpM*	*rmpM* deletion plasmid	This study
pCRII-Δ*mlp*	*mlp* deletion plasmid	This study
pMB25	*imp* deletion plasmid	3
pEN11-Imp	*Neisseria replicative* plasmid containing H44/76-derived *imp* under *lac* promoter control	3
pEN11-ComL	pEN11-Imp with *imp* replaced by HB-1 derived *comL*	This study
pEN11-BamE	pEN11-Imp with *imp* replaced by HB-1 derived *bamE*	This study
pEN11-BamD	pEN11-Imp with *imp* replaced by DH5α derived *bamD*	This study
pCRII-POTRA1	pCRII-TOPO vector carrying H44/76-derived *omp85* lacking the region encoding POTRA1	5
pEN11-HisOmp85	pEN11-Imp with *imp* replaced by a gene encoding 6xHis-Omp85	This study
pRV1300	*omp85* deletion plasmid	41

proteins encoded by genes cloned behind an isopropyl-β-D-1-thiogalactopyranoside (IPTG)-inducible promoter, *N. meningitidis* cells grown overnight on plates containing 1 or 10 μM IPTG as indicated, were resuspended in TSB without IPTG to an optical density at 550 nm (OD_{550}) of 0.1 and grown for 6 h. To induce expression of IPTG-regulated genes, 0.5 mM IPTG was added at the start of the liquid culture.

Antibiotic sensitivity

Meningococci grown overnight on GC agar plates were resuspended in 100 μl of TSB to an OD_{550} of 0.025 and plated on GC agar plates. Paper discs containing 30 μg vancomycin (BD Biosciences) were placed on top of the agar. The plates were incubated at 37°C for 24 h, after which growth-inhibition zones around the discs were measured in mm from the rim of the disk. All tests were repeated at least three times.

Plasmid and mutant constructions

Plasmids and primers used in this study are summarized in Table 1 and Table 2, respectively. Primers were designed based on the genome sequence of serogroup B strain MC58 (www.tigr.org), which belongs to the same clonal complex as the strain used in this study, H44/76. Deletion constructs of *bamC*, *comL, bamE, rmpM* and *mlp* were obtained by amplifying DNA fragments upstream and downstream of these genes by PCR using genomic DNA of HB-1 as template and primers indicated with Up-For and Up-Rev and Down-For and Down-Rev in Table 2. The fragments were cloned into pCRII-TOPO. Next, the upstream and downstream fragments of each gene were joined together in one plasmid using *Acc*I sites that were introduced via the primers and the *Xba*I site in the vector. A kanamycin-resistance gene (kan^R) cassette including the neisserial DNA uptake sequence, obtained from pMB25, was inserted in each plasmid after *Acc*I restriction, yielding pCRII-Δ*bamC*, pCRII-Δ*comL*, pCRII-Δ*bamE*, and pCRII-Δ*rmpM*. A chloramphenicol-resistance gene (cat^R) cassette was amplified by PCR from pACYC184 using primers P1 and P2 and cloned into pCRII-TOPO, yielding pCRII-*cat*. This cassette was used to create pCRII-Δ*mlp* by *Acc*I restriction and ligation. For allelic replacements, constructs containing the antibiotic-resistance cassette in the same transcriptional direction as the gene to be replaced were used. *N. meningitidis* was transformed as described (3) with PCR fragments obtained from the gene replacement constructs using primer pair M13Rev and M13For. When appropriate, 50 μM IPTG was added to the selection plates. The transformants were checked for the presence of the mutant alleles by PCR using the corresponding Up-For and Down-Rev primers and for the absence of the wild-type alleles by PCR using primers annealing within the removed coding sequence (indicated with –int in Table 2) and the corresponding Down-Rev primer and/or by immunoblot analysis. An insertional *rmpM* mutation was created in HB-1 by transferring the *rmpM::kan* allele from H44/76-Δcl4 into HB-1. To that end, HB-1 was transformed with a PCR product produced from H44/76-Δcl4 chromosomal DNA with primers RmpM-Up-For and RmpM-Down-Rev.

N. meningitidis comL and *bamE* genes were amplified by PCR using genomic DNA of HB-1 as template and primer pairs ComL-For/Rev and BamE-For/Rev, respectively. The resulting PCR products were cloned into pCRII-TOPO. The *comL* gene was subcloned into the neisserial replicative plasmid pEN11-Imp via *Nde*I/*Aat*II restriction and ligation, resulting in pEN11-ComL. The *bamE* gene was subcloned into this vector using *Nde*I/*Pvu*I sites, yielding pEN11-BamE. In this vector, expression of the inserted gene is driven by tandem *lac/tac* promoter/operator sequences. The *E. coli bamD* gene was PCR amplified from DNA of DH5α and primer pair BamD-For/Rev. After cloning the PCR product into pCRII-TOPO, *bamD* was subcloned into pEN11-Imp via *Nde*I /*Aat*II restriction and ligation, yielding pEN11-BamD.

Table 2. Primers used in this study. Restriction sites used for cloning are underlined

Primer name	Sequence (5'-3')	Restriction site
BamC-Up-For	ATGATGTGTTCCGCATCGTC	
BamC-Up-Rev	ATGTCGACGCAGCTTCCAAACAGA	*Acc*I
BamC-Down-For	ATGTCGACTCGGACGGCATGGCTATATT	*Acc*I
BamC-Down-Rev	ATGACGTCGGACGGCATCGTTGCCGTCG	
ComL-Up-For	ATGACGTCGAGCGACATTCGATATAGC	
ComL-Up-Rev	ATGTCGACGAGTGGCACAGGCACTCA	*Acc*I
ComL-Down-For	AAGTCGACATGCCTTGCCAGCACG	*Acc*I
ComL-Down-Rev	ATGTGGCTTGCCGATGTGTC	
BamE-Up-For	ATTTACCTCGCCGCACTTCACG	
BamE-Up-Rev	ATGTCGACGGTAGTGTAACACTGCTTGAATA	*Acc*I
BamE-Down-For	ATGTCGACAGGAACACACATGACACCGC	*Acc*I
BamE-Down-Rev	ATGCGCATTGTTTGAGGTCTCT	
Mlp-Up-For	CTTGGTAAACAGCCATTGTTCCCAG	
Mlp-Up-Rev	ATGTCGACGTTCGGAAGAGCCGCATC	*Acc*I
Mlp-Down-For	ATGTCGACATGTTACTACCTGCCAATAC	*Acc*I
Mlp-Down-Rev	AGTTCGCGGCAGAGGATGCGG	
RmpM-Up-For	GAGACCGAAACCACGCGCTTG	
RmpM-Up-Rev	ATGTCGACGAAGCGAGCAATGCAACG	*Acc*I
RmpM-Down-For	ATGTCGACAATCCGCAGCATCGTAAC	*Acc*I
RmpM-Down-Rev	TTAGGCTCAATCGCTGCAACTGACGG	
ComL-For	ATCATATGAAAAAAATTCTTTTAAC	*Nde*I
ComL-Rev	ATGACGTCTTATCAGTGCCAGTAACGCCAC	*Aat*II
BamE-For	ATCATATGGTGAACAAAACCCTCATCCT	*Acc*I
BamE-Rev	ATCGATCGTTATGGTTTGTCTGTGTT	*Pvu*I
BamC-int	GTCGACGGCAAGTCTCCTGC	
ComL-int	ACGCGGCGCATATATCGCCGC	
BamE-int	TACTGCGCGACGCATTCCAT	
Mlp-int	CGCCCGCATTACGACGAAAG	
BamD-For	ATCATATGATGACGCGCATGAAA	*Nde*I
BamD-Rev	ATGACGTCTTATGTATTGCTGCT	*Aat*II
His-up	GACTTCCACCACCACCACCACCACCAA GACTTCACCATCCAAGACATCCGC	
His-down	GTCTTGGTGGTGGTGGTGGTGGTGGAA GTCGGCAAGTGCCAAAGGCGA	
Omp85NotIF	AGCGGCCGCAAACCGCATTCCGCACCACAAGGAA	*Not*I
Omp85NotIR	TTTTAAGCTTTTAGAACGTCGTGCCGAGTTGGAAT	
P1	GTCGACGGATCCGTGTAGGCTGGAGCTGCTTC	*Acc*I
P2	GTCGACGGATCCATGCCGTCTGAACATATGAATATC CTCCTTA	*Acc*I
M13-For	GTAAAACGACGGCCAGT	
M13-Rev	CAGGAAACAGCTATGAC	

To engineer a His-tag at the N terminus of mature *N. meningitidis* Omp85, two overlapping DNA fragments were generated by PCR using primer pairs His-Up/Omp85NotIR and His-Down/Omp85NotIF and genomic DNA of HB-1 as template. The PCR products were purified and mixed for a second PCR with the external primers Omp85NotIF and Omp85NotIR, creating a DNA fragment encoding an Omp85 variant with an additional HHHHHHQDF amino-acid sequence between the signal sequence and the N terminus of the mature protein. The resulting PCR product was cloned into pCRII-TOPO. The 5'-fragment of the obtained *omp85* allele was excised using the *Not*I site upstream of *omp85* and a *Sal*I site within *omp85* and substituted for the corresponding fragment in pCRII-POTRA1, a plasmid encoding a mutant *N. meningitidis* Omp85 protein lacking its POTRA1 domain and containing an *Aat*II site at the 3'-end of *omp85*. The complete gene was subsequently introduced into pEN11-Imp using *NotI*/*Aat*II restriction, yielding pEN11-HisOmp85. The chromosomal copy of *omp85* in HB-1, containing pEN11-HisOmp85, was for the most part replaced by a kan^R cassette as described before (41).

Cell envelope isolation

To isolate cell envelopes, bacteria grown in TSB for 6 h were collected by centrifugation, resuspended in 50 mM Tris-HCl, 5 mM EDTA (pH 8.0) containing protease-inhibitor cocktail "Complete" (Roche) and stored overnight at -80°C. After ultrasonic disintegration (3 x 45 s at level 8, output 40%, Branson sonifier 450; Branson Ultrasonics Corporation), unbroken cells were removed by centrifugation (12,000 *g*, 15 min, 4˚C). Cell envelopes were collected by ultracentrifugation (170,000 *g*, 5 min, 4˚C), dissolved in 2 mM Tris-HCl (pH 7.6) and stored at –20°C.

Trypsin digestion

The protease susceptibility of Omp85 in cell envelopes was tested by incubating samples with 50 µg/ml of trypsin (Sigma) overnight at room temperature. The samples were denatured by boiling in sample buffer and analyzed by regular sodium dodecyl sulfate-polyacrylamide gel electrophoresis (SDS-PAGE) and immunoblotting.

Affinity purification

Cell envelopes were incubated in TBS (20 mM Tris-HCl, 150 mM NaCl pH 7.4), 2% Elugent (Calbiochem), 5 mM EDTA for 2 h at room temperature and centrifuged (20,800 *g*, 30 min, room temperature). The buffer of the supernatant was exchanged to TBS, 0.1% Elugent, 20 mM imidazole using PD-10 columns (GE Healthcare). The extract was mixed with Ni^{2+}-nitrilotriacetic acid (Ni^{2+}-NTA)-agarose beads (Qiagen) for 1-2 h at 4°C while rotating. The beads were washed in TBS, 0.05% *n*-dodecyl-ß-D-maltoside, 20 mM imidazole, for 1 h at 4°C while rotating. After settling of the beads by gravity, proteins were eluted with TBS, 200 mM imidazole, 0.05% *n*-dodecyl-ß-D-maltoside. The samples were analyzed by SDS-PAGE and immunoblotting. For immunoblotting, the fractions were concentrated 10-fold by precipitation with trichloroacetic acid.

SDS-PAGE and Western blot analysis

Protein samples were analyzed by regular SDS-PAGE (41). Alternatively, for semi-native SDS-PAGE, sample buffer lacking β-mercaptoethanol and containing only 1% SDS and running buffer containing 0.025% SDS (5) were used for analysis of Omp85 complexes, while sample buffer containing 0.1% SDS and no β-mercaptoethanol combined with running buffer containing 1% SDS was used for porin analysis. Furthermore, the gels contained no SDS and electrophoresis was carried out on ice at 12 mA. Proteins were visualized in the gels

with Coomassie Brilliant Blue or silver (1). To enhance epitope recognition on immunoblots, native proteins were denatured within the gels by leaving the gels in steam for 20 min prior to blotting. Blotting was performed in a Biorad Wet blotting system in 25 mM Tris, 192 mM glycine, 0.02% SDS in 20% methanol, pH 8.3. The membranes were blocked for 1 h in phosphate-buffered saline (pH 7.6), supplemented with 0.5% non-fat dried milk (Protifar, Nutricia) and 0.1% Tween-20. The blots were incubated for 1 h with primary antibodies, washed, and then probed for 1 h with goat anti-rabbit or goat anti-mouse IgG secondary antibodies conjugated with horseradish peroxidase or alkaline phosphatase (Southern Biotechnology Associates Inc.) diluted in the blocking buffer. The signal was visualized with enhanced chemiluminescense (Amersham). When alkaline phosphatase-conjugated antibodies were used, the blots were incubated in 0.1 M Tris-HCl (pH 9.5), 0.1 mg/ml Nitro Blue Tetrazolium, 0.5 mg/ml 5-bromo-4-chloro-3-indolyl phosphate (both from Sigma-Aldrich), until color developed.

Antisera

Rabbit antisera against the N-terminal (residues 22-464) (α-N-Omp85) or C-terminal (residues 455-797) (α-C-Omp85) parts of *N. meningitidis* Omp85 and against *E. coli* BamD were generously provided by Ralph Judd (University of Montana, USA) and by Naoko Yokota and Hajime Tokuda (University of Tokyo, Japan), respectively. A monoclonal antibody (Mab) directed against *N. meningitidis* Omp85 and anti-PilQ antiserum were provided by GlaxoSmithKline Biologicals (Rixensart, Belgium). Rabbit antisera were raised against synthetic peptides designed on the sequence of neisserial BamC (CDASALLGKLHSELR), ComL (CVLETNFPKSPFLKQ), and BamE (CAAEALKDRQNTDKP) at Genosphere Biotechnologies (Paris, France). Mabs directed against PorA, PorB and RmpM were provided by the Netherlands Vaccine Institute (Bilthoven, The Netherlands). The anti-Imp antiserum was previously described (3).

Results

Presence of genes encoding Bam components in neisserial genomes

In *E. coli,* Omp85 is associated with the accessory lipoprotein components BamB, BamC, BamD, and BamE (32, 46). We performed BLAST searches in the genome sequence of *N. meningitidis* strain MC58 using *E. coli* protein sequences to identify the genes encoding similar lipoproteins. For BamC, we found a homolog (locus tag NMB0928) with relatively low similarity (24% identity, 37% similarity), but in the same chromosomal location as *bamC* in *E. coli* (*i.e.*, downstream of the *dabA* gene). The homolog of BamD was identified previously in *N. gonorrhoeae* and designated ComL, since a transposon insertion in the corresponding gene resulted in decreased competence (12). ComL of strain MC58 (NMB0703) shares 38% identity and 59% similarity with its *E. coli* counterpart. Searches for BamE homologs yielded two candidates: NMB0204 (37% identity and 65% similarity) and NMB1898 (25% identity and 47% similarity). Comparison of flanking genes did not provide any further clue as to which ORF would encode the functional homolog of BamE: the genes flanking *bamE* in *E. coli*, *recN* and b2618, are not found near NMB0204 or NMB1898. Given its higher similarity to BamE, we will refer to the protein encoded by NMB0204 as the neisserial BamE homolog. The protein encoded by NMB1898 is annotated as Mlp, for meningococcal lipoprotein (47). We did not find a BamB homolog, neither in strain MC58, nor in any other neisserial genome sequence present in databases at the NCBI. In *E. coli*, the *bamB* (*yfgL)* gene is present in a locus comprising *yfgK*, *yfgL*, *yfgM*, and *hisS*. In the neisserial genomes, a similar locus is found but without *yfgL*. A conserved region in *E. coli* BamB was identified that is involved in interaction with Omp85 (42). Further BLAST

searches with this conserved region in the available neisserial genomes yielded no hits. BamB has also been shown to contain seven binding motifs for pyrroloquinoline-quinone (PQQ) (21). Their relevance is not clear, because *E. coli* does not possess any PQQ synthase (25). No proteins containing these domains are present in *N. meningitidis* (http://smart.embl.de/smart/show_motifs.pl?ID=P77774). Thus, no BamB-like protein appears to be present in the *Neisseriae*. Sequences and genetic organization of the *bamC, comL,* and *bamE* loci are highly conserved among the pathogenic *Neisseriae* as revealed by searches in the 19 currently available genome sequences of *N. gonorrhoeae* and *N. meningitidis* at the NCBI (data not shown) and as reported for *bamC* (7).

Construction of mutants defective in the synthesis of the accessory lipoproteins

To investigate whether the identified accessory lipoproteins would indeed function in OMP assembly in *N. meningitidis*, we attempted to create deletion mutants in HB-1 by replacing the corresponding genes with antibiotic-resistance cassettes. Strains, deficient for BamC and BamE were easily obtained, indicating that these proteins are not essential in *N. meningitidis* (Figure 1A and B). Growth of both mutants in liquid medium was not significantly different from that of HB-1 (data not shown). Introduction into HB-1Δ*bamE* of plasmid pEN11-BamE, which carries the *bamE* gene under control of an IPTG-inducible promoter, resulted in a strain demonstrating regulatable *bamE* expression (Figure 1B). To investigate the function of the second BamE homolog, Mlp, we also constructed a mutant lacking this gene and, additionally, a strain lacking both *bamE* and *mlp*. These mutants were easily obtained demonstrating that Mlp is essential neither in a wild type nor in a *bamE* background.

Contrary to the results described above, we were not able to inactivate the *comL* gene. We were only able to inactivate this gene on the chromosome in a strain that expressed a complementing copy of *comL* from plasmid, demonstrating that this gene is essential in *N. meningitidis*. Accordingly, normal growth of the resulting strain, designated HB-1Δ*comL*(pComL), was dependent on IPTG (Figure 1C). Interestingly, we could not inactivate the chromosomal *comL* gene when *bamD*, the *E. coli* homolog of *comL*, was present on the complementing plasmid, even though we could demonstrate expression of the *bamD* gene in the presence of IPTG on Western blot (Figure 1D). This result indicates a species-specific functioning of ComL/BamD. To obtain sufficient amounts of ComL-depleted cells for membrane preparations, HB-1Δ*comL*(pComL) was pre-grown overnight on plates containing 10 µM IPTG and subsequently in TSB for 6.5 h with or without IPTG. This procedure resulted in considerable growth in the absence of IPTG, yet cells became depleted for ComL as shown on immunoblot (Figure 1E). Collectively, these data show that BamC, BamE, and Mlp are not essential in *N. meningitidis*, whereas ComL is essential even though a viable *comL* transposon insertion mutation in *N. gonorrhoeae* has been described (12).

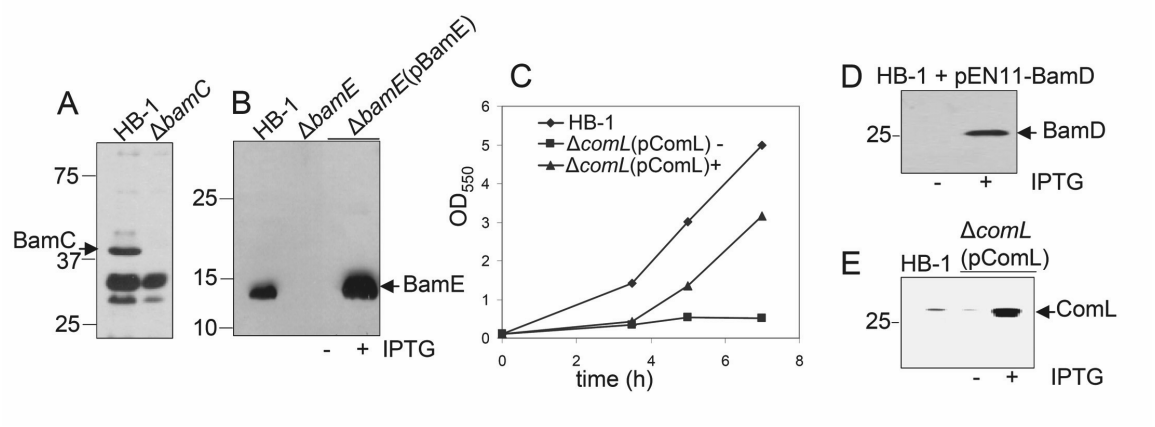

Figure 1

BamC, BamE and ComL mutants. (**A**) Cell envelopes derived from the strains indicated above the panel were separated by SDS-PAGE and immunoblotted with anti-BamC serum. The predicted MW of BamC is 39 kDa; the bands below the 37-kDa marker probably represent non-specific reactivity of the antiserum. (**B**) Cell lysates of the strains indicated above the panel were separated by SDS-PAGE and immunoblotted with anti-BamE serum. HB-1Δ*bamE*(pBamE) was analyzed after growth in the presence or absence of 0.5 mM IPTG. (**C**) Growth of HB-1 and HB-1Δ*comL*(pComL) in the absence (-) or presence (+) of 0.5 mM IPTG. HB-1 Δ*comL*(pComL) was pre-grown overnight on plates containing 1 μM IPTG. (**D**) Cell lysates of HB-1 carrying pEN11-BamD grown in the absence or presence of 0.5 mM IPTG were subjected to SDS-PAGE, blotted and probed with anti-BamD antiserum. (**E**) Immunoblot, probed with anti-ComL serum, of cell envelopes of HB-1 and HB-1Δ*comL*(pComL) grown in the absence (-) or presence (+) of 0.5 mM IPTG. In this case, HB-1Δ*comL*(pComL) was pre-grown overnight on plates containing 10 μM IPTG.

Role of the accessory lipoproteins in OMP assembly

Next, we tested the impact of the mutations on OMP assembly. Cell envelopes of the various mutants showed similar protein profiles when analyzed in denaturing SDS-PAGE (Figure 2A). The most abundant proteins in the meningococcal OM are the porins PorA and PorB, which normally assemble into trimers, which are detectable in semi-native SDS-PAGE. When OMP assembly in *N. meningitidis* is compromised due to Omp85 depletion, porins accumulate in their unassembled states and migrate at the positions of the denatured monomeric forms in semi-native SDS-PAGE (41). Using this assay we found accumulation of unassembled porins, most prominently in the ComL-depleted strain and, to a lesser extent, also in HB-1Δ*bamE* (Figure 2B). No unassembled porins were detected in the HB-1Δ*bamC* (Figure 2B) or HB-1Δ*mlp* (Figure 2C) strains. These observations were confirmed in immunoblots using anti-PorA and anti-PorB antibodies (Figure 2D). The assembly defects seen in the absence of BamE or upon depletion of ComL were complemented by expression of *bamE* or *comL in trans*. In the immunoblot analysis, the HB-1Δ*bamC* occasionally showed

a very slight defect in PorA assembly (Figure 2D), but this was poorly reproducible. We also tested the assembly of a non-prototypical OMP, PilQ. PilQ is a secretin that forms highly stable multimers, possibly homo-dodecamers, which are highly resistant to the denaturing effects of SDS and heat. PilQ assembly defects can therefore be detected in regular SDS-PAGE analysis by assessing the levels of monomeric PilQ (6, 9). PilQ assembly was unaffected in HB-1Δ*bamC*, since similar amounts of PilQ monomers were detected in this strain as in the parent strain (Figure 2E). However, in HB-1Δ*bamE* and in the ComL-depleted strain, PilQ assembly was clearly diminished (Figure 2E). Again, in both cases the defect was restored upon expression of *bamE* or *comL*, respectively, *in trans*.

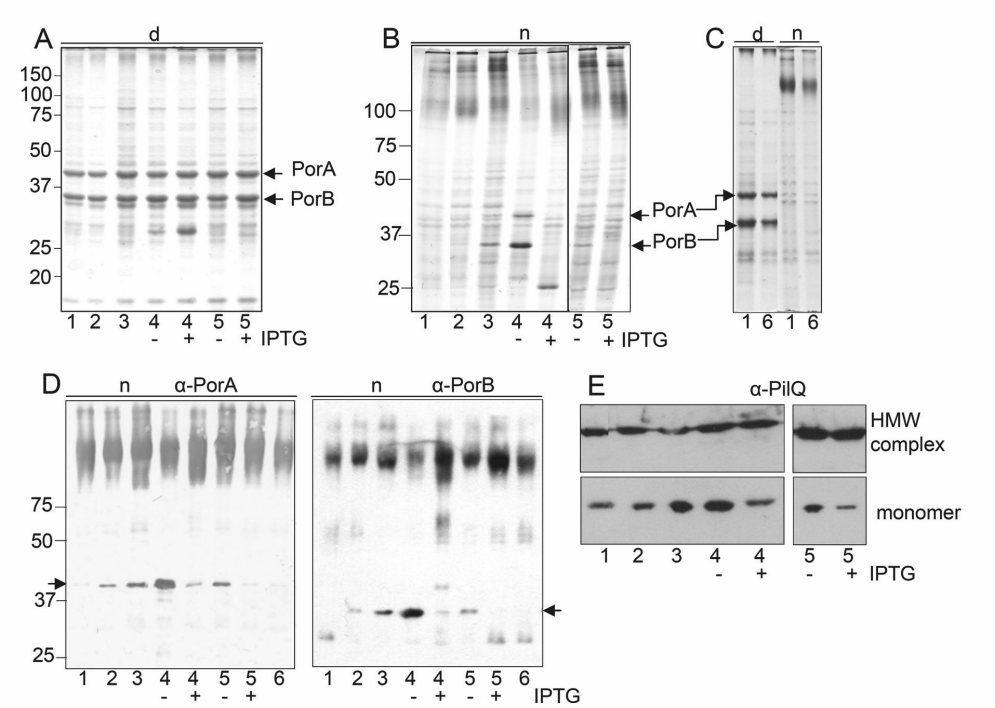

Figure 2

Role of putative Bam complex components in OMP assembly. (**A-D**) Cell envelopes were subjected to denaturing (d) or semi-native (n) SDS-PAGE and stained with Coomassie Brilliant Blue (A, B, C) or blotted and probed with anti-PorA or anti-PorB antibodies (D). Arrows point at unfolded porins. (**E**) Cell lysates were subjected to denaturing SDS-PAGE and immunoblotting with anti-PilQ antiserum. Only the relevant parts of the blot are shown. The strains are indicated below the panels as follows: 1: HB-1; 2: HB-1Δ*bamC*; 3: HB-1Δ*bamE*; 4: HB-1Δ*comL*(pComL); 5: HB-1Δ*bamE*(pBamE); 6: HB-1Δ*mlp*.

In *E. coli*, even mild OMP assembly defects can have a profound effect on the integrity of the OM, resulting in increased sensitivity to antibiotics (26, 32, 46). To evaluate whether the Δ*bamC* and Δ*mlp* mutants could have such mild assembly defects, which

remained undetected in the biochemical analyses described above, we tested the sensitivity of the strains to vancomycin in a disc diffusion assay. Like the wild-type strain, the Δ*bamC* and Δ*mlp* mutants appeared completely resistant to this antibiotic, whereas the deletion of *bamE* resulted in a clearly increased sensitivity, which was not enhanced by the simultaneous absence of *mlp* (Figure 3). Thus, together, our results demonstrate that ComL and BamE are required for OMP assembly, whereas BamC and Mlp have no obvious role in this process.

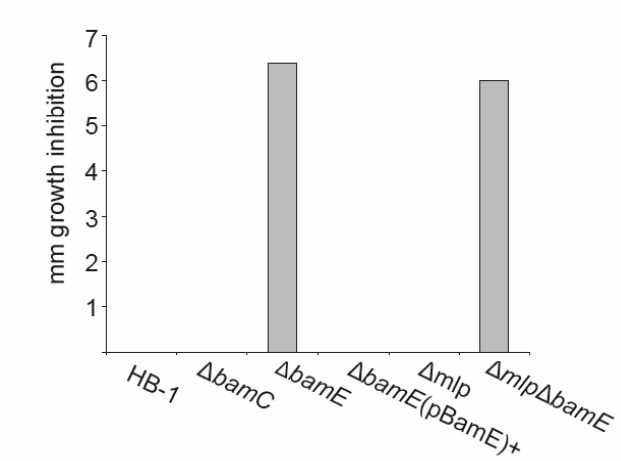

Figure 3

Vancomycin-sensitivity test. Sensitivity towards vancomycin was measured by a disc diffusion assay. Shown are sizes of growth clearing zones as measured in mm from the rim of the disk. Sensitivity of HB-1Δ*bamE*(pBamE) was assessed in the presence of 0.5 mM IPTG (+). Results of a representative experiment are shown.

Characterization of a high-molecular weight Omp85 complex

Next, we wished to determine whether BamC, ComL, and BamE form a complex with Omp85, like in *E. coli*. Previously, we found that Omp85 is mostly present in a high-molecular weight (HMW) complex when cell envelopes of *N. meningitidis* are analyzed by semi-native SDS-PAGE (41). To test whether this complex represents Omp85 with associated lipoproteins, we probed blots containing these complexes with antisera directed against Omp85 and the three lipoproteins. As expected, Omp85 was found in a HMW complex (Figure 4A). However, none of the three lipoproteins was detected at this position (Figure 4A). To verify the absence of the lipoproteins in the HMW Omp85 complex, we analyzed the electrophoretic mobility of this complex in cell envelopes of mutants, deficient in the Omp85-associated lipoproteins. Indeed, the electrophoretic mobility of the complex from the mutants was not altered (Figure 4B), confirming that BamC, BamE and ComL are not part of this complex. The absence of BamE and the depletion of ComL resulted in higher levels of unfolded monomeric Omp85, consistent with their roles in OMP assembly. This defect was for the most part restored upon expression of *bamE* or *comL in trans* (Figure 4B).

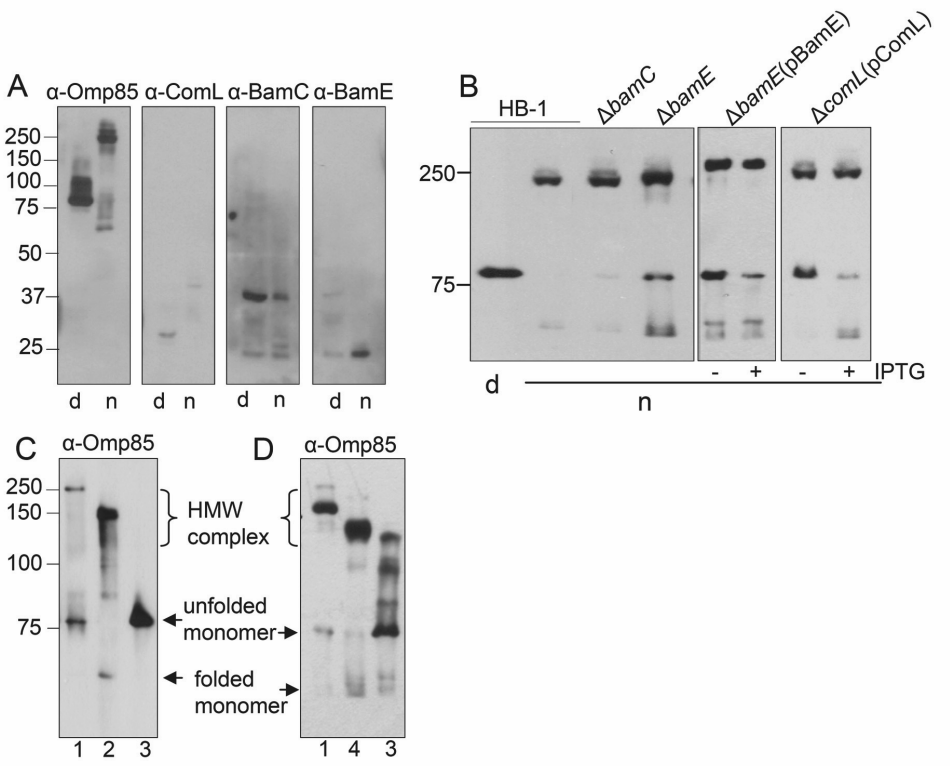

Figure 4

Composition of the HMW SDS-resistant Omp85 complex. (**A**) Cell envelopes from strain HB-1 were analyzed by denaturing (d) or semi-native (n) SDS-PAGE, blotted, and probed with antisera indicated above the panels. (**B**) Cell envelopes derived from the strains indicated above the panels were analyzed by denaturing (d) or semi-native (n) SDS-PAGE, blotted, and probed with an anti-Omp85 Mab. HB-1Δ*bamE*(pBamE) was grown in the presence or absence of 0.5 mM IPTG, as indicated. HB-1Δ*comL*(pComL) was pre-grown overnight on plates containing 10 μM IPTG and subsequently grown in TSB in the absence or presence of 0.5 mM IPTG. (**C-D**) Cell envelopes of 1: HB-1; 2: HB-1-Δcl4: 3: HB-1Δ*rmpM* and 4: H44/76-Δcl4 were analyzed by semi-native SDS-PAGE and immunoblotting using an anti-Omp85 Mab. The positions of various conformations of Omp85 are indicated in panels C and D.

Identification of RmpM in the HMW Omp85 complex

Since we could not detect the accessory lipoproteins in the HMW Omp85 complex, this complex represents either a homo-oligomer of Omp85 or a complex of Omp85 with (an)other protein(s). We previously found the RmpM protein to be associated with several neisserial OMP complexes, such as the porins and the lactoferrin receptor (19, 28). Therefore, we reasoned that perhaps this protein could also be present in the HMW Omp85 complex.

RmpM is a two-domain protein with a so-called OmpA domain, which is thought to associate non-covalently with the peptidoglycan layer, in its C-terminal end (17). The 40-amino-acid N-terminal domain of RmpM, which is linked to the C-terminal domain via a proline-rich hinge region, is too small to form a membrane-embedded β-barrel. Also, RmpM does not contain an N-terminal cysteine residue, which could be lipidated thereby forming a membrane anchor. Instead, RmpM is thought to be associated with the OM through binding via its N-terminal domain to integral OMPs (17).

To assess the presence of RmpM in the Omp85 complex, we transferred the *rmpM* allele from a previously constructed *rmpM* mutant (39) into strain HB-1, yielding HB-1-Δcl4. Western-blot analysis with an anti-RmpM Mab confirmed the absence of the wild-type RmpM in the mutant (data not shown). The Omp85 complex of this strain migrated substantially faster in the gel (Figure 4C, compare lanes 1 and 2), demonstrating that RmpM is part of this complex. However, Omp85 still migrated as a distinct complex at a position much higher than the monomer. We noticed that the *rmpM::kan* allele used to create this mutant was constructed by insertion of a kan^R cassette in the 3'-end of the gene, thereby disrupting the OmpA domain but leaving the 5'-end of *rmpM* intact. The resulting mutant allele could possibly encode a protein comprising the N-terminal 157 amino acids of RmpM, including the signal sequence. To test whether this protein would be sufficient for forming a complex with Omp85, we constructed an alternative *rmpM* mutant, designated HB-1Δ*rmpM*, which had only 49 nucleotides left at the 5'-end of the gene. Western blots of semi-native SDS-PAGE gels containing cell envelopes prepared from this mutant usually showed several separate HMW bands containing Omp85 plus significant quantities of denatured monomeric Omp85 (Figure 4D, lane 3). However occasionally, all Omp85 detected was found to migrate at its unfolded monomeric position (Figure 4C, lane 3). This variability is likely reflective of a very unstable complex. In contrast, mutants containing the *rmpM::kan* allele, either in an H44/76 or in an HB-1 background, reproducibly showed a distinct HMW Omp85 complex, migrating faster than that of the parental strain (middle lanes in Figure 4C and 4D). Apparently, the N terminus of RmpM is required for the formation of an Omp85 complex that is stable during semi-native SDS-PAGE analysis. However, RmpM is not absolutely required for complex formation, since HMW forms of Om85 were still detected in its absence suggesting that other, unknown, components are associated with Omp85 or that Omp85 migrates as homo-oligomers. The observed association of RmpM with Omp85 defines it as part of the Bam complex in *N. meningitidis.*

Role of RmpM in OMP assembly

Since RmpM is part of the Omp85 complex, we wished to determine whether it has any role in OMP assembly. From the analysis of H44/76-Δcl4, which contains the *rmpM::kan* allele, we postulated previously that RmpM stabilizes OMP complexes (19, 28). To re-address this issue and investigate any effects on OMP assembly in a strain completely lacking RmpM, we analyzed porin assembly in HB-1Δ*rmpM* and, for comparison, in HB-1-Δcl4. As shown in Figure 5A and Figure 5B, the overall protein profile of cell envelopes in denaturing conditions was unaffected by the partial or complete absence of RmpM, except for the presence of the full-length RmpM protein in the HB-1 strain which is best visualized when samples are heat-denatured without reducing agents (Figure 5A). In semi-native SDS-PAGE analysis, we did not detect unassembled porins in either *rmpM* mutant (Figure 5B), a finding confirmed for PorA in immunoblot analysis (Figure 5C). On this blot, cell envelopes of a ComL-depleted strain showing the PorA pattern of an OMP assembly mutant were included for comparison. These gels and blots showed that the porin trimers from the *rmpM* mutants migrated faster than those of the parent strain, consistent with the notion that these trimers in the wild-type strain actually represent hetero-oligomers consisting of porin trimers

and RmpM (19). Furthermore, the blots revealed the presence of dimeric and folded monomeric porin forms, which were not or in much lower amounts present in the sample of the parent strain (Figure 5C, D). These dimeric and folded monomeric forms were not detected in the assembly-defective ComL-depleted strain (Figure 5C, lane 4), indicating that their presence does not result from an assembly defect, but from decreased stability of assembled trimeric porins in the absence of RmpM. Overall, these data show that RmpM is not required for porin folding and assembly, but rather it stabilizes their trimeric forms. In the case of PorB, this stabilizing role appeared more important than in the case of PorA, since we did not detect any PorB trimers in the HB-1Δ*rmpM* mutant (Figure 5D).

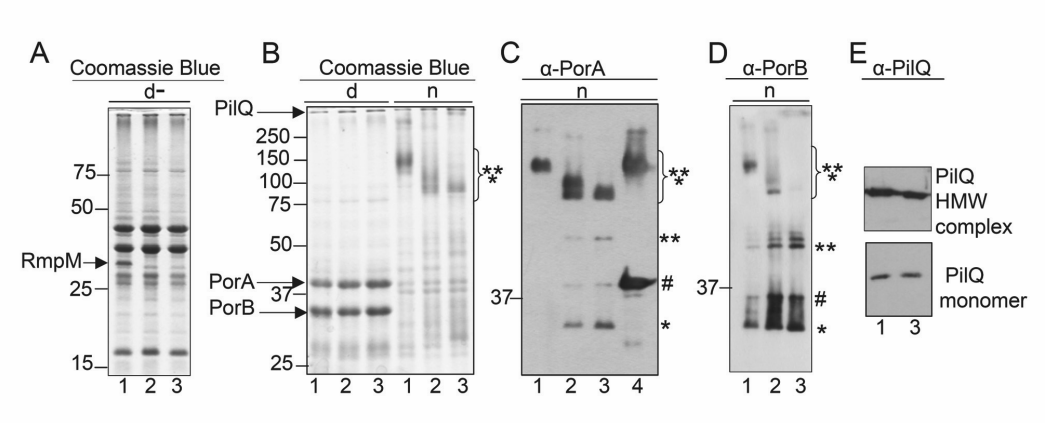

Figure 5

OMP assembly in RmpM mutants. (**A-D**) Cell envelopes were subjected to denaturing (d), denaturing without reducing agents (d-) or semi-native (n) SDS-PAGE and stained with Coomassie Blue (A, B), or blotted and probed with anti-PorA (C) or anti-PorB (D) antibodies. Cell envelopes were prepared from 1: HB-1; 2: HB-1-Δcl4; 3: HB-1Δ*rmpM*; 4: HB-1Δ*comL*(pComL) grown in the absence of IPTG. Folded porin monomers, dimers and trimers are indicated by single, double and triple asterisks, respectively. Unfolded monomeric porin is indicated by #. The ComL-depleted cell envelope sample is included as a control to show defective PorA assembly. (**E**) Cell lysates were subjected to denaturing SDS-PAGE and immunoblotting with anti-PilQ antiserum. Lane numbers refer to strains as in panels A-C.

The assembly of PilQ was totally unaffected by the absence of RmpM, since similar levels of PilQ multimers and monomers were detected in the membranes of HB-1Δ*rmpM* as in those of the parent strain (Figure 5E). Also, the PilQ complex did not migrate faster in the gel in the absence of RmpM (Figure 5B and 5E), demonstrating that RmpM is not associated with this complex. Thus, apparently, RmpM is not associated with all protein complexes in the OM.

Association of lipoproteins with the Bam complex

The absence of the lipoproteins from the HMW Omp85 complex detected in semi-native SDS-PAGE does not necessarily mean that they are not associated with Omp85 *in*

vivo. Possibly, they dissociate from the complex due to the prevailing conditions of semi-native SDS-PAGE. To further investigate the association of the lipoproteins with Omp85, we analyzed the protease accessibility of Omp85 in cell envelopes of the mutants, emanating from the idea that its protease sensitivity could increase when associated components are lost. Trypsin treatment of cell envelopes, followed by immunoblotting with an antiserum directed

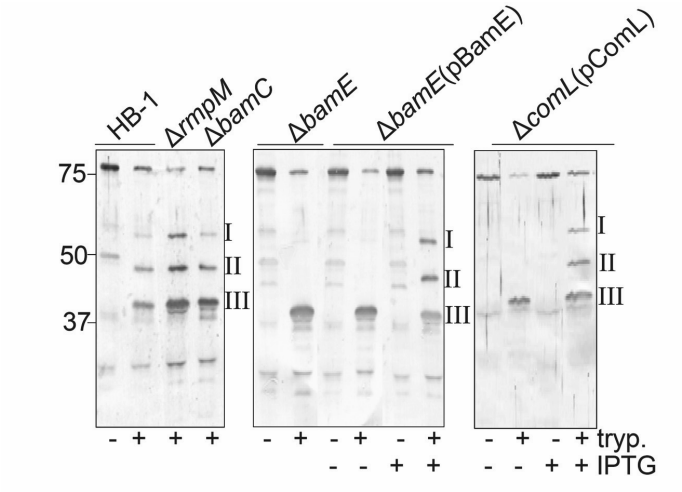

Figure 6

Protease accessibility of Omp85 in Bam complex mutants. Cell envelopes from the strains indicated above the lanes were treated with or without trypsin (tryp) and subjected to denaturing SDS-PAGE followed by immunoblotting with α-C-Omp85 antiserum. Tryptic fragments are indicated with I, II, and III. When relevant, the absence of presence of IPTG during growth of the strains is indicated.

against the C-terminal β-barrel domain of Omp85, resulted in the detection of three large distinct fragments with apparent molecular weights of approximately 58, 48 and 40 kDa (designated I, II and III, respectively, in Figure 6). In the case of the Δ*rmpM*, Δ*bamC*, and Δ*mlp* strains, similar digestion products were obtained as for the parent strain (Figure 6 and data not shown). Interestingly, in the Δ*bamE* strain only fragment III was detected, demonstrating that Omp85 is better accessible to trypsin in the absence of BamE. Also in the case of the ComL-depleted strain only fragment III was detected (Figure 6), indicating that newly inserted Omp85 proteins, which were handled by pre-existing functional Bam complexes, cannot a find a ComL partner molecule and therefore become more accessible to trypsin. This altered digestion profile was in both cases completely reversible when the plasmid-borne copies of *bamE* and *comL*, respectively, were expressed (Figure 6, middle and right panels).

To obtain additional evidence for the association of ComL, BamE and possibly BamC with Omp85, we purified the Bam complex from the Neisserial OM by means of pull-down assays using an N-terminally His-tagged Omp85 protein expressed in strain HB-1. The chromosomal copy of *omp85* was disrupted in this strain to ensure maximal co-purification of Omp85 complex components. In the presence of IPTG, this strain grew indistinguishably

from HB-1 (data not shown), demonstrating that the His-tagged version of Omp85 is functional. Detergent extracts of cell envelopes prepared from this strain were subjected to

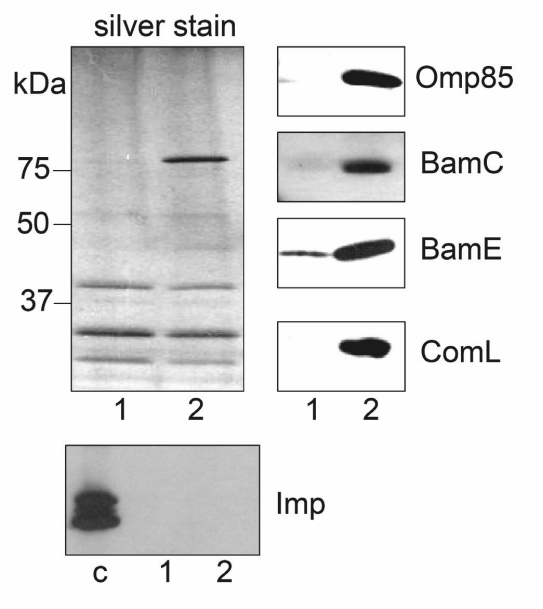

Figure 7

Omp85-associated proteins in *N. meningitidis*. Cell envelope extracts of strains expressing wild-type (1) or His-tagged (2) Omp85 were subjected to Ni^{2+}-NTA purification. Shown are elution fractions analyzed by denaturing SDS-PAGE and silver staining or immunoblotting, using antibodies against the indicated proteins. The lane indicated with c contains non-extracted cell envelopes of HB-1 as a control to show reactivity of the anti-Imp antiserum.

Ni^{2+}-NTA purification. As a control, we subjected extracts of cell envelopes from the parent strain HB-1 to similar procedures. Analysis of the elution fractions by SDS-PAGE and silver staining yielded only one specific band in the sample of the cells producing His-tagged Omp85 (Figure 7), which was confirmed to be Omp85 by immunoblotting (Figure 7). Next, the elution fractions were probed with antisera, directed against ComL, BamC, or BamE. All three lipoproteins were detected specifically in the elution fraction derived from the His-Omp85-expressing strain and not, or much less, in that of the control strain (Figure 7). The Imp protein, an OMP functioning in LPS transport to the cell surface (3), did not co-purify with Omp85 (Figure 7), further demonstrating the specificity of the assay. These results demonstrate that BamC, BamE, and ComL are associated with Omp85 in *N. meningitidis* but, apparently, this association does not withstand the conditions of semi-native SDS-PAGE.

Discussion

In this work, we addressed the composition of the Bam complex in *N. meningitidis* and identified homologs of the Bam complex components BamC, BamD, and BamE, while a

BamB homolog was not found. The absence of BamB in *Neisseria* was confirmed by searches using hidden Markov models developed for each of the Bam complex components of *E. coli* (14). Applied to α-proteobacteria, these searches demonstrated that *Brucella* species also lack BamB and, in addition, BamC. BamC was also not detected in *Caulobacter* and *Rickettsia* species (14). Homology searches indicated that even the essential lipoprotein ComL/BamD appears to be absent from species such as *Borrelia burgdorferi*. Thus, the Bam complex composition in Gram-negative bacteria is not very well conserved, except for the presence of Omp85, reinforcing its key function in the OMP assembly process.

The BamD homolog ComL was found to be essential in *N. meningitidis* as it is in *E. coli*. In the *comL* depletion strain, severe assembly defects of the porins and the secretin PilQ were observed, indicative of a general OMP assembly defect. Remarkably, a viable *comL* mutant has been described for *Neisseria gonorrhoeae* (12). This mutant contains a transposon insertion in *comL*, potentially resulting in expression of a truncated ComL protein, containing only 96 out of the 251 amino-acid residues of the mature part of the protein. Possibly, the essential part of ComL is comprised within these N-terminal 96 residues. On the other hand, we cannot exclude the possibility that species-specific differences exist in BamD/ComL dependency of bacteria. In this respect, it is interesting to note that a viable *bamD* knockout was recently described also in a close relative of *E. coli*, *i.e., Salmonella enterica* (11). The gonococcal *comL* mutant demonstrated a severe defect in transformation, but not in DNA uptake or in piliation (10). These observations, together with data suggesting that ComL might be covalently attached to the peptidoglycan layer, since it was not released from this layer by boiling in 4% SDS, led to the suggestion that ComL functions in periplasmic DNA transport and perhaps acts as a "space-maker" (10, 12). Such a function could also be important for the periplasmic transport of OMPs.

The *bamC* mutant showed virtually no defects in OMP assembly. Similarly, *E. coli bamC* mutants demonstrated only very mild phenotypes: they were shown to be selectively sensitive only to rifampin (26) and to show detectable defects in growth and OMP assembly only when combined with mutations in other OMP assembly components (26, 32, 46). Of note, such synthetic defects in *E. coli* were observed when *bamB* and *bamC* mutations were combined (46), while the *bamC* mutation in *N. meningitidis*, which does not possess a *bamB* gene, has no phenotype. The *bamE* mutant, in contrast, demonstrated a clear defect in OMP assembly and a severely compromised OM integrity. Consistently, an increased sensitivity of a *bamE* mutant to the cationic peptide polymyxin was reported before (38). Also in *E. coli*, *bamE* mutations compromised OM integrity (32, 36), but such mutants displayed only very mild OMP assembly defects (32). However, *bamE* and *bamB* mutations were synthetically lethal in *E. coli* (32), while a *bamE* mutation could easily be introduced in the *bamB*-deficient background of *N. meningitidis.* Thus, while *bamE* is an essential gene in an *E. coli bamB* mutant, this is not the case in *N. meningitidis*. This discrepancy is not due to the presence in *N. meningitidis* of a second *bamE* homolog, designated *mlp*, since a *bamE mlp* double mutant did not display any synthetic defects. We did not observe any phenotype of an *mlp* mutant in OMP assembly or OM integrity at all. Hence, the function of Mlp remains to be resolved. In a microarray analysis, the gene was found to be induced under iron-limitation (16), which, however, we could not confirm in a recent proteomic analysis (40). Remarkably, all *N. gonorrhoeae* strains analyzed so far contain a frameshift mutation 72 bp into the coding sequence of *mlp*, resulting in premature termination of the reading frame (47, data not shown), hence its name *mlp*, for meningococcal lipoprotein. Both BamE and Mlp consist of a so-called SmpA_OmlA domain. Interestingly, the closest homologs of Mlp in many bacteria, such as a 31-kDa protein from *Haemophilus somnus* (45), are extended with an OmpA domain, a peptidoglycan-binding domain thought to function in cell envelope stabilization.

Protease-accessibility experiments and pull-down assays clearly demonstrated that Omp85, BamC, ComL, and BamE form a complex in *N. meningitidis*. The observation that *E. coli* BamD could not substitute ComL might be due to failure to incorporate the heterologous protein into the neisserial Bam complex. Importantly, we did not co-purify the Imp protein in the pull-down assays, demonstrating that the LPS transport machinery is not, or at least not strongly, associated with the OMP assembly machinery in *N. meningitidis*. This finding argues against a suggestion that one of the POTRA domains of *E. coli* BamA may bind Imp (22). Possibly, Imp-Omp85 association may be different in *E. coli,* but then, a His-tagged BamB protein also did not pull-down Imp in this species (46).

Another component of the Bam complex of *N. meningitidis*, RmpM, was identified by the analysis of an Omp85-containing HMW complex detected in semi-native SDS-PAGE. BamC, ComL, and BamE were not detected in this complex presumably because they dissociated from this complex in the sample buffer, which contained 1% SDS. RmpM was previously shown to be present in oligomeric complexes of porins and TonB-dependent receptors in the neisserial OM (19, 28). Possibly, the association of RmpM with these OMPs is established while they are engaged with the Bam complex. Lack of RmpM did not result in general defects in OMP assembly, as inferred from porin and PilQ assembly. Rather, RmpM appears to stabilize oligomeric OMP complexes (19, 28) as was confirmed for the porins in the present study. Similarly, we observed that the HMW Omp85 complex was dramatically less stable in the Δ*rmpM* mutant since large amounts of monomeric Omp85 were detected (Figure 4C and D). Interestingly, our results indicated that RmpM is not associated with the PilQ complex, perhaps reflecting structural differences between PilQ and classical β-barrel OMPs. Consistently, the stability of the oligomeric PilQ complex appeared unaffected in the *rmpM* mutant,

Even in the absence of RmpM, Omp85 was detected in HMW forms. Possibly, other, still unknown components are associated with Omp85, or Omp85 is present in this complex as homo-oligomers. This latter possibility would be consistent with our previous findings that *in vitro* refolded *E. coli* Omp85 appeared to form tetramers (29). Moreover, several members of the Omp85 superfamily, such as mitochondrial Tob55 (27), chloroplast Toc75 (31), and the two-partner secretion component HMW1B from *Haemophilus influenzae* (35), behave as multimers after extraction from the membrane.

In conclusion, the Bam complex of *N. meningitidis* consists at least of Omp85, BamC, ComL, BamE, and RmpM, and differs from that of *E. coli* by the absence of a BamB homolog and the presence of RmpM. Like in *E. coli*, Omp85 and ComL/BamD are essential components, while the relative importance of the non-essential components BamC and BamE differs. The RmpM protein stabilizes the complex.

Acknowledgements

We would like to acknowledge the contributions of Rome Voulhoux and Jeroen Geurtsen in initial experiments. We thank Ralph Judd, Naoko Yokota, Hajime Tokuda, the Netherlands Vaccine Institute and GlaxoSmithKline for donation of antibodies. This work was supported by the Netherlands Research Councils for Chemical Sciences (CW) and Earth and Life Sciences (ALW) of the Netherlands organization for Scientific Research (NWO).

References

1. **Blum, H., H. Beier, and H. J. Gross.** 1987. Improved silver staining of plant proteins, RNA and DNA in polyacrylamide gels. Electrophoresis **8:**93-99.
2. **Bos, M. P., and J. Tommassen.** 2005. Viability of a capsule- and lipopolysaccharide-deficient mutant of *Neisseria meningitidis*. Infect. Immun. **73:**6194-6197.
3. **Bos, M. P., B. Tefsen, J. Geurtsen, and J. Tommassen**. 2004. Identification of an outer membrane protein required for the transport of lipopolysaccharide to the bacterial cell surface. Proc. Natl. Acad. Sci. USA **101:**9417-9422.
4. **Bos, M. P., V. Robert, and J. Tommassen.** 2007. Biogenesis of the Gram-negative bacterial outer membrane. Annu. Rev. Microbiol. **61:**191-214.
5. **Bos, M. P., V. Robert, and J. Tommassen.** 2007. Functioning of outer membrane protein assembly factor Omp85 requires a single POTRA domain. EMBO Rep. **8:**1149-1154.
6. **Carbonnelle, E., S. Hélaine, L. Prouvensier, X. Nassif, and V. Pelicic.** 2005. Type IV pilus biogenesis in *Neisseria meningitidis*: PilW is involved in a step occurring after pilus assembly, essential for fibre stability and function. Mol. Microbiol. **55:**54-64.
7. **Delgado, M., D. Yero, O. Niebla, S. González, Y. Climent, Y. Pérez, K. Cobas, E. Caballero, D. García, and R. Pajón.** 2007. Lipoprotein NMB0928 from *Neisseria meningitidis* serogroup B as a novel vaccine candidate. Vaccine **25:**8420-8431.
8. **Doerrler, W. T., and C. R. H. Raetz.** 2005. Loss of outer membrane proteins without inhibition of lipid export in an *Escherichia coli* YaeT mutant. J. Biol. Chem. **280:**27679-27687.
9. **Drake, S. L., S. A. Sandstedt, and M. Koomey.** 1997. PilP, a pilus biogenesis lipoprotein in *Neisseria gonorrhoeae*, affects expression of PilQ as a high-molecular-mass multimer. Mol. Microbiol. **23:**657-668.
10. **Facius, D., M. Fussenegger, and T. F. Meyer.** 1996. Sequential action of factors involved in natural competence for transformation of *Neisseria gonorrhoeae*. FEMS Microbiol. Lett. **137:**159-164.
11. **Fardini, Y, J. Trotereau, E. Bottreau, C. Souchard, P. Velge, and I. Virlogeux-Payant**. 2009. Investigation of the role of the BAM complex and SurA chaperone in outer membrane protein biogenesis and T3SS expression in *Salmonella.* Microbiology **155:**1613-1622.
12. **Fussenegger, M., D. Facius, J. Meier, and T. F. Meyer.** 1996. A novel peptidoglycan-linked lipoprotein (ComL) that functions in natural transformation competence of *Neisseria gonorrhoeae*. Mol. Microbiol. **19:**1095-1105.
13. **Galloway, S. M., and C. R. H. Raetz.** 1990. A mutant of *Escherichia coli* defective in the first step of endotoxin biosynthesis. J. Biol. Chem. **265:**6394-6402.
14. **Gatsos, X., A. J. Perry, K. Anwari, P. Dolezal, P. P. Wolynec, V. A. Likić, A. W. Purcell, S. K. Buchanan, and T. Lithgow.** 2008. Protein secretion and outer membrane assembly in *Alphaproteobacteria*. FEMS Microbiol. Rev. **32:**995-1009.
15. **Gentle, I., K. Gabriel, P. Beech, R. Waller and T. Lithgow.** 2004. The Omp85 family of proteins is essential for outer membrane biogenesis in mitochondria and bacteria. J. Cell. Biol. **164:**19-24.
16. **Grifantini, R., S. Sebastian, E. Frigimelica, M. Draghi, E. Bartolini, A. Muzzi, R. Rappuoli, G. Grandi, and C. A. Genco.** 2003. Identification of iron-activated and –repressed Fur-dependent genes by transcriptome analysis of *Neisseria meningitidis* group B. Proc. Natl. Acad. Sci. USA **100:**9542-9547.
17. **Grizot, S., and S. K. Buchanan.** 2004. Structure of the OmpA-like domain of RmpM from *Neisseria meningitidis*. Mol. Microbiol. **51:**1027-1037.
18. **Holten J.** 1979. Serotypes of *Neisseria meningitidis* isolated from patients in Norway during the first six months of 1978. J. Clin. Microbiol. **9:**186-188.
19. **Jansen C., A. Wiese, L. Reubsaet, N. Dekker, H. de Cock, U. Seydel, and J. Tommassen.** 2000. Biochemical and biophysical characterization of in vitro folded outer membrane porin PorA of *Neisseria meningitidis*. Biochim. Biophys. Acta **1464:**284-298.

20. **Johansen, J.**, **A.A. Rasmussen, M. Overgaard and P. Valentin-Hansen.** 2006. Conserved small non-coding RNAs that belong to the σ^E regulon: role in down-regulation of outer membrane proteins. J. Mol Biol. **364:**1-8.
21. **Khairnar, N. P., V. A. Kamble, S. H. Mangoli, S. K. Apte, and H. S. Misra.** 2007. Involvement of a periplasmic protein kinase in DNA strand break repair and homologous recombination in *Escherichia coli*. Mol. Microbiol. **65:**294-304.
22. **Kim, S., J. C. Malinverni, P. Sliz, T. J. Silhavy, S. C. Harrison, and D. Kahne.** 2007. Structure and function of an essential component of the outer membrane protein assembly machine. Science **317:**961-964.
23. **Kozjak, V., N. Wiedemann, D. Milenkovic, C. Lohaus, H. E. Meyer, B. Guiard, C. Meisinger, and N. Pfanner.** 2003. An essential role of Sam50 in the protein sorting and assembly machinery of the mitochondrial outer membrane. J. Biol. Chem. **278:**48520-48523.
24. **Malinverni, J. C., J. Werner, S. Kim, J. G. Sklar, D. Kahne, R. Misra, and T. J. Silhavy.** 2006. YfiO stabilizes the YaeT complex and is essential for outer membrane protein assembly in *Escherichia coli*. Mol. Microbiol. **61:**151-164.
25. **Matsushita, K., J. C. Arents, R. Bader, M. Yamada, O. Adachi, and P. W. Postma.** 1997. *Escherichia coli* is unable to produce pyrroloquinoline quinone (PQQ). Microbiology **143:**3149-3156.
26. **Onufryk, C., M. L. Crouch, F. C. Fang, and C. A. Gross.** 2005. Characterization of six lipoproteins in the σ^E regulon. J. Bacteriol. **187:**4552-4561.
27. **Paschen, S. A., T. Waizenegger, T. Stan, M. Preuss, M. Cyrklaff, K. Hell, D. Rapaport, and W. Neupert.** 2003. Evolutionary conservation of biogenesis of β-barrel membrane proteins. Nature **426:**862-866.
28. **Prinz, T., and J. Tommassen.** 2000. Association of iron-regulated outer membrane proteins of *Neisseria meningitidis* with the RmpM (class 4) protein. FEMS Microbiol. Lett. **183:**49-53.
29. **Robert, V., E. B. Volokhina, F. Senf, M. P. Bos, P. Van Gelder, and J. Tommassen.** 2006. Assembly factor Omp85 recognizes its outer membrane protein substrates by a species-specific C-terminal motif. PLoS Biol **4:**e377.
30. **Ruiz, N., and T. J. Silhavy.** 2005. Sensing external stress: watchdogs of the *Escherichia coli* cell envelope. Curr. Opin. Microbiol. **8:**122-126.
31. **Schleiff, E., J. Soll, M. Küchler, W. Kühlbrandt, and R. Harrer.** 2003. Characterization of the translocon of the outer envelope of chloroplasts. J. Cell. Biol. **160:**541-551.
32. **Sklar, J. G., T. Wu, L. S. Gronenberg, J. C. Malinverni, D. Kahne, and T. J. Silhavy.** 2007. Lipoprotein SmpA is a component of the YaeT complex that assembles outer membrane proteins in *Escherichia coli*. Proc. Natl. Acad. Sci. USA **104:**6400-6405.
33. **Steeghs, L., H. de Cock, E. Evers, B. Zomer, J. Tommassen, and P. van der Ley**. 2001. Outer membrane composition of a lipopolysaccharide-deficient *Neisseria meningitidis* mutant. EMBO J. **20:**6937-6945.
34. **Steeghs, L., R. den Hartog, A. den Boer, B. Zomer, P. Roholl, and P. van der Ley.** 1998. Meningitis bacterium is viable without endotoxin. Nature **392:**449-450.
35. **Surana, N. K., S. Grass, G. G. Hardy, H. Li, D. G. Thanassi, and J. W. St. Geme III.** 2004. Evidence for conservation of architecture and physical properties of Omp85-like proteins throughout evolution. Proc. Natl. Acad. Sci. USA **101:**14497-14502.
36. **Tamae C., A. Liu, K. Kim, D. Sitz, J. Hong, E. Becket, A. Bui, P. Solaimani, K. P. Tran, H. Yang and J. H. Miller.** 2008. Determination of antibiotic hypersensitivity among 4,000 single-gene knockout mutants of *Escherichia coli*. J. Bacteriol. **190:**5981-5988.
37. **Tashiro, Y., N. Nomura, R. Nakao, H. Senpuku, R. Kariyama, H. Kumon, S. Kosono, H. Watanabe, T. Nakajima, and H. Uchiyama.** 2008. Opr86 is essential for viability and is a potential candidate for a protective antigen against biofilm formation by *Pseudomonas aeruginosa*. J. Bacteriol. **190:**3969-3978.
38. **Tzeng Y. L., K. D. Ambrose, S. Zughaier, X. Zhou, Y. K. Miller, W. M. Shafer, and D. S. Stephens.** 2005. Cationic antimicrobial peptide resistance in *Neisseria meningitidis.* J. Bacteriol. **187:**5387-5396.
39. **van der Voort, E. R., P. van der Ley, J. van der Biezen, S. George, O. Tunnela, H. van Dijken, B. Kuipers, and J. Poolman.** 1996. Specificity of human bactericidal antibodies

against PorA P1.7,16 induced with a hexavalent meningococcal outer membrane vesicle vaccine. Infect. Immun. **64:**2745-2751.

40. **van Ulsen P., K. Kuhn, T. Prinz, H. Legner, P. Schmid, C. Baumann, and J. Tommassen.** 2009. Identification of proteins of *Neisseria meningitidis* induced under iron-limiting conditions using the isobaric tandem mass tag (TMT) labelling approach. Proteomics **9:**1771-1781.
41. **Voulhoux, R., M. P. Bos, J. Geurtsen, M. Mols, and J. Tommassen.** 2003. Role of a highly conserved bacterial protein in outer membrane protein assembly. Science **299:**262-265.
42. **Vuong, P., D. Bennion, J. Mantei, D. Frost, and R. Misra.** 2008. Analysis of YfgL and YaeT interactions through bioinformatics, mutagenesis, and biochemistry. J. Bacteriol. **190:**1507-1517.
43. **Walther, D. M., D. Papic, M. P. Bos, J. Tommassen, and D. Rapaport.** 2009. Signals in bacterial β-barrel proteins are functional in eukaryotic cells for targeting to and assembly in mitochondria. Proc. Natl. Acad. Sci. USA **106:**2531-2536.
44. **Werner, J., and R. Misra.** 2005. YaeT (Omp85) affects the assembly of lipid-dependent and lipid-independent outer membrane proteins of *Escherichia coli*. Mol. Microbiol. **57:**1450-1459.
45. **Won, J., and R. W. Griffith**.1993. Cloning and sequencing of the gene encoding a 31-kilodalton antigen of *Haemophilus somnus*. Infect. Immun. **61:**2813-2821.
46. **Wu, T., J. Malinverni, N. Ruiz, S. Kim, T. J. Silhavy, and D. Kahne.** 2005. Identification of a multicomponent complex required for outer membrane biogenesis in *Escherichia coli*. Cell **121:**235-245.
47. **Yang, Q. L., C. R. Tinsley, and E. C. Gotschlich.** 1995. Novel lipoprotein expressed by *Neisseria meningitidis* but not by *Neisseria gonorrhoeae*. Infect. Immun. **63:**1631-1636.

Chapter 3

Role of the periplasmic chaperones Skp and SurA in outer membrane protein biogenesis in *Neisseria meningitidis*

Elena B. Volokhina, Michiel Stork, Jan Tommassen and Martine P. Bos

Department of Molecular Microbiology and Institute of Biomembranes, Utrecht University, Padualaan 8, 3584 CH Utrecht, The Netherlands

Abstract

The periplasmic chaperones Skp and SurA are implicated in the biogenesis of outer membrane proteins (OMPs) in *Escherichia coli*. In this work we investigated whether these chaperones exert similar functions in *Neisseria meningitidis*. An initially generated mutant, in which the entire *skp* gene was replaced with a kanamycin-resistance cassette demonstrated protein leakage into the extracellular medium and increased sensitivity to antibiotics, indicative of a compromised outer membrane. Moreover, the assembly of the OMPs PorA and PilQ was affected in this mutant. However, these characteristics were not restored upon complementation with an *skp* gene in trans. Further investigation by qPCR revealed that the expression of at least two downstream genes, *lpxD* and *fabZ* involved in lipid A and fatty-acid biosynthesis, respectively, was strongly affected by the mutation. A subsequently constructed insertional *skp* mutant, containing a kanamycin-resistance cassette inserted at the 5' end of *skp*, did not show protein leakage into the extracellular medium, but showed lower levels of porins. This defect was restored upon expression of *skp* in trans, demonstrating that Skp functions in porin biogenesis in *N. meningitidis*, like it does in *E. coli*. However, *E. coli* Skp could not functionally substitute Skp in *N. meningitidis*, indicating that it functions in a species-specific manner. In contrast, no phenotype was found for the *surA* mutant. Moreover, while *skp* and *surA* mutations are synthetically lethal in *E. coli*, a *skp surA* double mutant could be constructed and was viable in *N. meningitidis*. Our results demonstrate an important role for Skp, but not for SurA, in OMP biogenesis in *N. meningitidis*.

Introduction

Bacterial outer membrane proteins (OMPs) are synthesized in the cytoplasm with an N-terminal signal sequence that directs them to the Sec translocon for transport through the inner membrane (IM) (12). After crossing the periplasm, they are assembled into the outer membrane (OM) by a machinery that, in *Neisseria meningitidis*, consists at least of the central component Omp85 (37), the essential lipoprotein ComL, two non-essential lipoproteins NlpB and SmpA, and the RmpM protein (Chapter 2). In *Escherichia coli*, this machinery was recently re-named Bam (β-barrel assembly machinery) and is similarly composed of Omp85 (BamA), NlpB (BamC), YfiO (BamD, a homolog of ComL), SmpA (BamE), and, additionally, YfgL (BamB), a lipoprotein that has no homolog in *Neisseria* (30, 41, Chapter 2). The functional homolog of RmpM, i.e. OmpA, has, so far, not been demonstrated to be present in the Bam complex in *E. coli*.

Several chaperones have been identified that play a role in OMP biogenesis during transit of the periplasm. Among them, Skp and SurA appear to be the most prominent ones. In *E. coli*, Skp was initially demonstrated to bind specifically to the unfolded chains of various OMPs (8, 10), although also some other proteins may act as substrates for binding (6, 17). The protein was shown to bind OMPs at the surface of the plasma membrane even before their translocation via the Sec translocon was completed (14). It was shown to stimulate the release of these substrates from the IM and the formation of soluble periplasmic intermediates of these proteins (28). The crystal structure of Skp revealed a homotrimer with a basket-like shape, which seems suitable to transiently shield substrates from the environment and thereby prevent their aggregation (20, 39).

The SurA protein was named after its first identified role, i.e., survival protein A, because its absence decreased survival of *E. coli* in stationary phase (34). *E. coli* SurA contains two peptidyl-prolyl isomerase (PPIase) domains flanked by N- and C-terminal sequences. The PPIase domains are dispensable for SurA's chaperone activity (1). Its crystal structure shows a core module formed by the N- and C-terminal segments and the PPIase 1 domain, with the PPIase 2 domain extending away from this core (2). Consistent with its proposed OMP-specific chaperone activity, SurA preferentially binds peptides *in vitro* containing two consecutive aromatic residues or two aromatic residues separated by one other residue, a motif regularly present in OMPs (15).

In *E. coli*, neither *skp* nor *surA* is an essential gene. Their individual absence causes rather similar phenotypes, i.e., a decrease in OMP levels and increased membrane permeability (8, 21, 27, 28). Interestingly, *surA* and *skp* mutations are synthetically lethal, meaning that the simultaneous absence of both genes is not tolerated, suggesting that they might act in parallel, complementary pathways (26). However, there is an alternative explanation for this synthetic lethality (5). In contrast to the case of Skp, there is no biochemical evidence that SurA associates with the IM. Cross-linking experiments showed that SurA, but not Skp, can be found in close association to the Bam complex (29, 38); thus, Skp and SurA appear to act in different parts of the periplasmic compartment. Also, the structure of Skp was found to resemble that of prefoldin, a cytosolic molecular chaperone belonging to a family of chaperones sometimes referred to as "holdases". These chaperones do not facilitate folding of their substrates but protect them from aggregation by holding them in their cavities, whereafter substrate release is thought to be triggered by interaction with downstream folding systems (20, 39). Consistently, the β-barrel domain of OmpA was found to be maintained in an unfolded state inside the Skp cavity (40). SurA, however, appears to be a "folding" chaperone since its absence strongly reduced the kinetics of the formation of folded OMPs (21, 27). The demand for a holding chaperone, such as Skp, may be limited under conditions of efficient OMP folding. However, when the folding process is

compromised, e.g. in a *surA* mutant, such a demand could be so high that the absence of Skp is not tolerated. Conversely, the demand for an efficient folding chaperone is high in the absence of the holding chaperone. These considerations provide an alternative explanation for the synthetic lethality of *skp* and *surA* mutations.

The roles of Skp and SurA have been almost exclusively studied in the *Enterobacteraceae*. Recently, it was reported that *surA* could not be inactivated in *Bordetella pertussis*, suggesting that it is an essential gene in that species (16). Thus, the OMP assembly process in *E. coli* is not the paradigm for all bacteria. In this respect, *N. meningitidis* has already revealed some insightful differences with *E. coli*: in contrast to *E. coli*, this Gram-negative bacterium can survive and assemble OMPs when the synthesis or transport of lipopolysaccharide (LPS) is disturbed (4, 31). Apparently, the OMP assembly pathway operates independently of LPS biogenesis in this bacterium. The structure of *E. coli* Skp shows a potential LPS-binding site (39), perhaps explaining the LPS connection to OMP assembly. This LPS-binding motif consists of five amino-acid residues that are strikingly well conserved (39). Interestingly, one basic residue of the LPS-binding motif of Skp (a lysine) is substituted by a glutamine in *N. meningitidis* Skp, possibly affecting its potential to bind LPS. Also, the composition of the Bam complex in *N. meningitidis* is not similar to that of *E. coli* (Chapter 2) and the phenotype of mutants depleted of Bam components is different in either species. In *E. coli*, the σ^E response is activated in such mutants, resulting in the degradation of unfolded OMPs by the periplasmic protease DegP and the inhibition of their synthesis by small regulatory RNAs (5). This regulatory pathway is missing in *N. meningitidis* (5), and unassembled OMPs accumulate in the periplasm when OMP assembly is compromised (37). Lack of such of feedback mechanisms may allow for a clearer interpretation of mutant phenotypes.

Comparison of the workings of fundamental processes, such as OMP assembly, in different organisms is likely to reveal novel insights. Since *N. meningitidis* has proven to be very informative as a model organism in studies to understanding OM biogenesis, we have now undertaken a systematic study into the role of the major periplasmic chaperones Skp and SurA in *N. meningitidis*.

Materials and methods

Bacterial strains and growth conditions

E. coli strains TOP10F' (Invitrogen) and DH5α (laboratory stock) were grown at 37˚C either on LB agar plates or in liquid LB medium on a shaker. When appropriate, 25 μg/ml of chloramphenicol or 50 μg/ml of kanamycin were added to the medium for plasmid maintenance. *N. meningitidis* strain HB-1, an unencapsulated derivative of serogroup B strain H44/76 (3), was grown at 37°C in candle jars on GC agar plates (Oxoid) supplemented with Vitox (Oxoid) and, when necessary, with 10 μg/ml of chloramphenicol or 80 μg/ml of kanamycin. The liquid cultures were grown in tryptic soy broth (TSB) (Becton Dickinson).

DNA manipulations

The primers and plasmids used in this study are summarized in Tables 1 and 2, respectively. All *N. meningitidis* DNA fragments were obtained by PCR using genomic DNA from strain HB-1 as the template. The *N. meningitidis skp* (*skp1*) and *surA* deletion mutants were made by replacing the entire genes by kanamycin-resistance (kan^R) cassettes. To that end, the upstream and downstream regions of these genes were amplified by PCR. The following primer couples were used to amplify upstream and downstream fragments of the genes to generate deletion constructs: NMB0182F/A and C/NMB0180R, respectively, for *skp*; and D/NMB0280R and NMB0281F/G, respectively, for *surA*. The fragments were cloned into

pCRII-TOPO, yielding plasmids pCRII-180 and pCRII-182 for the *skp1* inactivation construct and pCRII-280 and pCRII-281 for the *surA* inactivation construct, respectively. After verifying the desired orientation of the inserts in pCRII-TOPO, the *Sac*I-*Sal*I fragment of pCRII-180 was introduced into *Sac*I-*Sal*I-digested pCRII-182, yielding pCRII-180/182. The latter construct was digested with *Sal*I to allow for the insertion of a kan^R cassette, obtained as a *Sal*I-restricted fragment from pMB25, yielding pCRII-*skp::kan*. Similarly, the *Sac*I-*Acc*I fragment of pCRII-280 was ligated into pCRII-281, cut with *Sac*I-*Acc*I, yielding pCRII-280/281, followed by insertion of the kan^R cassette excised from pMB25 or a chloramphenicol-resistance cassette excised from pCRII-*cat* by *Acc*I restriction, yielding pCRII-*surA::kan* and pCRII-*surA::cat*, respectively. The chloramphenicol-resistance gene cassette was amplified by PCR from pACYC184 using primers P1 and P2 and cloned into pCRII-TOPO, yielding pCRII-*cat*. In all cases, the transcription direction of the cassette was similar to that of the replaced gene.

Table 1. Primers used in this study; restriction sites are underlined

Primer	Sequence	Restriction site
A	ATGACGTCGTGGCAGAACACCTGACC	
NMB0182F	ATGTCGACCTGAAGGGCTTCAGACGGCATT	*Sal*I
C	ATGACGGTGTGCGAACCGATT	
NMB0180R	ATGTCGACTTCAGACGGCATACCGAAC	*Sal*I
B	ATCATATGACCCGTTTGACCC	*Nde*I
SkpRev	ATGACGTCTCATCAGCGGGCGT	*Aat*II
D	TACGGCAACGACAGGATTA	
NMB0280R	ATGTCGACACGGTGCTCCTGCCAGGTT	*Acc*I
NMB0281F	ATGTCGACGAGCAGGCGGGAATCCGGTT	*Acc*I
G	ATGACGTCGGCAACTTCTGAATCGTC	
F	ATTGTTGTTGCTTCGGATAA	
E	ATGACGTCTTAGCGGATGTCGACATACGCGC	
A'	ATGCCGTCTGAACGCCGAAATCGAA	
B'	TTTGGACTAGGTGTCGACGTGCGCGC	*Acc*I
C'	ACGTCGACACCTAGTCCAAAAAATCG	*Acc*I
D'	ATGCCGTCTGAAAACAGGCGGGCGACTTTGG	
skpcoliF	ATCATATGCTGACAAAATTGCA	*Nde*I
skpcoliR	ATGACGTCTTATTTAACCTGTTTC	*Aat*II
rmpMF	CAGGCTCCGCAATATGTTGA	
rmpMR	GTTGTCTTGAGCTTCGGCG	
lpxDF	GGACATTTCCGTTACCGCC	
lpxDR	CTGTCGTGGACTTCGGCTTT	
fabZF	ATCCAAAAACTCATCCCCCAC	
fabZR	GGTGACGTTTTTAATCGCGGT	
P1	GTCGACGGATCCGTGTAGGCTGGAGCTGCTTC	*Acc*I
P2	GTCGACGGATCCATGCCGTCTGAACATATGAATATCCTCCTTA	*Acc*I

Table 2. Plasmids used in this study

Plasmid	Description	Reference
pCRII-TOPO	TA-cloning vector	Invitrogen
pCRII-180	pCRII-TOPO with *skp* upstream fragment	This study
pCRII-182	pCRII-TOPO with *skp* downstream fragment	This study
pCRII-180/182	pCRII-TOPO with *skp* upstream and downstream fragments	This study
pCRII-*skp::kan*	*skp1* knock-out construct	This study
pCRII-280	pCRII-TOPO with *surA* upstream fragment	This study
pCRII-281	pCRII-TOPO with *surA* downstream fragment	This study
pCRII-280/281	pCRII-TOPO with *surA* upstream and downstream fragments	This study
pCRII-*skp*-A'B'	pCRII-TOPO with 3'-region of *omp85* and 5'-region of *skp*	This study
pCRII-*skp*-C'D'	pCRII-TOPO with 3'-region of *skp* and 5'-region of *lpxD*	This study
pCRII-*skp2*	*skp2* knock-out construct	This study
pMB25	pCRII-TOPO with *imp* inactivation construct	4
pACYC184	source of chloramphenicol-resistance cassette	New England Biolabs
pCRII-*cat*	pCRII-TOPO with chloramphenicol-resistance cassette, flanked by *Acc*I sites	This study
pCRII-*surA::kan*	*surA* knock-out construct (kanamycin-resistance cassette)	This study
pCRII-*surA::cat*	*surA* knock-out construct (chloramphenicol-resistance cassette)	This study
pCRII-skp_{Nm}	pCRII-TOPO with complete *N. meningitidis skp*	This study
pCRII-skp_{Ec}	pCRII-TOPO with *E. coli skp* without its signal sequence	This study
pEN11-*imp*	*Neisseria* replicative plasmid containing H44/76 *imp* under *lac* promoter control	4
pEN11-skp_{Nm}	pEN11-*imp* with *imp* replaced by *N. meningitidis skp*	This study
pFP10-c-*lbpA*	*Neisseria* replicative plasmid containing the *lbpA* gene of H44/76 and its upstream sequence under *lac* promoter control	24
pFP10-skp_{Ec}	pFP10-c-*lbpA* with the mature LbpA-encoding part replaced by that for *E. coli* Skp	This study

To create an insertional *skp* mutant (*skp2*), a fragment consisting of the 3'-region of *omp85* and 5'-region of *skp* was amplified using primers A' and B', and another fragment consisting of the 3'-region of *skp* and 5'-region of *lpxD* was amplified using primers C' and D'. The fragments were cloned into pCRII-TOPO, yielding pCRII-*skp*-A'B' and pCRII-*skp*-C'D', respectively. The *Acc*I-*Spe*I fragment of pCRII-*skp*-C'D' was then ligated into *Acc*I-*Spe*I-restricted pCRII-*skp*-A'B' together with the *Acc*I-restricted kan^R cassette released from pMB25, yielding pCRII-*skp2*. The final construct contained a mutant *skp* allele with a kan^R cassette inserted after nucleotide 68 in the same transcriptional direction as *skp* and a 2-nucleotide insertion directly downstream of the cassette.

For complementation experiments, *N. meningitidis skp* was obtained by PCR using primers B and SkpRev and cloned into pCRII-TOPO, yielding pCRII-skp_{Nm}. From there, the *skp* gene was excised with *Nde*I and *Aat*II and subcloned into *Nde*I/*Aat*II-digested pEN11-*imp*, producing pEN11-skp_{Nm}. *E. coli skp* was amplified by PCR from genomic DNA of strain DH5a using primers skpcoliF and skpcoliR and cloned into pCRII-TOPO, producing pCRII-skp_{Ec}. From there, the *skp* gene was excised with *Nde*I and *Aat*II and subcloned into *Nde*I/*Aat*II-digested pFP10-c-*lbpA*, producing pFP10-skp_{Ec}. As result of the cloning strategy, the signal sequence of the *E. coli* Skp in the resulting gene product was replaced by that of the *N. meningitidis* lactoferrin-binding protein A (LbpA) (MNKKHSFPLTLTALAIATAFPSYA).

Meningococci were transformed on plate by adding 100 ng of PCR product or plasmid in 10 mM $MgCl_2$ for 3-5 h to a few freshly restreaked colonies. Thereafter, bacteria were plated on GC agar plates containing appropriate antibiotics for mutant selection.

Antibiotic sensitivity assay

Meningococci from overnight GC agar plates were resuspended in 100 µl of TSB to an optical density at 550 nm (OD_{550}) of 0.025 and plated on GC agar plates. Paper discs containing antibiotics (BD Biosciences) or 10 µl of 1% sodium dodecyl sulfate (SDS) plus 0.5 mM ethylenediaminetetraacetic acid (EDTA) solution were placed on top of the agar. The plates were incubated at 37°C for 24 h, after which the zones of clearing around the disks were measured in mm from the rim of the disks.

Cell fractionation

To isolate cell envelopes, bacteria grown in TSB for 6 h were collected by centrifugation, resuspended in 50 mM Tris-HCl, 5 mM EDTA (pH 8.0) containing protease inhibitor cocktail "Complete" (Roche) and stored overnight at -80°C. After ultrasonic disintegration (3 x 45 s at level 8, output 40%, Branson sonifier 450; Branson Ultrasonics Corparation), unbroken cells were removed by centrifugation (12,000 *g*, 15 min, 4˚C). Cell envelopes were collected by ultracentrifugation (170,000 *g*, 5 min, 4˚C), dissolved in 2 mM Tris-HCl (pH 7.6) and stored at –20°C. Extracellular media were collected from cultures grown for 6 h in TSB. Bacteria were removed by centrifugation (6,000 *g*, 10 min, room temperature) and proteins were precipitated from the supernatant with 10 % trichloroacetic acid.

LPS quantification

The amount of LPS in cell envelopes was quantified by 3-deoxy-d-manno-octulosonic acid measurement (35).

SDS-PAGE and Western blot analysis

Protein samples were analyzed by standard SDS-polyacrylamide electrophoresis (SDS-PAGE). Alternatively, for semi-native SDS-PAGE (37), sample buffer containing only 1% SDS and no β-mercaptoethanol and running buffer containing 0.025% SDS were used. These gels contained no SDS and electrophoresis was carried out on ice at 12 mA. Protein bands in gels were stained with Coomassie Brilliant Blue.

To enhance epitope recognition on immunoblots, native proteins were denatured within the semi-native SDS-PAGE gels by leaving the gels in steam for 20 min prior to blotting. Blotting was performed in a Biorad Wet blotting system in 25 mM Tris, 192 mM glycine (pH 8.3), 0.02% SDS in 20% methanol. The membranes were blocked for 1 h in phosphate-buffered saline (PBS) (pH 7.6), supplemented with 0.5% non-fat dried milk

(Protifar, Nutricia) and 0.1% Tween-20. The blots were incubated for 1 h with primary antibodies, washed, and then probed for 1 h with goat anti-rabbit or goat anti-mouse IgG secondary antibodies conjugated with horseradish peroxidase (Southern Biotechnology Associates Inc.) diluted in the blocking buffer. The signal was visualized with enhanced chemiluminescense (Amersham).

Rabbit antiserum against the N-terminal region (residues 22-464) of *N. meningitidis* Omp85 (α-N-Omp85) was generously provided by Ralph Judd (University of Montana, USA). Monoclonal antibodies against PorA, PorB, and RmpM were provided by the Netherlands Vaccine Institute (Bilthoven, The Netherlands). Rabbit antiserum against *N. meningitidis* Imp was described before (4). Mouse antiserum directed against PilQ was provided by GlaxoSmithKline Biologicals (Rixensart, Belgium). Rabbit antiserum against *E. coli* Skp was a kind gift from Mathias Müller (Universität Freiburg, Germany) (33).

Quantitative real-time PCR

Quantitative real-time PCR (qRT-PCR) was performed using an Applied Biosystems 7900HT Fast Real-Time PCR System and SYBR green master mix (Applied Biosystems) according to the manufacturer's recommendations. Total RNA was isolated by resuspending approximately $4x10^9$ *N. meningitidis* cells in 3 ml Trizol (Invitrogen). After the addition of 600 µl of chloroform and centrifugation, the upper phase was mixed 1:1 with 75% ethanol. The mixture was passed through a nucleospin RNA II column (Macherey-Nagel), washed with buffer R3 from the nucleospin RNA II kit and eluted in 100 µl of water. The RNA was then treated with Turbo DNA-Free (Ambion) to yield DNA-free RNA. To generate cDNA, 1 µg of total RNA was reverse transcribed from random hexamers using the Transcriptor High Fidelity cDNA synthesis kit (Roche) according to the manufacturer's recommendations. As a control, parallel samples were processed, in which the reverse transcriptase was omitted from the reaction mixture. PCRs were performed in triplicate in a 25-µl volume in a 96-well plate (Applied Biosystems) with the following cycle parameters: 95°C for 10 min, followed by 40 cycles of 95°C for 15 s and 60°C for 1 min, using primer couples lpxDF/lpxDR, fabZF/fabZR, and rmpMF/rmpMR (Table 1) to amplify the cDNAs of *lpxD*, *fabZ* and *rmpM*, respectively. A melting plot was performed to ensure that the signal originated from the specific amplicon. Data analysis was performed using the comparative cycle threshold method (Applied Biosystems) to determine relative expression levels. The *rmpM* transcript was used to normalize all data.

Reverse transcriptase PCR

For reverse transcriptase PCR, RNA was isolated as described above. cDNA was produced from *skp* mRNA using primer SkpRev and the Transcriptor High Fidelity cDNA synthesis kit (Roche) followed by 35 cycles of PCR amplification using primer B and primer SkpRev.

Results

Complete *skp* and *surA* deletions in *N. meningitidis*

To investigate the roles of Skp and SurA in *N. meningitidis*, the *skp1* and *surA* mutants were constructed by replacing the entire *skp* and *surA* genes by a kan^R cassette (Figure 1A). The mutations were verified in a series of PCRs (Figure 1A and 1B). Correct mutants were easily obtained showing that neither of these genes is essential. When the mutants were grown in liquid medium, the *surA* mutant displayed a slight but reproducible growth defect, but a more significant defect was observed in the case of the *skp1* mutant (Figure 2A). We noticed that the colonies formed by the *skp1* mutant were more opaque

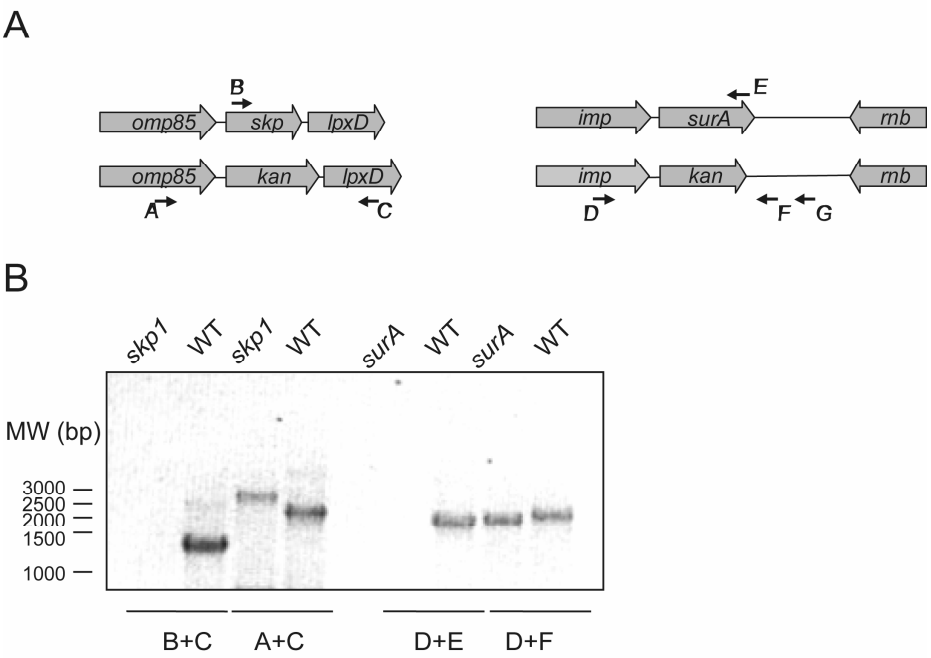

Figure 1

Construction of the *skp1* and *surA* deletion mutant strains. (**A**) Genomic organization of the *skp* and *surA* loci. To create deletion mutants, the complete *surA* and *skp* genes were replaced by *kan*^{R} cassettes via homologous recombination. PCR fragments generated with primer pairs A/C or D/G were used to transform the parent strain HB-1. (**B**) PCR products obtained from parent (WT) and mutant cells. The primer pairs used in the PCRs are indicated below the lanes. Primer pairs B/C and D/E yielded the expected fragments of 1291 base pairs (bp) and 1871 bp, respectively, from the parent strain and no fragments in the respective mutants, consistent with the absence of the binding sites for primers B and E, respectively. PCR analysis with primer pair A/C resulted in a 2157-bp fragment for the parent and the expected larger fragment of 2844 bp for the *skp1* mutant. Primer pair D/F yielded a 2168-bp fragment for the parent strain and the expected smaller fragment of 2027 bp for the *surA* mutant. The DNA fragments were analyzed by agarose gel electrophoresis and SYBR® Safe DNA gel staining (Invitrogen). The positions of size markers are shown at the left. Primer sequences are given in Table 1.

compared to those of the parent strain or the *surA* mutant. This opacity was unlikely due to phase-variable Opa protein expression, since the opacity was completely homogeneous, and no transparent phase variants were ever observed. This feature rather resembles the opacity seen before in *imp* and *msbA* mutants (4, 32), which contain a compromised OM, leak periplasmic proteins, and contain very low levels LPS as a result of LPS transport defects. Similarly, the *skp1* mutant released much more protein into the medium than the parent strain or the *surA* mutant (Figure 2B), indicating that its OM integrity is compromised. However, the *skp1* mutant did not produce detectably less LPS than the parent (data not shown).

Another consequence of a compromised OM is an increased susceptibility to antimicrobial agents. *E. coli surA* and *skp* mutants were shown to be more sensitive to antibiotics and to SDS plus EDTA (1, 21, 28). Therefore, we tested the sensitivity of the *skp1* and *surA* mutants to such agents (Figure 2C). The *skp1* mutant was indeed more sensitive to vancomycin and chloramphenicol than the parent strain. However, no increased sensitivity to vancomycin, chloramphenicol or SDS/EDTA was found in the case of the *surA* mutant (Figure 2C).

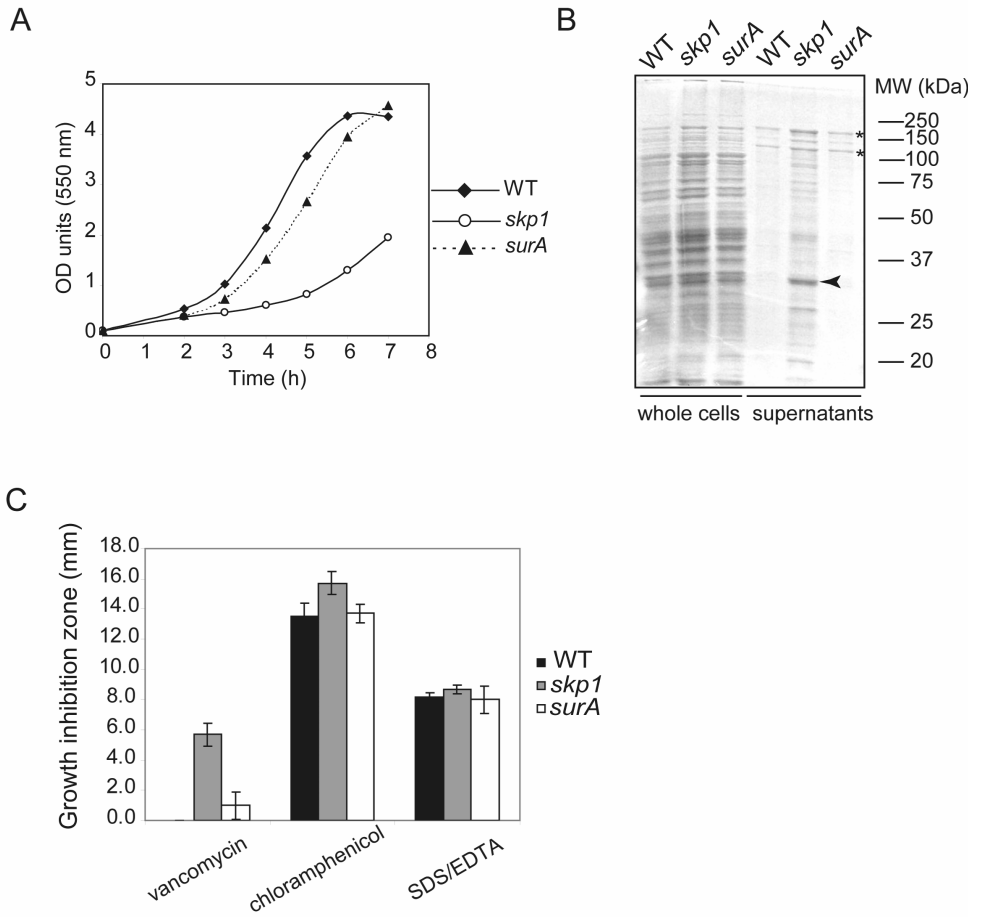

Figure 2

Phenotypes of the *skp1* and *surA* mutants. (**A**) Growth curves of parent (WT) and mutant strains in TSB. (**B**) Protein profiles of cells and culture supernatants observed by SDS-PAGE followed by Coomassie Brilliant Blue staining. The positions of molecular weight standard proteins are shown at the right. The major bands in the extracellular medium of the parent (WT) and *surA* mutant strains (indicated with asterisks) are two different secreted forms of IgA protease (36). The major band in the extracellular medium of the *skp1* mutant (arrowhead) is the periplasmic iron-binding protein FbpA (4). (**C**) Antibiotic sensitivity assays. Data represent mean values ±SD of growth inhibition zones around discs containing the indicated compounds from three independent experiments.

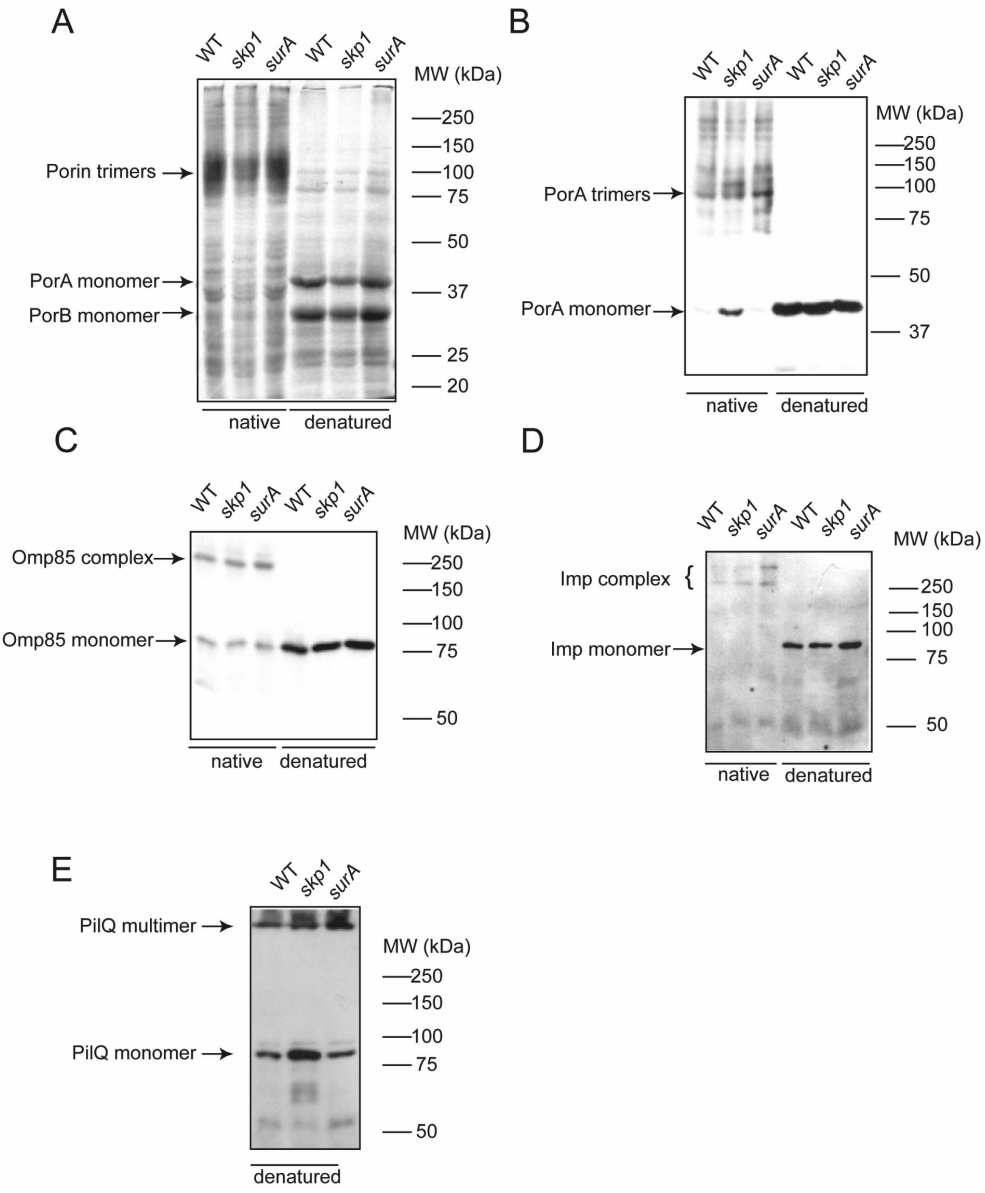

Figure 3

OMP assembly in the *skp1* and *surA* mutants. Cell envelopes were analyzed by SDS-PAGE under denaturing or semi-native conditions followed by Coomassie Brilliant Blue staining (**A**) or immunoblotting using antibodies against PorA (**B**), Omp85 (**C**), Imp (**D**), or PilQ (**E**). Monomers and oligomeric complexes of the various OMPs are indicated. The positions of molecular weight markers are indicated at the right of each panel.

OMP assembly in the *skp* and *surA* deletion mutants

Next, we analyzed OMP assembly in the *skp1* and *surA* mutants (Figure 3). It appeared that both porins produced by *N. meningitidis*, PorA and PorB, were correctly assembled into trimers in the mutants as analyzed by semi-native SDS-PAGE and Coomassie Brilliant Blue staining, although the total amount of porin trimers seemed to be somewhat decreased in the *skp1* mutant (Figure 3A). Furthermore, an immunoblot revealed the presence of some unassembled monomeric PorA in the *skp1* mutant (Figure 3B). Besides porins, several other OMPs were analyzed. Under semi-native electrophoresis conditions, Omp85 migrates as a high-molecular weight (HMW) complex in SDS-PAGE (37). This characteristic was unaffected in the mutants (Figure 3C). Also, the assembly of the Imp protein, which is required for LPS transport to the outer leaflet of the OM (4) and whose gene is located in an operon with *surA* (Figure 1A), was studied. Under semi-native SDS-PAGE conditions, Imp was detected in two HMW bands, which probably represent the native conformation of the protein and suggest that Imp is present in a complex in *N. meningitidis* (Figure 3D). This conformation was apparently poorly recognized by our antiserum, resulting in a relatively weak signal. The similar intensity of the HMW bands and the lack of the signal corresponding to the unfolded form after semi-native SDS-PAGE suggest that all the Imp protein in the *skp1* and *surA* mutants is assembled into this native conformation (Figure 3D). The secretin PilQ is assembled into multimers, which are stable and do not denature completely even upon boiling in 2% SDS (7, 11). The ratio between multimer and monomer appearance in denaturing SDS-PAGE can thus be taken as measure of the assembly status of PilQ. Using this assay, more unassembled monomeric PilQ was detected in the *skp1* mutant than in the parent strain and the *surA* mutant (Figure 3E) indicating that the assembly of PilQ is affected in the *skp1* deletion mutant. Overall, no impact of the absence of SurA was observed. In contrast, the deletion of *skp* clearly resulted in a defective OM and less efficient assembly of several OMPs.

Effect of the *skp* deletion on the expression of downstream genes

To confirm that the phenotype of the *skp1* deletion mutant was indeed caused by the lack of Skp, we introduced a copy of *skp* under the control of an isopropyl-β-D-thiogalactopyranoside (IPTG)-inducible promoter on plasmid pEN11-skp_{Nm} into the mutant. Remarkably, growth of the resulting strain in the presence of IPTG was not restored to wild-type levels (Figure 4A). Also the amount of protein released in the medium was not decreased upon growth in the presence of IPTG (Figure 4B). To ensure that Skp was produced upon IPTG induction, the presence of *skp* transcripts was assessed by reverse transcriptase PCR. The *skp* mRNA was detectable in HB-1 and in the complemented *skp1* mutant strain grown in the presence or absence of IPTG, but, as expected, not in the *skp1* mutant (Figure 4C). The observation that *skp* was expressed from pEN11-skp_{Nm} also in the absence of IPTG indicates that the *lac* promoter present in the construct is somewhat leaky. It should be noted, however, that this reverse transcriptase PCR assay is not quantitative. Thus, even though the plasmid copy of *skp* was transcribed, it did not complement the chromosomal deletion.

The *skp* deletion might have a polar effect on the expression of neighboring genes. The *skp* gene is present in an operon containing several genes involved in OMP assembly (*omp85*) and LPS and fatty acid synthesis (*lpxD, fabZ, lpxA*) (Figure 4D) (13). Omp85 synthesis was not affected in the mutant as evidenced in the immunoblot analysis (Figure 3C). Due to the unavailability of specific antisera, we could not test protein levels of LpxD or FabZ; instead we measured mRNA levels using qRT-PCR. The levels of *lpxD* and *fabZ* transcripts were ~30 and ~9 times lower in the *skp* mutant than in the parent strain,

demonstrating that the replacement of the *skp* gene by the *kan*^{R} cassette exerted a strong polar effect on the expression of the downstream genes.

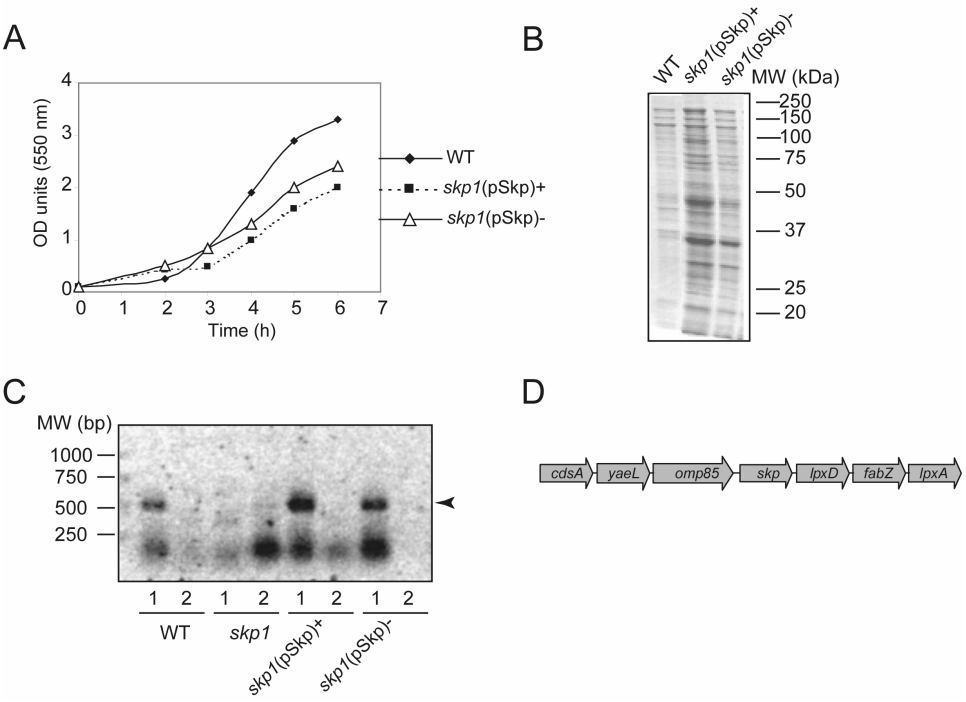

Figure 4

Lack of complementation of the *skp1* deletion mutant by *skp* expression *in trans*. The parent strain HB-1 (WT) and the *skp1* mutant containing pEN11-*skp*$_{Nm}$ (pSkp) grown in the presence [*skp1*(pSkp)+] or absence [*skp1*(pSkp)-] of 1 mM IPTG were analyzed. (**A**) Growth curves of the indicated strains in TSB. (**B**) Extracellular protein profiles analyzed by SDS-PAGE and Coomassie Brilliant Blue staining. The positions of molecular weight standard proteins are shown at the right. (**C**) Expression of *skp* detected by reverse transcriptase PCR (lanes 1). Control samples, which were processed without reverse transcriptase, are shown in lanes 2. The positions of size markers are shown at the left. The position of the *skp* cDNA PCR product is indicated with an arrowhead. The DNA fragments were analyzed by agarose gel electrophoresis and SYBR® Safe DNA gel staining. (**D**) Transcriptional unit comprising the *skp* gene in strain H44/76 (13), the encapsulated parent of HB-1.

Insertional *skp* mutant

Next, we constructed an alternative *skp* mutant to circumvent the polar effect brought about by replacement of the entire *skp* gene. To that end, a *kan*^{R} cassette was inserted into the 5'-part of the *skp* gene without concomitant deletion of *skp* sequences (Figure 5A). Interestingly, colonies of the resulting *skp2* mutant were not opaque and the strain did not release more protein into the medium than its parental strain (Figure 5B), nor was it

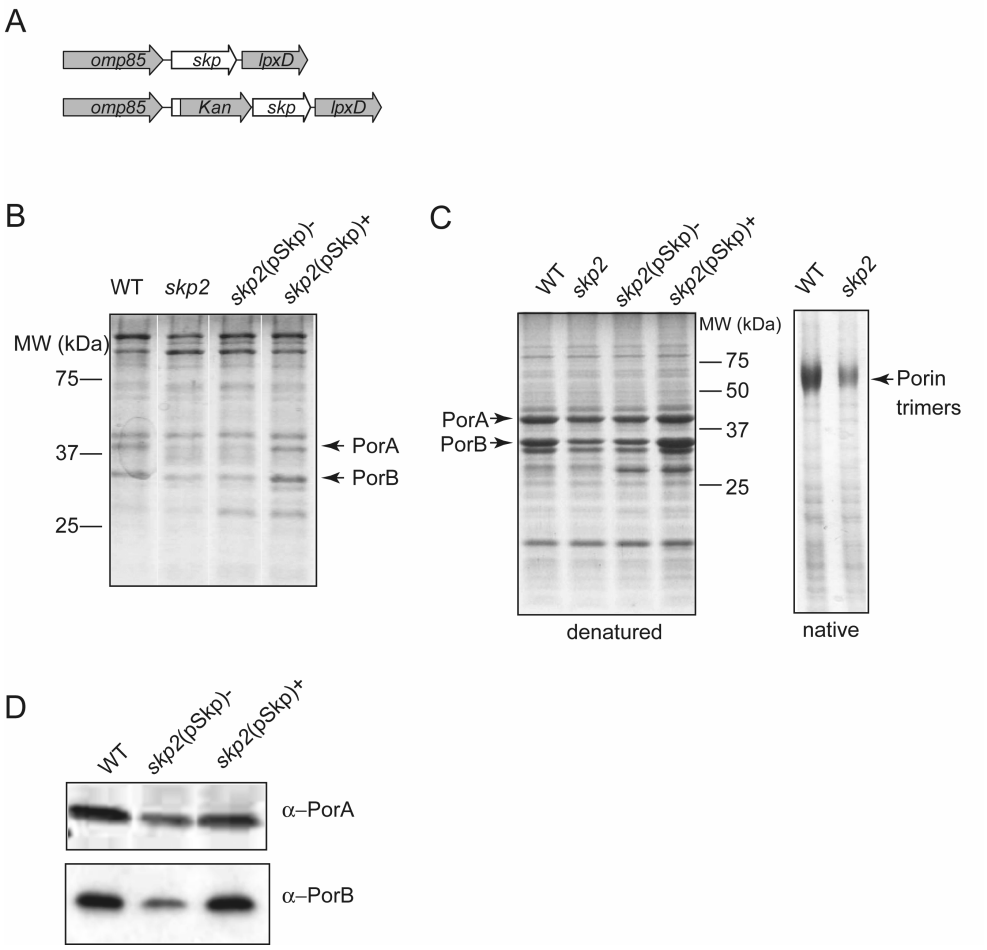

Figure 5

Comparison of protein profiles of the parental strain HB-1 (WT), the insertional *skp2* mutant and the *skp2* mutant containing pEN11-skp_{Nm} (pSkp) grown in the presence [*skp2*(pSkp)+] or absence [*skp2*(pSkp)-] of 1 mM IPTG. (**A**) Construction of the *skp2* mutant. A kan^R cassette was inserted after the first 68 nucleotides of the *skp* gene in the same transcriptional orientation as *skp*. (**B**) The *skp2* mutation does not cause protein leakage. Shown are the protein profiles of the extracellular media of the strains . After SDS-PAGE, the protein bands were visualized by Coomassie Brilliant Blue staining. The positions of PorA and PorB monomers are indicated. (**C**) The *skp2* mutation affects porin levels. Cell envelopes from the strains were analyzed by denaturing SDS-PAGE and Coomassie Brilliant Blue staining (left panel). Molecular weight markers are indicated on the right. The positions of PorA and PorB monomers are indicated. The right panel shows a semi-native SDS-PAGE analysis of cell envelopes of strain HB-1 and the *skp2* mutant. The position of the porin trimers is indicated. (**D**) Immunoblots of cell lysates of the strains were probed with antibodies against PorA (upper panel) and PorB (lower panel).

significantly more sensitive to vancomycin than the parent (data not shown). Also, the *skp2* mutant did not demonstrate any growth defect (data not shown). However, SDS-PAGE analysis of cell envelopes showed decreased levels of porins, particularly of PorB (Figure 5C). To verify that this defect was due to the absence of Skp, pEN11-skp_{Nm} was introduced into this strain. SDS-PAGE analysis of cell envelopes of the complemented strain showed decreased levels of porins when grown in the absence of IPTG and restoration of this defect after growth in the presence of IPTG (Figure 5C). No accumulation of porin monomers was observed when the envelopes were analyzed by semi-native SDS-PAGE, demonstrating that all porins detected in the absence of Skp were in the trimeric state (Figure 5C). To verify the decreased porin levels in the absence of Skp, we compared carefully equalized numbers of cells, based on OD_{550}, on immunoblots using anti-PorA and anti-PorB monoclonal antibodies (Figure 5D). These experiments clearly showed that the total levels of both porins were reduced in the absence of Skp. We did not find increased levels of porins in the extracellular medium (Figure 5B), demonstrating that the lower cellular levels are not due to enhanced OM blebbing of the bacteria. The levels of porins found in the medium due to blebbing, which is typical of neisserial strains, actually reflected the different levels found in the cells, related to the absence or presence of Skp (compare Figures 5B and 5D).

The *surA* and *skp* mutations are not synthetically lethal in *N. meningitidis*

In *E. coli*, the simultaneous absence of Skp and SurA is not tolerated (26). To test whether *skp* and *surA* mutations are synthetically lethal also in *N. meningitidis*, we transformed a *surA::cat* mutant with the insertional *skp::kan* (*skp2*) construct. Correct transformants were as easily obtained as in a wild-type background, demonstrating that, unlike in *E. coli*, both *skp* and *surA* can be inactivated in *N. meningitidis* at the same time.

E. coli Skp does not complement a neisserial *skp* mutant

E. coli-derived Skp was reported to bind the neisserial autotransporter NalP with high affinity *in vitro* (25). To determine whether *E. coli* Skp can substitute for *N. meningitidis* Skp *in vivo*, we introduced a copy of *E. coli skp* under the control of an IPTG-inducible promoter on plasmid pFP10-skp_{Ec} into the *skp2* mutant. Porin levels were not restored upon induction of expression of the *E. coli skp* gene, whereas this was clearly the case when neisserial *skp* was present on the plasmid (Figure 6A). Immunoblot analysis of cell envelopes confirmed that *E. coli* Skp was indeed produced upon IPTG induction. Two bands were specifically detected with the antiserum raised against *E. coli* Skp, probably corresponding to the precursor and mature forms of Skp (Figure 6B). Thus, *E. coli* Skp is not able to functionally substitute *N. meningitidis* Skp.

Discussion

In this work we investigated the possible role of Skp and SurA in OMP biogenesis in *N. meningitidis*. Substitution of the complete *skp* gene by a kan^R cassette negatively affected the transcription of the downstream genes *lpxD* and *fabZ*, and presumably also of *lpxA*, which is located downstream of *fabZ* (Figure 4D) in the same transcriptional unit (13). Therefore, and also because an *skp* gene provided *in trans* failed to complement the *skp1* mutation, the observed phenotype of the *skp1* mutant is likely the combined result of Skp deficiency and reduced expression of the downstream genes. LpxD and LpxA are acyltransferases involved in the biosynthesis of the LPS component lipid A (9, 18), whereas FabZ is involved in fatty acid biosynthesis (22). The *skp1* mutant, therefore, might be affected in LPS and/or phospholipid biosynthesis, although we could not detect altered levels of LPS. The latter observation implicates that LpxA and LpxD levels are not limiting for LPS biosynthesis in the wild-type strain. The phenotype of the *skp1* mutant included a reduced assembly

efficiency of at least two OMPs, PorA and PilQ, which could not be attributed to reduced Omp85 production, which appeared unaffected. The low levels of unassembled PorA and the enhanced release of proteins into the medium together with colony opacity are all features observed also in mutants that produce no or low levels of LPS, such as *lpxA*, *imp* and *msbA* mutants (4, 32). Thus, these features are likely consequences of a disturbed phospholipid/LPS balance in the OM, as well as of the absence of Skp.

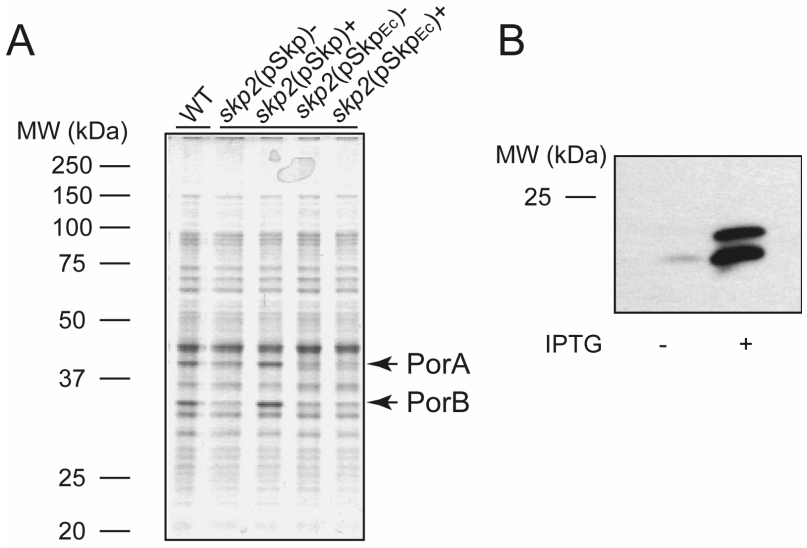

Figure 6

Functionality of *E. coli* Skp in *N. meningitidis*. (**A**) Protein profiles of total cell lysates of HB-1 (WT) and of the *skp2* mutant strain carrying either pEN11-skp_{Nm} [*skp2*(pSkp)] or pFP10-skp_{Ec} [*skp2*($pSkp_{Ec}$)]. The plasmid-containing strains were grown in the presence or absence of 1 mM IPTG as indicated by the plus and minus sign, respectively. The lysates were analyzed by denaturing SDS-PAGE and Coomassie Brilliant Blue staining. The positions of PorA and PorB are indicated. (**B**) Synthesis of *E. coli* Skp in *N. meningitidis*. Cell envelopes of HB-1 carrying pFP10-skp_{Ec}, grown in the presence or absence of 1 mM IPTG, were analyzed by denaturing SDS-PAGE and immunoblotting with antiserum directed against *E. coli* Skp.

The polar effect of the *skp1* mutation is likely related to the sequence at the 5'-side of the *lpxD* gene. In the *skp1* mutant, 28 bp upstream of *lpxD* were left intact, which should be sufficient to preserve the *lpxD* ribosome-binding site (Figure 7). There might be regulatory sequences, perhaps an additional promoter, present in the 3'-end of the *skp* gene, affecting *lpxD* and *fabZ* transcription. Apparently, the promoter present in the kan^R cassette does not compensate for the loss of this sequence.

The enhanced release of proteins into the medium was not observed in the insertional *skp2* mutant, indicating that it is not attributable to Skp deficiency. However, lower levels of porins were clearly due to the absence of Skp, since they were restored upon expression of

skp in trans. These results define the role of Skp as a chaperone in OMP assembly also in *N. meningitidis*. The decreased porin levels in the *skp2* mutant are likely due to proteolytic degradation of unprotected, unfolded intermediates in the periplasm. *N. meningitidis* does not appear to respond to accumulation of unfolded OMPs in the same way as *E. coli* does. When OMP assembly is compromised in *E. coli*, the σ^E response is activated, which leads to sRNA-mediated suppression of OMP synthesis (5) and to enhanced expression of the protease DegP, which degrades unassembled OMPs in the periplasm. Both processes result in severely lower OMP levels. *N. meningitidis* lacks most of the components of this σ^E response system (5) and, consistently, accumulates unfolded OMPs in the periplasm when OMP assembly is compromised, such as when Omp85 levels are depleted (37). Although *N. meningitidis* does not contain a *degP* homolog, it does contain a gene, NMB0532 in strain MC58 (www.tigr.org), putatively encoding a DegQ homolog, which is another member of the HtrA family of proteases to which DegP belongs (19). In *E. coli*, DegQ was identified as a multicopy suppressor of *degP* mutations and *degQ* mutants do not display any phenotype on their own. Possibly, this DegQ protease is responsible for the degradation of unfolded porins in the *skp* mutant of *N. meningitidis*.

TAATCCCGCAAATGCCGTCTGAAGCCCTTCAG*ACGGCATTTCGCGGCAACATTCGAAGGAGTT
TTACC**ATG**ACCCGTTTGACCCGCGCGTTTGCCGCGGCTCTGATCGGTTTGTGCTGCACCGCAGGC
GCGCACGTCGAC**ACCTAGTCCAAAAAATCGGCTTTATCAACACCGAGCGCATCTACCTCGAA
TCCAAGCAGGCGCGCAAGATTCAAAAAACGCTGGACAGCGAATTTTCCGCTCGTCAGGACGAAT
TGCAAAAACTGCAACGCGAAGGTCTGGATTTGGAAAGGCAGCTTGCCGAAGGCAAACTCAGAA
ACGCAAAAAAGGCGCAAGCCGAAGAAAAATGGCGCGGGCTGGTCGCAGCGTTCCGCAAAAAAC
AGGCGCAGTTTGAAGAAGACTACAACCTCCGCCGCAACGAAGAGTTTGCCTCCCTCCAGCAAAA
CGCCAACCGCGTCATCGTCAAAATCGCCAAACAGGAAGGTTACGATGTCATTTTGCAGAACGTG
ATTTACGTCAACACCCAATACGACGTTACCGACAGCGTCATTAAAGAAATGAACGCCCGC**TGA**C
CCT*TTCAGACGGCATACCGAACAGGAAAACC***ATG***

Figure 7

Sequence of the *skp* locus in strain HB-1. The stop codon of *omp85* is indicated in regular boldface, the start and stop codons of *skp* are indicated in underlined boldface, and the start codon of *lpxD* in italic boldface. The insertion site of the *kan*^{R} cassette in the *skp2* mutant is indicated by **, and the region replaced by the *kan*^{R} cassette in the *skp1* mutant is framed by * on each side. A 16-bp inverted repeat, which includes a neisserial DNA uptake sequence, is shown in grey.

But then, why are unassembled porins degraded in the *skp2* mutant, but not during Omp85 depletion? One can envision three destinations for nascent OMPs arriving in the periplasm: assembly into the OM, or, when this route is compromised, accumulation in aggregates or proteolytic degradation. The balance between these alternative pathways may be different depending on the severity of the assembly defect. With a mild assembly defect as in the *skp2* mutant, the DegQ protease encoded by the NMB0532 locus could probably degrade the unassembled OMPs in the periplasm. However, when there is a severe assembly defect as in the Omp85-depletion strain, the protease cannot cope with the massive accumulation of unassembled OMPs, which then will form aggregates.

Skp does not demonstrate much species specificity *in vitro*, as *E. coli*-derived Skp binds neisserial OMPs (25). Nevertheless, *E. coli* Skp could not functionally substitute its homolog in *N. meningitidis*. This suggests that Skp might interact with another component of

the OMP biogenesis machinery and that such interaction possibly happens in a species-specific manner.

While the role we found for Skp in OMP biogenesis in *N. meningitidis* is consistent with its role in *E. coli,* a more surprising result of this study is the apparent absence of a role for SurA in this process. It has been suggested even that SurA is the major periplasmic chaperone for OMP biogenesis in *E. coli*, whereas Skp acts in a parallel rescue pathway that deals only with substrates that fall off from the SurA pathway (29). We actually anticipated that it might not be possible to obtain a *surA* mutant in *N. meningitidis*, since this organism does not contain a homolog of YfgL (BamB) (Chapter 2), a lipoprotein implicated in OMP assembly in *E. coli*. A double *yfgL surA* knock-out was shown to be synthetically lethal in *E. coli* (23). Also, the absence of synthetic lethality of the *skp2* and *surA* mutations in *N. meningitidis* constitutes another difference with the situation in *E. coli*, but is consistent with the fact that we did not observe any phenotype of the *surA* mutation at all. The different function of SurA in *N. meningitidis* as compared to that in *E. coli* is probably reflected in its different structure. The *N. meningitidis* SurA sequence contains remarkable tri-amino-acid repeats (AAK/VAK) directly after the signal sequence in the beginning of the mature domain of the protein. The number of these repeats is highly variable among the SurA proteins of *Neisseria* strains of which the genome sequence is available, and their function is obscure. More important with respect to function probably is that *N. meningitidis* SurA lacks one out of the two PPIase domains found in *E. coli* SurA. Based on sequence alignments (data not shown), the PPIase 1 domain, which together with the N- and C-terminal parts forms the core of the protein in the crystal structure of *E. coli* SurA (2), is missing while the PPIase 2 domain, which forms a satellite relative to the core, is present. Although it has been reported that the PPIase domains are dispensable for function (1), an important role has been assigned to the PPIase 1 domain. *E. coli* SurA has been shown to selectively bind peptides that are rich in aromatic residues and characteristic for OMPs (15), and it was subsequently demonstrated that the recognition of these peptides is imparted by the PPIase 1 domain (42). Thus, SurA of *N. meningitidis* may fail to specifically recognize OMP substrates because it misses the PPIase 1 domain. Interestingly, the SurA proteins of several other bacteria, such as those of *Haemophilus influenzae* and *Pasteurella multocida*, were also recognized to lack the PPIase 1 domain (2), and we speculate that also in these bacteria SurA has no particular role in OMP biogenesis.

The possibility to inactivate *skp* and *surA* at the same time suggests that OMPs in *N. meningitidis* may cross the periplasm unassisted. Perhaps, this is related to the absence of the σ^E response, allowing a broader time span for the Omp85 machinery to deal with unassembled periplasmic OMP intermediates. Alternatively, we cannot exclude the possibility that there is another periplasmic chaperone, which is redundant to Skp and/or SurA in *N. meningitidis*, but has no or only a marginal role in *E. coli*.

Acknowledgements

This work was supported by the Netherlands Research Councils for Chemical Sciences (CW) and Earth and Life Sciences (ALW) from the Netherlands Organization for Scientific Research (NWO).

References

1. **Behrens, S., R. Maier, H. de Cock, F. X. Schmid, and C. A. Gross.** 2001. The SurA periplasmic PPIase lacking its parvulin domains functions *in vivo* and has chaperone activity. EMBO J. **20:**285-294.
2. **Bitto, E., and D. B. McKay.** 2002. Crystallographic structure of SurA, a molecular chaperone that facilitates folding of outer membrane porins. Structure **10:**1489-1498.
3. **Bos, M. P., and J. Tommassen.** 2005. Viability of a capsule- and lipopolysaccharide-deficient mutant of *Neisseria meningitidis*. Infect. Immun. **73:**6194-6197.
4. **Bos M. P.**, **B. Tefsen**, **J. Geurtsen**, **and J. Tommassen.** 2004. Identification of an outer membrane protein required for the transport of lipopolysaccharide to the bacterial cell surface. Proc. Natl. Acad. Sci. U S A **101:**9417-9422.
5. **Bos, M. P., V. Robert, and J. Tommassen.** 2007. Biogenesis of the gram-negative bacterial outer membrane. Annu. Rev. Microbiol. **61:**191-214.
6. **Bothmann, H., and A. Plückthun.** 1998. Selection for a periplasmic factor improving phage display and functional periplasmic expression. Nat. Biotechnol. **16:**376-380.
7. **Carbonnelle, E., S. Hélaine, L. Prouvensier, X. Nassif, and V. Pelicic.** 2005. Type IV pilus biogenesis in *Neisseria meningitidis*: PilW is involved in a step occurring after pilus assembly, essential for fibre stability and function. Mol. Microbiol. **55:**54-64.
8. **Chen, R., and U. Henning.** 1996. A periplasmic protein (Skp) of *Escherichia coli* selectively binds a class of outer membrane proteins. Mol. Microbiol. **19:**1287-1294.
9. **Coleman**, **J., and C. R. H. Raetz.** 1988. First committed step of lipid A biosynthesis in *Escherichia coli*: sequence of the *lpxA* gene. J. Bacteriol. **170:**1268-1274.
10. **de Cock, H., U. Schäfer, M. Potgeter, R. Demel, M. Müller, and J. Tommassen.** 1999. Affinity of the periplasmic chaperone Skp of *Escherichia coli* for phospholipids, lipopolysaccharides and non-native outer membrane proteins. Role of Skp in the biogenesis of outer membrane protein. Eur. J. Biochem. **259:**96-103.
11. **Drake, S. L., S. A. Sandstedt, and M. Koomey.** 1997. PilP, a pilus biogenesis lipoprotein in *Neisseria gonorrhoeae*, affects expression of PilQ as a high-molecular-mass multimer. Mol. Microbiol. **23:**657-668.
12. **Driessen, A. J. M., and N. Nouwen.** 2008. Protein translocation across the bacterial cytoplasmic membrane. Annu. Rev. Biochem. **77:**643-667.
13. **Genevrois, S., L. Steeghs, P. Roholl, J. Letesson, and P. van der Ley.** 2003. The Omp85 protein of *Neisseria meningitidis* is required for lipid export to the outer membrane. EMBO J. **22:**1780–1789.
14. **Harms, N., G. Koningstein, W. Dontje, M. Müller, B. Oudega, J. Luirink, and H. de Cock.** 2001. The early interaction of the outer membrane protein PhoE with the periplasmic chaperone Skp occurs at the cytoplasmic membrane. J. Biol. Chem. **276:**18804-18811.
15. **Hennecke, G., J. Nolte, R. Volkmer-Engert, J. Schneider-Mergener, and S. Behrens.** 2005. The periplasmic chaperone SurA exploits two features characteristic of integral outer membrane proteins for selective substrate recognition. J. Biol. Chem. **280:**23540-23548.
16. **Hodak, H., A. Wohlkönig, C. Smet-Nocca, H. Drobecq, J. M. Wieruszeski, M. Sénéchal, I. Landrieu, C. Locht, M. Jamin, and F. Jacob-Dubuisson.** 2008. The peptidyl–prolyl isomerase and chaperone Par27 of *Bordetella pertussis* as the prototype for a new group of parvulins. J. Mol. Biol. **376:**414-426.
17. **Jarchow S.**, **C. Lück**, **A. Görg**, **and A. Skerra.** 2008. Identification of potential substrate proteins for the periplasmic *Escherichia coli* chaperone Skp. Proteomics **8:**4987-4994.
18. **Kelly, T. M.**, **S. A. Stachula**, **C. R. H. Raetz**, **and M. S. Anderson.** 1993. The *firA* gene of *Escherichia coli* encodes UDP-3-0-(R-3-hydroxymyristoyl)-glucosamine N-acyltransferase. The third step of endotoxin biosynthesis. J. Biol. Chem. **268:**19866-19874.
19. **Kim, D. Y., and K. K. Kim.** 2005. Structure and function of HtrA family proteins, the key players in protein quality control. J. Biochem. Mol. Biol. **38:**266-274.

20. **Korndörfer, I. P., M. K. Dommel, and A. Skerra.** 2004. Structure of the periplasmic chaperone Skp suggests functional similarity with cytosolic chaperones despite differing architecture. Nat. Struct. Mol. Biol. **11:**1015-1020.
21. **Lazar, S. W., and R. Kolter.** 1996. SurA assists the folding of *Escherichia coli* outer membrane proteins. J. Bacteriol. **178:**1770-1773.
22. **Marrakchi, H., Y.-M. Zhang, and C. O. Rock.** 2002. Mechanistic diversity and regulation of Type II fatty acid synthesis. Biochem. Soc. Trans. **30:**1050-1055.
23. **Onufryk, C., M. L. Crouch, F. C. Fang, and C. A. Gross.** 2005. Characterization of six lipoproteins in the σ^E regulon. J. Bacteriol. **187:**4552-4561.
24. **Pettersson, A., J. Kortekaas, V. E. Weynants, P. Voet, J. T. Poolman, M. P. Bos, and J. Tommassen.** 2006. Vaccine potential of the *Neisseria meningitidis* lactoferrin-binding proteins LbpA and LbpB. Vaccine **24:**3545-3557.
25. **Qu, J., C. Mayer, S. Behrens, O. Holst, and J. H. Kleinschmidt.** 2007. The trimeric periplasmic chaperone Skp of *Escherichia coli* forms 1:1 complexes with outer membrane proteins via hydrophobic and electrostatic interactions. J. Mol. Biol. **374:**91-105.
26. **Rizzitello, A. E., J. R. Harper, and T. J. Silhavy.** 2001. Genetic evidence for parallel pathways of chaperone activity in the periplasm of *Escherichia coli*. J. Bacteriol. **183:**6794-6800.
27. **Rouvière, P. E., and C. A. Gross.** 1996. SurA, a periplasmic protein with peptidyl-prolyl isomerase activity, participates in the assembly of outer membrane porins. Genes Dev. **10:**3170-3182.
28. **Schäfer, U., K. Beck, and M. Müller.** 1999. Skp, a molecular chaperone of gram-negative bacteria, is required for the formation of soluble periplasmic intermediates of outer membrane proteins. J. Biol. Chem. **274:**24567-24574.
29. **Sklar, J. G., T. Wu, D. Kahne, and T. J. Silhavy.** 2007. Defining the roles of the periplasmic chaperones SurA, Skp, and DegP in *Escherichia coli*. Genes Dev. **21:**2473-2484.
30. **Sklar, J. G., T. Wu, L. S. Gronenberg, J. C. Malinverni, D. Kahne, and T. J. Silhavy.** 2007. Lipoprotein SmpA is a component of the YaeT complex that assembles outer membrane proteins in *Escherichia coli*. Proc. Natl. Acad. Sci. U S A **104:**6400-6405.
31. **Steeghs, L., R. den Hartog, A. den Boer, B. Zomer, P. Roholl, and P. van der Ley.** 1998. Meningitis bacterium is viable without endotoxin. Nature **392:**449-450.
32. **Tefsen, T., M. P. Bos, F. Beckers, J. Tommassen, and H. de Cock.** 2005. MsbA is not required for phospholipid transport in *Neisseria meningitidis*. J. Biol. Chem. **280:**35961-35966.
33. **Thome, B. M., H. K. Hoffschulte, E. Schiltz, and M. Müller.** 1990. A protein with sequence identity to Skp (FirA) supports protein translocation into plasma membrane vesicles of *Escherichia coli*. FEBS Letters **269:**113-116.
34. **Tormo, A., M. Almirón, and R. Kolter.** 1990. *surA*, an *Escherichia coli* gene essential for survival in stationary phase. J. Bacteriol. **172:**4339-4347.
35. **van Alphen L., A. Verkleij, J. Leunissen-Bijvelt, and B. Lugtenberg.** 1978. Architecture of the outer membrane of *Escherichia coli*. III. Protein-lipopolysaccharide complexes in intramembraneous particles. J. Bacteriol. **134:**1089-1098.
36. **van Ulsen, P., L. van Alphen, J. ten Hove, F. Fransen, P. van der Ley, and J. Tommassen.** 2003. A Neisserial autotransporter NalP modulating the processing of other autotransporters. Mol. Microbiol. **50:**1017-1030.
37. **Voulhoux, R., M. P. Bos, J. Geurtsen, M. Mols, and J. Tommassen.** 2003. Role of a highly conserved bacterial protein in outer membrane protein assembly. Science **299:**262-265.
38. **Vuong, P., D. Bennion, J. Mantei, D. Frost, and R. Misra.** 2008. Analysis of YfgL and YaeT interactions through bioinformatics, mutagenesis, and biochemistry. J. Bacteriol. **190:**1507-1517.
39. **Walton, T. A., and M. C. Sousa.** 2004. Crystal structure of Skp, a prefoldin-like chaperone that protects soluble and membrane proteins from aggregation. Mol. Cell **15:**367-374.
40. **Walton, T. A., C. M. Sandoval, C. A. Fowler, A. Pardi, and M. C. Sousa.** 2009. The cavity-chaperone Skp protects its substrate from aggregation but allows independent folding of substrate domains. Proc. Natl. Acad. Sci. U S A **106**:1772-1777.

41. **Wu, T., J. Malinverni, N. Ruiz, S. Kim, T. J. Silhavy, and D. Kahne.** 2005. Identification of a multicomponent complex required for outer membrane biogenesis in *Escherichia coli*. Cell **121:**235-245.

42. **Xu, X., S. Wang, Y-X. Hu, and D. B. McKay.** 2007. The periplasmic bacterial molecular chaperone SurA adapts its structure to bind peptides in different conformations to assert a sequence preference for aromatic residues. J. Mol. Biol. **373:**367-381.

Chapter 4

Species specificity of the Omp85 component of the bacterial outer membrane protein-assembly machinery

Elena B. Volokhina[1], Frank Beckers[1], Erica Lindh[1], Viviane Robert[2], Jan Tommassen[1] and Martine P. Bos[1]

[1] Department of Molecular Microbiology and Institute of Biomembranes, Utrecht University, Padualaan 8, 3584 CH Utrecht, The Netherlands

[2] Faculté des Sciences et Techniques, Université Paul Cézanne- Aix-Marseille III, Marseille, France

Abstract

The Omp85 protein is the key component of the outer membrane protein (OMP)-assembly machinery in Gram-negative bacteria and in mitochondria. We previously demonstrated that Omp85 recognizes its OMP substrates in a species-specific manner *in vitro*. In this work, we further studied species specificity *in vivo* by testing the functioning of the Omp85 homologs of *Neisseria meningitidis*, *Neisseria gonorrhoeae*, *Bordetella pertussis*, *Burkholderia mallei*, and *Escherichia coli* in *E. coli* and in *N. meningitidis*. We found that neither heterologous Omp85 functioned in either species, except for *N. gonorrhoeae* Omp85, which fully complemented a *N. meningitidis omp85* mutant. The heterologous Omp85 proteins were assembled into the outer membrane of *E. coli* to a significant extent and, at least in the case of the *N. meningitidis* homolog, also associated with BamD, an essential accessory lipoprotein of the endogenous OMP assembly machinery. Thus, insufficient substrate recognition appears to be the major reason for the lack of heterologous Omp85 functioning in *E. coli*. Omp85 is thought to consist of two domains: an N-terminal periplasmic part and a C-terminal membrane-embedded β-barrel. Various chimeras comprising swapped domains of *N. meningitidis* and *E. coli* Omp85 proteins were also not functional in either host, although some of them appeared to be inserted in the outer membrane. The lack of functionality of the chimeric proteins indicates that the two domains of Omp85 need to be compatible in order to function.

Introduction

Gram-negative bacteria are characterized by a cell envelope consisting of an inner membrane and an outer membrane (OM), which are separated by the peptidoglycan-containing periplasm. While the integral inner membrane proteins are α-helical, all but one known integral OM proteins (OMPs) are β-barrels (7, 14). All OMPs are synthesized in the cytosol with an N-terminal signal sequence that directs them to the Sec translocon for transport through the inner membrane (8). Extensive genetic and biochemical research brought to light many aspects of protein translocation across the inner membrane; however, details about protein assembly into the OM have remained obscure.

Previously, we showed the Omp85 protein to be an essential part of the OMP insertion machinery in *Neisseria meningitidis*. Depletion of this essential protein in a conditional mutant strain resulted in the accumulation of unassembled forms of all OMPs analyzed (28), demonstrating that Omp85 is required for OMP assembly. Later, a similar function was shown for the Omp85 homologs YaeT (recently re-named BamA) in *Escherichia coli* (6, 30, 31) and Opr86 in *Pseudomonas aeruginosa* (27). Interestingly, an Omp85 homolog is also present and required for OMP assembly in mitochondria (10, 15, 19). In *E. coli*, four lipoproteins associated with Omp85 have been identified: BamB (formerly YfgL), BamC (NlpB), BamD (YfiO), and BamE (SmpA) (23, 31). BamB, BamC and BamE are not essential in *E. coli*, but phenotypes of deletion mutants suggest that these proteins are important for efficient OMP assembly (23, 31). We established that meningococcal Omp85 is also associated with BamC, BamD and BamE, and, additionally, with the RmpM protein (Chapter 2). BamB is not present in neisserial strains. Like Omp85, BamD is an essential component of the OMP assembly machinery in *E. coli* (17, 31). Its depletion results in a phenotype similar to that of an Omp85–depleted strain. In *N. meningitidis*, the BamD homolog, ComL, was also shown to be essential and to be involved in OMP assembly (Chapter 2).

The Omp85 protein was predicted to consist of a 12-stranded membrane-embedded β-barrel in its C-terminal part and an N-terminal part localized in the periplasm (28). In the predicted periplasmic part, five polypeptide-transport-associated (POTRA) domains are located; such domains are also found in several other proteins involved in protein translocation (22). A complete Omp85 structure is not yet available, but two crystal structures and one NMR structure of POTRA domain-containing fragments of *E. coli* BamA have been solved (9, 12, 13). They show a similar fold for all POTRA domains: three β-sheets overlaid with a pair of antiparallel α-helices. The 12-stranded β-barrel topology prediction leaves a 61-amino-acid region between the barrel and the POTRA domains, which we designated the hinge region (4). The crystal structure of the two-partner secretion-system component FhaC of *Bordetella pertussis*, which shares limited sequence similarity with Omp85, was recently solved. This protein turned out to consist of two POTRA domains and a 16-stranded β-barrel (5). This indicates the possibility of the Omp85 β-barrel containing 16 β-strands as well, with four additional β-strands located in the hinge region.

Many β-barrel OMPs carry a C-terminal signature sequence. This sequence is characterized by a phenylalanine or a tryptophan at the C-terminal position, a hydrophobic amino-acid residue, preferably a tyrosine, at the position -3 from the C terminus, and hydrophobic residues at the positions -5, -7, and -9 from the C terminus (26). This signature sequence was shown *in vitro* to interact with *E. coli* BamA (21), likely via the POTRA domains, which, indeed, have been shown to bind peptides derived from the OMP PhoE (13).

Refolded BamA interacted with *E. coli*-derived C-terminal signature sequences, but not with those found in neisserial OMPs, the defining difference being the nature of the penultimate C-terminal amino acid (21). These results are consistent with the observation that

neisserial β-barrel OMPs are not efficiently assembled in *E. coli*. Apparently, despite the fact that the OMP assembly pathway is conserved among the Gram-negatives, the Omp85 machinery is not able to efficiently recognize OMPs from other bacteria indicating that species-specific adaptation has occurred during evolution.

Here, we investigated whether Omp85 homologs from various Gram-negative bacteria are able to substitute each other *in vivo*.

Materials and Methods

Bacterial strains and growth conditions

E. coli strains TOP10F' (Invitrogen), DH5α (laboratory collection), and the BamA-depletion strain AG100ΔyaeT pARAyaeT (24) were grown either on LB agar plates or in liquid LB medium on a shaker at 37˚C, except for complementation assays, when the bacteria were grown at 30˚C. The BamA-depletion strain has the first 1667 nucleotides of the chromosomal *bamA* replaced by a kanamycin-resistance cassette and contains an intact copy of *bamA* on a plasmid under control of an arabinose-inducible promoter (24). When necessary, the media were supplemented with an appropriate antibiotic (25 μg/ml chloramphenicol or 50 μg/ml kanamycin) for plasmid maintenance. Liquid cultures were grown in LB, supplemented with 0.02% arabinose for the BamA-depletion strains, or with 0.4% glucose for pRV2000-HisOmp85-containing strains (see below), to an optical density at 600 nm (OD_{600}) of 0.5, when 0.5 mM of isopropyl-β-D-thiogalactopyranoside (IPTG) was added for 2 h to induce the expression of the plasmid-encoded genes. *N. meningitidis* strain HB-1 (3), an unencapsulated derivative of the serogroup B strain H44/76, and *Neisseria gonorrhoeae* strain FA1090 from our laboratory collection were grown at 37°C in candle jars on GC agar plates (Oxoid), supplemented with Vitox (Oxoid), and, when necessary, with an antibiotic (10 μg/ml chloramphenicol or 80 μg/ml kanamycin). Liquid cultures were obtained by growing *N. meningitidis* for 6 h in tryptic soy broth (Becton Dickinson) in the absence or presence of 1 mM IPTG.

Plasmid constructions

The plasmids and primers used are listed in Tables 1 and 2, respectively. DNA fragments containing *omp85* genes were obtained by PCR using genomic DNA templates from *N. meningitidis* HB-1, *N. gonorrhoeae* FA1090*, Burkholderia mallei* Bogor (provided by the Central Veterinary Institute, Lelystad, The Netherlands), *B. pertussis* Tohama I (provided by the Netherlands Vaccine Institute, Bilthoven, The Netherlands) and *E. coli* DH5α, and cloned into pCRII-TOPO. We used the sequences of the locus tags NMB0182, NGO1801, BMA1547, BP1427 and b0177, respectively, (http://www.tigr.org) to design primers for the PCR amplifications. The primers carried restriction sites allowing for subcloning of the *omp85* genes behind the IPTG-inducible promoter on plasmid pFP10-c-*lbpA*, which is able to replicate in *N. meningitidis* as well as in *E. coli*. As a result of the cloning strategy, the original signal sequences were substituted by that of the lactoferrin-binding protein A (LbpA) of *N. meningitidis* (MNKKHSFPLTLTALAIATAFPSYA). The *Nde*I-*Aat*II fragments, carrying *N. meningitidis*, *N. gonorrhoeae*, and *E. coli omp85* genes were ligated into *Nde*I-*Aat*II-digested pFP10-c-*lbpA*, yielding pFP10-$omp85_{Nm}$, pFP10-$omp85_{Ng}$, and pFP10-$omp85_{Ec}$, respectively. The fragments containing *B. pertussis* and

Table 1. Plasmids used in this study

Plasmid	Characteristics[a]	Reference
pARAyaeT	*Ec bamA* behind an arabinose-inducible promoter	(24)
pRV1300	*Nm omp85::kan* gene replacement construct	(28)
pCRII-TOPO	TA-cloning vector	Invitrogen
pCRII-*omp85*$_{Nm}$	pCRII-TOPO carrying *Nm omp85*	
pFP10-c-*lbpA*	*Neisseria* plasmid containing the *lbpA* gene behind an IPTG-inducible promoter	(20)
pFP10-*omp85*$_{Nm}$	pFP10 carrying *Nm omp85* fused to the fragment of *lbpA* encoding the signal sequence	This study
pFP10-*omp85*$_{Ng}$	pFP10 carrying *Ng omp85* fused to the fragment of *lbpA* encoding the signal sequence	This study
pFP10-*omp85*$_{Bm}$	pFP10 carrying *Bm omp85* fused to the fragment of *lbpA* encoding the signal sequence	This study
pFP10-*omp85*$_{Bp}$	pFP10 carrying *Bp omp85* fused to the fragment of *lbpA* encoding the signal sequence	This study
pFP10-*omp85*$_{Ec}$	pFP10 carrying *Ec bamA* fused to the fragment of *lbpA* encoding the signal sequence	This study
pFP10-$Y_{479}O$	pFP10 carrying a chimera encoding the LbpA signal sequence and amino acids 21-479 of *Ec* BamA fused to amino acids 480-797 of *Nm* Omp85	This study
pFP10-$O_{480}Y$	pFP10 carrying a chimera encoding the LbpA signal sequence and amino acids 22-480 of *Nm* Omp85 fused to amino acids 481-810 of *Ec* BamA	This study
pFP10-$Y_{423}O$	pFP10 carrying a chimera encoding the LbpA signal sequence and amino acids 21-423 of *Ec* Omp85 fused to amino acids 424-797 of *Nm* Omp85	This study
pFP10-$O_{423}Y$	pFP10 carrying a chimera encoding the LbpA signal; sequence and amino acids 22-423 of *Nm* Omp85 fused to amino acids 424-810 of *Ec* Omp85	This study
pEN11-His-Omp85	pFP10-derived plasmid encoding N-terminally His-tagged *Nm* Omp85	Chapter 2
pRV2000	pBR322-based plasmid, encoding *Nm* Omp85 under the control of an IPTG-inducible promoter	(28)
pRV2000-HisOmp85	pRV2000 encoding N-terminally His-tagged *Nm* Omp85	This study

[a] *Ec, E. coli*; *Nm*, *N. meningitidis*; *Ng, N. gonorrhoeae*; *Bm, B. mallei*; *Bp, B. pertussis*

B. mallei omp85 were excised using the *Nde*I site introduced by the forward primers and the *Kpn*I site of pCRII-TOPO and introduced into *Nde*I-*Kpn*I-digested pFP10-*omp85*$_{Ec}$, thereby substituting the major part of *E. coli bamA*, which has a *Kpn*I site in the 3'-region, by the entire heterologous *omp85*, yielding pFP10-*omp85*$_{Bp}$ and pFP10-*omp85*$_{Bm}$, respectively.

Table 2. Primers used in this study. Restriction sites used for cloning are underlined

Primer name	Sequence	Restriction site
BmF	ATCATATGCAACGGCGCCCTTCG	*Nde*I
BmR	ATGACGTCTCAGAACGCCGTCC	
BpF	ATCATATGCCTTCGAGCCCTTTGT	*Nde*I
BpR	ATGACGTCTCAGAAACCCGTGCC	
NmF	ATCATATGCCGACTTCACCATCCA	*Nde*I
NmR	ATGACGTCTTAGAACGTCGTGCC	*Aat*II
EcF	ATCATATGCCGCTGAAGGGTTCGTAGTGAAAGAT	*Nde*I
EcR	ATGACGTCTTACCAGGTTTTACCGATGTTA	*Aat*II
HingeF	CCGTACTTCACGGCAGACGGCGTCAGCCTGGG	
EcNmF	GTAAAAGAGCGCAACACCGGTTCCCTGGATTTGAGCGCG	
NmEcR	CCAAAGTTGAAGCTACCGGTGGAACGTTCGGTCAGACTC	
HingeR	CCCAGGCTGACGCCGTCTGCCGTGAAGTACGG	
Omp85R2	CAAAGAAGGGGATTTCTTTG	
Omp85F3	GGCGGACGTTTCCGTTGGGG	
Omp85F4	ATACCTCGGGCGCGGCAAAC	
Omp85R7	GCCCGGTTCGATGTGCAGGACGAA	
G	TTTGCCGTCTGAACCCTTTAAAATCACAACCGTTGCCGG	

The N- and C-terminal domains of the *N. meningitidis* Omp85 and BamA were swapped resulting in chimeras. Two chimeric *omp85* genes were designed encoding proteins in which the N-terminal and C-terminal domains of *N. meningitidis omp85* and *E. coli bamA* were exchanged within a small region of high homology around the start of the predicted 12-stranded β-barrel (28). The construct designated $Y_{479}O$ encodes a protein carrying the N-terminal part of BamA and the C-terminal part of *N. meningitidis* Omp85, while the $O_{480}Y$ encodes the reverse chimera. The *E. coli* Omp85 homolog BamA was formerly known as YaeT, hence the letter Y in the designations of the chimera. The numbers indicate the most C-terminal amino acid of the Omp85 domain present in the N-terminal part of the chimera, counting the N-terminal signal sequence. For the $Y_{479}O$ construct two overlapping PCR products were made: one using the EcF and HingeR primers and pFP10-$omp85_{Ec}$ as template and the other using the HingeF and NmR primers and pFP10-$omp85_{Nm}$ as template. The purified PCR products were mixed, melted and annealed and combined with EcF and NmR as external primers in a second PCR to obtain the complete chimeric genes. For the $O_{480}Y$ chimera, also two PCR products were generated: one using NmF and HingeR as primers and pFP10-$omp85_{Nm}$ as template, and the other with HingeF and EcR as primers and pFP10-$omp85_{Ec}$ as template. The second PCR was performed using purified PCR fragments and NmF and EcR as external primers. The obtained chimeras were introduced into pCRII-TOPO. The *Nde*I-*Aat*II fragments were subsequently ligated into pFP10-c-*lbpA*, digested with *Nde*I and *Aat*II yielding constructs pFP10-$Y_{479}O$ and pFP10-$O_{480}Y$.

Chimeras designated $Y_{423}O$ and $O_{423}Y$ were constructed to produce hybrid proteins where domain exchange occurred at the C terminus of the predicted POTRA5 domain (12) with the N-terminal domain of the chimera comprising 423 amino-acid residues. To make the $Y_{423}O$ construct, a megaprimer was created using primers EcNmF and Omp85R2, and pFP10-$omp85_{Nm}$ as the template. The purified megaprimer was combined with the EcF primer and pFP10-$omp85_{Ec}$ as the template for a second PCR and the product was cloned into pCRII-TOPO. The chimeric fragment was then introduced into pFP10-$omp85_{Nm}$, using the *Nde*I site

and the *Kpn*I site present in the *N. meningitidis omp85* gene, yielding pFP10-$Y_{423}O$. For the $O_{423}Y$ chimera, megaprimer1 was generated using primers NmEcR and Omp85F3 and pFP10-$omp85_{Nm}$ as the template. For the second PCR, megaprimer1 was combined with the EcR primer and pFP10-$omp85_{Ec}$ as the template. The chimeric fragment obtained was cloned into pCRII-TOPO, yielding pCRII-$O_{423}Ya$. Megaprimer2 was produced using primers Omp85F4 and Omp85R7 and pFP10-$omp85_{Nm}$ as template. Megaprimer2 was then combined with EcR and pCRII-$O_{423}Ya$ as template in a PCR. The resulting PCR product was cloned into pCRII-TOPO, yielding pCRII-$O_{423}Yb$. The missing 5'-part of *omp85* was added through insertion of a *Sal*I-*Not*I fragment of pCRII-$omp85_{Nm}$, a precursor of pFP10-$omp85_{Nm}$, into *Sal*I-*Not*I-restricted pCRII-$O_{423}Yb$, yielding pCRII-$O_{423}Yc$. Finally, an *Nde*I-*Kpn*I fragment of pCRII-$O_{423}Yc$ was ligated into *Nde*I-*Kpn*I-digested pFP10-Ec, yielding pFP10-$O_{423}Y$.

Plasmid pRV2000-HisOmp85 was created by insertion of a *Not*I-*Aat*II fragment, encoding *N. meningitidis* Omp85 with an additional HHHHHHQDF amino-acid sequence between the signal sequence and the N terminus of the mature Omp85 protein from pEN11-His-Omp85 into *Not*I-*Aat*II restricted pRV2000.

Complementation assays

To test whether various Omp85 variants could complement BamA deficiency in *E. coli*, pFP10-based plasmids containing *omp85* variants under the control of an IPTG-inducible promoter were introduced into the BamA-depletion strain, which produces BamA from an arabinose-inducible promoter (24). The bacteria were first plated on LB agar supplemented with 0.02% arabinose and incubated overnight at 30°C to induce the expression of BamA and then streaked on plates without arabinose plus 0.5 mM IPTG and grown for 48 h at 30ºC. Cells were also streaked on plates containing 0.02% arabinose plus or minus IPTG. To evaluate Omp85 complementation in *N. meningitidis*, it was tested whether the chromosomal copy of *N. meningitidis omp85* could be disrupted, while various *omp85* variants were expressed from the pFP10-derived plasmids. To this end, pRV1300 was used as the template to generate a PCR product containing a fragment upstream of *N. meningitidis omp85*, a kanamycin-resistance cassette and a 3'-fragment of *omp85*. The PCR fragment was used to transform HB-1 cells carrying *omp85* variants on a plasmid. Transformations were done in the presence of IPTG and transformants were selected on GC agar plates supplemented with 1 mM IPTG and kanamycin and analyzed by PCR using primer pair G and Omp85R2 that hybridize upstream and in the 3'-fragment of *omp85*.

Cell envelope isolation

To isolate cell envelopes, bacteria from liquid cultures were collected by centrifugation, resuspended in 50 mM Tris-HCl, 5 mM EDTA (pH 8.0) containing protease inhibitor cocktail “Complete” (Roche) and stored overnight at -80°C. After ultrasonic disintegration (3 x 45 s at level 8, output 40%, Branson sonifier 450; Branson Ultrasonics Corporation), unbroken cells were removed by centrifugation (12,000 *g*, 15 min, 4˚C). Cell envelopes were collected by ultracentrifugation (170,000 x *g*, 5 min, 4˚C), dissolved in 2 mM Tris-HCl (pH 7.6) and stored at –20°C.

Urea extraction

Thirty-µl samples of cell envelope preparations were incubated in 1 ml of 20 mM Tris-HCl, 100 mM glycine (pH 7.6), 6 M urea for 1 h at room temperature (RT) while rotating. The insoluble material was separated from the soluble fraction by ultracentrifugation (200,000 x *g*, 1 h, 4˚C). The pellet was dissolved in 30 µl of 2 mM Tris-HCl (pH 7.6), while the solubilized proteins were precipitated from the supernatant with 10% trichloroacetic acid (TCA) and dissolved in 30 µl H_2O.

Trypsin digestion

The trypsin sensitivity of Omp85 variants expressed in *N. meningitidis* was tested by incubating cell envelopes with 50 μg/ml trypsin (Sigma) overnight at RT. The samples were denatured by boiling in sample buffer and analyzed by sodium dodecyl sulfate-polyacrylamide gel electrophoresis (SDS-PAGE) and immunoblotting.

SDS-PAGE and Western blot analysis

Proteins were analyzed by standard denaturing SDS-PAGE or by semi-native SDS-PAGE (28). These latter conditions were obtained by using sample buffer containing only 1% SDS and lacking β-mercaptoethanol and running buffer containing only 0.025% SDS. Furthermore, the gels contained no SDS and electrophoresis was carried out on ice at 12 mA. To enhance epitope recognition on immunoblots, native proteins were denatured within the gels by leaving the gels in steam for 20 min prior to blotting. Proteins were blotted onto nitrocellulose membranes in 25 mM Tris, 192 mM glycine, 0.02% SDS, 20% methanol, using a Biorad wet blotting apparatus. The membranes were blocked for 1 h in phosphate-buffered saline (PBS) (pH 7.6), supplemented with 0.5% non-fat dried milk (Protifar, Nutricia) and 0.1% Tween-20. The blots were incubated for 1 h with primary antibodies, washed and then probed for 1 h with goat anti-rabbit IgG secondary antibodies conjugated with horseradish peroxidase or alkaline phosphatase (Southern Biotechnology Associates Inc.) diluted in the blocking buffer. The signal was visualized with enhanced chemiluminescense (Amersham) in the case of horseradish peroxidase-conjugated secondary antibodies. When alkaline phosphatase-conjugated antibodies were used the blot was incubated in 0.1 M Tris-HCl (pH 9.5), 0.1 mg/ml Nitro Blue Tetrazolium (Sigma-Aldrich), and 0.5 mg/ml of 5-bromo-4-chloro-3-indolyl phosphate (Sigma-Aldrich), until color developed.

BamA was detected with a rabbit antiserum raised against the denatured full-length protein (21). Rabbit antisera against the N-terminal regions (residues 22-464) of *N. meningitidis* Omp85 (α-N-Omp85) and of *N. gonorrhoeae* Omp85 *(*α-Ng-Omp85) and against the C-terminal region (residues 455-797) of *N. meningitidis* Omp85 (α-C-Omp85) were generously provided by R. Judd (University of Montana, USA). In some cases, α-Ng-Omp85 was mixed with α-C-Omp85 producing α-Omp85 mix. The antisera against *E. coli* BamD and BamB were generous gifts of Naoko Yokota and Hajime Tokuda (University of Tokyo, Japan).

To visualize proteins in gels, they were stained with Coomassie Brilliant Blue or with silver (2).

Affinity purification

Cell envelopes of DH5α containing pRV2000-HisOmp85 were extracted with 2% Elugent (Calbiochem) in TBS (20 mM Tris-HCl, 150 mM NaCl, pH 7.4), 5 mM EDTA for 2 h at RT followed by centrifugation (20,800 x *g*, 30 min, RT). The buffer composition of the supernatant was exchanged to TBS, 0.1% Elugent, 20 mM imidazole using PD-10 columns (GE Healthcare). Approximately 0.5-2.0 ml of 50% Ni^{2+}-nitrilotriacetic acid-agarose (Ni^{2+}-NTA) beads (Qiagen) were added to the supernatant followed by incubation at 4°C for 1-2 h while rotating. The beads were allowed to settle by gravity and washed in TBS, 20 mM imidazole, 0.05% *n*-dodecyl-ß-D-maltoside for 1 h at 4°C while rotating. Proteins were eluted in TBS, 200 mM imidazole, 0.05% n-dodecyl-ß-D-maltoside and analyzed by SDS-PAGE and immunoblotting. For immunoblot analysis, fractions were concentrated 10-fold by TCA precipitation.

Results

N. meningitidis and *E. coli* Omp85 homologs cannot substitute each other *in vivo*

To determine whether or not the *E. coli* and *N. meningitidis* Omp85 homologs could substitute each other *in vivo*, a plasmid containing the *bamA* (*omp85*) gene of *E. coli* under control of a *lac* promoter was introduced into *N. meningitidis* strain HB-1. This resulted in IPTG-dependent expression of *bamA* in HB-1 (Figure 1A). As a control, HB-1 was also transformed with a similar plasmid containing *N. meningitidis omp85*. Next, we attempted to disrupt the chromosomal *omp85* copy in the transformants. Correct transformants were easily obtained when *N. meningitidis omp85* was expressed from plasmid. In contrast, PCR analysis showed that the few kanamycin-resistant transformants that were obtained from the cells expressing *bamA* still contained the wild-type copy of *omp85* on the chromosome. Apparently, BamA cannot substitute *N. meningitidis* Omp85. To determine whether BamA was inserted into the neisserial OM, we tested its extractability with urea from these membranes. Correctly inserted OMPs are not usually extracted with urea, as demonstrated for the neisserial porins in Figure 1B. However, the vast majority of BamA present in neisserial cell envelopes was extractable with urea (Figure 1B). Correctly assembled β-barrel domains of OMPs are also usually resistant to proteases. Accordingly, the intact C-terminal β-barrel domain of BamA can be obtained by treating *E. coli* cell envelopes with trypsin (21), whereas endogenous *N. meningitidis* Omp85 produces trypsin-resistant fragments of ~40 and 48 kDa, reactive with α-C-Omp85 in neisserial cell envelopes (Figure 1C, left panel). However, when neisserial cell envelopes containing BamA were treated with trypsin, no protected fragment was found (Figure 1C, right panel), indicating that no part of BamA is properly assembled into the OM. Together, these data demonstrate that BamA, for the most part, is not inserted in the neisserial OM and, therefore, cannot be expected to functionally replace Omp85.

For the reciprocal experiment, we used the *E. coli* BamA-depletion strain AG100ΔyaeT pARAyaeT (24). In this strain, a part of the chromosomal *bamA* gene is replaced by a kanamycin-resistance cassette, whereas an intact copy of *bamA* is located on the pARAyaeT plasmid under an arabinose-inducible promoter. Plasmid pFP10-$omp85_{Nm}$ carrying the *N. meningitidis omp85* gene was introduced into this strain and the cells were grown on plates in the absence of arabinose to deplete the endogenous BamA, while *N. meningitidis* Omp85 synthesis was induced with IPTG. Under these conditions, the strain failed to form colonies (Figure 2A), while in similar conditions a control strain containing *bamA* under IPTG control on pFP10-$omp85_{Ec}$ did grow (data not shown, but see also Figure 4E and 5E). The expression of *N. meningitidis omp85* in response to IPTG induction was confirmed on immunoblots, using cell envelopes of cells grown in the presence of arabinose and IPTG (Figure 2B). Thus, Omp85 of *N. meningitidis* does not function in *E. coli*. The insertion of *N. meningitidis* Omp85 into the *E. coli* OM was assessed by extracting cell envelopes with urea. A substantial portion of the protein was found to be extractable

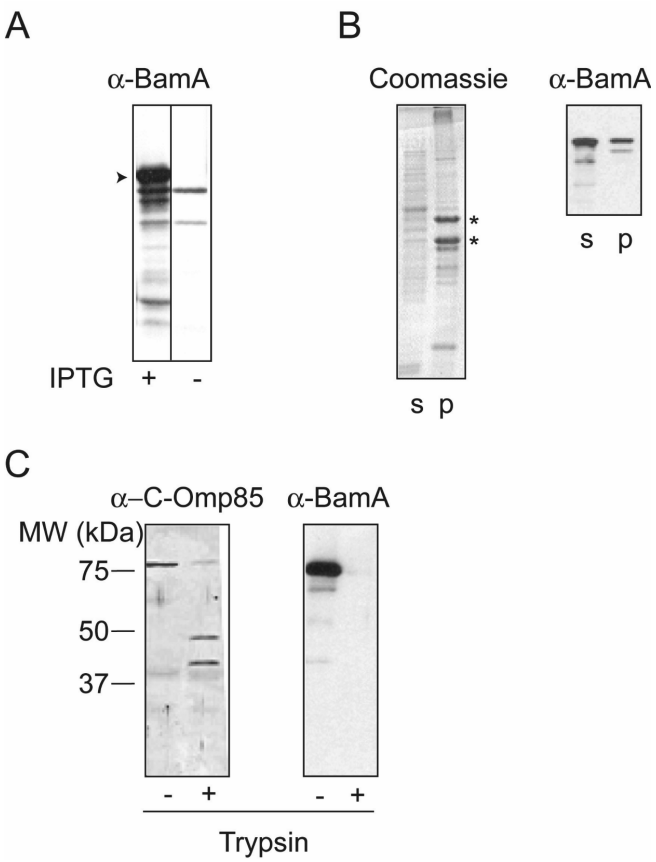

Figure 1

Expression and assembly of BamA in *N. meningitidis*. Samples were analyzed by denaturing SDS-PAGE followed by immunoblotting using the indicated antisera or by Coomassie Brilliant Blue staining. (**A**) Immunoblots of cell envelopes of uninduced (-) or induced (+) HB-1 cells containing pFP10-*omp85*$_{Ec}$ carrying *bamA* under an IPTG-inducible promoter. BamA is indicated with an arrowhead. (**B**) Cell envelopes of HB-1 expressing BamA were extracted with urea and the urea-soluble (s) and -insoluble (p) fractions were analyzed by SDS-PAGE followed by Coomassie Brilliant Blue staining (left panel) or immunoblotting (right panel). Neisserial porins are indicated with asterisks. (**C**) Cell envelopes of HB-1 (left panel) or HB-1 expressing BamA (right panel) were treated with trypsin at RT and processed for immunoblot analysis. The positions of molecular weight marker proteins are shown at the left.

(Figure 2C). As a control, however, we then also tested the extractability of *N. meningitidis* Omp85 from neisserial cell envelopes and found, quite surprisingly, that also in that case a considerable proportion of the protein was solubilized, while the porins were not extracted (Figure 2C). Apparently, Omp85 behaves different from porins in this respect; therefore,

since the results showed that ~half of the protein produced was not extracted from the *E. coli* membranes, our data suggests that *N. meningitidis* Omp85 is at least partially inserted into the *E. coli* membrane.

In *N. meningitidis*, Omp85 forms a high molecular-weight (HMW) complex in the OM, which can be detected by semi-native SDS-PAGE (28; Figure 2D, left panel). HMW complexes of *N. meningitidis* Omp85 were also found in the *E. coli* membrane (Figure 2D, right panel), although they demonstrated a higher electrophoretic mobility. This lower apparent molecular weight of the complex can be explained by the absence in *E. coli* of the RmpM protein, which is part of the HMW Omp85 complex in *N. meningitidis* (Chapter 2). Indeed, in a neisserial *rmpM* mutant, the HMW Om85 complex migrates with an apparent molecular weight (M_r) of 150 kDa (Chapter 2), which is very similar to the M_r of the Omp85 complex in *E. coli* (Figure 2D). Apart from the HMW complex, an unfolded monomeric form of *N. meningitidis* Omp85 was detected in the *E. coli* membranes, while this was not the case in the neisserial membrane preparation (Figure 2D). This difference might be due to less efficient assembly of Omp85 in a heterologous host or, again, by the absence of RmpM, which was shown to stabilize the Omp85 complex in *N. meningitidis* (Chapter 2). Together, this data suggests that at least a proportion of the neisserial Omp85 produced is correctly assembled into the *E. coli* OM.

BamA was shown to be associated with several lipoproteins: BamB, BamC, BamD and BamE (23, 31). A failure to associate with these lipoproteins could possibly explain the lack of function of neisserial Omp85 in *E. coli*. To test this possibility, pRV2000-HisOmp85 encoding *N. meningitidis* Omp85 with a His-tag at the N terminus of the mature protein was introduced into *E. coli* DH5α and expression of the recombinant protein was induced with IPTG. Cell envelopes were extracted with Elugent and the His-tagged Omp85 was affinity purified with Ni^{2+}-NTA beads under native conditions (Figure 2E). As a control, a mock purification was done on cells not producing the His-tagged Omp85. Remarkably, substantial amounts of *E. coli* BamD co-purified with the neisserial Omp85 (Figure 2E). The specificity of the co-purification of BamD was evidenced by its absence in the mock. In contrast to the essential lipoprotein BamD, the non-essential lipoprotein BamB did not co-purify with Omp85 (Figure 2E). The other accessory lipoproteins of the Bam complex could not be assessed since specific antisera were not available. These results enforce the notion that at least a portion of the Omp85 produced in *E. coli* is correctly assembled.

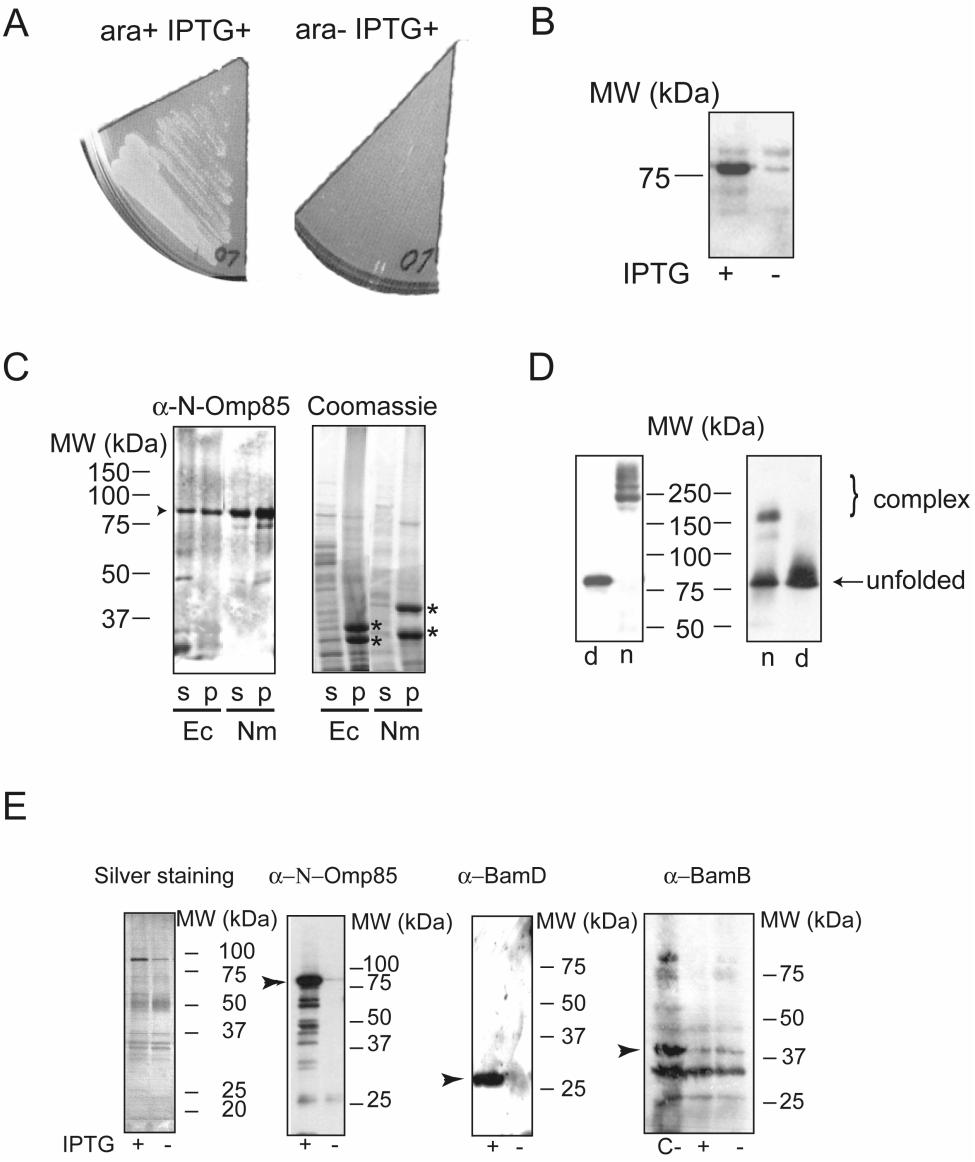
A
ara+ IPTG+
ara- IPTG+
B
MW (kDa)
75
IPTG + -
C
α-N-Omp85
Coomassie
MW (kDa)
150
100
75
50
37
s p s p
Ec Nm
s p s p
Ec Nm
D
MW (kDa)
250
150
100
75
50
d n
n d
complex
unfolded
E
Silver staining
α–N–Omp85
α–BamD
α–BamB
MW (kDa)
100
75
50
37
25
20
IPTG + -
+ -
+ -
C- + -

Figure 2

Expression, assembly, and functionality of *N. meningitidis* Omp85 in *E. coli*. (**A**) Growth of *E. coli* strain AG100ΔyaeT carrying on plasmids *bamA* under an arabinose-inducible promoter and *N. meningitidis omp85* under an IPTG-inducible promoter. The cells were grown on plates containing 0.5 mM IPTG and either or not 0.02% arabinose (ara) as indicated. (**B**) Immunoblot containing cell envelopes of *E. coli* strain AG100ΔyaeT pARAyaeT containing pFP10-$omp85_{Nm}$ grown in LB containing 0.02% arabinose and either or not IPTG to induce expression of *N. meningitidis* Omp85. The blot was probed with α-Omp85 mix. (**C**) Urea extraction of cell envelopes of *E. coli* AG100ΔyaeT pARAyaeT, expressing *N. meningitidis* Omp85 from pFP10-$omp85_{Nm}$ (Ec), and of HB-1 (Nm). Urea-soluble (s) and -insoluble (p) fractions were analyzed by SDS-PAGE and immunoblot analysis with α-N-Omp85 (left panel) or Coomassie Brilliant Blue staining (right panel). An arrowhead indicates Omp85. Porins are indicated with asterisks. (**D**) High molecular weight *N. meningitidis* Omp85 complex in *N. meningitidis* (left panel) and in *E. coli* AG100ΔyaeT pARAyaeT containing pFP10-$omp85_{Nm}$ (right panel). Cell envelopes were analyzed under denaturing (d) or semi-native (n) conditions and probed with α-Omp85 mix. Various Omp85 forms are indicated. (**E**) Co-purification of Bam-complex components with His-tagged *N. meningitidis* Omp85 in *E. coli*. Extracts of cell envelopes of *E. coli* DH5α cells containing pRV2000-HisOmp85, either induced or not with IPTG, were solubilized with detergent, and His-tagged Omp85 with associated proteins was bound to Ni^{2+}-NTA and subsequently eluted. Elution fractions were analyzed by SDS-PAGE followed by silver staining (left panel) or immunoblotting. Immunoblots were performed with 10x concentrated elution fractions and probed with the indicated antisera. As a positive control for BamB detection, cell envelopes derived from strain DH5α were analyzed (C-). The relevant proteins are indicated with arrowheads.

Functionality of chimeras of *N. meningitidis* and *E. coli* Omp85

As described above, the *N. meningitidis* and *E. coli* Omp85 proteins cannot functionally replace each other. To determine which part of the Omp85 proteins could be dictating this species specificity, the N- and C-terminal domains of the *N. meningitidis* Omp85 and BamA were swapped resulting in chimeras. Two sets of chimeras were made. For the first couple, designated $Y_{479}O$ and $O_{480}Y$, the site of the domain exchange was based on a previously proposed topology model, which predicts the presence of a 12-stranded β-barrel in the C-terminal part of Omp85 (28) separated from the POTRA domains by a hinge region (Figure 3A). The site of exchange was chosen just upstream of this β-barrel domain (Figure 3A). However, the recently resolved structure of FhaC, a distant homolog of Omp85, revealed a 16-stranded β-barrel (5), suggesting that also Omp85 might possess a 16-stranded β-barrel and that the predicted hinge region might in fact be part of this barrel. Therefore, another set of chimeras, designated $Y_{423}O$ and $O_{423}Y$, was made, where the domains were swapped directly after the C terminus of POTRA5 (Figure 3A). This latter set of chimeras eliminates the risk that the β-barrel structure would be affected by the domain exchange. The domain exchanges in chimeras $Y_{479}O$ and $O_{480}Y$ were made upstream and downstream, respectively, of residue 480 (Figure 3B). In the chimeras $Y_{423}O$ and $O_{423}Y$, the fusion sites are directly after the residue 423 (Figure 3B).

The chimeric genes were cloned behind an IPTG-inducible promoter and introduced into *N. meningitidis* and *E. coli*. Synthesis of all hybrid proteins was detected in *N. meningitidis* when immunoblots with cell envelopes were probed with appropriate antisera

(Figure 4A). Remarkably, both chimeras comprising the C-terminal region of neisserial Omp85 were expressed to much higher levels than those containing the C-terminal part of BamA, as judged from Coomassie Brilliant Blue staining of gels containing cell envelope preparations (Figure 4B). This higher production might be diagnostic of a better assembly of the former chimeras, as unassembled chimeras would likely be degraded in the periplasm.

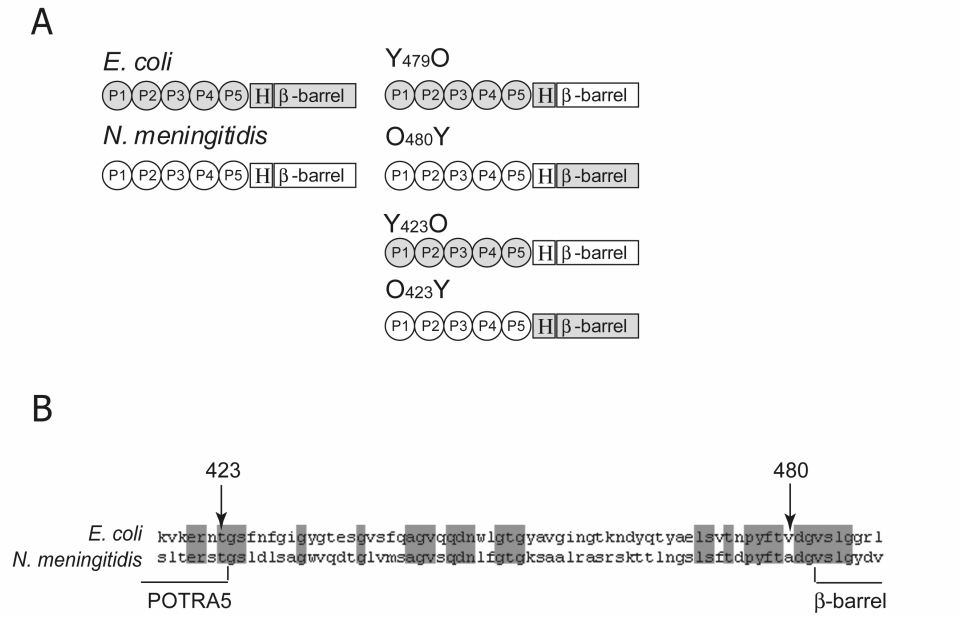

Figure 3

Construction of Omp85 chimeras. (**A**) Schematic representation of the Omp85 proteins of *E. coli* (grey) and *N. meningitidis* (white) and the two sets of chimeric proteins. POTRA domains P1-P5, a 12-stranded β-barrel, and the hinge region in between (H) are specified. (**B**) Partial sequences (residues 417-489, counting the signal sequence) of *N. meningitidis* Omp85 and *E. coli* BamA. Grey boxes indicate identical amino acids. Arrows point at amino-acid residue 423, *i.e.*, the C terminus of POTRA5 (12), and at residue 480, *i.e.*, the N terminus of the predicted 12-stranded β-barrel (28).

The trypsin-sensitivity profile of the different chimeras was consistent with this notion. As before (Figure 1C), trypsin treatment of wild-type membranes yielded two prominent bands of ~40 and 48 kDa, both detected with the α-C-Omp85 antiserum (Figure 4C). Interestingly, the membranes containing the $Y_{423}O$ or $Y_{479}O$ chimera yielded extra 37-kDa and 30-kDa fragments, respectively, which were both reactive with the α-C-Omp85 antiserum (Figure 4C), indicating that C-terminal β-barrel domain of these chimeras was assembled into the OM. In contrast, no trypsin-resistant fragments reactive with the α-BamA antiserum were obtained from cell envelopes containing the $O_{423}Y$ chimera (Figure 4C), suggesting that this chimera was not assembled. The $O_{480}Y$ chimera also was not assembled into the OM, since it was fully extractable with urea from the *N. meningitidis* cell envelopes (Figure 4D). Thus,

only the chimeras containing the C-terminal part of Omp85 appeared to be assembled in the OM. However, the chromosomal copy of *omp85* could not be inactivated during expression of either these or the reverse chimeras indicating that all four chimeras are non-functional in *N. meningitidis*.

In contrast to the control strain expressing BamA from pFP10-*omp85*$_{Ec}$, the *E. coli* BamA-depletion strain expressing chimeras $Y_{479}O$ or $O_{480}Y$ grew significantly worse on plates without arabinose plus IPTG than on plates with arabinose plus IPTG (Figure 4E). The background growth on the plates without arabinose might result from the residual presence of BamA after depletion. Similarly, the chimeras $Y_{423}O$ and $O_{423}Y$ appeared inactive in *E. coli*, since the BamA-depletion strains expressing them did not grow in the presence of IPTG when arabinose was absent (Figure 4E, right panel). However, these strains also grew poorly on plates containing both arabinose and IPTG (data not shown), indicating that the expression of these chimeras is toxic for *E. coli*. This growth defect was temperature dependent. At 37˚C, these strains could be grown in the presence of arabinose and IPTG, and the chimeras $Y_{423}O$ and $O_{423}Y$ produced under these conditions appeared to be inserted into the *E. coli* OM to some extent, since they were only partially extractable with urea (Figure 4F). Nevertheless, neither of the chimeras complemented endogenous BamA in *E. coli*.

Substitution of *N. meningitidis* and *E. coli* Omp85 proteins by other homologs

The absence of functional complementarities between BamA and Omp85 described above could be related to the large evolutionary distance between *E. coli*, belonging to the class of γ-proteobacteria, and *N. meningitidis*, a β-proteobacterium. Therefore, we next investigated whether Omp85 from other β-proteobacteria, *i.e.* those of *Bordetella pertussis*, *Burkholderia mallei* and *Neisseria gonorrhoeae*, could functionally substitute Omp85 in *N. meningitidis*. Strain HB-1 was transformed with plasmids containing these *omp85* genes under *lac* promoter control, and expression of the proteins was evaluated by SDS-PAGE analysis of cell envelopes from transformants grown in the presence of IPTG. The *B. mallei*-derived Omp85 protein (Figure 5A) and the gonococcal one (data not shown) were detectable on Coomassie-stained gels, which may indicate that these proteins are assembled in the OM. In contrast, the *B. pertussis*-derived Omp85 was not detectable (Figure 5A). Next, we tested whether the chromosomal *omp85* gene could be inactivated while the cells were kept in the presence of IPTG. We only succeeded to obtain correct mutants when the gonococcal *omp85* was expressed from plasmid. Thus, apparently, the meningococcal Omp85 protein can be functionally replaced by Omp85 of the closely related species *N. gonorrhoeae* but not by Omp85 of *B. pertussis* or *B. mallei.*

We evaluated also whether the various Omp85 proteins could substitute for *E. coli* BamA. The cross-reactivity of the antibodies raised against neisserial Omp85 with the *B. pertussis* and *B. mallei* homologs allowed us to evaluate the expression of these proteins by Western-blot analysis. These proteins as well as the gonococcal homolog could indeed be detected in the *E. coli* BamA-depletion strain grown in the presence of IPTG (Figure 5B). It is not clear whether the weaker band of *B. mallei* Omp85 is due to lower expression levels or to weaker cross-reactivity with the antiserum. A large proportion of *B. pertussis* Omp85 appears to be degraded in *E. coli* into polypeptides with slightly lower apparent molecular weights (Figure 5B).

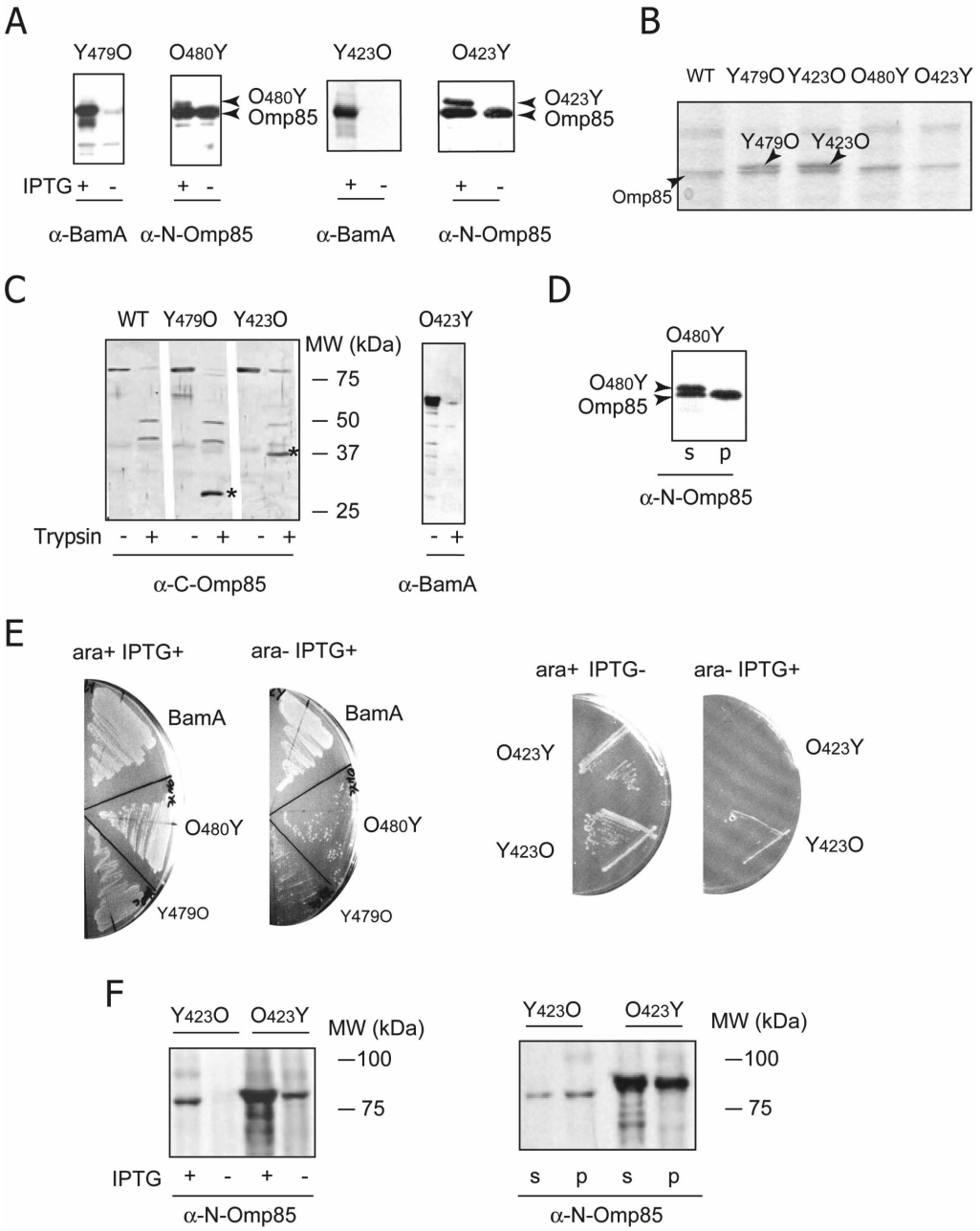
A
Y479O
O480Y
Y423O
O423Y
O480Y
Omp85
O423Y
Omp85
IPTG + - + - + - + -
α-BamA
α-N-Omp85
α-BamA
α-N-Omp85
B
WT Y479O Y423O O480Y O423Y
Y479O Y423O
Omp85
C
WT Y479O Y423O
O423Y
MW (kDa)
— 75
— 50
— 37
— 25
Trypsin - + - + - + - +
α-C-Omp85
α-BamA
D
O480Y
O480Y
Omp85
s p
α-N-Omp85
E
ara+ IPTG+
ara- IPTG+
BamA
O480Y
Y479O
BamA
O480Y
Y479O
ara+ IPTG-
ara- IPTG+
O423Y
Y423O
O423Y
Y423O
F
Y423O O423Y
MW (kDa)
—100
— 75
IPTG + - + -
α-N-Omp85
Y423O O423Y
MW (kDa)
—100
— 75
s p s p
α-N-Omp85

Figure 4

Expression, assembly and functionality of Omp85 chimeras in *E. coli* and in *N. meningitidis*. In all blots, the antisera used are indicated below the panels. (**A**) Immunoblots showing IPTG-induced expression of Omp85/BamA chimeras in *N. meningitidis*. Strain HB-1 containing plasmids encoding the chimeras indicated above the panels was grown with or without IPTG and cell envelopes were isolated and analyzed by SDS-PAGE and immunoblotting. In the case of the chimeras $O_{480}Y$ and $O_{423}Y$, also the endogenous Omp85 is detected with α-N-Omp85. (**B**) Expression of Omp85/BamA chimeras in *N. meningitidis.* Cell envelopes were isolated from strain HB-1 (WT) and its derivatives expressing the Omp85 chimeras indicated after growth in the presence of IPTG and analyzed by SDS-PAGE and staining with Coomassie Brilliant Blue. Positions of *N. meningitidis* Omp85, $Y_{479}O$ and $Y_{423}O$ are indicated by arrowheads. (**C**) Trypsin sensitivity of Omp85 variants in *N. meningitidis* cell envelopes. Cell envelopes of strain HB-1 expressing the Omp85/BamA chimeras indicated were treated with or without trypsin at RT and analyzed on immunoblot. WT indicates the parent strain HB-1. The additional digestion products of $Y_{479}O$ and $Y_{423}O$ are indicated by asterisks. (**D**) Extractability of chimera $O_{480}Y$ from cell envelopes with urea. Cell envelopes of *N. meningitidis* strain HB-1 expressing $O_{480}Y$ were extracted with urea and the urea-soluble (s) and -insoluble (p) fractions were analyzed by SDS-PAGE and immunoblotting. Endogenous Omp85 and $O_{480}Y$ are indicated. (**E**) Growth of *E. coli* strain AG100ΔyaeT carrying on plasmids *bamA* under control of an arabinose-inducible promoter and *omp85* variants under control of an IPTG-inducible promoter. Cells were grown on plates with arabinose and/or IPTG as indicated. (**F**) Expression and membrane insertion of Omp85/BamA chimeras in *E. coli*. Cell envelopes were isolated from *E. coli* strain AG100ΔyaeT pARAyaeT expressing $Y_{423}O$ and $O_{423}Y$ upon IPTG-induction from plasmid. The cell envelopes were directly analyzed by SDS-PAGE and immunoblotting (left panel) or extracted with urea after which the urea-soluble (s) and -insoluble (p) fractions were analyzed (right panel).

This might indicate a folding defect of the protein in the heterologous host. However, the protein was detected in HMW complexes upon semi-native SDS-PAGE (Figure 5C), suggesting that at least some of the protein was correctly assembled into the OM. *N. gonorrhoeae* Omp85 was for a large proportion non-extractable with urea from cell envelopes (Figure 5D) and migrated as a HMW complex in semi-native SDS-PAGE (Figure 5C), demonstrating that this protein is also at least partially inserted in the *E. coli* OM. Assembly of the *B. mallei* Omp85 protein could not reliably be assessed for lack of sufficient reactivity with the available antisera, and no HMW complex was observed on semi-native samples of *E. coli* cells (Figure 5C). Nevertheless, although all three Omp85 variants were expressed and, at least two of them assembled to some extent in the OM, none of them allowed growth of the BamA-depletion strain in the absence of arabinose (Figure 5E), demonstrating that they cannot functionally substitute BamA.

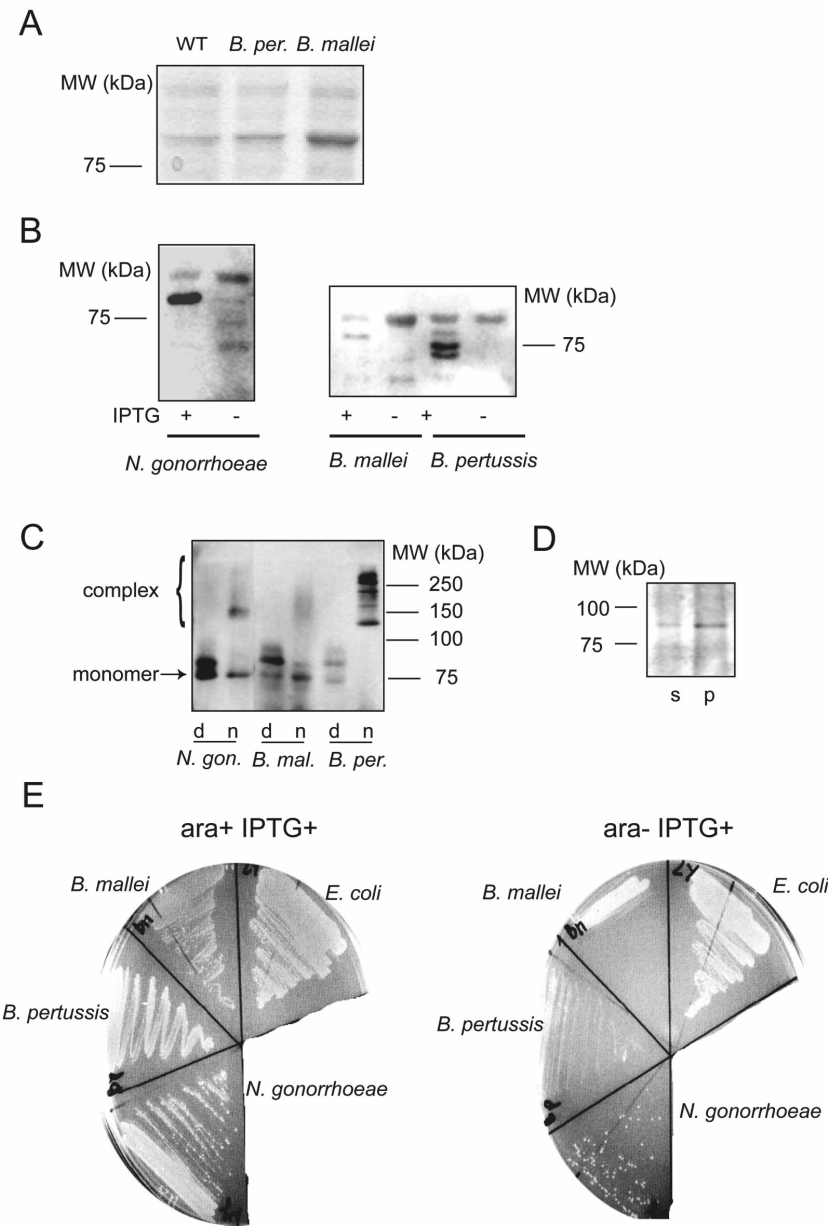
A
WT
B. per.
B. mallei
MW (kDa)
75
B
MW (kDa)
75
IPTG + -
N. gonorrhoeae
MW (kDa)
75
+ - + -
B. mallei
B. pertussis
C
complex
monomer
MW (kDa)
250
150
100
75
d n d n d n
N. gon.
B. mal.
B. per.
D
MW (kDa)
100
75
s p
E
ara+ IPTG+
B. mallei
E. coli
B. pertussis
N. gonorrhoeae
ara- IPTG+
B. mallei
E. coli
B. pertussis
N. gonorrhoeae

Figure 5

Expression, assembly and functionality of *B. mallei*, *B. pertussis* and *N. gonorrhoeae* Omp85 in *N. meningitidis* and in *E. coli*. (**A**) Cell envelopes of *N. meningitidis* strain HB-1 (WT) and its derivatives producing *B. pertussis* (*B. per.*) and *B. mallei* Omp85 proteins from plasmids after growth of the bacteria with IPTG were analyzed by SDS-PAGE and Coomassie Brilliant Blue staining. (**B**) Immunoblots showing IPTG-induced synthesis of the *N. gonorrhoeae*, *B. mallei* and *B. pertussis* Omp85 proteins in *E. coli*. *E. coli* strain AG100ΔyaeT pARAyaeT containing the relevant plasmids was grown in the presence of arabinose and either with or without IPTG, and cell envelopes were isolated and analyzed by SDS-PAGE and Western blotting. For detection, the α-Omp85 mix antiserum was used. (**C**) HMW complex formation by *N. gonorrhoeae* (*N. gon.*), *B. mallei* (*B. mal.*) and *B. pertussis* (*B. per.*) Omp85 in *E. coli*. Cell envelopes of *E. coli* strain AG100ΔyaeT pARAyaeT producing Omp85 variants from plasmid were analyzed by SDS-PAGE either under denaturing (d) or semi-native conditions (n). After electrotransfer to a nitrocellulose membrane, the blot was probed with the α-Omp85 mix antiserum. The positions of HMW Omp85 complexes and unfolded monomers are indicated. (**D**) Extractability of *N. gonorrhoeae* Omp85 from *E. coli* cell envelopes with urea. Cell envelopes of *E. coli* strain AG100ΔyaeT pARAyaeT expressing *N. gonorrhoeae omp85* from plasmid were extracted with urea and the urea-soluble (s) and -insoluble (p) fractions were analyzed by immunoblotting using the α-N-Omp85 antiserum. (**E**) Growth of *E. coli* strain AG100ΔyaeT carrying on plasmid *bamA* under control of an arabinose-inducible promoter and *omp85* derived from the species indicated under control of an IPTG-inducible promoter. The bacteria were grown on plates with arabinose and/or IPTG as indicated.

Discussion

In this work we studied the species-specific functioning of Omp85, the central component of the OMP insertion machinery, which is essential and conserved in Gram-negative bacteria. Remarkably, we found this species specificity to be fairly strict, since even Omp85 homologs within one class of proteobacteria were generally not exchangeable.

Several factors might contribute to the lack of the interchangeability of Omp85 homologs: insufficient assembly of the foreign Omp85 into the OM, an inability to form a fully functional OMP-insertion machinery because the accessory lipoproteins of the Bam complex are not bound, or failure of the heterologous Omp85 to efficiently recognize various OMP substrates.

In *N. meningitidis*, BamA was not assembled into the OM and therefore could obviously not compensate for the absence of neisserial Omp85. In contrast, *N. meningitidis* Omp85 appeared to be inserted into the *E. coli* OM, at least to a substantial extent. Previously, we showed that neisserial OMPs are only poorly inserted into the *E. coli* OM. This defect was related to the nature of the penultimate amino acid of the OMP: in *Neisseria* this residue is almost invariably a positively charged one, whereas in *E. coli* this is only rarely the case (21; Table 3). Replacing the lysine present in this position in the neisserial porin PorA by glutamine greatly enhanced PorA assembly in *E. coli* (21). Omp85 is one of the few neisserial OMPs that does not have a positively charged residue at the penultimate position (Table 3); therefore it might be sufficiently recognized by the Bam complex to be inserted in

the *E. coli* OM. Neisserial Omp85 was even able to associate in the *E. coli* OM with the essential Bam-complex component BamD but not with BamB. This is consistent with the absence of a BamB homolog in *N. meningitidis* (Chapter 2).

Table 3. C-terminal amino acid sequences of selected OMPs of *E. coli*, *N. meningitidis*, *B. mallei* and *B. pertussis*

Protein	Function	Distance from C terminus 10 9 8 7 6 5 4 3 2 1	Accession number
***E. coli* OMPs**			
PhoE	Porin	I V A V G M T Y Q F	AAC73345
OmpC	Porin	I V A L G L V Y Q F	AAC75275
OmpF	Porin	T V A V G I V Y Q F	AAC74015
LamB	Maltoporin	T F G A Q M E I W W	AAC77006
OmpT	Protease	I T T A G L K Y T F	AAC73666
PagP	Lipid A palmitoyl transferase	V Y F A W M R F Q F	AAC73723
Tsx	Nucleoside channel	G G Y L V V G Y N F	AAC73514
FadL	Long-chain fatty acid transporter	L F G T N F N Y A F	AAC75404
Hbp	Autotransporter	A I N A N I R Y S F	CAA11507
Pet	Autotransporter	A I N A N F R Y S F	AAC26634
FhuA	Siderophore receptor	Q V V A T A T F R F	AAC73261
BamA		Q F Q F N I G K T W	b0177
***N. meningitidis* OMPs**			
PorA	Porin	A A S V G L R H K F	NMB1429
PorB	Porin	A G G V G L R H K F	NMB2039
NspA	unknown	E L S A G V R V K F	NMB0663
Opa	Adhesin	E V S L G M R Y R F	NMB0926
Opc	Adhesin	E Y G L R V G I K F	NMB1053
IgA protease	Autotransporter	S G Q I K I Q I R F	NMB0700
App	Autotransporter	S A G I K L G Y R W	NMB1985
FrpB	Siderophore receptor	D V R L G V N Y K F	NMB1988
Omp85		R F Q F Q L G T T F	NMB0182

***Burkholderia mallei* OMPs**			
Porin	Porin OmpF like	A V R A A I R H K F	BMAA1286
Porin	Porin PorA like	D I R I G M R H S F	BMAA0486
OpcP	Porin PorB like	A A T V G L R H R F	BMAA1353
FhuA	Siderophore receptor	T V I A T A K Y N W	BMA1178
FhuA	Siderophore receptor	Q V S L L T T L Q F	BMAA1180
FhuA	Siderophore receptor	S A E L V A T L R F	BMA2036
	Autotransporter	A V Q G S L H W K F	BMAA1263
Omp85		K F Q F Q I G T A F	BMA1547
***Bordetella pertussis* OMPs**			
Porin	porin	A V A V G L R H R F	BP2851
PagP	Lipid A palmitoyl transferase	V L F M F G R W E F	BP3006
Porin	Porin PorA like	A V G V G I R H R F	BP0840
Porin	Porin PorB like	A V A V G L R H R F	BP2851
Iga/BrkA	Autotransporter	S F H A G Y R Y S F	BP3494
Iga/Prn	Autotransporter	T F H A G Y R Y S W	BP1054
IgA protease	Autotransporter	S A N L G L R V A Y	BP0529
SphB1	Autotransporter subtilisin-like protease	Q L S A S L T Y R Y	BP0216
FrpB/hemC	Siderophore receptor	N I K L S I A Q R F	BP0456
FhuA/BfrH	Siderophore receptor	S I K A S L R Y R W	BP1138
FhuA/BfrF	Siderophore receptor	T V L G R V T Y K W	BP0736
FhuA/fauA	Siderophore receptor	N V M L N L R A Q Y	BP2463
FhuA/bfrC	Siderophore receptor	S I S R Y P D I W I	BP3663
OmpQ	Porin	T R F G V M T Q R F	BP3405
Omp85		A F Q F Q I G T G F	BP1427

Thus, despite assembly into the OM and association with at least the other essential Bam complex component, neisserial Omp85 could not functionally replace BamA, possibly because of relatively poor recognition of *E. coli* OMP substrates, making efficient OMP assembly impossible. Of note, we recently showed that *E. coli* OMPs could be assembled in the OM of mitochondria (29). However, this assembly was efficient only when the bacterial OMP was expressed at a low level, whereas large amounts of unfolded protein accumulated in the mitochondria at higher expression conditions. It seems likely that also neisserial Omp85 can handle *E. coli* OMP substrates to some extent. However, due to poor recognition, it cannot deal with the massive amounts of OMPs produced under maximal growth conditions, resulting in the lethal accumulation of periplasmic OMP aggregates. Possibly, functional activity of neisserial Omp85 in *E. coli* could be detected under conditions of slow growth, *i.e.*, when the capacity of the machinery is not so much challenged.

Chimeric proteins, comprising Omp85 domains derived from *N. meningitidis* and *E. coli* were not functional in either host. However, all evidence indicated that the two chimeras containing the C-terminal part of *N. meningitidis* Omp85 were inserted into the neisserial OM, in contrast to those containing the BamA C-terminal region and full-length BamA. These results demonstrate that the β-barrel part of Omp85, which includes the C-terminal signature sequence, contains the species-specific information required for OM insertion.

Since both $Y_{423}O$ and $Y_{480}O$ were inserted, both proteins should contain an intact β-barrel. This indicates that the β-barrel consists of only 12 β-strands, as proposed in the

original topology model (28). Further support for this notion is derived from the tryptic digestion patterns. Trypsin digestion of cell envelopes containing the $Y_{423}O$ chimera yielded a specific fragment with an M_r of 37 kDa, which could correspond to the Omp85-derived part of the hybrid (*i.e.*, the hinge and the β-barrel according to the topology model) with a calculated molecular mass of 40.6 kDa. The boundary between the two segments in the $Y_{423}O$ chimera comprises the sequence KERNT. We previously showed that intact BamA is cleaved by trypsin between K and ERNT (21), so possibly the $Y_{423}O$ chimera is cleaved at the same position. Since the predicted hinge region has a molecular mass of 6.4 kDa and β-barrels are generally highly resistant to proteases, the specific fragment with an M_r of 30 kDa detected in the tryptic digest of cell envelopes containing the $Y_{479}O$ chimera than most likely consists of an intact β-barrel of which the hinge region, derived in this hybrid from BamA, is cleaved off. The boundary of the BamA and Omp85 fragments in the $Y_{479}O$ chimera, however, does not contain a Lys or Arg residue, necessary for trypsin cleavage. Therefore, more information on the exact composition of the tryptic fragments will be necessary to draw definite conclusions regarding the topology model. If, indeed, the β-barrel of Omp85 consists of 12 β-strands, it would mean that different members of the Omp85 superfamily not only differ with respect to the number of POTRA domains they contain, but also with respect to the size of the β-barrel. It should be noted, in this respect, that the β-barrel of another member of this superfamily, YftM of *E. coli*, was suggested to contain only eight β-strands (25).

Trypsin digestion of native Omp85 embedded within the membranes yielded considerably larger fragments than digestion of the $Y_{423}O$ and $Y_{479}O$ chimeras. Therefore, the POTRA domains in the wild-type protein are not fully accessible to the protease, either because of compact folding or because they are shielded by other parts of the Bam complex. The smaller fragments obtained after digestion of the hybrids therefore indicate that the POTRA domains are not properly assembled into the Bam complex, which, amongst others, could be an explanation for the lack of functionality of the hybrids in *N. meningitidis*. The incorrect assembly of these POTRA domains could be due to misfolding or to the failure to interact with other parts of the Bam complex. It seems unlikely that the POTRA domains of *E. coli* BamA cannot fold properly in *N. meningitidis*. Furthermore, since Omp85 expressed in *E. coli* could recruit the endogenous BamD, it seems likely that the BamA-derived POTRA domains of the chimeras can also recruit the neisserial Bam components. Therefore, the misassembly of the POTRA domains of the hybrids may be due to inappropriate interaction with the β-barrel domain. The crystal structure of FhaC, another member of the Omp85 superfamily, showed extensive interactions between the β-barrel and the adjacent POTRA domain (5) and it seems likely that similar extensive interaction occurs between the β-barrel of Omp85 and the POTRA5 domain. Such interaction may not be possible in the hybrids, which would explain the increased protease sensitivity of the hybrids compared to wild-type Omp85. This improper assembly and/or inefficient substrate recognition explain the lack of function of the $Y_{423}O$ and $Y_{479}O$ chimeras in *N. meningitidis*, even although they were inserted into the membrane.

We expected the $Y_{423}O$ and $Y_{479}O$ chimeras to function in *E. coli*. They were expected to insert into the OM, since also the wild-type Omp85 was found to do so and, indeed, $Y_{423}O$ was only partly extractable with urea. These chimeric proteins should have no problem recognizing *E. coli* OMP substrates or recruit accessory Bam components, because they contain the *E. coli* POTRA domains. However, these features were apparently not sufficient to allow for complete functioning. Again, inappropriate interaction between POTRA5 and the β-barrel might explain the lack of function of these hydrids in *E. coli.*

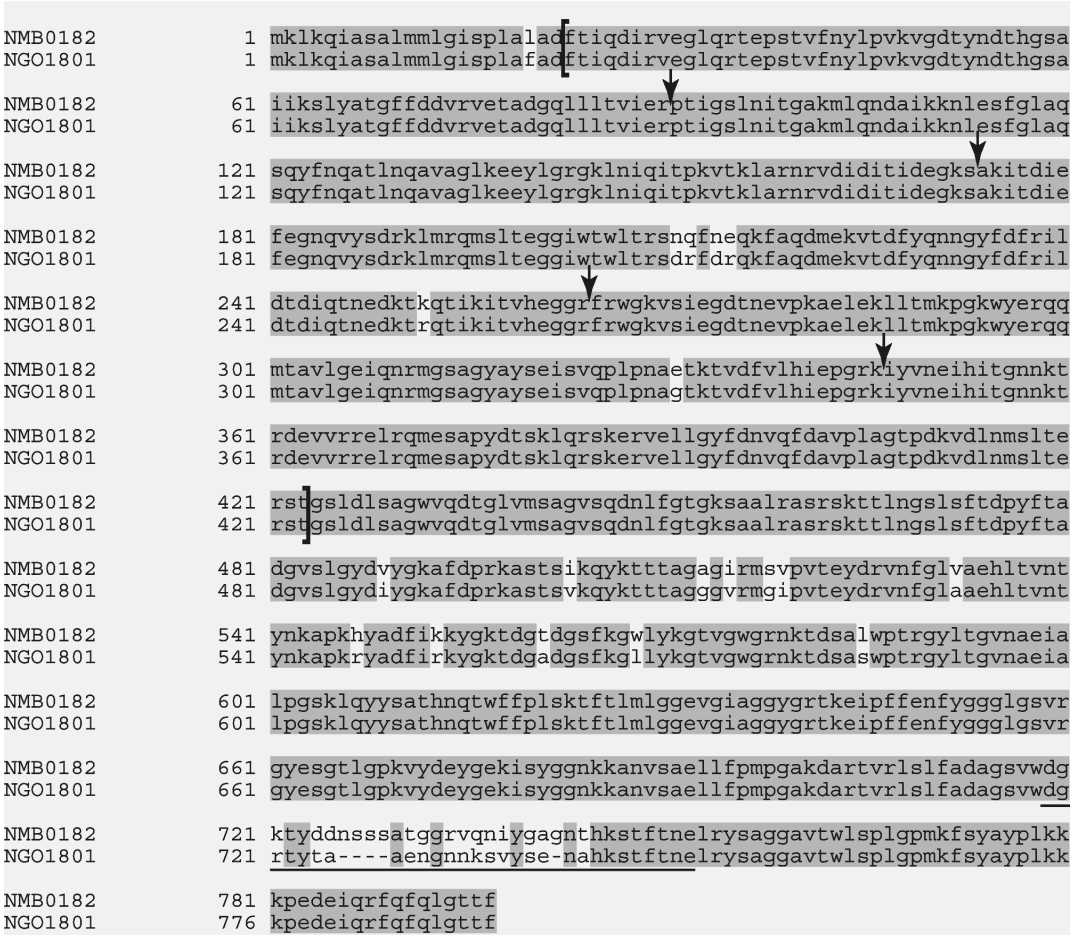

Figure 6

Alignment of amino acid sequences of the mature Omp85 proteins from *N. meningitidis* (NMB0182) and *N. gonorrhoeae* (NGO1801). The region containing the POTRA domains is marked by parentheses, and boundaries of the separate POTRA domains are indicated by arrows in accordance with the structure of the BamA fragment (12). Identical residues are indicated by grey boxes. Amino acids corresponding to the predicted loop 5 in the 12-stranded β-barrel model of Omp85 are underlined (28).

Since *N. meningitidis* and *E. coli* belong to different classes of the proteobacteria, we considered that their Omp85 proteins might be too diverse to allow for interspecies complementation. Therefore, we investigated whether the Omp85 proteins of *B. pertussis, B. mallei* and *N. gonorrhoeae,* which, like *N. meningitidis,* belong to the γ-proteobacteria, could substitute for Omp85 in *N. meningitidis.* However, whereas the Omp85 of *N. gonorrhoeae* is indeed very similar to that of *N. meningitidis* (Figure 6), those from *B. pertussis* and *B. mallei*

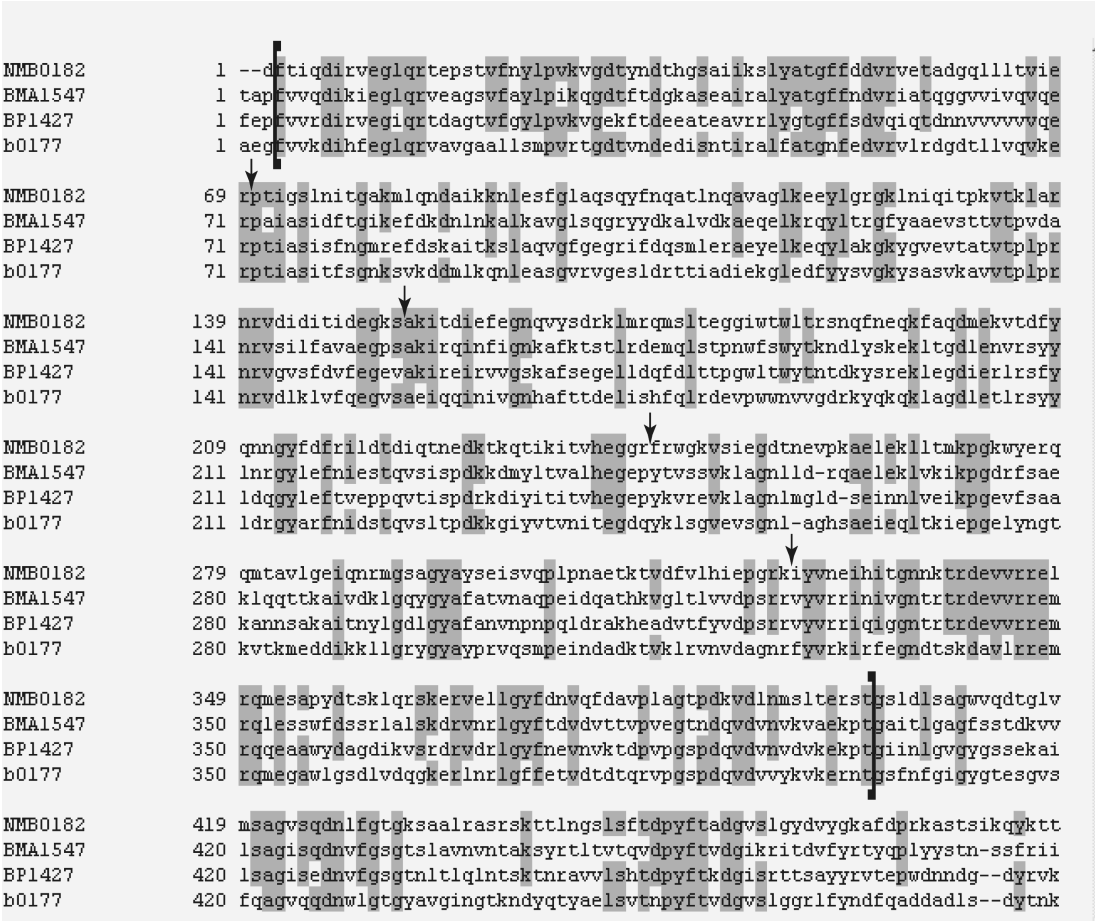

Figure 7

Alignment of amino acid sequences of the N-terminal Omp85 fragments from *N. meningitidis* (NMB0182), *B. mallei* (BMA1547), *B. pertussis* (BP1427), and *E. coli* (b0177). The region containing the POTRA domains is marked by parentheses and boundaries of the separate POTRA domains are indicated by arrows in accordance with the structure of the BamA fragment (12). Identical residues are indicated by grey boxes.

share only slightly more similarity with *N. meningitidis* Omp85 than does the *E. coli* homolog (Table 4, Figure 7). When different Omp85 domains are compared, particularly the POTRA1 and POTRA5 domains seem more similar. Interestingly, the POTRA5 domain was shown to be the only POTRA domain essential for the functioning of *N. meningitidis* Omp85 (4). We also compared the Omp85 substrates in the different species (Table 3). Substrate recognition by Omp85 is for an important part mediated by the C-terminal signature sequence of OMPs (21). Inspection of a number of OMP sequences of *B. pertussis* and *B. mallei* showed that these OMPs also often, but not as consistently as the *N. meningitidis* OMPs, contain a

positively charged residue at the -2 position from the C terminus. This observation, together with the relatively high conservation of the essential POTRA5 domain sequence made us anticipate that the Omp85 proteins of these species might function in *N. meningitidis*. However, they did not. Their higher expression levels might indicate that the *B. mallei* and *N. gonorrhoeae* Omp85 homologs were assembled into *N. meningitidis* OM. However, only the Omp85 protein of *N. gonorrhoeae* was functional, while the more distant *B. mallei* Omp85 homolog was not. We could not further assess the assembly of *B. mallei* Omp85 into the neisserial OM, because specific antisera were not available.

Table 4. Identity/similarity comparison of Omp85 proteins and their fragments. Mature proteins, the regions containing all five POTRA domains and separate POTRA domains were compared using the BLAST engine for two sequences (www.ncbi.nlm.nih.gov). POTRA domains were taken from ref. 4. The comparisons were done relative to *N. meningitidis* Omp85 (A) or *E. coli* BamA (B)

A

Omp85	Mature protein	All POTRAs	POTRA1	POTRA2	POTRA3	POTRA4	POTRA5
B. mallei	37/58%	39/62%	53/73%	35/59%	32/55%	32/58%	53/76%
B. pertussis	36/57%	37/61%	47/72%	38/59%	33/58%	23/48%	49/72%
E. coli	33/51%	33/55%	45/58%	34/57%	26/46%	31/57%	40/64%
N. gonorrhoeae	95/97%	98/99%	100/100%	100/100%	94/98%	98/98%	100/100%

B

Omp85	Mature protein	All POTRAs	POTRA1	POTRA2	POTRA3	POTRA4	POTRA5
B. mallei	37/53%	46/62%	50/65%	37/51%	53/67%	39/62%	50/65%
B. pertussis	35/51%	40/60%	37/60%	38/54%	42/66%	32/53%	50/68%
N. meningitidis	33/51%	33/55%	45/58%	34/57%	26/46%	31/57%	40/64%
N. gonorrhoeae	33/51%	33/55%	45/58%	34/57%	25/46%	30/56%	40/64%

In *E. coli*, the *B. mallei, B. pertussis* and *N. gonorrhoeae* Omp85 homologs were not functional, even though at least two of them appeared to be assembled into the OM. Insufficient substrate recognition is again the most likely explanation for their lack of functionality.

There are several protein insertion/translocation machineries in bacteria. The machineries are ancient and are highly conserved, but nevertheless, are not always able to handle substrates from other species. For example, the Sec machinery, which translocates unfolded proteins across the IM of bacteria, was shown to accept foreign signal peptides (11, 18). Nevertheless, its preference for cognate signal peptides has been described (16). Similarly, one of the other systems known to translocate at least some heterologous proteins less efficiently than the endogenous ones is the Tat system, which translocates folded substrates across the IM. It has been reported, for example, that the Tat system of *E. coli* translocates the periplasmic glucose-fructose oxidoreductase precursor of *Zymomonas mobilis*, another Gram-negative bacterium, across the IM only when it carries a signal peptide derived from *E. coli* (1). Therefore, the species-specific functioning of Omp85, shown in this work, is not a unique particularity of the OMP insertion machinery.

Acknowledgements

We offer our special thanks to Christian Andersen for providing the *E. coli* AG100ΔyaeT pARAyaeT strain, to Naoko Yokota and Hajime Tokuda for the generous gift of antisera against *E. coli* BamD and BamB, and to Ralph Judd for providing the anti-Omp85 sera. This work was supported by the Netherlands Research Councils for Chemical Sciences (CW) and Earth and Life Sciences (ALW) of the Netherlands Organization for Scientific Research (NWO).

References

1. **Blaudeck, N., G. A. Sprenger, R. Freudl, and T. Wiegert.** 2001. Specificity of signal peptide recognition in Tat-dependent bacterial protein translocation. J. Bacteriol. **183:**604-610.
2. **Blum, H., H. Beier, H. J. Gross.** 1987. Improved silver staining of plant proteins, RNA and DNA in polyacrylamide gels. Electrophoresis **8:**93-99.
3. **Bos, M. P., and J. Tommassen.** 2005. Viability of a capsule- and lipopolysaccharide-deficient mutant of *Neisseria meningitidis*. Infect. Immun. **73:**6194-6197.
4. **Bos, M. P., V. Robert, and J. Tommassen.** 2007. Functioning of outer membrane protein assembly factor Omp85 requires a single POTRA domain. EMBO Rep. **8:**1149-1154.
5. **Clantin, B., A. S. Delattre, P. Rucktooa, N. Saint, A. C. Méli, C. Locht, F. Jacob-Dubuisson, and V. Villeret.** 2007. Structure of the membrane protein FhaC: a member of the Omp85-TpsB transporter superfamily. Science **317:**957-961.
6. **Doerrler**, **W. T., and C. R. H. Raetz.** 2005. Loss of outer membrane proteins without inhibition of lipid export in an *Escherichia coli* YaeT mutant. J. Biol. Chem. **280:**27679-27687.
7. **Dong, C., K. Beis, J. Nesper, A. L. Brunkan-Lamontagne, B. R. Clarke, C. Whitfield, and J. H. Naismith.** 2006. Wza the translocon for *E. coli* capsular polysaccharides defines a new class of membrane protein. Nature **444:**226-229.
8. **Driessen, A. J., and N. Nouwen.** 2008. Protein translocation across the bacterial cytoplasmic membrane. Annu. Rev. Biochem. **77:** 643-667.
9. **Gatzeva-Topalova, P. Z., T. A. Walton, and M. C. Sousa.** 2008. Crystal structure of YaeT: conformational flexibility and substrate recognition. Structure **16:**1873–1881.
10. **Gentle, I., K. Gabriel, P. Beech, R. Waller, and T. Lithgow.** 2004. The Omp85 family of proteins is essential for outer membrane biogenesis in mitochondria and bacteria. J. Cell Biol. **164:**19-24.
11. **Gray, G. L.**, **J. S. Baldridge**, **K. S. McKeown**, **H. L. Heyneker**, **and C. N. Chang.** 1985. Periplasmic production of correctly processed human growth hormone in *Escherichia coli*: natural and bacterial signal sequences are interchangeable. Gene **39:**247-254.
12. **Kim, S., J. C. Malinverni, P. Sliz, T. J. Silhavy, S. C. Harrison, and D. Kahne.** 2007. Structure and function of an essential component of the outer membrane protein assembly machine. Science **317:**961-964.
13. **Knowles, T. J., M. Jeeves, S. Bobat, F. Dancea, D. McClelland, T. Palmer, M. Overduin, and I. R. Henderson.** 2008. Fold and function of polypeptide transport-associated domains responsible for delivering unfolded proteins to membranes. Mol. Microbiol. **68:**1216-1227.
14. **Koebnik, R., K. P. Locher, and P. Van Gelder.** 2000. Structure and function of bacterial outer membrane proteins: barrels in a nutshell. Mol. Microbiol. **37:**239-253.
15. **Kozjak, V., N. Wiedemann, D. Milenkovic, C. Lohaus, H. E. Meyer, B. Guiard, C. Meisinger, and N. Pfanner.** 2003. An essential role of Sam50 in the protein sorting and assembly machinery of the mitochondrial outer membrane. J. Biol. Chem. **278:**48520-48523.
16. **Lam, S. L., S. Kirby, and A. B. Schryvers.** 2003. Foreign signal peptides can constitute a barrier to functional expression of periplasmic proteins in *Haemophilus influenzae*. Microbiology **149:**3155–3164.
17. **Malinverni, J. C., J. Werner, S. Kim, J. G. Sklar, D. Kahne, R. Misra, and T. J. Silhavy.** 2006. YfiO stabilizes the YaeT complex and is essential for outer membrane protein assembly in *Escherichia coli*. Mol. Microbiol. **61:**151-164.
18. **Meens, J., E. Frings, M. Klose, and R. Freudl.** 1993. An outer membrane protein (OmpA) of *Escherichia coli* can be translocated across the cytoplasmic membrane of *Bacillus subtilis*. Mol. Microbiol. **9:**847-855.
19. **Paschen, S. A., T. Waizenegger, T. Stan, M. Preuss, M. Cyrklaff, K. Hell, D. Rapaport, and W. Neupert.** 2003. Evolutionary conservation of biogenesis of β-barrel membrane proteins. Nature **426:**862-866.

20. **Pettersson, A., J. Kortekaas, V. E. Weynants, P. Voet, J. T. Poolman, M. P. Bos, and J. Tommassen.** 2006. Vaccine potential of the *Neisseria meningitidis* lactoferrin-binding proteins LbpA and LbpB. Vaccine **24:**3545-3557.
21. **Robert, V., E. B. Volokhina, F. Senf, M. P. Bos, P. Van Gelder, and J. Tommassen.** 2006. Assembly factor Omp85 recognizes its outer membrane protein substrates by a species-specific C-terminal motif. PLoS Biol. **4:**e377.
22. **Sánchez-Pulido, L., D. Devos, S. Genevrois, M. Vicente, and A. Valencia.** 2003. POTRA: a conserved domain in the FtsQ family and a class of β-barrel outer membrane proteins. Trends Biochem. Sci. **28:**523-526.
23. **Sklar, J. G., T. Wu, L. S. Gronenberg, J. C. Malinverni, D. Kahne, and T. J. Silhavy.** 2007. Lipoprotein SmpA is a component of the YaeT complex that assembles outer membrane proteins in *Escherichia coli*. Proc. Natl. Acad. Sci. U S A **104:**6400-6405.
24. **Stegmeier, J. F., and C. Andersen.** 2006. Characterization of pores formed by YaeT (Omp85) from *Escherichia coli*. J. Biochem. (Tokyo) **140:**275-283.
25. **Stegmeier, J. F., A. Glück, S. Sukumaran, W. Mäntele, and C. Andersen.** 2007. Characterisation of YtfM, a second member of the Omp85 family in *Escherichia coli*. Biol. Chem. **388:**37-46.
26. **Struyvé, M., M. Moons, and J. Tommassen.** 1991. Carboxy-terminal phenylalanine is essential for the correct assembly of a bacterial outer membrane protein. J. Mol. Biol. **218:**141-148.
27. **Tashiro, Y., N. Nomura, R. Nakao, H. Senpuku, R. Kariyama, H. Kumon, S. Kosono, H. Watanabe, T. Nakajima, and H. Uchiyama.** 2008. Opr86 is essential for viability and is a potential candidate for a protective antigen against biofilm formation by *Pseudomonas aeruginosa*. J.Bacteriol. **190:**3969-3978.
28. **Voulhoux, R., M. P. Bos, J. Geurtsen, M. Mols, and J. Tommassen.** 2003. Role of a highly conserved bacterial protein in outer membrane protein assembly. Science **299:**262-265.
29. **Walther, D. M., D. Papic, M. P. Bos, J. Tommassen, and D. Rapaport.** 2009. Signals in bacterial β-barrel proteins are functional in eukaryotic cells for targeting to and assembly in mitochondria. Proc. Natl. Acad. Sci. U S A **106:**2531-2536.
30. **Werner, J., and R. Misra.** 2005. YaeT (Omp85) affects the assembly of lipid-dependent and lipid-independent outer membrane proteins of *Escherichia coli*. Mol. Microbiol. **57:**1450-1459.
31. **Wu, T., J. Malinverni, N. Ruiz, S. Kim, T. J. Silhavy, and D. Kahne.** 2005. Identification of a multicomponent complex required for outer membrane biogenesis in *Escherichia coli.* Cell **121:**235-245.

Chapter 5

Purification and structural characterization of the Omp85 proteins of *N. meningitidis* and *E. coli* and their sub-domains

Elena B. Volokhina[1], Lucy Rutten[2], Freya Senf[1], Patrick Van Gelder[3], Piet Gros[2], Martine P. Bos[1] and Jan Tommassen[1]

[1] Department of Molecular Microbiology and Institute of Biomembranes, Utrecht University, Utrecht, The Netherlands.

[2] Department of Crystal and Structural Chemistry, Bijvoet Center for Biomolecular Research, Utrecht University, Utrecht, The Netherlands.

[3] Department of Molecular and Cellular Interactions, Flanders Interuniversity Institute for Biotechnology (VIB), Free University Brussels, Brussels, Belgium.

Part of the results in this chapter has been published:
Robert, V., E. B. Volokhina, F. Senf, M. P. Bos, P. Van Gelder, and J. Tommassen. 2006. Assembly factor Omp85 recognizes its outer membrane protein substrates by a species-specific C-terminal motif. PLoS Biol. **4:**e377.

Abstract

The Omp85 protein is essential for the insertion and assembly of bacterial outer membrane proteins. Its exact role and functional mechanism remain enigmatic. In this work we have developed methods to obtain large quantities of the Omp85 proteins of *N. meningitidis* and *E. coli* as well as of sub-domains thereof. The full-length proteins were produced in inclusion bodies and folded into their native conformation *in vitro*. An initial characterization showed that these proteins form oligomers *in vitro*, which, in the case of the *E. coli* homolog, could be visualized by electron microscopy as donut-like structures with an apparent central cavity. Protease-digestion experiments confirmed the two-domain model of Omp85 and yielded a protease-resistant C-terminal fragment that was purified in the case of the *E. coli* protein and shown by circular dichroism spectroscopy to have a high β-sheet content, consistent with its proposed integral outer membrane location. The presumed periplasmic N-terminal fragments of both Omp85 proteins were produced separately and appeared to have mutually different properties. The *N. meningitidis* Omp85 fragment formed inclusion bodies and had to be folded *in vitro*, whereas the *E. coli* Omp85 fragment remained soluble and could be purified in its native form from the lysate. Initial crystallization trials yielded crystals for several of the proteins produced, which were, however, of insufficient quality to solve the structures.

Introduction

Omp85 is an essential protein, responsible for outer membrane protein (OMP) insertion and assembly in Gram-negative bacteria. The function of Omp85 was initially characterized in *Neisseria meningitidis*, where Omp85-depleted bacteria showed impaired assembly of all OMPs examined (26). Later, Omp85 was described as essential and indispensable for OMP biogenesis also in *Escherichia coli* and *Pseudomonas aeruginosa* (5, 25, 27, 28) and, strikingly, in mitochondria (8, 12, 16). In *E. coli*, Omp85 was formerly known as YaeT and it was recently re-named BamA (for β-barrel assembly machinery component A). For convenience, we will use $Omp85_{Nm}$ and $Omp85_{Ec}$ to designate the *N. meningitidis* and *E. coli* Omp85 homologs, respectively, in this and the next chapter. $Omp85_{Ec}$ is associated with at least four lipoproteins: BamB (formerly known as YfgL), BamC (NlpB), BamD (YfiO), and BamE (SmpA) (21, 28). In *N. meningitidis*, we found $Omp85_{Nm}$ associated with three of these lipoproteins, i.e. BamC, BamD, and BamE, and with a major outer membrane (OM)-associated protein known as Reduction-modifiable protein M (RmpM) (Chapter 2). Similar to Omp85, BamD (also known as ComL in *Neisseria*) is essential and important for OMP assembly in both *E. coli* and in *N. meningitidis*, while the roles of the other three lipoproteins and RmpM in OMP assembly are less pronounced (14, 21, 28, Chapter 2). The Omp85 proteins in Gram-negative bacteria are predicted to consist of two domains: an N-terminal periplasmic domain and a C-terminal β-barrel domain embedded in the membrane (26). The periplasmic domain was predicted to contain five repeated polypeptide-transport-associated (POTRA) domains (18). Recently, the structure of an N-terminal fragment containing the first four POTRA domains of $Omp85_{Ec}$ was reported (10). These POTRA domains share a similar structure: a 3-stranded β-sheet overlaid with two antiparallel α-helices and together form a fishhook-like shape (10). Later, a structure of the same fragment but in an extended conformation was presented (7). The differences between two structures indicate conformational flexibility in the N-terminal region of $Omp85_{Ec}$ between POTRA2 and POTRA3. The relative importance of distinct POTRA domains for Omp85 function and viability of the cell was shown by studying mutants, expressing mutant Omp85 variants in *N. meningitidis* and *E. coli* (2, 10). Nuclear magnetic resonance studies revealed binding of $Omp85_{Ec}$ POTRA domains to synthetic peptides derived from the canonical $Omp85_{Ec}$ substrate PhoE, indicating that POTRA domains are involved in interaction with substrate proteins (11). No structure is available so far of the membrane-embedded part of Omp85. Bacterial Omp85 proteins were predicted to contain a 12-stranded β–barrel at the C terminus (26), but experimental evidence to support this model is still lacking. Of note, the crystal structure of the membrane-embedded part of *Bordetella pertussis* FhaC, a distantly related member of the Omp85 superfamily involved in protein secretion across the OM, showed a 16-stranded, rather than a 12-stranded β-barrel (3). This indicates that Omp85 might contain a 16-stranded β-barrel as well. The $Omp85_{Nm}$ β-barrel domain was shown to be essential and could not be replaced by another neisserial β-barrel of a similar size (2), demonstrating that it not simply functions as a membrane anchor for the POTRA domains.

These studies provided valuable information about structure-function relationships of various domains in Omp85. Nevertheless, understanding of the mechanism of OMP insertion is still limited. Insight into the structural, biochemical and biophysical properties of purified Omp85 molecules *in vitro* could significantly increase our understanding of their function. Previously, it was shown in our group that the purified $Omp85_{Ec}$, reconstituted in planar lipid bilayers, forms pores and that it specifically interacts with *E. coli* OMPs but not with an OMP from *N. meningitidis*. The interaction was monitored as a change in pore activity upon addition of OMPs or their C-terminal peptides (17). In this work, we purified the complete

Omp85 proteins and separate sub-domains thereof from both *E. coli* and *N. meningitidis* to enable their structural and functional characterization.

Materials and Methods

Bacterial strains and growth conditions

E. coli strains TOP10F' (Invitrogen), DH5α (laboratory stock), BL21(DE3) (Novagen) and BL21 Star™ (DE3) (Novagen) were grown either on LB/agar plates or in liquid LB medium on a shaker at 37°C in the presence of 100 μg/ml of ampicillin or 50 μg/ml of kanamycin if necessary for plasmid maintenance. *N. meningitidis* strains HB-1 (1) and MC58 from laboratory stock were grown at 37°C in candle jars on GC agar plates (Oxoid) supplemented with 2% Vitox (Oxoid) or as liquid cultures in tryptic soy broth (TSB) (Becton Dickinson).

Plasmid constructions

DNA fragments encoding mature $Omp85_{Nm}$ and $Omp85_{Ec}$ or their N-terminal domains (Nt-$Omp85_{Nm}$ and Nt-$Omp85_{Ec}$) were obtained by PCR and cloned into pCRII-TOPO (Invitrogen). The primers that were used (Table 1) carried restriction sites for further subcloning into expression vectors. *N. meningitidis omp85* without its signal sequence-encoding part was PCR amplified from genomic DNA of strain MC58 using primers Omp85F and Omp85R and subcloned via pCRII-TOPO into pET11a (Novagen) after *Nde*I/*Bam*HI restriction, producing pET11a-Δss$Omp85_{Nm}$. The pET11ΔssyaeT plasmid carrying *bamA* of *E. coli* was constructed before in a similar manner (17). The gene fragment encoding Nt-$Omp85_{Nm}$ was obtained by PCR using pET11a-Δss$Omp85_{Nm}$ as the template and primers EV5 and EV6. These primers contained *Nde*I and *Xho*I restrictions sites, respectively, which allowed subcloning into the pET26b vector (Novagen), yielding pET26b-Nt-$Omp85_{Nm}$. The resulting protein contained 460 amino acids of mature $Omp85_{Nm}$ with a C-terminal 6xHis-tag. The gene fragment encoding the N-terminal 460 amino acids of mature $Omp85_{Ec}$ was PCR amplified using pET11ΔssyaeT as the template and the primers EV7 and EV8. These primers contained *Nde*I and *Bam*HI sites, respectively, for subcloning into pET11a yielding pET11a-Nt-$Omp85_{Ec}$.

Table 1. Primers used in this study. The restriction sites used for cloning are underlined and restriction enzymes are indicated

Primer	Sequence	Restriction site
Omp85F	ATGC<u>CATATG</u>GACTTCACCATCCAAGAC	*Nde*I
Omp85R	ATCG<u>GGATCC</u>TTAGAACGTCGTGCCGAGTTG	*Bam*HI
EV5	AT<u>CATATG</u>GACTTCACCATCC	*Nde*I
EV6	AT<u>CTCGAG</u>GTCTGCCGTGAAG	*Xho*I
EV7	GCTA<u>CATATG</u>GAAGGGTTCGTAGTG	*Nde*I
EV8	AT<u>GGATCC</u>TTAATCTACGGTGAAGTACGG	*Bam*HI

Expression of recombinant Omp85 proteins

Strain BL21(DE3) containing pET11a-Δss$Omp85_{Nm}$ or pET11a-Nt-$Omp85_{Ec}$ and strain BL21 Star™ (DE3) containing pET11ΔssyaeT or pET26b-Nt-$Omp85_{Nm}$ were used to produce proteins. The cells were grown to an OD_{600} of 0.7, when 1 mM isopropyl-β-D-

thiogalactopyranoside (IPTG) was added to induce the expression of the plasmid-encoded genes. After 90 min of induction, cells were harvested by centrifugation and frozen at –20°C.

Protein isolation

Bacterial cell pellets were resuspended in 10 mM Tris-HCl (pH 8.0), 3 mM EDTA, supplemented with protease inhibitor cocktail "Complete" (Roche) and disrupted by sonication (3 x 5 min at level 8, output 40%, Branson sonifier 450; Branson Ultrasonics Corporation). The inclusion bodies formed were collected by centrifugation (2000 *g*, 10 min, 4°C), and solubilized in 8 M urea, 20 mM Tris-HCl (pH 8.0), 100 mM glycine. The remaining insoluble material and membranes were removed by ultracentrifugation (100,000 *g*, 1 h, 4°C). The preparations obtained contained 5 mg/ml $Omp85_{Nm}$, 20 mg/ml Nt-$Omp85_{Nm}$ and 2.5 mg/ml $Omp85_{Ec}$ as estimated by UV absorption measurements or using the Pierce protein assay kit (Pierce Biotechnology). The yield per 1-liter culture was 25 mg for $Omp85_{Nm}$, 100 mg for Nt-$Omp85_{Nm}$ and 12.5 mg for $Omp85_{Ec}$, respectively. Nt-$Omp85_{Ec}$ did not form inclusion bodies and was produced as a soluble protein and purified as described in the following paragraph.

In vitro folding and purification of proteins

Refolding of full-length Omp85 proteins was initiated by 10-fold dilution of solubilized inclusion bodies in refolding buffer and incubation overnight at 4°C. The refolding buffer for $Omp85_{Nm}$ contained 0.5% (w/v) lauryldimethylamine-oxide (LDAO), 55 mM Tris-HCl (pH 8.2), 0.44 M L-arginine, 1.1 M guanidine, and 21 mM NaCl. $Omp85_{Ec}$ was refolded in 0.5% (w/v) n-dodecyl-N,N-dimethyl-1-ammonio-3-propanesulfonate (SB-12) (Fluka) and 20 mM Tris-HCl as described (17) except that the pH was increased to pH 8.5 to allow more efficient binding to the Q-Sepharose column during purification. Prior to use, SB-12 was dissolved in methanol/chloroform (1:1) and purified using an Al_2O_3 column.

Nt-$Omp85_{Nm}$ was refolded by 20-fold dilution of solubilized inclusion bodies in 5 mM phosphate buffer (pH 7.4) supplemented with 0.2% SB-12 and incubation overnight at room temperature (RT).

$Omp85_{Ec}$ and its tryptic fragment (Ct-$Omp85_{Ec}$), obtained as described below, were purified by anion-exchange chromatography on a Q-Sepharose column (Pharmacia), equilibrated with 20 mM Tris-HCl (pH 8.5), supplemented with 0.06% n-decylpentaoxyethylene ($C_{10}E_5$) or 0.06% LDAO. The proteins were eluted with a linear gradient of 0-500 mM NaCl in the equilibration buffers. The final preparations yielded 4.5 mg of purified $Omp85_{Ec}$ and 1.5 mg of Ct-$Omp85_{Ec}$ per 1-liter culture as estimated by UV absorption measurement.

Cells expressing Nt-$Omp85_{Ec}$ were harvested by centrifugation (2000 *g*, 20 min, 4°C), resuspended in 10 mM Tris-HCl (pH 8.0), 3 mM EDTA, supplemented with protease inhibitor cocktail "Complete" (Roche) and homogenized by sonication (2 x 5 min at level 7, output 40%, Branson sonifier 450). The homogenate was centrifuged twice (700 *g*, 10 min, 4°C and 2500 *g*, 2 h, 4°C) and the supernatant was passed through a 0.45-µm filter (Millipore) to remove solid particles. The filtered supernatant was loaded on a Resource Q column (GE Healthcare). After washing with 20 mM Tris-HCl (pH 8.0), 0.06% LDAO, the protein was eluted with a linear gradient of 0-1 M NaCl in the same buffer. The yield of purified Nt-$Omp85_{Ec}$ produced per 1-liter culture was 0.5 mg, according to UV absorption measurements.

All protein preparations were aliquoted and stored at -20ºC.

Electron microscopy

Purified $Omp85_{Ec}$ was used at 0.3 mg/ml in 20 mM Tris-HCl (pH 8.5), 15 mM NaCl, 0.06% $C_{10}E_5$. A 5-µl drop was applied to a glow-discharged copper grid covered with a thin layer of continuous carbon film and incubated for 2 min at RT. The excess liquid was removed and the grid was washed over two drops of distilled water, stained with 1% (w/v) uranyl acetate aqueous solution for 30 s and air-dried. The samples were examined using a Tecnai 10 electron microscope (FEI Electron Optics, Eindhoven, The Netherlands) at 120 kV acceleration voltage.

Cell envelope isolation

Cells of *N. meningitidis* or *E. coli* were collected by centrifugation, resuspended in 50 mM Tris-HCl (pH 8.0), 5 mM EDTA, containing protease inhibitor cocktail "Complete" (Roche), and stored overnight at -80°C. After ultrasonic disintegration (3 x 45 s at level 8, output 40%, Branson sonifier 450), unbroken cells were removed by centrifugation (12,000 *g*, 15 min, 4°C) and cell envelopes were collected by ultracentrifugation (170,000 *g*, 5 min, 4°C). The obtained pellets were dissolved in 2 mM Tris-HCl (pH 7.6) and stored at -20°C.

Proteolytic digestion

Protease resistance of $Omp85_{Nm}$ in cell envelopes and after *in vitro* folding was tested by incubating samples with various concentrations of proteinase K (Sigma) for 15 min either at 37˚C (cell envelopes) or on ice (refolded). The reactions were terminated by adding 1 mM phenylmethylsulfonyl fluoride (PMSF) and incubating on ice for 10 min. The samples were denatured by boiling in sample buffer and analyzed by SDS-PAGE. *E. coli* cell envelopes or refolded $Omp85_{Ec}$ were treated with 25 µg/ml of trypsin (Sigma) for 1 h at RT or with 50 µg/ml of proteinase K for 15 min at 37˚C, whereupon the proteases were inactivated with 1 mM PMSF. The *in vitro* folded proteins were used at 0.5 mg/ml.

SDS-PAGE and Western blot analysis

Proteins were analyzed by SDS-PAGE under denaturing or semi-native conditions (26). To obtain semi-native conditions, SDS was omitted from the gels and added to the running and sample buffers in varying amounts, as indicated in the Figure legends. The sample buffer did not contain any reducing agent and samples were prepared and run at 4ºC at 12 mA.

In Western blot experiments, the proteins were transferred from gels onto nitrocellulose membranes in 25 mM Tris, 192 mM glycine (pH 8.3), 20% methanol, 0.025% SDS using the Biorad wet blotting system. To denature folded proteins, the gels were heated with steam for 20 min prior to blotting. The membranes were blocked for 1 h in phosphate-buffered saline (PBS) (pH 7.6) supplemented with 0.5% non-fat dried milk (Protifar, Nutricia) and 0.1% Tween-20. The blots were incubated for 1 h with a primary antiserum, washed and then incubated for 1 h with a goat anti-rabbit IgG secondary antiserum conjugated to horseradish peroxidase (Biosource International), diluted in the blocking buffer. The signal was visualized using enhanced chemiluminescence (Amersham Biosciences). $Omp85_{Ec}$ was detected with a rabbit α-BamA antiserum raised against the full-length protein (17). Rabbit antisera against the N-terminal regions (residues 22-464) of *N. meningitidis* Omp85 (α-N-Omp85) and of *N. gonorrhoeae* Omp85 *(*α-Ng-Omp85) and against the C-terminal region (residues 455-797) of *N. meningitidis* Omp85 (α-C-Omp85) were generously provided by R. Judd (University of Montana, USA). In some cases, α-Ng-Omp85 was mixed with α-C-Omp85 producing α-Omp85 mix.

Molecular weight determination by SDS-PAGE

A calibration curve was obtained by plotting the migration distances of standard molecular weight proteins (Biorad All blue marker) against logarithms of their molecular weights. The molecular weights of the obtained Omp85 protease-resistant fragments were calculated from this calibration curve.

Blue Native PAGE

Blue Native PAGE (BN-PAGE) was done as described previously (19) with some modifications: 6-aminohexanoic acid was omitted from the system and samples, containing 0.5 mg/ml of protein, were mixed with an equal volume of sample buffer [25 mM imidazole-HCl (pH 7.0), 17.4% (v/v) glycerol, 0.05% (w/v) Coomassie Brilliant Blue G-250] prior to loading on a linear gradient gel [running gel, 5% to 20% (w/v) acrylamide; stacking gel, 3% (w/v) acrylamide].

CD spectroscopy

Circular dichroism (CD) spectra of Ct-Omp85$_{Ec}$ [0.3 mg/ml in 2 mM Tris-HCl (pH 8.5), 0.06% $C_{10}E_5$] and of Nt-Omp85$_{Nm}$ (1 mg/ml in 5 mM phosphate buffer, 0.2% SB-12) were recorded at RT over a wavelength range of 190-250 nm using a 0.5-mm path cell in an Olis CD instrument (Olis, Inc.USA). The data of 10 spectra were averaged and the contributions of the buffer were subtracted. The signals were converted to molar ellipticity.

Size exclusion chromatography

Refolded Omp85$_{Nm}$ was dialyzed overnight against a buffer consisting of 0.5% (w/v) LDAO, 20 mM Tris-HCl (pH 8.2), 0.3 M guanidine, and 21 mM NaCl. A 500-µl sample of the resulting Omp85 solution was passed through a Superdex 200 column (Pharmacia) at a fixed flow rate of 0.5 ml/min. Elution of the standard proteins (Amersham Bioscience) and Omp85 from the column was monitored by UV light absorption at 280 nm (Uvicord; Amersham Bioscience). Fractions of 1 ml were collected (RediFrac collector; Amersham Bioscience) and analyzed by standard SDS-PAGE. Omp85$_{Nm}$ was detected on the gels by Coomassie Brilliant Blue staining.

Dynamic light scattering

Dynamic light scattering (DLS) analyses were performed using a Laser-Spectroscatter 201 (RiNA netzwerk RNA technologien) at 532 nm with a scattering angle of 90°. Thirty µl of 1 mg/ml purified Omp85$_{Ec}$ in 20 mM Tris-HCl (pH 8.5), 0.06% LDAO or Ct-Omp85$_{Ec}$ in 20 mM Tris-HCl (pH 8.5), 0.06% $C_{10}E_5$ were measured. Prior to analysis**,** samples were centrifuged at 20,000 *g* for 1 h to remove aggregates. Ten data sets were recorded and the size distributions were analyzed using the software CONTIN.

N-terminal sequencing

For N-terminal sequencing, Ct-Omp85$_{Ec}$ was blotted from an SDS-PAGE gel onto a polyvinylidene difluoride membrane (Millipore). The blot was stained with Coomassie Brilliant Blue G-250, and the appropriate band was excised. This sample was subjected to five steps of Edman degradation at the Protein Sequencing Facility, Utrecht University, using a protein sequencer model 476 A (Perkin Elmer).

Crystallization trials

Proteins were concentrated to 5-10 mg/ml with a Centricon concentrator (Amicon). Concentrated Omp85$_{Ec}$ and Ct-Omp85$_{Ec}$ were dialyzed against 2 mM Tris-HCl (pH 8.5),

supplemented with 0.05% LDAO or $C_{10}E_5$ and $Omp85_{Nm}$ was dialyzed against its refolding buffer to remove excessive detergent. Crystallization trials were performed using the hanging-drop vapor diffusion method. Droplets containing equal amounts of protein preparation and mother liquor were equilibrated against the reservoir solution.

Results

In vitro folding of *N. meningitidis* Omp85

Previously, large quantities of folded $Omp85_{Ec}$ were obtained by producing the protein in cytoplasmic inclusion bodies and refolding it *in vitro* (17). Here, we assessed whether also the *N. meningitidis* homolog could be produced in a similar way. Refolding was tested by analyzing heat-modifiability of the protein, a typical feature of folded β-barrel OMPs, in semi-native SDS-PAGE (4, 9, 15). Like $Omp85_{Ec}$, $Omp85_{Nm}$ produced without its signal sequence in *E. coli* accumulated in inclusion bodies. However, $Omp85_{Nm}$ did not refold in the same conditions as used for $Omp85_{Ec}$ (data not shown). Different refolding conditions were tested by use of the Pierce Protein Refolding Kit (Pierce Biotechnology). The most efficient refolding was obtained in a buffer containing 55 mM Tris-HCl (pH 8.2), 21 mM NaCl, 1.1 M guanidine and 0.44 M L-arginine, supplemented with 0.5% SB-12 or LDAO. The refolded protein migrated substantially faster than the denatured protein in semi-native SDS-PAGE (Figure 1, left panel). This shift was comparable to that observed for $Omp85_{Nm}$ present in cell envelopes (Figure 1, right panel), suggesting that $Omp85_{Nm}$ acquired its native conformation after refolding. A refolding efficiency of ~80% was assessed from the gels. Attempts to remove guanidine completely after refolding resulted in precipitation of the protein. It was possible to decrease the guanidine content to 0.3 M and to remove L-arginine completely by dialysis while $Omp85_{Nm}$ remained soluble.

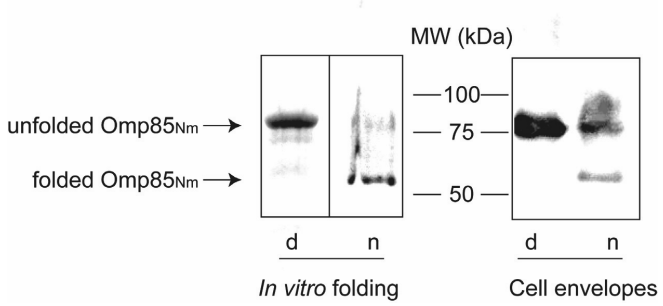

Figure 1

In vitro folding of $Omp85_{Nm}$ assessed by semi-native SDS-PAGE. Left panel: *in vitro* folded $Omp85_{Nm}$ was denatured by boiling in sample buffer containing 2% SDS and analyzed with 0.1% SDS in the running buffer (lane d), or resuspended in sample buffer containing 0.1% SDS and, without prior heating, analyzed with 0.01% SDS in the running buffer (lane n). The protein bands were visualized by Coomassie Brilliant Blue staining. Right panel: *N. meningitidis* cell envelopes were boiled with 2% SDS in the sample buffer (lane d) or incubated on ice with sample buffer containing 0.1% SDS (lane n) and analyzed with 0.05% SDS in the running buffer. Omp85 was visualized by Western blotting with α-N-Omp85 antiserum. The folded and unfolded forms of $Omp85_{Nm}$ are indicated and the positions of molecular weight marker proteins are shown in the middle.

Omp85 forms oligomers

$Omp85_{Ec}$ (17) and several other members of the Omp85 superfamily, such as mitochondrial Tob55 (16), chloroplast Toc75 (20), and *Haemophilus influenzae* HMW1B (24), were reported to form oligomers. Therefore, the oligomeric state of *in vitro* folded $Omp85_{Nm}$ was assessed in BN-PAGE. The electrophoretic mobility of $Omp85_{Ec}$ was analyzed as a control. As found before (17), this protein was detected in four distinct bands, which could correspond to monomers, dimers, trimers, and tetramers, suggesting that $Omp85_{Ec}$ formed tetramers that are in equilibrium with smaller oligomers, an equilibrium that might be influenced by the binding of Coomassie Brilliant Blue to the subunit interface. However, we found only two bands for $Omp85_{Nm}$, probably corresponding to the monomer and one of the oligomeric forms (Figure 2A). An estimation of the molecular weight of the oligomer is difficult, because the contributions of detergent and Coomassie Brilliant Blue are unknown.

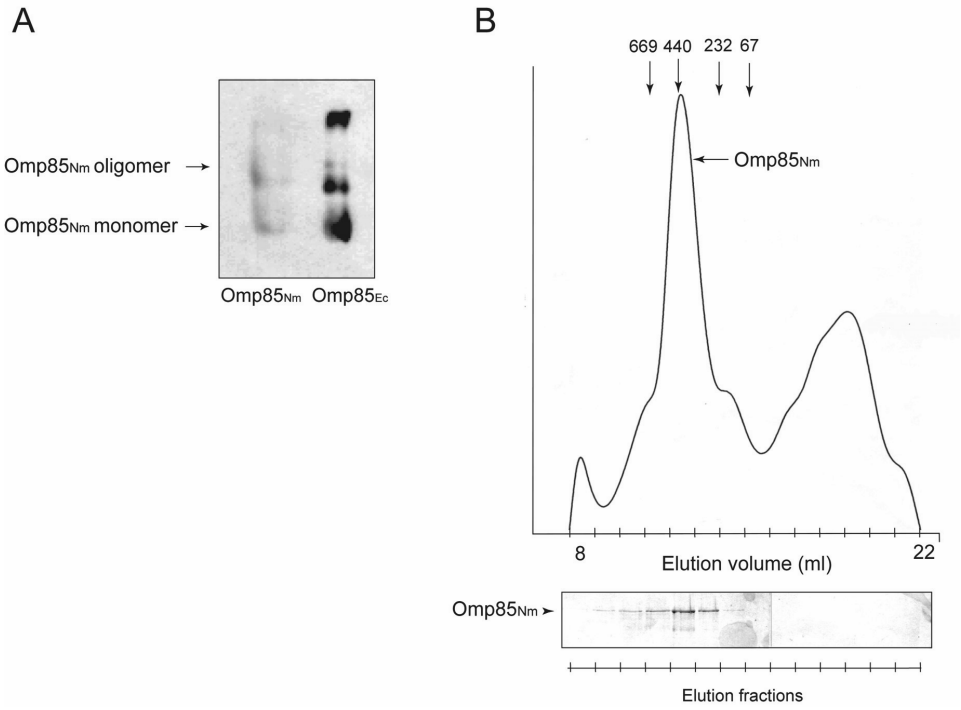

Figure 2

$Omp85_{Nm}$ forms oligomers. (**A**) Western blot after BN-PAGE containing refolded $Omp85_{Nm}$ and $Omp85_{Ec}$. The blot was probed with an α-N-Omp85 antiserum, washed, and then probed with α-BamA antiserum. Monomeric and oligomeric $Omp85_{Nm}$ forms are indicated. (**B**) Size exclusion chromatography of refolded $Omp85_{Nm}$. Elution volumes of the molecular weight standard proteins thyroglobulin (669 kDa), ferritine (440 kDa), catalase (232 kDa), and ovalbumin (67 kDa) are indicated. SDS-PAGE analysis of the elution fractions is given below the elution profile; an arrowhead specifies the position of Omp85, which was visualized by Coomassie Brilliant Blue staining.

We performed size exclusion chromatography to further analyze the *in vitro* folded $Omp85_{Nm}$ oligomers. Refolded $Omp85_{Nm}$ eluted in a single peak corresponding to a molecular weight of 438 kDa from a gel filtration column (Figure 2B) suggesting that all of the $Omp85_{Nm}$ protein in the sample was oligomeric. The second peak visible in Figure 2B did not contain $Omp85_{Nm}$ as shown by the SDS-PAGE analysis. The monomer seen on semi-native SDS-PAGE gel and on BN-PAGE (Figure 1 and 2A) likely results from dissociation of the oligomeric complex during electrophoresis. The estimated molecular weight of $Omp85_{Nm}$ is 86.2 kDa and that of an LDAO micelle is 21.8 kDa (23). It is not clear how many detergent micelles are bound per $Omp85_{Nm}$ oligomer but, if we assume that there is one micelle present per $Omp85_{Nm}$ molecule, than the calculated molecular weight of an $Omp85_{Nm}$ tetramer would be 432 kDa, which is very close to our experimental finding and indicates that the $Omp85_{Nm}$ oligomer is probably a tetramer. The estimated size of the $Omp85_{Nm}$ multimer is only slightly different from that found for the *in vitro* folded $Omp85_{Ec}$, i.e., ~473 kDa, which was suggested to form tetramers as well (17). This difference in size could be explained by the different molecular weights of $Omp85_{Ec}$ and $Omp85_{Nm}$, which are 88.4 kDa and 86.2 kDa, respectively, and by the different detergents used, i.e. LDAO and $C_{10}E_{5,}$ which form micelles of 21.8 and 27.6 kDa, respectively (13, 23). The calculated molecular weight of an $Omp85_{Ec}$ tetramer in $C_{10}E_5$ would be 464 kDa, which corresponds to the experimental data (17) and is slightly higher than the molecular weight predicted for the $Omp85_{Nm}$ tetramer.

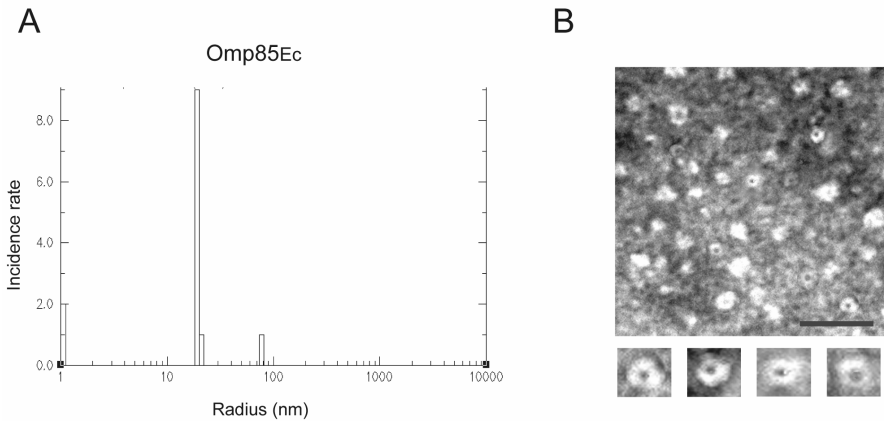

Figure 3

$Omp85_{Ec}$ particle characterization. (**A**) DLS histogram of refolded $Omp85_{Ec}$ (**B**) Electron microscopic images of negatively stained purified $Omp85_{Ec}$. The sample was applied to a grid, negatively stained with 1% uranyl acetate and visualized by EM. Scale bar represents 50 nm. Enlarged images of single $Omp85_{Ec}$ particles are given underneath the total view.

Further characterization of the oligomers of full-length Omp85 could be achieved, for example, by electron microscopy (EM) and X-ray crystallography. For both of these approaches, however, it is important that the sample is monodisperse. The gel filtration results presented previously for $Omp85_{Ec}$ (17) and here for $Omp85_{Nm}$ (Figure 2B) show a

symmetrical single elution peak, meaning that all of the Omp85 in the sample is in the same conformation, probably a tetramer. On the other hand, the BN-PAGE data showed multiple bands, arguing against the sample being homogenous. To obtain more information about homogeneity of the $Omp85_{Ec}$ preparation, we performed a DLS experiment. The intensity histograms obtained represent the hydrodynamic radii distribution in the sample. Most of the registered particles were found in one peak (Figure 3A), suggesting the Omp85 population in this sample to be monodisperse and to have a particle diameter of approximately 40 nm.

The experimental data obtained for $Omp85_{Ec}$ so far suggest that it is a protein with the ability to form pores (17, 22). We examined the $Omp85_{Ec}$ preparation using negative-stain electron microscopy (Figure 3B). The single particles observed had diameters of approximately 17 nm. The heavily stained center of these particles suggested the presence of pores of approximately 2.5 nm. This diameter is in line with the dimensions found in liposome swelling assays for $Omp85_{Ec}$ (17).

Two-domain structure of Omp85 proteins

The Omp85 proteins are predicted to be composed of two domains: an N-terminal moiety located in the periplasm containing five POTRA domains, which are possibly involved in the interaction with unfolded OMPs, and a C-terminal part supposedly forming a β-barrel, which is embedded in the OM. Compactly folded β-barrels are usually highly resistant to proteolytic digestion. To assess the two-domain model as well as the correct conformation of the *in vitro* folded proteins, we determined the protease sensitivity of the *E. coli* and *N. meningitidis* Omp85 proteins. The apparent molecular weights of the $Omp85_{Ec}$ and $Omp85_{Nm}$ full-length proteins on SDS-PAGE gels are 87.3 kDa and 85.7, respectively, which is close to their calculated molecular weights given in Table 2. We, therefore, used SDS-PAGE analysis to estimate the sizes of the proteolytic fragments obtained.

Table 2. Calculated molecular masses of $Omp85_{Ec}$ and $Omp85_{Nm}$ variants lacking 0, 1, 2, 3, 4, or 5 POTRA domains and of the predicted 12-stranded β-barrel domains. The POTRA domains are defined according to the structure of the $Omp85_{Ec}$ N-terminal fragment (10) and the 12-stranded β-barrels are defined according to the Omp85 topology model (26). The molecular weights are calculated using the ProParam tool (6)

Fragment description	$Omp85_{Ec}$	$Omp85_{Nm}$
Full-length (mature)	88.4 kDa	86.2 kDa
Δ POTRA1	80.7 kDa	78.5 kDa
Δ POTRA1-2	71.6 kDa	69.5 kDa
Δ POTRA1-3	61.1 kDa	58.7 kDa
Δ POTRA1-4	52.1 kDa	49.4 kDa
Δ POTRA1-5	43.1 kDa	40.5 kDa
12-stranded β-barrel	36.9 kDa	34.5 kDa

Proteolytic digestion of $Omp85_{Ec}$ in cell envelopes produced two major fragments with apparent molecular weights of 45 kDa and 56 kDa after trypsin treatment and 58 and 68 kDa after proteinase K treatment (Figure 4A). Protease digestion of *in vitro* folded $Omp85_{Ec}$ yielded a 45-kDa fragment after digestion with trypsin and a 47-kDa fragment after digestion with proteinase K (Figure 4A). The sizes of the latter fragments are close to the theoretical molecular weight of $Omp85_{Ec}$ lacking all five POTRA domains (43.1 kDa), but considerably larger than that of the predicted 12-stranded β-barrel (36.9 kDa) (Table 2), suggesting that the protease-resistant part of $Omp85_{Ec}$ could correspond to the C-terminal β-barrel part and that

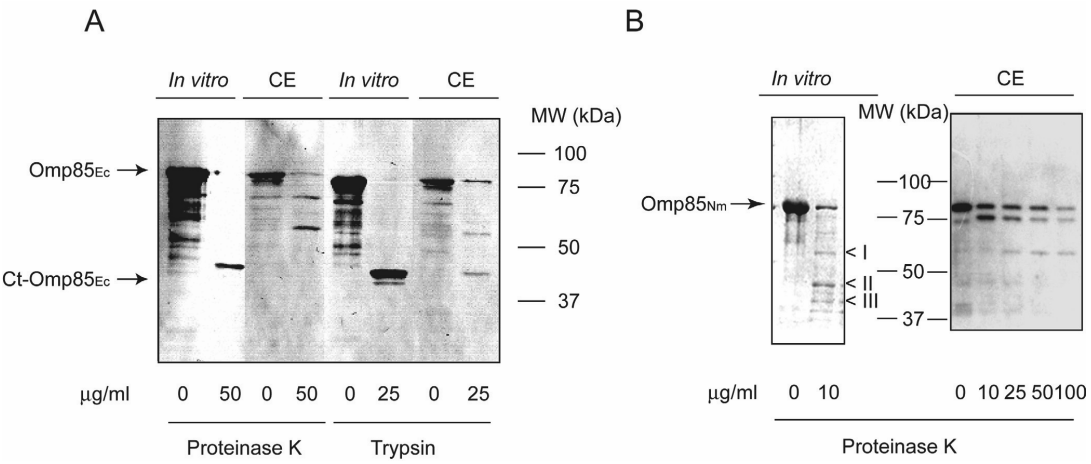

Figure 4

Protease susceptibility of $Omp85_{Ec}$ and $Omp85_{Nm}$. (**A**). Proteinase K and trypsin digestion profiles of $Omp85_{Ec}$, folded *in vitro* or in *E. coli* cell envelopes (CE). Fragments were detected using α-BamA antiserum. $Omp85_{Ec}$ and Ct-$Omp85_{Ec}$ are indicated. (**B**) Proteinase K digestion profiles of $Omp85_{Nm}$, folded *in vitro* or in *N. meningitidis* cell envelopes (CE). Roman numbers indicate proteolytic fragments of the refolded protein. The blot was probed with α-Omp85 mix.

this part is larger than originally predicted (26). For further characterization, the 45-kDa tryptic fragment, designated Ct-$Omp85_{Ec}$, was purified using ion-exchange chromatography and analyzed by semi-native SDS-PAGE and by CD spectroscopy (Figure 5A and 5B). The fragment showed heat-modifiability in semi-native SDS-PAGE and its CD spectrum revealed a typical β-structure curve with a minimum at 217 nm, indicating that it indeed represents the folded β-barrel domain. N-terminal sequence analysis of the Ct-$Omp85_{Ec}$ fragment revealed the amino-acid sequence ERNTG, which corresponds to the C terminus of the last predicted POTRA domain (10) (Figure 5C). Based on its apparent molecular weight, the 56-kDa fragment found in the cell envelopes after trypsin treatment could contain the β-barrel with POTRA5, possibly extended with a part of the POTRA4 domain (Table 2). If we assume that the 47-kDa proteinase K-resistant fragment of *in vitro* folded $Omp85_{Ec}$ also contains the C-terminal β-barrel fragment, than the 68- and 58-kDa $Omp85_{Ec}$ fragments found in the cell envelopes after treatment with proteinase K might correspond the proteolytic removal of the first two and three POTRA domains, respectively (Table 2).

To determine whether the Ct-$Omp85_{Ec}$ sample could be suitable for further experiments, such as crystallization trials, its homogeneity was assessed by DLS. Most of the detected particles in the sample were found in a peak corresponding to a diameter of ~12 nm (Figure 5D). However, much larger particles were also observed, suggesting some aggregation in the sample, but not enough to discourage crystallization attempts, described below. The molecular weight of the particles in the major peak was estimated to be 392 kDa, indicative of oligomerization. However, because the DLS data provide only a rough estimation of particle size and because the detergent contribution is not known, the exact amount of β-barrel molecules in the oligomer cannot be determined from this assay.

Proteinase K digestion of *N. meningitidis* cell envelopes produced two Omp85 digestion products: one of 79 kDa migrating just below the intact Omp85 and a smaller one

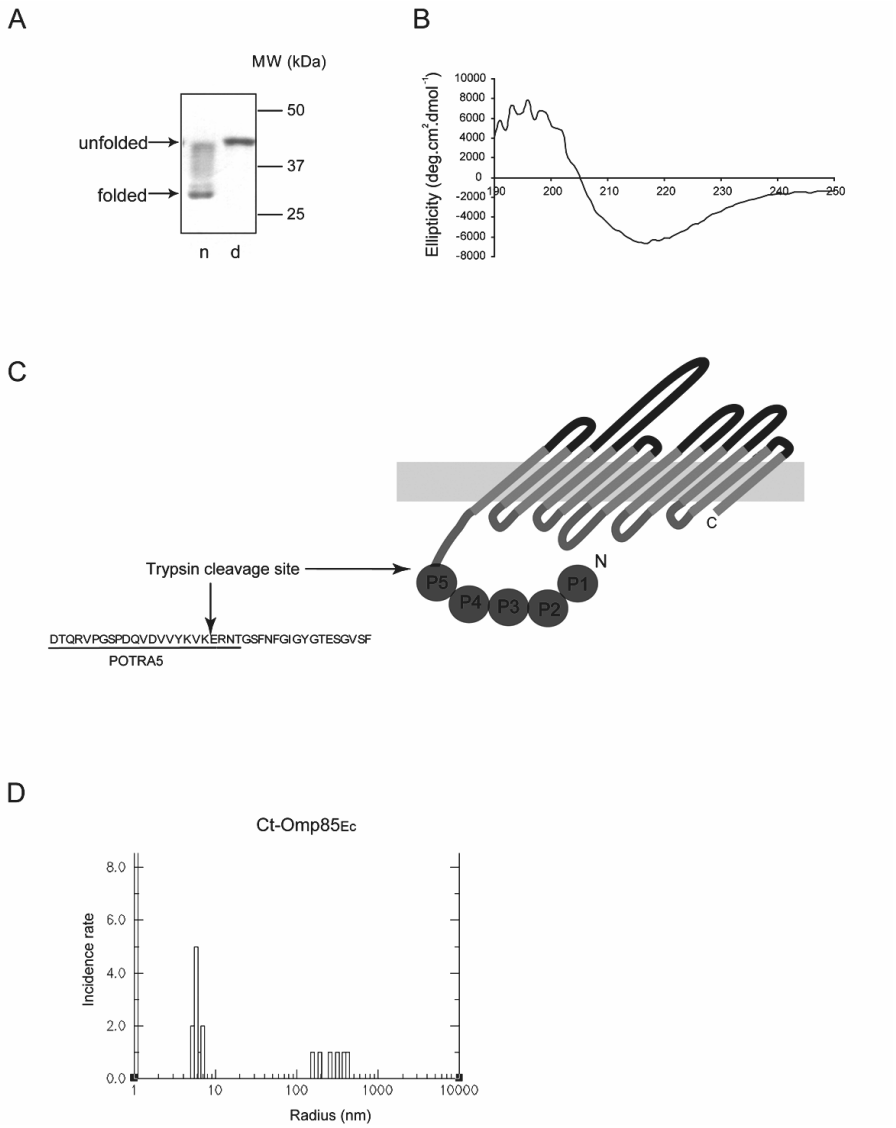

Figure 5

Characterization of Ct-Omp85$_{Ec}$. (**A**) Heat-modifiability of Ct-Omp85$_{Ec}$. The sample was incubated on ice in sample buffer with 0.1% SDS (n) or boiled in sample buffer with 2% SDS (d) and electrophoresed on a gel without SDS using running buffer containing 0.1% SDS. The protein bands were visualized by Coomassie Brilliant Blue staining. Folded and unfolded forms are indicated. (**B**) CD spectrum of the folded Ct-Omp85$_{Ec}$. The spectrum has a minimum around 217 nm, which is typical for a β-stranded protein. (**C**) Topology model of Omp85$_{Ec}$ based on that of Omp85$_{Nm}$ (26). The predicted periplasmic part with five POTRA domains (P1-P5) and the membrane-embedded β-barrel domain are shown. The trypsin-cleavage site in Omp85$_{Ec}$ as determined by N-terminal sequencing is indicated in the topology model and in the amino acid sequence of the relevant part of Omp85$_{Ec}$. (**D**) DLS histogram of Ct-Omp85$_{Ec}$.

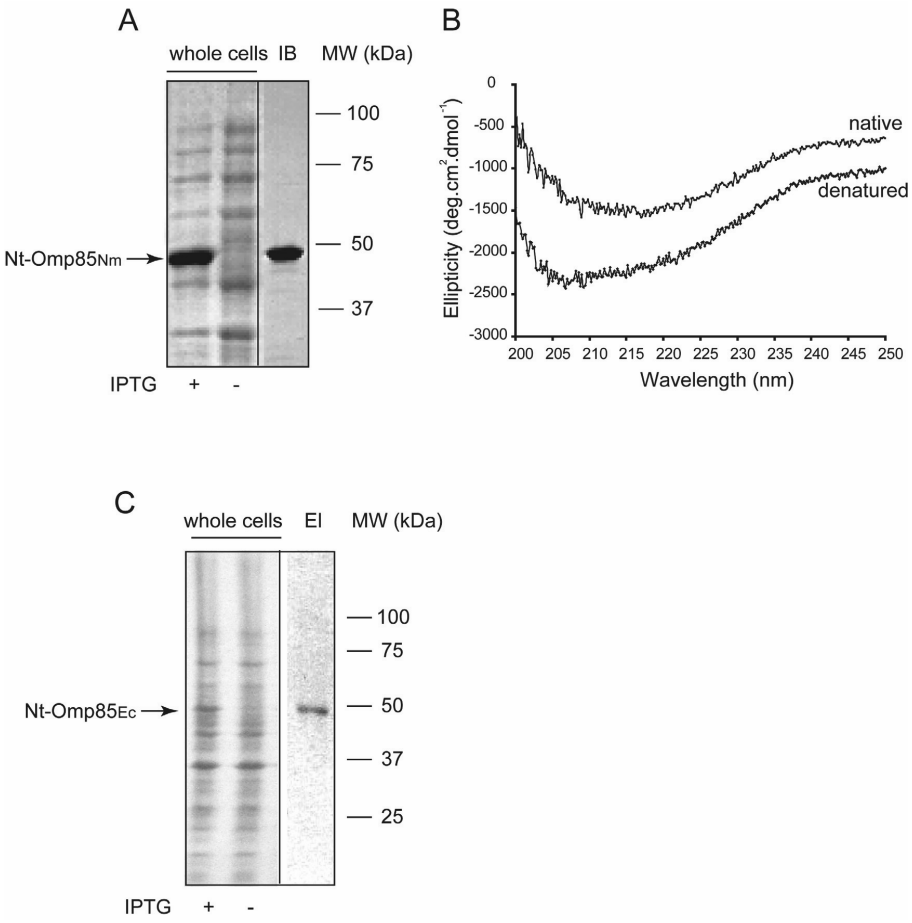

Figure 6

Purification of Nt-Omp85$_{Nm}$ and Nt-Omp85$_{Ec}$. (**A**) Expression and purification of Nt-Omp85$_{Nm}$. Lysates of cells grown in the presence or absence of IPTG and purified inclusion bodies (IB) are shown. Proteins are visualized by Coomassie Brilliant Blue staining. The position of Nt-Omp85$_{Nm}$ is indicated. (**B**) CD spectra of native and denatured refolded Nt-Omp85$_{Nm}$. (**C**) Expression and purification of Nt-Omp85$_{Ec}$. Lysates of cells grown in the presence or absence of IPTG and purified Nt-Omp85$_{Ec}$ (El) are shown. The gels are stained with Coomassie Brilliant Blue and the position of Nt-Omp85$_{Ec}$ is indicated.

of 65 kDa (Figure 4B). These fragments could result from the proteolytic removal of one and two POTRA domains, respectively (Table 2). Digestion of the *in vitro* folded *N. meningitidis* Omp85 yielded other prominent bands with estimated molecular weights of 58 kDa, 44 kDa, and 39 kDa, indicated as I, II, and III in Figure 4B. The 44-kDa fragment is the most

prominent one and it migrates at a similar position as the $Omp85_{Ec}$ tryptic fragment. Therefore, it might correspond to the C-terminal fragment of $Omp85_{Nm}$ lacking all POTRA domains, the predicted molecular weight of which is 40.5 kDa (Table 2). The 39-kDa band would than result from cleavage further downstream in the sequence in between the POTRA5 domain and the predicted 12-stranded β-barrel, although, based upon its apparent molecular weight, it is also possible that this fragment, rather than the 44-kDa fragment, corresponds to the entire C-terminal domain lacking only the five POTRA domains. The 58-kDa band might correspond to the fragment resulting from the proteolytic removal of three POTRA domains.

From the protease-sensitivity analysis several conclusions can be drawn. Both refolded *N. meningitidis* and *E. coli* homologs yielded distinct fragments upon proteolytic digestion, suggesting that they are in the folded conformation. For $Omp85_{Ec}$ we have shown that Ct-$Omp85_{Ec}$ contains a β-barrel. Our data suggest that the C-terminal part of Omp85 is resistant to proteolytic cleavage, unlike the N terminus, supporting the two-domain model predicted for Omp85.

Purification of the N-terminal fragments of the Omp85 proteins

The data described above are consistent with the hypothesis that the C-terminal part of Omp85 forms a β-barrel, which anchors Omp85 into the OM. The N-terminal POTRA-containing part might interact with OMP substrates. To study the substrate-binding properties of the Omp85 N-terminal part, we produced the predicted periplasmic domains (26) of both *N. meningitidis* and *E. coli* Omp85 without their signal sequences in *E. coli*. The Nt-$Omp85_{Nm}$ was produced with a C-terminal His-tag to facilitate purification. Because of its predicted cellular location, we expected this protein to be water-soluble. Strikingly, however, Nt-$Omp85_{Nm}$ formed inclusion bodies at high yields (Figure 6A). We solubilized the protein from these inclusion bodies and refolded it in the presence of detergent. Unlike in the case of β-barrels, we could not rely on heat-modifiability in semi-native PAGE to analyze the refolding of the N-terminal fragments. Therefore, we performed CD spectroscopy (Figure 6B). We compared spectra of the folded sample and of a sample that was boiled with 2% SDS. The native sample showed a spectrum corresponding to a protein consisting of both α-helices and β-strands, consistent with the reported crystal structure for an N-terminal fragment of $Omp85_{Ec}$ (10). When the sample was boiled in 2% SDS, the CD spectrum obtained was shifted, indicative of changes in the protein conformation, likely due to denaturation. A similar spectrum was obtained when SDS was added to the sample without boiling indicating that the refolded Nt-$Omp85_{Nm}$ fragment is highly sensitive to SDS.

In contrast to Nt-$Omp85_{Nm}$, Nt-$Omp85_{Ec}$ remained soluble when expressed in *E. coli*. Because most of the protein remained soluble and was not degraded by cytosolic proteases, we assumed that it is correctly folded. We purified the protein under native conditions by anion-exchange chromatography from the *E. coli* lysate (Figure 6C).

Crystallization trials

In order to gain insight into the Omp85 structure, crystallization trials were performed. Initial trials were done using Hampton research screen kits (Hampton research). The most promising conditions obtained in those screens were optimized by varying crystallization parameters, such as compound concentrations, precipitant type, and pH. We were able to obtain crystals for $Omp85_{Nm}$ in LDAO solution (Figure 7, right panel), for $Omp85_{Ec}$ both in LDAO (result not shown) and in $C_{10}E_5$ (Figure 7, left panel) and for Ct-$Omp85_{Ec}$ in LDAO and in $C_{10}E_5$ (not shown). Crystals were harvested from droplets with cryo-loops and directly cooled into liquid nitrogen. X-ray data were collected at 100 K on a CCD detector at ID-14 EH4 beamline at the European Synchrotron Radiation Facility (ERSF)

in Grenoble, France. However, none of the obtained crystals diffracted to a resolution that allowed structural determinations.

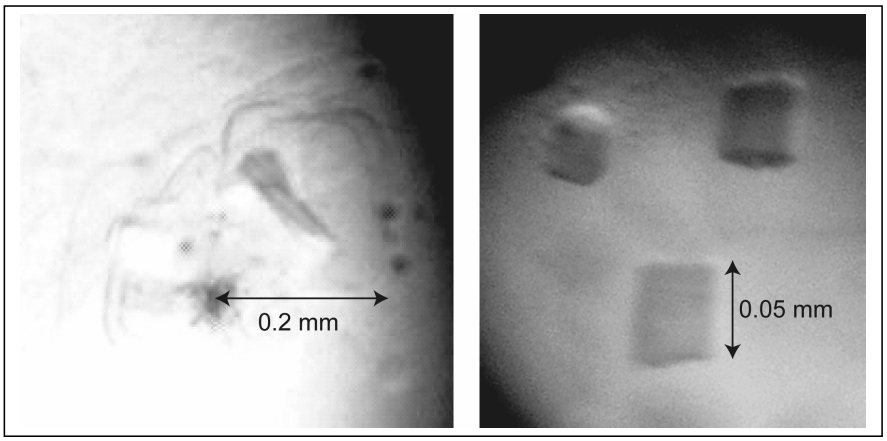

Figure 7

Omp85 crystals. Crystals obtained for $Omp85_{Ec}$ (left panel) and $Omp85_{Nm}$ (right panel) are shown. $Omp85_{Ec}$ was crystallized in 80 mM $(NH_4)_2HPO_4$, 5% polyethylenglycol (PEG) 2000, pH 7.0, 0.06% $C_{10}E_5$. $Omp85_{Nm}$ was crystallized in 30% PEG 3350, 10 mM $(NH_4)_2SO_4$, 0.06% LDAO. The dimensions of the crystals are indicated.

Discussion

Refolding of *N. meningitidis* Omp85

In this work we determined conditions to fold $Omp85_{Nm}$ *in vitro* from inclusion bodies. Although the $Omp85_{Nm}$ and $Omp85_{Ec}$ proteins are close homologs, they did not fold under the same conditions. In contrast to its *E. coli* counterpart, $Omp85_{Nm}$ required the presence of agents suppressing protein aggregation, such as L-arginine and guanidine for *in vitro* folding. Attempts to remove all such reagents completely after refolding by dialysis resulted in the precipitation of the protein. Thus, the Omp85 proteins of these two species appear to contain intrinsically different properties. Possibly, the neisserial homolog contains more areas of high hydrophobicity, which could be causing its enhanced tendency to aggregate.

Omp85 forms oligomers

We have shown before that *in vitro* folded $Omp85_{Ec}$ forms oligomers (17). These oligomers likely are tetramers as inferred from the particle size found using gel filtration, the migration pattern of the protein in BN-PAGE revealing bands likely corresponding to dimers, trimers, and tetramers, and pore activity recordings, which suggested conductivity steps generated by monomers and tetramers (17). Consistently, our EM results reveal particles of ~17 nm, which are likely to represent $Omp85_{Ec}$ oligomers (Figure 3B). $Omp85_{Nm}$ also forms oligomers (Figure 2A and B). The particle size of 438 kDa, estimated by size exclusion chromatography, suggests that $Omp85_{Nm}$ likely forms tetramers as well (Figure 2B). In this respect, the two Omp85 homologs appear similar.

Pore formation by Omp85

Previously, liposome swelling assays and planar lipid bilayer measurements showed that $Omp85_{Ec}$ forms pores (17, 22). The current DLS results indicated that the $Omp85_{Ec}$ preparation was homogeneous and it was, therefore, further examined by EM. The EM images revealed particles of ~17 nm in diameter with an apparent pore of approximately 2.5 nm. This pore diameter is similar to the pore dimension found in liposome swelling assay of $Omp85_{Ec}$, but much larger than the pores identified in planar lipid bilayer experiments, which might correspond to pores within the individual β-barrels (17).

Two-domain architecture of Omp85

In this work we showed that Omp85 consists of a protease-resistant and a protease-sensitive domain. Ct-$Omp85_{Ec}$ shows typical features of a β-barrel, as inferred from its heat-modifiability in semi-native SDS-PAGE and its CD spectrum. We found that this protease protected fragment starts at the C terminus of the last predicted POTRA domain. According to our topology model (26), a 12-stranded β-barrel of Omp85 is separated from the POTRA5 domain by a hinge region of 61 amino acid residues. The conformation of this region is still not clear. One possibility is that the hinge region is in fact a part of the β-barrel. The only structure of an Omp85 protein superfamily member solved up to date is that of the *Bordetella pertussis* FhaC (3). This protein is the membrane component of a two-partner secretion system and shares limited sequence homology with Omp85. It serves the translocation of a cognate substrate protein across the OM, while Omp85 is a general OMP assembly factor. The FhaC structure revealed the presence of 16 and not 12 β-strands. It is, therefore, possible that the bacterial Omp85 β-barrels also contain more than the 12 predicted β-strands and include the hinge region. However, there is no obvious sequence similarity between the amino acid sequences of the presumed linker region of Omp85 proteins and the first β-strands of FhaC to substantiate this possibility. The other possibility is that the hinge region is located in the periplasm, but is folded into a protease-resistant state. The proteinase K treatment of $Omp85_{Nm}$ yields a 44-kDa fragment, which is of a similar size as the protease-resistant fragment of $Omp85_{Ec}$. This fragment might represent the *N. meningitidis* Omp85 β-barrel. We also observed several fragments that are larger than the β-barrel fragment for both Omp85 homologs particularly upon protease digestion in cell envelopes, indicating that the periplasmic domain is more resistant to proteases in the *in vivo*-folded proteins than in the *in vitro*-folded proteins. One possibility is that cleavage sites available in the *in vitro* folded proteins are shielded *in vivo*, for example by interaction with the other Omp85 complex components. Alternatively, we cannot exclude the possibility that the N-terminal domains of the full-length proteins are not properly folded *in vitro*. Omp85 contains two domains, which reside in completely different environments: periplasm and OM. The refolding conditions were optimized based on heat-modifiability of the refolded protein, a property that is related to the β-barrel domain, which indeed was properly folded as appears from its protease resistance, but they don't provide a clue for the conformation of the N-terminal domain. The estimations made above for *N. meningitidis* Omp85 are based on the assumption that the β-barrel of this protein is resistant to digestion by proteinase K in the same way as the β-barrel of $Omp85_{Ec}$ is resistant to trypsin. However, cleavage in the loops of the β-barrel cannot be excluded, meaning that the observed fragments could be degraded at the C terminus as well as at the N terminus.

Surprisingly, Nt-$Omp85_{Ec}$ and Nt-$Omp85_{Nm}$ demonstrated different properties. While Nt-$Omp85_{Ec}$ was soluble, its *N. meningitidis* counterpart formed inclusion bodies. A difference in solubility was also found for the *in vitro* folded full-length proteins, which than might be caused by the differences in the solubility of the N-terminal domains. The Nt-

$Omp85_{Ec}$ and Nt-$Omp85_{Nm}$ both contained POTRA domains as well as the hinge region. As discussed above, we cannot exclude the possibility that this region is actually a part of the β-barrel and, therefore, contributes to the poor solubility of Nt-$Omp85_{Nm}$. To test this possibility, we have also constructed a shorter Nt-$Omp85_{Nm}$ variant that only contained the five POTRA domains (data not shown). However, also this variant was not soluble, indicating that the insolubility is due to the POTRA domains of Nt-$Omp85_{Nm}$.

In this study we developed an efficient way to obtain pure refolded $Omp85_{Nm}$ and we studied the two-domain structure and the oligomeric nature of this and the previously obtained $Omp85_{Ec}$. We also obtained and characterized the membrane part of the $Omp85_{Ec}$. These proteins as well as N-terminal fragments of both Omp85 homologs were used for further functional studies described in Chapter 6 of this thesis.

Acknowledgements

This work was supported by the Netherlands Research Councils for Chemical Sciences (CW) and Earth and Life Sciences (ALW) from the Netherlands Organization of Scientific Research (NOW) and by a short-term fellowship from the Federation of European Biochemical Sciences (FEBS) to E. B. Volokhina.

References

1. **Bos, M. P., and J. Tommassen.** 2005. Viability of a capsule- and lipopolysaccharide-deficient mutant of *Neisseria meningitidis*. Infect. Immun. **73:**6194-6197.
2. **Bos, M. P., V. Robert, and J. Tommassen.** 2007. Functioning of outer membrane protein assembly factor Omp85 requires a single POTRA domain. EMBO Rep. **8:**1149-1154.
3. **Clantin, B., A. S. Delattre, P. Rucktooa, N. Saint, A. C. Méli, C. Locht, F. Jacob-Dubuisson, and V. Villeret.** 2007. Structure of the membrane protein FhaC: a member of the Omp85-TpsB transporter superfamily. Science **317:**957-961.
4. **Dekker, N., K. Merck, J. Tommassen, and H. M. Verheij.** 1995. In vitro folding of *Escherichia coli* outer-membrane phospholipase A. Eur. J. Biochem. **232:**214-219.
5. **Doerrler, W. T., and C. R. Raetz.** 2005. Loss of outer membrane proteins without inhibition of lipid export in an *Escherichia coli* YaeT mutant. J. Biol. Chem. **280:**27679-27687.
6. **Gasteiger E., C. Hoogland, A. Gattiker, S. Duvaud, M. R. Wilkins, R. D. Appel, and A. Bairoch.** 2005. Protein identification and analysis tools on the ExPASy server, p. 571-607. *In* John M. Walker (ed), The Proteomics Protocols Handbook, Humana Press.
7. **Gatzeva-Topalova, P. Z., T. A. Walton, and M. C. Sousa.** 2008. Crystal structure of YaeT: conformational flexibility and substrate recognition. Structure **16:**1873–1881.
8. **Gentle, I., K. Gabriel, P. Beech, R. Waller, and T. Lithgow.** 2004. The Omp85 family of proteins is essential for outer membrane biogenesis in mitochondria and bacteria. J. Cell Biol. **164:**19-24.
9. **Jansen, C., A. Wiese, L. Reubsaet, N. Dekker, H. de Cock, U. Seydel, and J. Tommassen.** 2000. Biochemical and biophysical characterization of in vitro folded outer membrane porin PorA of *Neisseria meningitidis*. Biochim. Biophys. Acta **1464:**284-298.
10. **Kim, S., J. C. Malinverni, P. Sliz, T. J. Silhavy, S. C. Harrison, and D. Kahne.** 2007. Structure and function of an essential component of the outer membrane protein assembly machine. Science **317:**961-964.
11. **Knowles, T. J., M. Jeeves, S. Bobat, F. Dancea, D. McClelland, T. Palmer, M. Overduin, and I. R. Henderson.** 2008. Fold and function of polypeptide transport-associated domains responsible for delivering unfolded proteins to membranes. Mol. Microbiol. **68:**1216-1227.
12. **Kozjak, V., N. Wiedemann, D. Milenkovic, C. Lohaus, H. E. Meyer, B. Guiard, C. Meisinger, and N. Pfanner.** 2003. An essential role of Sam50 in the protein sorting and assembly machinery of the mitochondrial outer membrane. J. Biol. Chem. **278:**48520-48523.
13. **le Maire, M., P. C. Jesper, and V. Möller.** 2000. Interaction of membrane proteins and lipids with solubilizing detergents. Biochim. Biophys. Acta **1508:**86-111.
14. **Malinverni, J. C., J. Werner, S. Kim, J. G. Sklar, D. Kahne, R. Misra, and T. J. Silhavy.** 2006. YfiO stabilizes the YaeT complex and is essential for outer membrane protein assembly in *Escherichia coli*. Mol. Microbiol. **61:**151-164.
15. **Nakamura, K., and S. Mizushima.** 1976. Effects of heating in dodecyl sulfate solution on the conformation and electrophoretic mobility of isolated major outer membrane proteins from *Escherichia coli* K-12. J. Biochem. **80:**1411-1422.
16. **Paschen, S. A., T. Waizenegger, T. Stan, M. Preuss, M. Cyrklaff, K. Hell, D. Rapaport, and W. Neupert.** 2003. Evolutionary conservation of biogenesis of β-barrel membrane proteins. Nature **426:**862-866.
17. **Robert, V., E. B. Volokhina, F. Senf, M. P. Bos, P. Van Gelder, and J. Tommassen.** 2006. Assembly factor Omp85 recognizes its outer membrane protein substrates by a species-specific C-terminal motif. PLoS Biol. **4:**e377.
18. **Sánchez-Pulido, L., D. Devos, S. Genevrois, M. Vicente, and A. Valencia.** 2003. POTRA: a conserved domain in the FtsQ family and a class of β-barrel outer membrane proteins. Trends Biochem. Sci. **28:**523-526.
19. **Schagger, H.** 2001. Blue-native gels to isolate protein complexes from mitochondria. Methods Cell Biol. **65:**231-244.
20. **Schleiff, E., J. Soll, M. Këchler, W. Këhlbrandt, and R. Harrer.** 2003. Characterization of the translocon of the outer envelope of chloroplasts. J. Cell Biol. **160:**541-551.

21. **Sklar, J. G., T. Wu, L. S. Gronenberg, J. C. Malinverni, D. Kahne, and T. J. Silhavy.** 2007. Lipoprotein SmpA is a component of the YaeT complex that assembles outer membrane proteins in *Escherichia coli*. Proc. Natl. Acad. Sci. U S A **104:**6400-6405.
22. **Stegmeier, J. F., and C. Andersen.** 2006. Characterization of pores formed by YaeT (Omp85) from *Escherichia coli*. J. Biochem. (Tokyo) **140:**275-283.
23. **Strop, P., and A. T. Brunger.** 2005. Refractive index-based determination of detergent concentration and its application to the study of membrane proteins. Protein Sci. **14:**2207-2211.
24. **Surana, N. K., S. Grass, G. G. Hardy, H. Li, D. G. Thanassi, and J. W. Geme, 3rd.** 2004. Evidence for conservation of architecture and physical properties of Omp85-like proteins throughout evolution. Proc. Natl. Acad. Sci. U S A **101:**14497-14502.
25 **Tashiro, Y., N. Nomura, R. Nakao, H. Senpuku, R. Kariyama, H. Kumon, S. Kosono, H. Watanabe, T. Nakajima, and H. Uchiyama.** 2008. Opr86 is essential for viability and is a potential candidate for a protective antigen against biofilm formation by *Pseudomonas aeruginosa*. J. Bacteriol. **190:**3969-3978.
26. **Voulhoux, R., M. P. Bos, J. Geurtsen, M. Mols, and J. Tommassen.** 2003. Role of a highly conserved bacterial protein in outer membrane protein assembly. Science **299:**262-265.
27. **Werner, J., and R. Misra.** 2005. YaeT (Omp85) affects the assembly of lipid-dependent and lipid-independent outer membrane proteins of *Escherichia coli*. Mol. Microbiol. **57:**1450-1459.
28. **Wu, T., J. Malinverni, N. Ruiz, S. Kim, T. J. Silhavy, and D. Kahne.** 2005. Identification of a multicomponent complex required for outer membrane biogenesis in *Escherichia coli*. Cell **121:**235-245.

Chapter 6

Functional studies of *N. meningitidis* and *E. coli* Omp85 proteins and their sub-domains

Elena B. Volokhina[1*], Patrick Van Gelder[2*], Frank Beckers[1], Martine P. Bos[1], Lucy Rutten[3], Piet Gros[3] and Jan Tommassen[1]

[1] Department of Molecular Microbiology and Institute of Biomembranes, Utrecht University, Utrecht, The Netherlands

[2] Department of Molecular and Cellular Interactions, Flanders Interuniversity Institute for Biotechnology (VIB), Free University Brussels, Brussels, Belgium

[3] Department of Crystal and Structural Chemistry, Bijvoet Center for Biomolecular Research, Utrecht University, Utrecht, The Netherlands

* Contributed equally to this work

Abstract

Omp85 is an essential component of the machinery required for the assembly of bacterial outer membrane proteins (OMPs). In this work we investigated functional properties of purified *Neisseria meningitidis* and *Escherichia coli* Omp85 proteins and their sub-domains *in vitro*. Liposome-swelling assays and planar lipid bilayer experiments showed that *N. meningitidis* Omp85, like Omp85 of *E. coli*, forms pores, but its electrophysiological properties were different from those of the *E. coli* protein. The two-domain model for Omp85, with the C-terminal part forming a membrane-embedded pore and the N-terminal moiety extending in the periplasm and being responsible for substrate recognition, was confirmed by demonstrating the pore-forming capacity of a C-terminal fragment of *E. coli* Omp85 and the interaction of an N-terminal fragment of *N. meningitidis* Omp85 with OMPs and peptides derived from them. Furthermore, we found that the N-terminal fragment of *N. meningitidis* Omp85 is able to interact with lipid monolayers, unlike its *E. coli* counterpart, suggesting functional differences.

Introduction

Omp85 is an essential protein required for outer membrane protein (OMP) insertion and assembly in Gram-negative bacteria, as was first demonstrated in *Neisseria meningitidis* (22). The protein was suggested to be composed of two domains: a C-terminal part embedded in the outer membrane (OM) and an N-terminal moiety located in the periplasm (22). *Escherichia coli* Omp85, formerly known as YaeT, was recently re-named BamA. For the sake of clarity, we will use Omp85 as generic name and refer to the Omp85 proteins of *N. meningitidis* and *E. coli* as $Omp85_{Nm}$ and $Omp85_{Ec}$, respectively, in this chapter.

A C-terminal fragment of $Omp85_{Ec}$ (Ct-$Omp85_{Ec}$), obtained by trypsin digestion of *in vitro* folded protein, demonstrated typical β-barrel features consistent with its proposed membrane location (12; Chapter 5, this thesis). Also *in vitro* folded $Omp85_{Nm}$ ($Omp85_{Nm}$) contains a protease-resistant domain, which likely corresponds to the membrane-embedded β-barrel (Chapter 5). The Omp85 β-barrel domain was predicted to contain 12 β-strands (22). However, the crystal structure of FhaC of *Bordetella pertussis*, a component of a two-partner secretion system and member of the Omp85 superfamily with limited sequence homology to Omp85, revealed a 16-stranded β-barrel (1). Therefore, the exact conformation of the membrane-embedded part of Omp85 awaits structural resolution.

The majority of bacterial OMPs carries a C-terminal signature sequence. This sequence is characterized by a phenylalanine or a tryptophan at the C-terminal position, a hydrophobic amino acid residue, preferably a tyrosine, at the position -3 from the C terminus, and hydrophobic residues at positions -5, -7, and -9 from the C terminus (19). When reconstituted in planar lipid bilayers, *in vitro* folded $Omp85_{Ec}$ formed pores (12, 18). Changes in pore conductivity were observed when *E. coli* OMPs or peptides containing the OMP C-terminal signature sequences were added to the $Omp85_{Ec}$-containing bilayers, strongly indicating a direct interaction between Omp85 and its substrates (12). Moreover, since an OMP of *N. meningitidis* did not affect the conductivity of the $Omp85_{Ec}$-containing bilayers, this interaction appeared to be species-specific (12).

The N-terminal region of Omp85 is predicted to be located in the periplasm. It carries five polypeptide-transport-associated (POTRA) domains, which were suggested to be involved in substrate recognition (15). Previously, we have demonstrated that the exchange of the N-terminal segments between *N. meningitidis* and *E. coli* Omp85 resulted in chimeric Omp85 proteins that were not functional, neither in *N. meningitidis* nor in *E. coli* (Chapter 4), an observation consistent with the species-specific recognition of substrates by Omp85.

In Chapter 5 of this thesis, we described the purification of $Omp85_{Nm}$ and various sub-fragments of the *N. meningitidis* and *E. coli* Omp85 proteins. In this work, we further characterized these proteins. Particularly, we were interested to determine whether $Omp85_{Nm}$, like $Omp85_{Ec}$, forms pores in lipid bilayers, whether the C-terminal part of the Omp85 proteins is responsible for pore formation, and whether the N-terminal part is responsible for substrate recognition.

Materials and Methods

Protein preparations and synthetic peptides

All proteins and peptides used in this study are described in Table 1. *N. meningitidis* PorA P1.17,16 was produced according to (5) and dialyzed against phosphate-buffered saline (PBS) (pH 7.4), 0.06% lauryldimethylamine-oxide (LDAO) before use. *In vitro* folded *Salmonella typhimurium* LpxR was prepared as described before (14).

Table 1. Proteins and peptides used in this study

Protein	Species	Abbreviation	Stock solution	Source
Full-length Omp85	*N. meningitidis*	$Omp85_{Nm}$	0.5 mg/ml in 18 mM Tris-HCl (pH 8.2), 0.36 M L-arginine, 1.0 M guanidine, and 20 mM NaCl, 0.4 M urea, 0.45% LDAO	Chapter 5
N-terminal fragment consisting of amino acids 22-481 of $Omp85_{Nm}$	*N. meningitidis*	Nt-$Omp85_{Nm}$	2.3 mg/ml in 4.8 mM phosphate buffer (pH 7.4), 0.2% SB-12	Chapter 5
Full-length BamA ($Omp85_{Ec}$)	*E. coli*	$Omp85_{Ec}$	1 mg/ml in 20 mM Tris-HCl (pH 8.5), 0.5% SB-12	12
N-terminal fragment consisting amino acids 22-481 of $Omp85_{Ec}$	*E. coli*	Nt-$Omp85_{Ec}$	2.3 mg/ml in 20 mM Tris-HCl (pH 8.0), 0.06% LDAO	Chapter 5
C-terminal fragment consisting of amino acids 420-810 of $Omp85_{Ec}$	*E. coli*	Ct-$Omp85_{Ec}$	9 mg/ml in 20 mM Tris-HCl (pH 8.5), 0.06% $C_{10}E_5$	Chapter 5
FrpB	*N. meningitidis*		0.5 mg/ml in HEPES (pH 7.5), 0.3% SB-12	8
PorA P1.17, 16	*N. meningitidis*		10 mg/ml in PBS (pH 7.4), 0.06% LDAO	5
PorA P1.6	*N. meningitidis*		8 mg/ml in 20 mM ethanolamine (pH 10.5), 1% SB-12	5
PhoE	*E. coli*		0.36 mg/ml in 10 mM Tris-HCl (pH 8.0), 0.46 mM Tween-20	5
DDIVAVGMTYQF	*E. coli*	CterPhoE12	10 mM in 0.075% NH_3OH	Sigma
AVGMTYQF	*E. coli*	CterPhoE8	10 mM in 0.075% NH_3OH	Sigma
GMTYQF	*E. coli*	CterPhoE6	10 mM in 0.075% NH_3OH	Sigma
DVTIGFYVMDAQ		RandomPhoE[a]	10 mM in 0.075% NH_3OH	Sigma
AASVGLRHKF	*N. meningitidis*	CterPorA	10 mM in 2% CH_3COOH	Sigma
LpxR	*S. typhimurium*		8 mg/ml in 2 mM Tris (pH 7.5), 0.06% $C_{10}E_5$	14

[a]This peptide consists of the same 12 amino acid residues as CtermPhoE12, but in a randomized order.

Liposome-swelling assay

Liposome-swelling assays were performed as described (20). In short, liposomes were prepared from 4 μM 1,2-dioleoyl-sn-glycero-3-phosphocholine (DOPC) (Avanti Polar Lipids, Alabaster) and 1 μM egg phosphatidyl-DL-glycerol (Avanti). After addition of protein, proteoliposomes were generated in 5 mM Tris-HCl (pH 7.6) containing 17% dextran T40 (Amersham Biosciences). The isotonic concentration was determined by diluting the proteoliposomes into various concentrations of raffinose in 5 mM Tris-HCl (pH 7.6). The test

solutes [all in 5 mM Tris-HCl (pH 7.6)] for diffusion into the proteoliposomes were all from Sigma. Swelling of the proteoliposomes was monitored at 500 nm. The pore activities of PorA P1.7,16 and LpxR were measured as positive and negative controls, respectively. All measurements were repeated at least three times.

Planar lipid bilayer measurements

Planar lipid bilayers were produced as described (20). In brief, lipid membranes were formed from 1% (w/v) L-α-lecithin (Sigma) in hexane at room temperature across an orifice (50–150 μM diameter) in a Teflon septum, separating two electrolyte-containing chambers of 2.5 ml each. The pore activity of Ct-Omp85$_{Ec}$ was measured using 10 mM Tris-HCl (pH 7.4), 1 M KCl, 5 mM $CaCl_2$, and that of Omp85$_{Nm}$, which appeared to form more stable channels at lower pH, in 10 mM sodium acetate buffer (pH 5.0), 1 M KCl, 5 mM $CaCl_2$. Protein (5–10 μg) was added to the aqueous subphase, and insertions were monitored after applying a transmembrane potential of 50-200 mV. The channel conductance of the pores was determined from the stepwise conductance increments. The pore radii were calculated by applying

$$G=k[\pi a^2/(d+\pi a/2)]$$

where G is the conductance, k the bulk conductance (11.3 S/m), a the pore radius and d the membrane thickness (4 nm) (21).

Far Western blotting

The capacity of the periplasmic part of *N. meningitidis* Omp85 (Nt-Omp85$_{Nm}$) to bind various OMPs was tested in a Far Western blot assay. Purified *E. coli* PhoE, *N. meningitidis* PorA P1.6, or *N. meningitidis* FrpB were denatured by boiling in sample buffer containing 2% SDS and β-mercaptoethanol, subjected to sodium dodecyl sulfate-polyacrylamide gel electrophoresis (SDS-PAGE), and transferred onto nitrocellulose membranes. The membranes were blocked for 1 h in PBS (pH 7.6), 0.5% non-fat dried milk (Protifar, Nutricia), 0.1% Tween-20. The blots were incubated for at least 2 h at 4ºC with either native Nt-Omp85$_{Nm}$ diluted 1:100 in refolding buffer (4.8 mM phosphate, 0.2% SB-12, pH 7.4) or denatured Nt-Omp85$_{Nm}$. To denature the protein, the stock solution (Table 1) was boiled with 2% SDS and diluted in refolding buffer supplemented with 2% SDS. After that, the membranes were washed and probed for 1 h with a rabbit polyclonal antiserum raised against the N-terminal part of Omp85$_{Nm}$ (residues 22-464), which was generously provided by Ralph Judd (University of Montana, USA). After washing, the blot was incubated with alkaline phosphatase-conjugated goat anti-rabbit IgG secondary antibodies (Southern Biotechnology Associates Inc.). To visualize the signal, the blot was incubated in 0.1 M Tris-HCl (pH 9.5), 0.1 mg/ml Nitro Blue Tetrazolium, 0.5 mg/ml 5-bromo-4-chloro-3-indolyl phosphate (both from Sigma-Aldrich), until color appeared, whereafter the reaction was terminated by rinsing the blot with water.

Tryptophan fluorescence experiments

For tryptophan fluorescence measurements, the Nt-Omp85$_{Nm}$ preparation was diluted two-fold in PBS, yielding a final protein concentration of 1.2 mg/ml. Emission spectra were from 300 to 450 nm recorded at 25ºC using an excitation wavelength of 280 nm using a Perkin Elmer LS55 luminescence spectrometer. Kd values were determined by Scatchard plot analysis. Peptides were added to the cuvette in a step-wise manner.

Lipid monolayer surface tension measurements

A lipid mix containing 60 µg DOPC, 20 µg 1,2-dioleoyl-sn-glycero-3-phosphoethanolamine, 20 µg 1,2-dioleoyl-sn-glycero-3-phosphoserine was dried under nitrogen flow, dissolved in 200 µl hexane and diluted 10-fold in PBS. Lipid monolayers were spread from this solution at the air–water interface in a Teflon well (2 mL volume). Seven µl of Nt-Omp85$_{Nm}$ or Nt-Omp85$_{Ec}$ were injected at 2.3 mg/ml with a microsyringe directly into the subphase composed of PBS. Changes in surface tension were recorded using a Langmuir-tensiometer (Kibron micro-troughX) (2).

Modeling of the *N. meningitidis* Omp85 N-terminal domain

A structural model for the fragment encompassing POTRA1-4 of Omp85$_{Nm}$ was built using the known structure of the corresponding part of Omp85$_{Ec}$ (3) (PDB accession number 3EFC). The amino acid sequences of the N-terminal parts of the proteins were aligned using T-COFFEE (http://tcoffee.vital-it.ch/cgi-bin/Tcoffee/tcoffee_cgi/index.cgi?stage1=1&daction=TCOFFEE::Regular). The alignment was submitted to the SWISS-MODEL server (http://swissmodel.expasy.org) to generate a 3D model of the Omp85$_{Nm}$ fragment. Surface distribution of the hydrophobic residues was visualized by using browser plug-in MDL Chime Pro 2.6 SP7 (http://www.mdl.com/downloads/public/chime/2.6.SP7/MDLChime26SP7.jsp).

Results

Pore activity of *N. meningitidis* Omp85

Omp85$_{Ec}$ forms pores when reconstituted in liposomes and in planar lipid bilayers (12, 18). Here we evaluated whether Omp85$_{Nm}$ similarly has pore-forming capacities. Channel formation by Omp85$_{Nm}$ was determined by measuring the swelling rate of proteoliposomes suspended in an iso-osmotic arabinose solution. The permeability of liposomes containing Omp85$_{Nm}$ towards arabinose was proportional to the amount of Omp85$_{Nm}$ added, with the maximum reached at 8 µg of protein (Figure 1A). The *bona-fide* porin PorA P1.7,16 of *N. meningitidis*, which was previously shown to form pores in this assay (5), behaved similarly as Omp85$_{Nm}$ (Figure 1B). The LPS-modifying enzyme LpxR on the other hand, which is a membrane-embedded β-barrel without an internal channel as shown by its recent crystal structure resolution (14), did not mediate any proteoliposome swelling (Figure 1A and 1B). The size of the Omp85$_{Nm}$ pores was estimated by plotting the diffusion rates of solutes of various sizes (Figure 1C). From this plot, it was calculated that a solute with a mass of 403.5 Da would result in 10% of the swelling rate of arabinose. This value can be used to calculate the pore diameter (11), which was estimated to be 1.9 nm.

The Omp85$_{Nm}$ channels were further characterized in planar lipid bilayer experiments, where opening and closing of pores was observed (Figure 1D). Most of the conductance steps corresponded to 1.3 nS (Figure 1E), but also channels of 1.0 nS and 1.6 nS were observed, suggestive of the presence of various subconductance states. Assuming that Omp85$_{Nm}$ forms a perfect cylinder, the pore diameter calculated from its 1.3-nS conductivity, would be 0.82 nm.

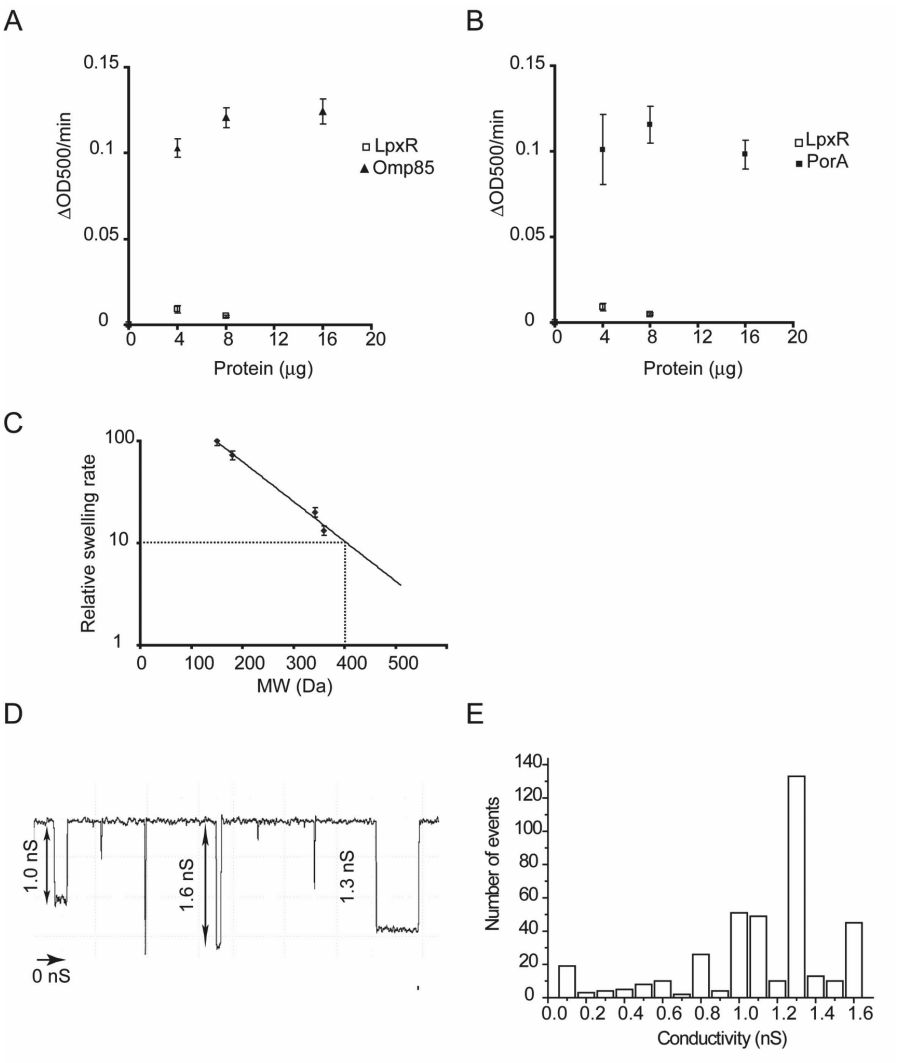

Figure 1

Pore activity of $Omp85_{Nm}$. (**A**) and (**B**) Swelling rates of proteoliposomes containing $Omp85_{Nm}$, PorA or LpxR in an iso-osmotic solution of L-arabinose. (**C**) Relative swelling rates of proteoliposomes containing $Omp85_{Nm}$ in solutions of sugars of various molecular weights. The sugars used were arabinose (150 Da), glucose (180 Da), saccharose (342 Da), maltose (360 Da). The data are shown relative to the swelling rate in arabinose solution and are the average values of at least three independent measurements; standard deviations are shown. The swelling rate corresponding to 10% of that in arabinose is indicated and served to estimate the size of the channel. (**D**) Channel recording in planar lipid bilayers at +100 mV. The zero-conductance level is indicated. (**E**) Amplitude histogram of channel opening and closing events in planar lipid bilayers. The data of seven independent recordings at +100 mV, -100 mV, +120 mV, -80 mV, and +140 mV were pooled and 402 events were analyzed.

Pore activity of the *E. coli* Omp85 C-terminal domain

Omp85 is predicted to have a two-domain structure with the C-terminal part being embedded in the OM (12, 22). We were interested in obtaining experimental support for this model. Previously we produced a trypsin-resistant C-terminal fragment of $Omp85_{Ec}$, designated Ct-$Omp85_{Ec}$ (12, Chapter 5). Ct-$Omp85_{Ec}$ showed features of a β-barrel according to CD spectra and semi-native SDS-PAGE (12, Chapter 5) and is therefore likely the part of the protein that mediates pore formation. To address this notion we performed planar lipid bilayer experiments with the purified Ct-$Omp85_{Ec}$. Pore openings and closings were indeed observed (Figure 2A). However, the electrophysiological characteristics of these pores were different from those of the full-length protein. The smallest conductance steps observed were 0.05 nS, but steps of 0.1, 0.15, and 0.2 nS, were also recorded with most of the steps being ~0.2 nS (Figure 2B). *In vitro* folded $Omp85_{Ec}$ appeared to form tetramers as deduced from size-exclusion chromatography experiments and as reflected in conductivity studies, which revealed conductance steps of 0.12 nS and 0.5 nS, supposedly corresponding to monomers and tetramers, respectively (12). Therefore, it is possible that the steps of 0.05 nS observed for Ct-$Omp85_{Ec}$ represent the conductivity of monomers and those of 0.1 nS, 0.15 nS, and 0.2 nS, of dimers, trimers, and tetramers, respectively. However, the conductivity of the Ct-$Omp85_{Ec}$ pores is much lower than that of the full-length protein pores, suggesting that the Omp85 fragment has a smaller pore diameter. This difference is apparently caused by the absence of the periplasmic POTRA domains, which might influence the conformation of the β-barrel and the charge distribution within it, leading to lower conductance steps.

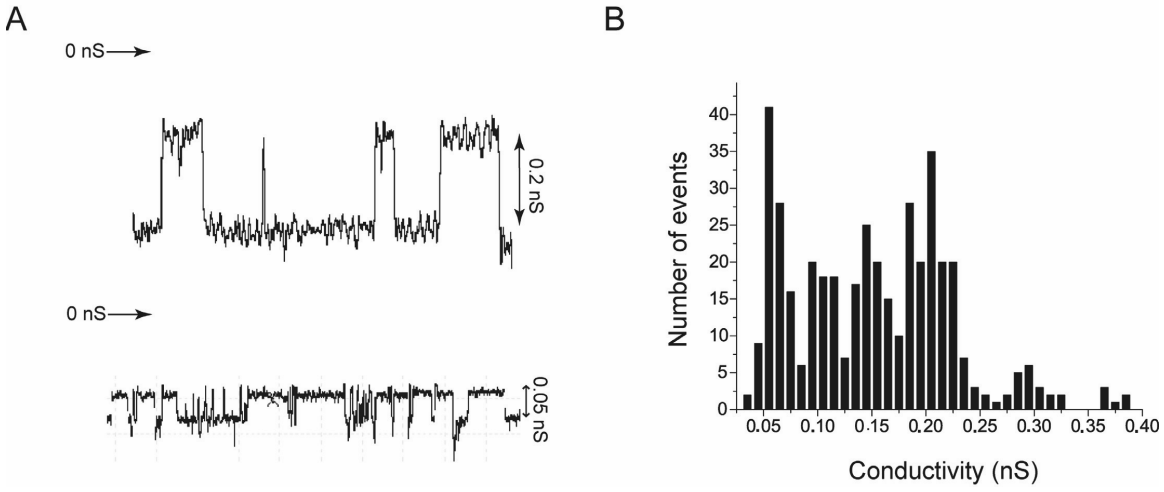

Figure 2

Pore activity of Ct-$Omp85_{Ec}$. (**A**) Two independent channel recordings in planar lipid bilayers measured at -50 mV (top) and -150 mV (bottom). Zero-conductance levels are indicated. (**B**) Amplitude histogram of channel opening and closing events. A total of 434 events were analyzed, using data from three independent recordings at -50 mV and -150 mV.

Substrate recognition is mediated by the N-terminal domain of Omp85

While the C-terminal domain of Omp85 is embedded in the membrane and forms pores, the N-terminal domain might function in substrate recognition. To investigate this concept, we purified the N-terminal fragment of $Omp85_{Nm}$ (Nt-$Omp85_{Nm}$) (Table 1) and studied its properties *in vitro*. Potential substrate recognition by Nt-$Omp85_{Nm}$ was investigated in Far Western-blotting assays, where the binding of Nt-$Omp85_{Nm}$ was tested first on the denatured neisserial OMP FrpB. Native Nt-$Omp85_{Nm}$ did indeed recognize FrpB (Figure 3A). The observation that denatured Nt-$Omp85_{Nm}$ did not bind FrpB indicated the specificity of the interaction. Species specificity in substrate recognition was not observed in this qualitative assay since native Nt-$Omp85_{Nm}$ bound similarly to both meningococcal OMPs (FrpB, PorA) and to an *E. coli* OMP (PhoE) (Figure 3B).

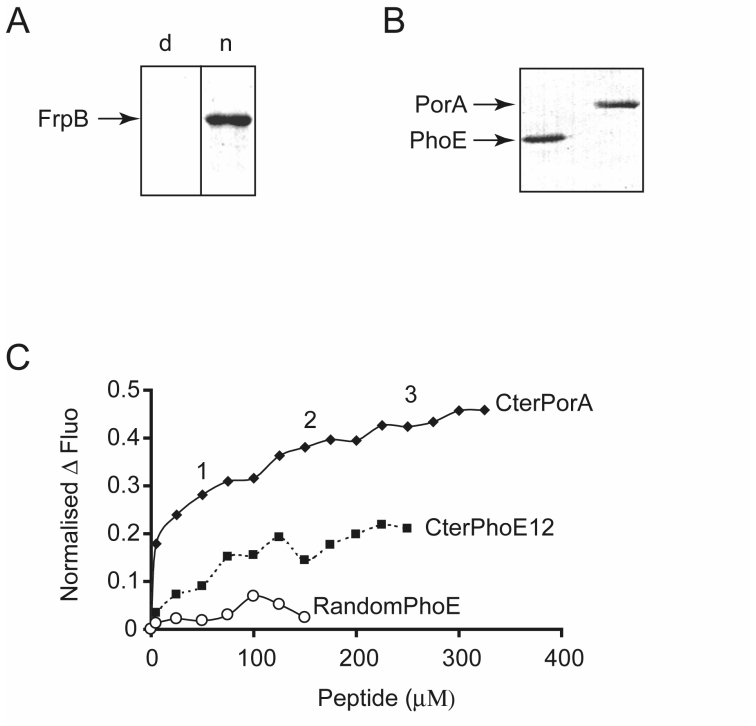

Figure 3

Substrate recognition by Nt-$Omp85_{Nm}$. (**A**) Blots containing purified denatured FrpB of *N. meningitidis* were incubated with refolded (n) or denatured (d) Nt-$Omp85_{Nm}$ and subsequently probed with antiserum directed against an N-terminal fragment of Omp85. (**B**) Blot containing denatured *N. meningitidis* PorA and *E. coli* PhoE was incubated with refolded Nt-$Omp85_{Nm}$ and probed as in panel A. (**C**) Quenching of the intrinsic tryptophan fluorescence of refolded Nt-$Omp85_{Nm}$ by the synthetic peptides CterPorA, CterPhoE12, and RandomPhoE. The peptides are described in detail in Table 1. Steps in fluorescence decrease in response to addition of CterPorA are indicated (1-3).

To obtain quantitative data, we also studied substrate binding of Nt-Omp85$_{Nm}$ by tryptophan fluorescence measurements (Figure 3C). As substrates we made use of synthetic peptides corresponding to the C-terminal signature sequences of OMPs, which were previously shown to interact in a species-specific manner with Omp85$_{Ec}$ in planar lipid bilayer experiments, thereby affecting the Omp85$_{Ec}$ pore activity (12). Dose-dependent changes in the intrinsic fluorescence of a protein upon addition of an interacting compound can be used to measure binding affinities. Step-wise addition of a C-terminal peptide of neisserial PorA (CterPorA) to Nt-Omp85$_{Nm}$ resulted in a decrease in tryptophan fluorescence. The results suggested the presence of several binding sites, one with high affinity and possibly two with lower affinity for the peptide (indicated by 1, 2 and 3 in Figure 3C). Kd values of 4.4 μM, 131 μM and 337 μM, respectively, were calculated from these curves using Scatchard plot analysis. The *E. coli*-derived PhoE peptide (CterPhoE12) bound with much lower affinity (Kd 73 μM), indicating that also Omp85$_{Nm}$ recognizes its substrates in a species-specific manner. No significant binding was observed for a scrambled version of CterPhoE12, indicating that the low level of binding of CterPhoE12 represents significant interaction.

Minimal substrate recognition sequence

Previously we found that a peptide comprising the C-terminal 12 amino acids of PhoE was recognized by Omp85$_{Ec}$ in planar lipid bilayers, whereas the experiments above demonstrated that a peptide comprising the C-terminal 10 amino acids of PorA was already sufficient for recognition by Omp85$_{Nm}$. To find the minimal fragment needed for recognition, we reconstituted Omp85$_{Ec}$ in planar lipid bilayers and measured changes in conductivity upon

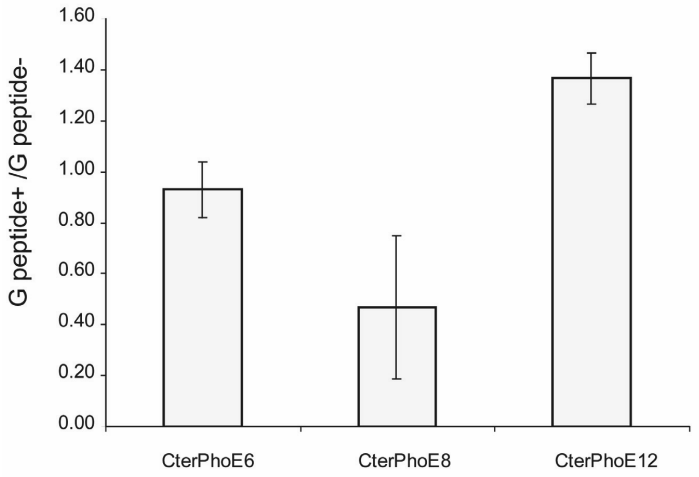

Figure 4

Determination of the minimal substrate recognition sequence for Omp85$_{Ec}$. All membrane conductivities were recorded at +100 mV. Bars represent the ratio of conductivities measured in the presence versus absence of 100 μM of the indicated peptide. PhoE peptides CterPhoE12, CterPhoE8, and CterPhoE6 (Table 1) were tested. All measurements were performed at least three times, and standard deviations are indicated.

addition of C-terminal PhoE peptides of various lengths. As reported before, the addition of the 12-amino-acid peptide CterPhoE12 caused an increase in pore activity (Figure 4). In contrast, an 8-amino acid peptide (CterPhoE8) resulted in a decrease in pore activity. This result demonstrates that also this peptide is recognized by $Omp85_{Ec}$, although the resulting interaction affected the Omp85 channels differently. When a peptide of 6 amino acids (CterPhoE6) was added, no significant changes in pore activity were observed (Figure 4).

Interaction between Omp85 N-termini and lipid monolayers

The experiments described above are consistent with the two-domain model of Omp85, which postulates that the C-terminal part is embedded in the OM and responsible for pore formation, while the N-terminal part extends in the periplasm and interacts with the substrates. However, the observation that expression of Nt-$Omp85_{Nm}$ in *E. coli* resulted in the formation of inclusion bodies (Chapter 5) indicates that this part of the protein might be membrane active as well. In contrast, expression of Nt-$Omp85_{Ec}$ yielded soluble protein, possibly indicative of a somewhat different functioning of the two protein domains. To investigate these possibilities, we studied the interaction of both Nt-$Omp85_{Nm}$ and Nt-$Omp85_{Ec}$ with lipid monolayers. Interestingly, while Nt-$Omp85_{Ec}$ had no effect, we found that the surface tension of the monolayer increased rapidly upon injection of Nt-$Omp85_{Nm}$ under the monolayer (Figure 5), indicating that Nt-$Omp85_{Nm}$ inserts between the lipids. The addition of buffers without protein did not affect surface tension of the monolayer, demonstrating that the detergents present in the solutions were not responsible for the observed effects (data not shown).

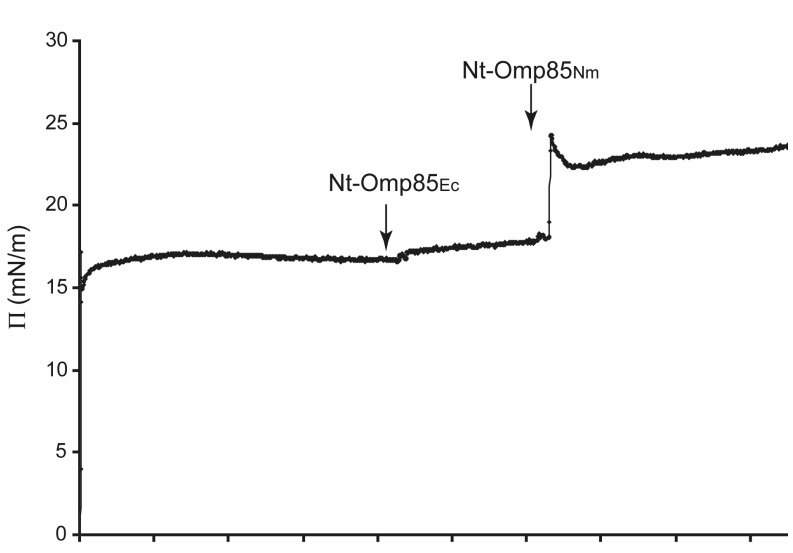

Figure 5

Interaction of N-terminal fragments of Omp85 with a lipid monolayer. Surface tension of the lipid monolayer was measured over time. Nt-$Omp85_{Ec}$ and Nt-$Omp85_{Nm}$ were injected under the monolayer at the indicated times.

The reason for the differences in physical properties of Nt-Omp85$_{Ec}$ and Nt-Omp85$_{Nm}$ might become clear from comparing the structures of the two protein fragments. More hydrophobic amino acid residues exposed on the surface of Nt-Omp85$_{Nm}$ could mediate its higher affinity for lipids and its tendency to aggregate. Two crystal structures of an Omp85$_{Ec}$ fragment, comprising the first four POTRA domains are available (3, 6). We modeled the corresponding part of Nt-Omp85$_{Nm}$ onto the most complete structure (3) of this fragment and compared them (Figure 6). Although there is some variation in the distribution of hydrophobic residues on the surfaces of both proteins, Nt-Omp85$_{Nm}$ does not appear to possess an overall higher surface hydrophobicity.

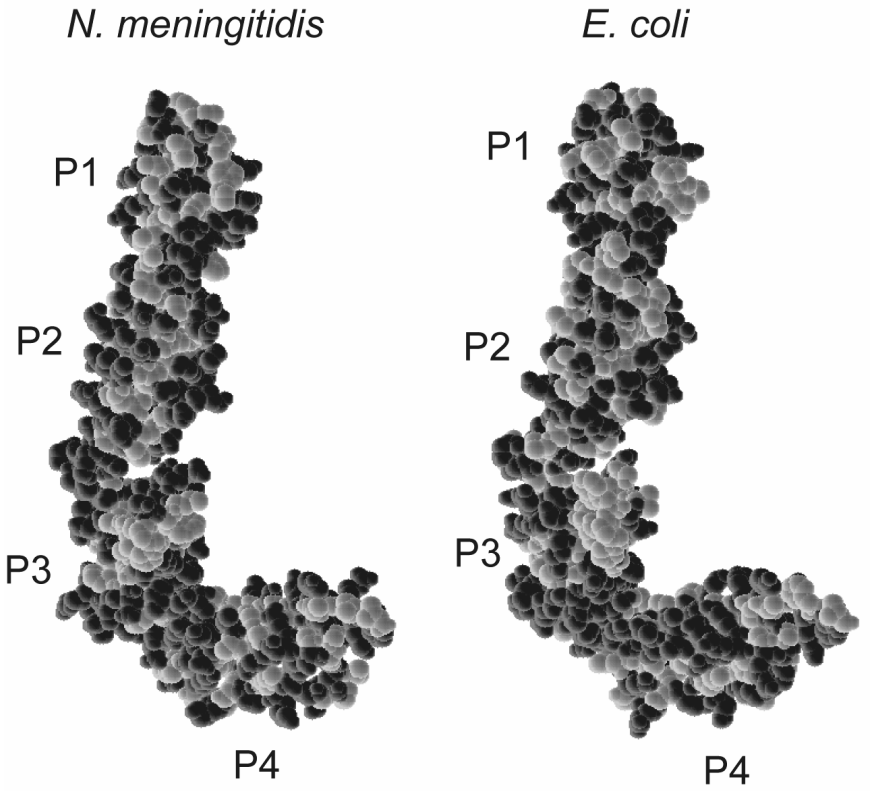

Figure 6

Space-filling representations of the POTRA domains 1-4 of *E. coli* and *N. meningitidis* Omp85. The solved structure POTRA1-4 of Omp85$_{Ec}$ (3) was used to create a model of the corresponding fragment of Omp85$_{Nm}$ using the Swiss Model Workspace server. The hydrophobic residues are shown in light grey; P1, P2, P3, and P4 indicate POTRA domains 1 through 4.

Discussion

In this work we found that *in vitro* folded $Omp85_{Nm}$ forms pores both in liposomes and in planar lipid bilayers. The conductance steps found for $Omp85_{Nm}$ (mostly 1.3 nS) are much larger than those of 0.12 nS found for $Omp85_{Ec}$ (12). It is not likely, however, that $Omp85_{Ec}$ really forms much smaller channels than $Omp85_{Nm}$, since these proteins, which show a high degree of sequence similarity, are expected to form very similar structures. Indeed, liposome-swelling assays suggest pore sizes of 2.5 nm for $Omp85_{Ec}$ (12) versus 1.9 nm for $Omp85_{Nm}$. More likely, the $Omp85_{Ec}$ channels are not fully open in planar lipid bilayers. A possibility would be that the channel of $Omp85_{Ec}$ is obstructed by more extensive interactions with the POTRA domains, but deletion of the POTRA domains, as in Ct-$Omp85_{Ec}$ resulted in even smaller pores. The crystal structure of FhaC, a distant member of the Omp85 superfamily, revealed a 16-stranded β-barrel, the internal channel of which is occupied by an N-terminal α-helix and an external loop, loop L6, which reaches through the barrel to the periplasmic side of the membrane (1). Although Omp85 doesn't have a fragment that could occupy a similar position as the N-terminal α-helix of FhaC, it does have a fragment with considerable sequence similarity to loop L6 of FhaC, which, therefore, could occupy a similar position within the barrel. Thus, one possibility is that this loop is fixed within the $Omp85_{Ec}$ β-barrel, thereby leaving only a very narrow channel, whereas it is more flexible in $Om85_{Nm}$, allowing the opening of much wider channels.

The calculated pore diameters found for $Omp85_{Nm}$ in liposomes and planar lipid bilayers were 1.9 nm and 0.82 nm, respectively. These results are close to the ones obtained for FhaC in similar assays, *i.e.*, 2.2 nm (4) and 0.82 nm (1), respectively. Calculations based on the FhaC structure indicate that a channel of 0.8 nm is possible when either the helix or the loop is not inserted in the barrel. Deletion of the α-helix did not affect FhaC channel conductivity (9), indicating that the α-helix was not inside the barrel during conductivity experiments with wild-type FhaC. Omp85 shares limited homology with FhaC, but it does not have an N-terminal α-helix, since the first POTRA domain of $Omp85_{Ec}$ was shown to start directly at the N terminus of the mature protein (3, 6). Nevertheless, $Omp85_{Ec}$ appears almost completely blocked in planar lipid bilayers. Therefore, our data suggests that Omp85 homologs have a smaller β-barrel than FhaC, possibly a 12-stranded β-barrel as predicted by the topology model (22), which can be completely blocked by the equivalent of L6 of FhaC alone.

In Chapter 5 we found evidence for the two-domain model of Omp85 by revealing a protease-sensitive N-terminal domain and protease-resistant C-terminal part. Here we characterized functions of the N-terminal and the C-terminal Omp85 fragments. Our hypothesis that the pore-forming activity of Omp85 is located in its C-terminal domain was confirmed by the observation that Ct-$Omp85_{Ec}$ formed channels in planar lipid bilayers. These results are consistent with the ones reported previously (18). The conductance steps for Ct-$Omp85_{Ec}$ were smaller than those found for the full-length protein: 0.05 and 0.2 nS, versus 0.12 and 0.5 nS, respectively. This is in contrast to the earlier data (18), where the authors reported no differences between the channels of full-length and C-terminal $Omp85_{Ec}$. In that study a fragment of 430 residues was used, while our Ct-$Omp85_{Ec}$ construct is only 390 amino acids long. Thus, the conformation of the longer fragment might have been more similar to the fold of the corresponding part in the full-length protein, which could explain its unaltered conductivity. The 0.05- and 0.2-nS conductivities we observed for Ct-$Omp85_{Ec}$ might correspond to those of monomers and tetramers, respectively. This is in line with dynamic light scattering data (Chapter 5), which also suggested oligomerization of Ct-$Omp85_{Ec}$. This would imply that POTRA domains are not required for the oligomerization of $Omp85_{Ec}$, a notion that is also substantiated by the monomeric behavior of a protein fragment

encompassing POTRA1 through POTRA5 of $Omp85_{Ec}$ in size exclusion chromatography and analytical ultracentrifugation experiments (7).

Consistent with the two-domain model, we also demonstrated that the N-terminal part of $Omp85_{Nm}$ is able to bind OMP substrates. Far Western-blotting assays demonstrated that refolded Nt-$Omp85_{Nm}$ could bind denatured OMPs. Tryptophan fluorescence measurements additionally showed that this fragment recognizes the C-terminal signature sequence of OMPs and that there is substantial species specificity in this activity, consistent with what we found before in planar lipid bilayer experiments for $Omp85_{Ec}$ (12). Besides a high-affinity binding site, the results suggested the presence of several weak binding sites in Nt-$Omp85_{Nm}$ for the PorA-derived peptide. Previously, NMR titration studies revealed weak binding of several internal PhoE-derived peptides to the POTRA domains in a protein fragment comprising POTRA1 and POTRA2 of $Omp85_{Ec}$ (7). In those experiments, a peptide comprising the C-terminal signature sequence was not included and, also, the Omp85 fragment used did not include POTRA5, the only POTRA domain that is essential for Omp85 function in *N. meningitidis.* We speculate that the high-affinity binding observed in our Trp fluorescence experiments reflects the binding of the PorA signature-sequence peptide to POTRA5, whereas the additional binding steps observed may correspond to the binding detected in the NMR experiments and reflect the interaction of the peptide with other POTRA domains.

So far, attempts to solve the crystal structure of Omp85 failed (Chapter 5). One way to obtain better crystals could be by performing co-crystallization experiments of Omp85 with a substrate. Obviously, using complete denatured OMPs as substrates for this purpose would not be very promising, but the use of C-terminal signature-sequence peptides could be a solution. Here we used the planar lipid bilayer method to determine the minimal peptide length needed for interaction with $Omp85_{Ec}$. As previously (12), the pore activity of $Omp85_{Ec}$ increased in response to the interaction with a peptide consisting of the C-terminal 12 amino acids of PhoE. In contrast, a shorter peptide, consisting of the C-terminal 8 amino acids resulted in a decrease in pore activity. This shows that $Omp85_{Ec}$ is able to interact also with the peptide of 8 amino acids, but apparently this interaction affects the Omp85 structure differently. The reason for this difference is not immediately clear. In the NMR studies cited above, the binding of a 15-mer peptide to a protein fragment consisting of two POTRA domains showed the formation of a binding platform involving the exposed edges of the β-sheets of two juxtaposed POTRA domains (7). Possibly, a similar platform is formed with a 12-mer peptide, but not with an 8-mer peptide, which could possibly bind to a single POTRA domain only, resulting in different conformational changes in Omp85 and in different effects on pore activity. A peptide of six amino acids did not affect the $Omp85_{Ec}$ pore activity. This does not necessarily imply that the peptide doesn't bind to Omp85, but it is not an obvious candidate for co-crystallization attempts. In contrast, both the 12-mer and the 8-mer peptides are interesting candidates, since they affect the Omp85 structure differently, thereby increasing the chance of obtaining suitable crystals.

Nt-$Omp85_{Nm}$ and Nt-$Omp85_{Ec}$ show some strikingly different physical properties: in Chapter 5 we showed that Nt-$Omp85_{Nm}$ forms inclusion bodies when expressed in *E. coli*, while Nt-$Omp85_{Ec}$ was expressed as a soluble protein, indicative of a possibly higher hydrophobicity of Nt-$Omp85_{Nm}$. Consistently, we demonstrated here that Nt-$Omp85_{Nm}$ but not Nt-$Omp85_{Ec}$ interacts with lipids in monolayer experiments. However, structural modeling exercises of POTRA1-4 did not reveal a higher number of hydrophobic residues exposed on the surface of Nt-$Omp85_{Nm}$ relative to Nt-$Omp85_{Ec}$ that could explain the differences in affinity for lipids. Both protein fragments include the POTRA5 domain and the hinge region located between this domain and the predicted 12-stranded β-barrel. This part of the proteins, which was not modeled, could possibly determine the different physical

properties of the two protein fragments. Anyhow, this feature might be relevant for Omp85 function. Possibly, the POTRA domains of $Omp85_{Nm}$ interact directly with the OM, in contrast to those of $Omp85_{Ec}$. We found that the composition of the Omp85 complex in *N. meningitidis* differs from that of *E. coli*, particularly in the absence of a homolog of *E. coli* BamB (YfgL) (Chapter 2, 16, 23). Interstingly, BamB of *E. coli*, contains a putative ALPS motive (P. Van Gelder, unpublished observation), a motive involved in protein-membrane interactions (10). Moreover, a *bamB* mutant in *E. coli* was shown to release decreased amounts of outer membrane vesicles (13), an observation, which also suggests a possible interaction of BamB with membranes. Thus, the absence of BamB in *N. meningitidis* might be compensated by an increased affinity of the N-terminal domain of Omp85 for membranes.

In conclusion, we have obtained more evidence to substantiate our two-domain Omp85 model, with the C-terminal domain being embedded in the OM and forming a pore, and the N-terminal domain being responsible for substrate recognition. Additionally, we found that $Omp85_{Nm}$ forms larger pores than $Omp85_{Ec}$ and that Nt-$Omp85_{Nm}$ is able to interact with lipid monolayers, while Nt-$Omp85_{Ec}$ is not.

Acknowledgements

This work was supported by the Netherlands Research Councils for Chemical Sciences (CW) and Earth and Life Sciences (ALW) with financial aid of the Netherlands Organization for Scientific Research (NWO). E. B. Volokhina also received a grant from the Federation of European Biochemical Sciences (FEBS). We also like to thank Dr. Fabrice Homblé from the ULB, Brussels for using his BLM equipment.

References

1. **Clantin, B., A. S. Delattre, P. Rucktooa, N. Saint, A. C. Méli, C. Locht, F. Jacob-Dubuisson, and V. Villeret.** 2007. Structure of the membrane protein FhaC: a member of the Omp85-TpsB transporter superfamily. Science **317:**957-961.
2. **Demel, R. A.** 1974. Monolayers-description of use and interaction. Methods Enzymol. **32:**539-544.
3. **Gatzeva-Topalova, P. Z., T. A. Walton, and M. C. Sousa.** 2008. Crystal structure of YaeT: conformational flexibility and substrate recognition. Structure **16:**1873–1881.
4. **Jacob-Dubuisson, F., C. El-Hamel, N. Saint, S. Guédin, E. Willery, G. Molle, and C. Locht.** 1999. Channel formation by FhaC, the outer membrane protein involved in the secretion of the *Bordetella pertussis* filamentous hemagglutinin. J. Biol. Chem. **274:**37731-37735.
5. **Jansen, C., A. Wiese, L. Reubsaet, N. Dekker, H. de Cock, U. Seydel, and J. Tommassen.** 2000. Biochemical and biophysical characterization of in vitro folded outer membrane porin PorA of *Neisseria meningitidis*. Biochim. Biophys. Acta **1464:**284-298.
6. **Kim, S., J. C. Malinverni, P. Sliz, T. J. Silhavy, S. C. Harrison, and D. Kahne.** 2007. Structure and function of an essential component of the outer membrane protein assembly machine. Science **317:**961-964.
7. **Knowles, T. J., M. Jeeves, S. Bobat, F. Dancea, D. McClelland, T. Palmer, M. Overduin, and I. R. Henderson.** 2008. Fold and function of polypeptide transport-associated domains responsible for delivering unfolded proteins to membranes. Mol. Microbiol. **68:**1216-1227.
8. **Kortekaas, J., S. A. Müller, P. Ringler, M. Gregorini, V. E. Weynants, L. Rutten, M. P. Bos, and J. Tommassen.** 2006. Immunogenicity and structural characterisation of an in vitro folded meningococcal siderophore receptor (FrpB, FetA). Microbes Infect. **8:**2145-2153.
9. **Méli A. C., H. Hodak, B. Clantin, C. Locht, G. Molle, F. Jacob-Dubuisson, and N. Saint.** 2006. Channel properties of TpsB transporter FhaC point to two functional domains with a C-terminal protein-conducting pore. J. Biol. Chem. **281:**158-166.
10. **Mesmin, B., G. Drin, S. Levi, M. Rawet, D. Cassel, J. Bigay, B. Antonny.** 2007. Two lipid-packing sensor motifs contribute to the sensitivity of ArfGAP1 to membrane curvature. Biochemistry **46:**1779-1790.
11. **Nikaido, H., K. Nikaido, and S. Harayama.** 1991. Identification and characterization of porins in *Pseudomonas aeruginosa*. J. Biol. Chem. **266:**770-779.
12. **Robert, V., E. B. Volokhina, F. Senf, M. P. Bos, P. Van Gelder, and J. Tommassen.** 2006. Assembly factor Omp85 recognizes its outer membrane protein substrates by a species-specific C-terminal motif. PLoS Biol. **4:**e377.
13. **Rolhion, N., N. Barnich, L. Claret, and A. Darfeuille-Michaud.** 2005. Strong decrease in invasive ability and outer membrane vesicle release in Crohn's disease-associated adherent-invasive *Escherichia coli* strain LF82 with the *yfgL* gene deleted. J. Bacteriol. **187:**2286-2296.
14. **Rutten, L., J. P. B. A. Mannie, C. M. Stead, C. R. H. Raetz, C. M. Reynolds, A. M. J. J. Bonvin, J. P. Tommassen, M. R. Egmond, M. S. Trent, and P. Gros.** 2009. Active-site architecture and catalytic mechanism of the lipid A deacylase LpxR of *Salmonella typhimurium*. Proc. Natl. Acad. Sci. U S A **106:**1960-1964.
15. **Sánchez-Pulido, L., D. Devos, S. Genevrois, M. Vicente, and A. Valencia.** 2003. POTRA: a conserved domain in the FtsQ family and a class of beta-barrel outer membrane proteins. Trends Biochem. Sci. **28:**523-526.
16. **Sklar, J. G., T. Wu, L. S. Gronenberg, J. C. Malinverni, D. Kahne, and T. J. Silhavy.** 2007. Lipoprotein SmpA is a component of the YaeT complex that assembles outer membrane proteins in *Escherichia coli*. Proc. Natl. Acad. Sci. U S A **104:**6400-6405.
17. **Sohn, J., and R. T. Sauer.** 2009. OMP peptides modulate the activity of DegS protease by differential binding to active and inactive conformations. Mol. Cell **33:**64-74.
18. **Stegmeier, J. F., and C. Andersen.** 2006. Characterization of pores formed by YaeT (Omp85) from *Escherichia coli*. J. Biochem. (Tokyo) **140:**275-283.

19. **Struyvé, M., M. Moons, and J. Tommassen.** 1991. Carboxy-terminal phenylalanine is essential for the correct assembly of a bacterial outer membrane protein. J. Mol. Biol. **218:**141-148.
20. **Van Gelder, P., F. Dumas, J. P. Rosenbusch, and M. Winterhalter.** 2000. Oriented channels reveal asymmetric energy barriers for sugar translocation through maltoporin of *Escherichia coli*. Eur. J. Biochem. **267:**79-84.
21. **Van Gelder, P., F. Dumas, and M. Winterhalter.** 2000. Understanding the function of bacterial outer membrane channels by reconstitution into black lipid membranes. Biophys. Chem. **85:**153–167.
22. **Voulhoux, R., M. P. Bos, J. Geurtsen, M. Mols, and J. Tommassen.** 2003. Role of a highly conserved bacterial protein in outer membrane protein assembly. Science **299:**262-265.
23. **Wu, T., J. Malinverni, N. Ruiz, S. Kim, T. J. Silhavy, and D. Kahne.** 2005. Identification of a multicomponent complex required for outer membrane biogenesis in *Escherichia coli*. Cell **121:**235-245.

Chapter 7

General and summarizing discussion

Gram-negative bacteria are characterized by a cell envelope consisting of an inner membrane (IM) and an outer membrane (OM), which are separated by the peptidoglycan-containing periplasm. The integral membrane proteins of the IM span this lipid bilayer by α-helical segments, whereas, with one exception (5), all integral outer membrane proteins (OMPs) are embedded in the OM in a β-barrel conformation composed of β-strands (19). All OMPs are synthesized in the cytosol with an N-terminal signal sequence, which is essential for their translocation across the IM by the Sec translocon (6). Several chaperones and folding factors, such as Skp and SurA, act in the periplasm and prevent OMPs from aggregation and facilitate folding of the OMPs. However, the actual process of assembly of OMPs into the OM is still poorly understood. Only in recent years, the existence of an OMP assembly machinery, which is now referred to as the Bam complex (for β-barrel assembly machinery), has become apparent.

Previously, the Omp85 protein was identified as an essential part of this Bam complex in *Neisseria meningitidis*. Depletion of this essential protein in a conditional mutant strain resulted in the periplasmic accumulation of unassembled forms of all OMPs analyzed (39). Later, a similar function was shown for the *Escherichia coli* Omp85 homolog BamA (4, 41, 42), and even in mitochondria, a homolog with a similar function was identified (11, 20, 27), probably reflecting the endosymbiont origin of these eukaryotic cell organelles. BamA was found to be associated with four lipoproteins: BamB, BamC, BamD, and BamE (34, 42). BamB, BamC, and BamE are not essential in *E. coli*, but their knockout phenotypes suggest that these proteins are important for efficient OMP assembly (34, 42). Like BamA, BamD is an essential component of the OMP-assembly machinery in *E. coli* (22, 42). Its depletion results in a phenotype similar to that of a BamA depletion strain.

The exact mechanistic of the process of OMP insertion into the OM remains enigmatic. Most of the work, which has been done so far, is focused on OMP assembly in *E. coli*. However, it is not known, to what extent the OMP assembly pathway is similar in all bacteria. There are some indications to believe that the OMP assembly pathway in *N. meningitidis* might differ from that of *E. coli*. The most important ones are: (i) the ability of *N. meningitidis* to survive and assemble OMPs in the absence of lipopolysaccharide (LPS) production or in the absence of a functional LPS transport system (1, 35, 36), and (ii) the absence of the σ^E response (2), which, in *E. coli*, is activated in response to periplasmic stress and prevents unassembled OMPs to accumulate in the periplasm (2, 31). Therefore, we studied in this work the OMP assembly process in *N. meningitidis*. Furthermore, we addressed species-specific features of the OMP assembly process and investigated functional properties of Omp85, the key component of the Bam complex.

OMP assembly in N. meningitidis: composition of the Bam complex

We characterized the Bam complex in *N. meningitidis* and found it to contain, besides Omp85, also BamC, the BamD homolog ComL, BamE, and RmpM (Chapter 2) (Figure 1). This composition differs from the Bam complex in *E. coli* (34, 42), in that it lacks BamB, but contains RmpM. There are more variations in the composition of Bam complex in Gram-negative bacteria; for example, a BamC homolog is absent in some of the α-proteobacteria, and at least one α-proteobacterial genome misses both *bamB* and *bamC* (9). Apparently, the accessory Bam complex components are not as well conserved throughout evolution as Omp85. Accordingly, the OMP assembly complex in mitochondria contains two accessory components, which, however, do not show any homology to the accessory components of the bacterial Bam complex (9).

The absence of one or more Bam complex components might be related to a lower demand of OMP insertion in some bacterial species. Indeed, α-proteobacterial genomes contain generally fewer predicted OMP-encoding genes than genomes of other classes of

proteobacteria (9); for example, *Rickettsia prowazekii* contains 17 of such genes, whereas *E. coli* contains 139 of them. Possibly, these bacteria do not require a highly efficient Bam complex.

In *N. meningitidis* at least several OMP complexes, including that of Omp85, contain RmpM protein (16, 28, Chapter 2). RmpM is a two-domain protein with a so-called OmpA domain, which is thought to associate non-covalently with the peptidoglycan layer, in its C-terminal end (12). It is possible that the presence of RmpM stabilizes the *N. meningitidis* Omp85 complexes (Chapter 2), possibly making the presence of BamB in this species unnecessary. It is not clear how such substitution is possible, since BamB and RmpM share no sequence similarities. However, *bamB* mutants in *E. coli* were shown to have an altered peptidoglycan biogenesis (7) and, therefore, BamB as RmpM, might interact with peptidoglycan.

Our analysis of an SDS-resistant high-molecular weight Omp85 complex from a neisserial mutant lacking the RmpM protein suggested that, possibly, yet other unknown components could be part of the Bam complex (Chapter 2). One possible candidate might be a lipoprotein encoded in *E. coli* by the *yraP* gene, which belongs to the σ^E regulon (25). In *E. coli*, a *surA yraP* double mutant is not viable, while both SurA and YraP individually are not essential (25). SurA is a periplasmic chaperone, involved, in *E. coli*, in OMP folding. The synthetic phenotype of a *surA yraP* double mutant suggests that the two proteins are involved in a similar process, possibly OMP insertion. YraP contains a lipobox and lacks an IM-retention signal, which means that it might act at the site of OMP insertion into the OM and be associated with Bam complex. A homolog of this 22-kDa protein is also present in *N. meningitidis*, where it is encoded by the NMB2091 locus in strain MC58 and, therefore, it might be associated with Omp85 in this organism.

The functions of the accessory Bam complex components are still not clear. We have shown that the Omp85 proteins can interact with their OMP substrates directly *in vitro* in the absence of any accessory component (30, Chapter 6), suggesting that these accessory components are not the primary receptors for the OMP substrates. The mitochondrial Omp85 homolog Tob55 was also shown to bind its substrates directly via its single POTRA domain; however, this POTRA domain was not essential for OMP assembly in mitochondria (13). Interestingly, a later study showed that in the mitochondrial OMP-assembly complex, substrates are not directly bound by Tob55, but by its associated component Tob38 (21). Therefore, it is still possible that the bacterial accessory components bind substrates and deliver them to Omp85, thereby increasing the efficiency of OMP assembly. It is also likely that the proteins that are associated with Omp85 create a more favorable environment for the folding and insertion of OMPs into the OM. A discussed above, RmpM is associated with peptidoglycan (12) and BamB might be involved in peptidoglycan biosynthesis (7). Furthermore, ComL of *N. gonorrhoeae* is covalently linked to the peptidoglycan layer (8) and BamE homologs of some bacteria carry a peptidoglycan-binding domain (24). Therefore, the BamA/Omp85-associated proteins might anchor the Bam complex to the peptidoglycan and possibly modulate peptidoglycan thereby facilitating OMP insertion. Such a role would explain the absence of homologs of the lipoproteins in the assembly machinery of mitochondria, where no peptidoglycan is present in the intermembrane space, *i.e.*, the equivalent of the bacterial periplasm.

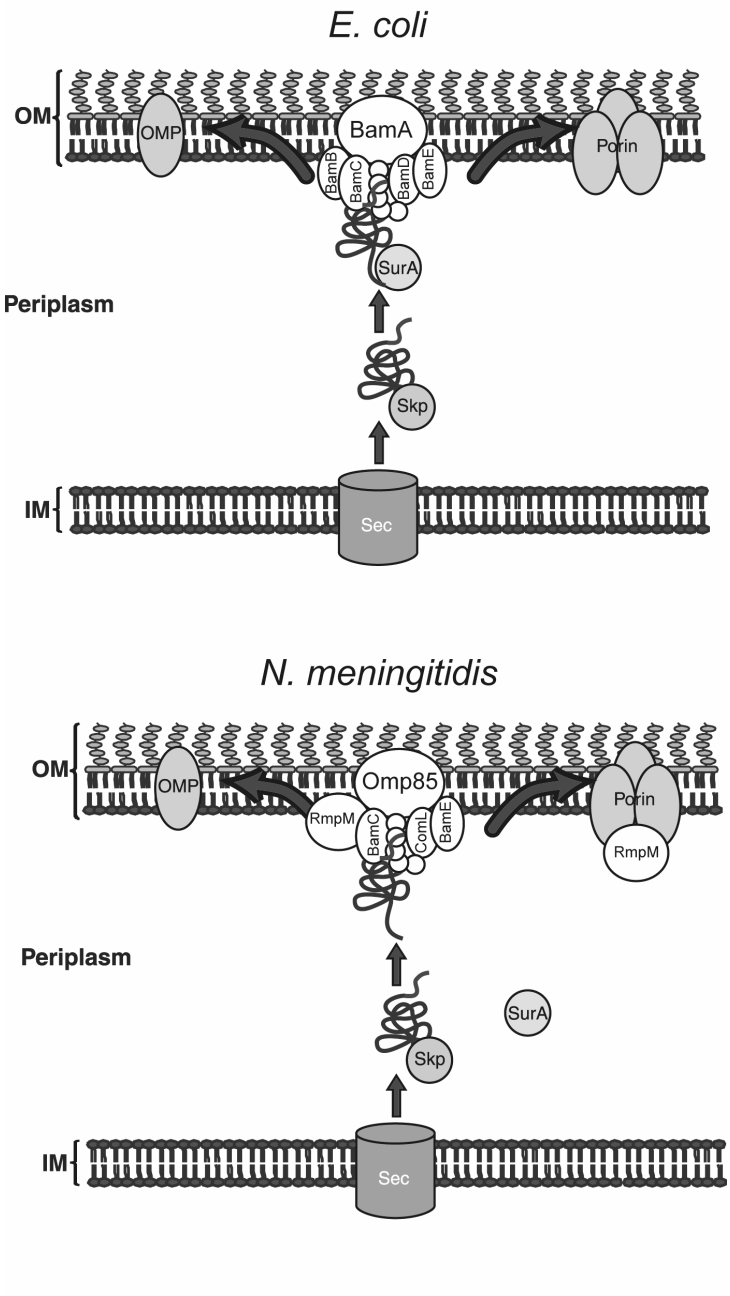
E. coli
OM
OMP
BamA
BamB
BamC
BamD
BamE
Porin
SurA
Periplasm
Skp
IM
Sec
N. meningitidis
OM
OMP
Omp85
RmpM
BamC
ComL
BamE
Porin
RmpM
Periplasm
SurA
Skp
IM
Sec

Figure 1

Biogenesis of OMPs in *E. coli* (upper panel) and *N. meningitidis* (lower panel). OMP precursors are synthesized in the cytosol with an N-terminal signal sequence and transported across the IM via the Sec machinery. The signal sequence is cleaved off by leader peptidase. In the periplasm, nascent OMPs interact with chaperones. In *E. coli* the chaperone Skp is shown to bind OMP precursors as soon as they emerge from the Sec machinery and to protect them from aggregation. SurA is considered to have an important role in *E. coli* OMP assembly, possibly as folding chaperone. Also in *N. meningitidis*, Skp is involved in OMP biogenesis, but we found no evidence for a role of SurA in this process. After crossing the periplasm, nascent OMPs interact with the Bam complex, consisting in *E. coli* of BamA, BamB, BamC, BamD, and BamB and in *N. meningitidis* of Omp85, BamC, the BamD homolog ComL, BamE, and RmpM. It is possible that BamA and Omp85 proteins are present as oligomers in the OM, in which case the neisserial Omp85 oligomer is more stable than that of BamA. OMP precursors bind to the BamA and Omp85 POTRA domains and are inserted into the OM. Several OMP complexes of neisserial OMPs, such as porins, also contain RmpM, which is suggested to help to maintain their stability.

OMP assembly in N. meningitidis: role of periplasmic chaperones

We characterized the functions of the periplasmic chaperones Skp and SurA in *N. meningitidis* (Chapter 3). We observed lower level of porins in an *skp* mutant and no phenotype for the *surA* mutant. This is different compared to *E. coli*, where deletion of *surA* has a more pronounced impact on OMP biogenesis than deletion of *skp* (33) (Figure 1). Moreover, an *skp surA* double mutant is viable in *N. meningitidis*, while this is not the case in *E. coli*. Furthermore, since a *bamB* homolog is missing in the *N. meningitidis* genome (Chapter 2) and a *surA bamB* double mutant of *E. coli* is not viable, we expected that SurA would be essential or at least important in *N. meningitidis*. However, this was not the case. As explained in Chapter 3, the limited function of SurA in *N. meningitidis* might be explained by the absence of the PPIase 1 domain in the meningococcal protein, which, in the *E. coli* protein, has been shown to facilitate selective binding of peptides that are rich in aromatic residues and characteristic for OMPs (14). The latter indicates that SurA's specific recognition of OMPs is impaired in *N. meningitidis*, where, apparently, this function is not needed or compensated by the presence of other chaperones. An alternative explanation derives from a recent proteomics study, which proposed that SurA is not a general OMP chaperone in *E. coli*, but rather acts on a subset of OMPs, particularly on the biogenesis of LptD (also known as Imp), an LPS transporter in the outer membrane (38). The abundance of this protein was decreased, while its mRNA levels remained the same, indicating that the decreased levels of LptD in the *surA* deletion strain are due to its assembly deficiency rather than to the down-regulation of transcription. LPS deficiency in *E. coli* triggers the σ^E periplasmic stress response, which inhibits the OMP biosynthesis (31). Thus, the severely decreased amounts of OMPs in an *E. coli surA* mutant may be due to the induction of the σ^E response and not related to a direct role of this chaperone in OMP biogenesis. In *N. meningitidis* no such stress response is present (2), and, thus, OMP biosynthesis and assembly can proceed also in the absence of LPS (1, 36). Therefore, *N. meningitidis* could be less vulnerable to *surA* depletion than *E. coli*.

Species specificity in OMP assembly

As discussed above, differences have occurred in OMP assembly among bacteria. Testing whether components of the OMP insertion pathway are able to substitute their homologs in other species is an excellent tool to characterize the evolutionary divergence. Earlier it was reported that BamB of *E. coli* could be substituted by BamB homologs from *Pseudomonas aeruginosa* and *Vibrio cholerae* (40). In this work, we studied whether Omp85 can replace its homologs in various bacterial species (Chapter 4) and whether BamD and Skp of *E. coli* can substitute their neisserial counterparts (Chapter 2 and Chapter 3). We found that the Omp85 homologs from *N. meningitidis, E. coli, Bordetella pertussis,* and *Burkholderia mallei* cannot substitute the authentic proteins in *N. meningitidis* and *E. coli* (Chapter 4). The species specificity of Omp85 might be due to the inefficient recognition of nascent OMPs from other bacteria, as we showed *in vitro* for neisserial Omp85 (Chapter 6) and previously for *E. coli* BamA (30). Alternatively, accessory Bam complex components and chaperones may not cooperate efficiently with foreign Omp85 proteins. This might be the underlying reason for the lack of functionality of *E. coli*-derived BamD and Skp in *N. meningitidis* (Chapters 2 and 3). Interestingly, *E. coli* Skp was shown to bind *N. meningitidis*-derived NalP with similar affinity as *E. coli*-derived OMPs *in vitro*, indicating that lack of substrate recognition is, in this case, not the cause of the species-specificity of functioning (29).

Characterization of Omp85

The Omp85 protein was originally predicted to consist of a 12-stranded membrane-embedded β-barrel at the C terminus and an N-terminal periplasmic part (39). Within the periplasmic part five polypeptide-transport-associated (POTRA) domains were predicted; such domains are also found in several other proteins involved in protein translocation (32). The presence of five POTRA domains in Omp85 was confirmed by crystal structures and small angle X-ray scattering data obtained for an N-terminal part of *E. coli* BamA (10, 17, 18). According to the topology prediction, postulating a 12-stranded β-barrel, there is a region between the C terminus of the POTRA5 domain and the first amino acid of the β-barrel of Omp85. In *N. meningitidis* and *E. coli* this so-called hinge region, for which no function has been suggested so far, is 61 amino acids long. A complete structure is known of a distant member of the Omp85 superfamily, the two-partner secretion system component FhaC of *Bordetella pertussis* (3). This protein consists of two POTRA domains and a 16-stranded β-barrel. This indicates the possibility of the Omp85 β-barrel containing 16 β-strands as well, with four additional β-strands located in the hinge region.

To gain more insight into the function of Omp85, we produced and purified the *N. meningitidis* and *E. coli* Omp85 proteins and their sub-domains (30, Chapter 5). Protease digestion assays indicated that both *N. meningitidis* and *E. coli* Omp85 homologs are composed of two sub-domains: a protease-resistant β-barrel fragment and a protease-sensitive N-terminal part (30, Chapter 5), in accordance with the predicted topology model. Both Omp85 homologs formed pores in liposome-swelling assays and in planar lipid bilayers (30, Chapter 6). We showed that the C-terminal fragment of *E. coli* BamA constitutes the pore-forming domain (Chapter 6). As mentioned above, the structure of this β-barrel part is still under debate. In the original topology model, a 12-stranded β-barrel was predicted, but the solved structure of FhaC showed a 16-stranded β-barrel. The FhaC structure revealed that the channel is blocked by the inwardly folded loop 6 and an N-terminal α-helix (3). Deletion of the loop 6 in FhaC altered its channel properties; furthermore, it abolished secretion of FhaC substrate (3). This loop 6 of FhaC is part of a region, designated motif 3, which is conserved among Omp85-family members (3, 23). Within this motif, a conserved fragment VRGY is

located at the tip of the loop, which reaches into the periplasm. *N. meningitidis* Omp85 also contains exactly the same sequence, but, in the original topology model, it is predicted to be part of the seventh β-strand in the barrel (39). Because loop 6 is important for the channel properties and function of an Omp85-family member (3) and part of the highly conserved motif, it might be logical to suspect that the VRGY residues would be located in a similar loop and not in a β-strand in other Omp85 homologs as well. Therefore, some deviation between the actual structure and original topology model of Omp85 might be expected and a revision of this model would be needed.

The pore activity of Omp85 might provide some insights into the size of the β-barrel, although the data have to be interpreted with care, since various parts of the protein might obstruct the channel. For the *N. meningitidis* Omp85, conductance steps of 1.3 nS found, that is much bigger than the conductance steps of 0.12 nS and 0.5 nS found previously for the *E. coli* BamA. It was suggested that the 0.5-nS conductances actually represent the activity of four 0.12-nS channels present in a tetramer of BamA. If this interpretation is correct, the BamA channel is almost completely obstructed by (an) element(s) that is apparently more flexible in the case of *N. meningitidis* Omp85. Which element(s) might block the BamA channel? As described above, the FhaC channel was obstructed in the crystal structure by an N-terminal α-helix and by the inwardly folded loop 6. Since a segment of Omp85/BamA has considerable sequence similarity to this loop 6 of FhaC, we might expect this segment to form a similar channel-obstructing loop in BamA. However, the bacterial Omp85 homologs do not have an N-terminal α-helix, since their first POTRA domain is starting directly after the signal sequence (32). Therefore, the BamA channel might have been obstructed only by the loop. If we propose that a single inwardly folded loop is sufficient to block the BamA channel and both the loop and the α-helix are required to block the FhaC channel, than we might suggest that the Omp85/BamA proteins have a smaller channel than FhaC, possibly formed by 12 β-strands in accordance with the previously proposed topology model (39). Consistently, the conductivity of the neisserial Omp85 of 1.3 nS and its pore diameter of 1.9 nm calculated from the liposome-swelling assays are very similar to those found for the 12-stranded β-barrel translocator domain of the *N. meningitidis* autotransporter NalP (26; Roussel-Jazede, unpublished results). Moreover, chimeric proteins carrying the predicted 12-stranded β-barrel of *N. meningitidis* Omp85 and the N-terminal fragment including the hinge of *E. coli* BamA and reciprocal constructs were inserted into the OM, indicating that the C-terminal 12 β-strands of Omp85 are able to form a membrane-anchoring β-barrel (Chapter 4). Additionally, protease-digestion patterns of these hybrids were suggestive of a protease-resistant fragment that could correspond in size with a 12-stranded β-barrel (Chapter 4). Therefore, the bacterial Omp85 proteins are possibly containing 12-stranded β-barrels, although more data is needed to confirm this proposal. Of note, the amount of β-strands in the C-terminal β-barrel appears to vary between members of the Omp85 superfamily. While the barrel of FhaC contains 16 strands and that of Omp85 possibly only 12, it was suggested previously that the Omp85-superfamily member YtfM from *E. coli* contains an 8-stranded β-barrel (37).

The POTRA domains located in the N-terminal part of Omp85 were expected to interact with nascent OMPs. In this work, we provide evidence for this notion by showing that the POTRA-domain-containing part of Omp85 interacts with unfolded OMPs and peptides derived from them (Chapter 6). Thus, all our data are consistent with a two-domain organization of Omp85, although it remains to be shown where the boundary between the two domains is exactly located. Intriguingly, we observed several distinctly different physical properties of the POTRA-repeat-containing domain of *E. coli* and *N. meningitidis* Omp85: the neisserial domain was less soluble and demonstrated a higher affinity for lipids than the

E. coli domain, suggesting that the surface of the former domain is more hydrophobic. This difference might also contribute to the lack of functional substitution *in vivo* (Chapter 4).

Like *E. coli* BamA, *N. meningitidis* Omp85 formed oligomers, probably tetramers, *in vitro* (Chapter 5). However, it remains to be proven whether Omp85 is present in an oligomeric conformation also in its native environment, the OM. The detection of several HMW forms of Omp85 in a neisserial RmpM mutant in semi-native SDS-PAGE may be indicative for the presence of such native Omp85 oligomers (Chapter 2). These presumed oligomers are not very stable though, since they were inconsistently observed in our assays (Chapter 2). We never observed similar complexes of BamA in *E. coli* membranes, whereas neisserial Omp85 expressed in *E. coli* did form HMW complexes. Possibly, Omp85 derived from *N. meningitidis* forms more stable oligomers than the *E. coli*-derived protein.

Although extensive research has revealed several important aspects of the OMP assembly pathway, the complete picture is still far from clear. Particularly, it is still not known exactly how OMP precursors are inserted into the OM and what the exact functions of the Bam complex components are. To gain more insights, further research should focus on determining the interactions between the pathway components and their substrates. Setting up an *in vitro* system using purified components of the OMP insertion machinery would be extremely valuable to study OMP assembly. Further, efforts should be continued to obtain the structure of the complete Omp85 alone and in combination with Bam accessory components and its OMP substrates. Such information will be essential to understand eventually the OMP assembly process.

References

1. **Bos M. P.**, **B. Tefsen**, **J. Geurtsen**, **and J. Tommassen.** 2004. Identification of an outer membrane protein required for the transport of lipopolysaccharide to the bacterial cell surface. Proc. Natl. Acad. Sci. U S A **101:**9417-9422.
2. **Bos, M. P., V. Robert, and J. Tommassen.** 2007. Biogenesis of the Gram-negative bacterial outer membrane. Annu. Rev. Microbiol. **61:**191-214.
3. **Clantin, B., A. S. Delattre, P. Rucktooa, N. Saint, A. C. Méli, C. Locht, F. Jacob-Dubuisson, and V. Villeret.** 2007. Structure of the membrane protein FhaC: a member of the Omp85-TpsB transporter superfamily. Science **317:**957-961.
4. **Doerrler**, **W. T., and C. R. H. Raetz.** 2005. Loss of outer membrane proteins without inhibition of lipid export in an *Escherichia coli* YaeT mutant. J. Biol. Chem. **280:**27679-27687.
5. **Dong, C., K. Beis, J. Nesper, A. L. Brunkan-Lamontagne, B. R. Clarke, C. Whitfield, and J. H. Naismith.** 2006. Wza the translocon for *E. coli* capsular polysaccharides defines a new class of membrane protein. Nature **444:**226-229.
6. **Driessen, A. J. M., and N. Nouwen.** 2008. Protein translocation across the bacterial cytoplasmic membrane. Annu. Rev. Biochem. **77:**643-667.
7. **Eggert, U.S., N. Ruiz, B. V. Falcone, A. A Branstrom, R. C. Goldman, T. J. Silhavy, and Kahne.** 2001 Genetic basis for activity differences between vancomycin and glycolipid derivatives of vancomycin. Science **294:**361-364.
8. **Fussenegger, M., D. Facius, J. Meier, T. F. Meyer.** 1996. A novel peptidoglycan-linked lipoprotein (ComL) that functions in natural transformation competence of *Neisseria gonorrhoeae*. Mol. Microbiol. **19:**1095-1105.
9. **Gatsos, X., A. J. Perry, K. Anwari, P. Dolezal, P. P. Wolynec, V. A. Likić , A. W. Purcell , S. K. Buchanan, and T. Lithgow.** 2008. Protein secretion and outer membrane assembly in *Alphaproteobacteria*. FEMS Microbiol. Rev. **32:**995-1009.
10. **Gatzeva-Topalova, P. Z., T. A. Walton, and M. C. Sousa.** 2008. Crystal structure of YaeT: conformational flexibility and substrate recognition. Structure **16:**1873–1881.
11. **Gentle, I., K. Gabriel, P. Beech, R. Waller, and T. Lithgow.** 2004. The Omp85 family of proteins is essential for outer membrane biogenesis in mitochondria and bacteria. J. Cell. Biol. **164:**19-24.
12. **Grizot, S., and S. K. Buchanan.** 2004. Structure of the OmpA-like domain of RmpM from *Neisseria meningitidis*. Mol. Microbiol. **51:**1027-1037.
13. **Habib, S. J., T. Waizenegger, A. Niewienda, S. A. Paschen, W. Neupert, and D. Rapaport.** 2007. The N-terminal domain of Tob55 has a receptor-like function in the biogenesis of mitochondrial β-barrel proteins. J. Cell. Biol. **176:**77-88.
14. **Hennecke, G., J. Nolte, R. Volkmer-Engert, J. Schneider-Mergener, and S. Behrens.** 2005. The periplasmic chaperone SurA exploits two features characteristic of integral outer membrane proteins for selective substrate recognition. J. Biol. Chem. **280:**23540-23548.
15. **Jacob-Dubuisson, F., C. El-Hamel, N. Saint, S. Guédin, E. Willery, G. Molle, and C. Locht.** 1999. Channel formation by FhaC, the outer membrane protein involved in the secretion of the *Bordetella pertussis* filamentous hemagglutinin. J. Biol. Chem. **274:**37731-37735.
16. **Jansen C., A. Wiese, L. Reubsaet, N. Dekker, H. de Cock, U. Seydel, and J. Tommassen.** 2000. Biochemical and biophysical characterization of in vitro folded outer membrane porin PorA of *Neisseria meningitidis*. Biochim. Biophys. Acta **1464:**284-298.
17. **Kim, S., J. C. Malinverni, P. Sliz, T. J. Silhavy, S. C. Harrison, and D. Kahne.** 2007. Structure and function of an essential component of the outer membrane protein assembly machine. Science **317:**961-964.
18. **Knowles, T. J., M. Jeeves, S. Bobat, F. Dancea, D. McClelland, T. Palmer, M. Overduin, and I. R. Henderson.** 2008. Fold and function of polypeptide transport-associated domains responsible for delivering unfolded proteins to membranes. Mol. Microbiol. **68:**1216-1227.
19. **Koebnik, R., K. P. Locher, and P. Van Gelder.** 2000. Structure and function of bacterial outer membrane proteins: barrels in a nutshell. Mol. Microbiol. **37:**239-253.

20. **Kozjak, V., N. Wiedemann, D. Milenkovic, C. Lohaus, H. E. Meyer, B. Guiard, C. Meisinger, and N. Pfanner.** 2003. An essential role of Sam50 in the protein sorting and assembly machinery of the mitochondrial outer membrane. J. Biol. Chem. **278:**48520-48523.
21. **Kutik, S., D. Stojanovski, L. Becker, T. Becker, M. Meinecke, V. Krüger, C. Prinz, C. Meisinger, B. Guiard, R. Wagner, N. Pfanner, and N. Wiedemann.** 2008. Dissecting membrane insertion of mitochondrial β-barrel proteins. Cell **132:**1011-1024.
22. **Malinverni, J. C., J. Werner, S. Kim, J. G. Sklar, D. Kahne, R. Misra, and T. J. Silhavy.** 2006. YfiO stabilizes the YaeT complex and is essential for outer membrane protein assembly in *Escherichia coli*. Mol. Microbiol. **61:**151-164.
23. **Moslavac S., O. Mirus, R. Bredemeier, J. Soll, A. von Haeseler, and E. Schleiff.** 2005. Conserved pore-forming regions in polypeptide- transporting proteins. FEBS J. **272:**1367-1378.
24. **Nardini, P. M., A. Mellors, and R. Y. Lo.** 1998. Characterization of a fourth lipoprotein from *Pasteurella haemolytica* A1 and its homology to the OmpA family of outer membrane proteins. FEMS Microbiol. Lett. **165:**71-77.
25. **Onufryk, C., M. -L. Crouch, F. C. Fang, and C. A. Gross.** 2005. Characterization of six lipoproteins in the σ^E regulon. J. Bacteriol. **187:**4552-4561.
26. **Oomen, C. J., P. van Ulsen, P. van Gelder, M. Feijen, J. Tommassen, and P. Gros.** 2004. Structure of the translocator domain of a bacterial autotransporter. EMBO J. **23:**1257-1266.
27. **Paschen, S. A., T. Waizenegger, T. Stan, M. Preuss, M. Cyrklaff, K. Hell, D. Rapaport, and W. Neupert.** 2003. Evolutionary conservation of biogenesis of β-barrel membrane proteins. Nature **426:**862-866.
28. **Prinz, T., and J. Tommassen.** 2000. Association of iron-regulated outer membrane proteins of *Neisseria meningitidis* with the RmpM (class 4) protein. FEMS Microbiol. Lett. **183:**49-53.
29. **Qu, J., C. Mayer, S. Behrens, O. Holst, and J. H. Kleinschmidt.** 2007. The trimeric periplasmic chaperone Skp of *Escherichia coli* forms 1:1 complexes with outer membrane proteins via hydrophobic and electrostatic interactions. J. Mol. Biol. **374:**91-105.
30. **Robert, V., E. B. Volokhina, F. Senf, M. P. Bos, P. Van Gelder, and J. Tommassen.** 2006. Assembly factor Omp85 recognizes its outer membrane protein substrates by a species-specific C-terminal motif. PLoS Biol. **4:**e377.
31. **Ruiz, N., and T. J. Silhavy.** 2005. Sensing external stress: watchdogs of the *Escherichia coli* cell envelope. Curr. Opin. Microbiol. **8:**122-126.
32. **Sánchez-Pulido, L., D. Devos, S. Genevrois, M. Vicente, and A. Valencia.** 2003. POTRA: a conserved domain in the FtsQ family and a class of β-barrel outer membrane proteins. Trends Biochem. Sci. **28:**523-526.
33. **Sklar, J. G., T. Wu, D. Kahne, and T. J. Silhavy.** 2007. Defining the roles of the periplasmic chaperones SurA, Skp, and DegP in *Escherichia coli*. Genes Dev. **21:**2473-2484.
34. **Sklar, J. G., T. Wu, L. S. Gronenberg, J. C. Malinverni, D. Kahne, and T. J. Silhavy.** 2007. Lipoprotein SmpA is a component of the YaeT complex that assembles outer membrane proteins in *Escherichia coli*. Proc. Natl. Acad. Sci. U S A **104:**6400-6405.
35. **Steeghs, L., R. den Hartog, A. den Boer, B. Zomer, P. Roholl, and P. van der Ley.** 1998. Meningitis bacterium is viable without endotoxin. Nature **392:**449-450.
36. **Steeghs, L., H. de Cock, E. Evers, B. Zomer, J. Tommassen, and P. van der Ley.** 2001. Outer membrane composition of a lipopolysaccharide-deficient *Neisseria meningitidis* mutant. EMBO J. **20:**6937-6945.
37. **Stegmeier, J. F., A. Glück, S. Sukumaran, W. Mäntele, and C. Andersen.** 2007. Characterisation of YtfM, a second member of the Omp85 family in *Escherichia coli*. Biol. Chem. **388:**37-46.
38. **Vertommen, D., N. Ruiz, P. Leverrier, T. J. Silhavy, and J. F. Collet.** 2009. Characterization of the role of the *Escherichia coli* periplasmic chaperone SurA using differential proteomics. Proteomics **9:**2432-2443.
39. **Voulhoux, R., M. P. Bos, J. Geurtsen, M. Mols, and J. Tommassen.** 2003. Role of a highly conserved bacterial protein in outer membrane protein assembly. Science 299:262-265.

40. **Vuong, P., D. Bennion, J. Mantei, D. Frost, and R. Misra.** 2008. Analysis of YfgL and YaeT interactions through bioinformatics, mutagenesis, and biochemistry. J. Bacteriol. **190:**1507-1517.
41. **Werner, J., and R. Misra.** 2005. YaeT (Omp85) affects the assembly of lipid-dependent and lipid-independent outer membrane proteins of *Escherichia coli*. Mol. Microbiol. **7:**1450-1459.
42. **Wu, T., J. Malinverni, N. Ruiz, S. Kim, T. J. Silhavy, and D. Kahne.** 2005. Identification of a multicomponent complex required for outer membrane biogenesis in *Escherichia coli*. Cell **121:**235-245.

Samenvatting

Samenvatting

Gram-negatieve bacteriën worden gekenmerkt door een celenveloppe, die bestaat uit een binnenmembraan en een buitenmembraan, welke gescheiden worden door het peptidoglycaan-bevattende periplasma. De binnenmembraan is een symmetrische bilaag van fosfolipiden. Daarentegen bevat de buitenmembraan alleen fosfolipiden aan de binnenkant, terwijl de buitenste laag lipopolysaccharides (LPS) bevat. De meeste Gram-negative bacteriën hebben dit LPS nodig om te overleven. De integrale eiwitten van de binnenmembraan traverseren deze membraan met α-helische segmenten, terwijl vrijwel alle bekende integrale buitenmembraaneiwitten (OMPs voor outer membrane proteins) als β-barrels in de buitenmembraan zijn verankerd. Bij Gram-negatieve bacteriën vormt de buitenmembraan het contactoppervlak tussen de bacterie en haar onmiddellijke omgeving. Als gevolg daarvan spelen OMPs een belangrijke rol in de interactie van de bacterie met haar omgeving en eventueel ook met andere bacteriën of gastheercellen.

Alle OMPs worden aangemaakt in het cytosol met een N-terminaal signaalpeptide, dat nodig is voor hun translocatie over de binnenmembraan door het Sec eiwittransportsysteem. Na het passeren van de binnenmembraan komen OMPs terecht in het periplasma. De passage van de OMPs door het periplasma is het best beschreven in *Escherichia coli*. In het periplasma worden OMPs gebonden door Skp, een chaperone die ervoor zorgt dat de hydrofobe delen van de OMPs niet aggregeren in de hydrofiele omgeving van het periplasma. Verder bevat het periplasma chaperones die van belang zijn voor het vouwen van OMPs. SurA is het best beschreven vouwingschaperone.

Aan de binnenkant van buitenmembraan komen OMPs in aanraking met de buitenmembraaneiwit assemblagemachine, die zorgt voor uiteindelijke vouwing van OMPs en hun insertie in de buitenmembraan. In *E. coli* wordt deze assemblagemachine Bam genoemd voor β-barrel assembly machinery.

Het eiwit Omp85 is het belangrijkste onderdeel van het Bam complex; zijn functie is voor het eerst beschreven in *Neisseria meningitidis* door onze groep. Omp85 is een essentieel eiwit, wat wil zeggen dat de bacterie het nodig heeft om te overleven. Depletie, of het omlaag brengen van de hoeveelheid Omp85 in de cel, leidde tot accumulatie van niet-gevouwen OMPs in het periplasma van *N. meningitidis*. Alle geteste OMPs bleken Omp85-afhankelijk te zijn voor hun assemblage. Later werd een soortgelijke functie aangetoond voor de *E. coli* Omp85 homoloog BamA. Genen, coderend voor Omp85 eiwitten zijn aanwezig in alle bekende genomen van Gram-negatieve bacteriën. Bovendien bevatten ook mitochondriën, eukaryotische celorganellen, die geëvolueerd zijn uit bacteriën, Omp85 homologen met eenzelfde functie als die in bacteriën.

BamA van *E. coli* bleek een complex te vormen met tenminste vier lipoproteïnen: BamB, BamC, BamD en BamE. BamB, BamC en BamE zijn niet essentieel in *E. coli* en hebben maar een beperkte rol in OMP assemblage. Daarentegen is BamD, net als BamA, een essentieel onderdeel van het Bam complex. In het geval van een OMP assemblage defect wordt er in *E. coli* een zogenaamde σ^E stressrespons geactiveerd. Deze respons leidt tot verhoogde productie van vouwingsfactoren, zoals periplasmatische chaperones en Bam componenten; tegelijkertijd onderdrukt het de productie van nieuwe OMPs en stimuleert het de productie van het periplasmatische enzym DegP, dat niet-geassembleerde OMPs afbreekt. In *N. meningitidis* ontbreekt zo'n respons en in het geval van een OMP assemblagedefect stapelen ongevouwen OMPs zich op in het periplasma.

Het exacte mechanisme van het proces van OMP insertie in de buitenmembraan is nog onduidelijk. Het merendeel van het werk, dat tot nu toe gedaan is, is gericht op OMP assemblage in *E. coli*. Het is echter niet bekend in hoeverre OMP assemblage gelijk is in alle Gram-negatieve bacteriesoorten. In sommige Gram-negatieve bacteriën (bijvoorbeeld in α-proteobacteriën) ontbreken bepaalde onderdelen van het Bam complex. Als OMPs uit andere

Gram-negatieve bacteriën in *E. coli* worden geproduceerd, worden ze vaak niet op efficiënte wijze geassembleerd.

Er zijn een aantal aanwijzingen dat de OMP assemblage in *N. meningitidis* anders verloopt dan in *E. coli*. Bijvoorbeeld OMPs van *N. meningitidis* worden vaak niet goed geassembleerd wanneer ze in *E. coli* worden geproduceerd. Het vermogen van *N. meningitidis* om te overleven in de afwezigheid van LPS, iets wat *E. coli* niet kan, wijst erop dat er belangrijke verschillen zijn tussen buitenmembraanbiogenese in *N. meningitidis* en *E. coli*, die ook betrekking kunnen hebben op de OMP assemblage. Bovendien houdt het ontbreken van de σ^E periplasmatische stressrespons in *N. meningitidis* in, dat deze bacterie een andere manier dan *E. coli* heeft om met OMP assemblagedefecten om te gaan.

Het doel van het onderzoek beschreven in dit proefschrift was het bestuderen van OMP assemblage in *N. meningitidis* om meer inzicht te krijgen in OMP biogenese in Gram-negatieve bacteriën.

In **hoofdstuk 2** werd de samenstelling van het Bam complex in *N. meningitidis* en de functie van de geïdentificeerde componenten bestudeerd. Uit analyse van genoomsequenties van *N. meningitidis* stammen bleek dat er geen genen codererend voor een BamB homoloog aanwezig zijn. We vonden echter wel genen coderend voor BamC, BamD (in *N. gonorrhoeae* eerder al beschreven als ComL), BamE, en een tweede homoloog van BamE, Mlp. Uit het feit dat ze mee gezuiverd werden met Omp85, werd geconcludeerd dat BamC, ComL en BamE in de cel een complex vormen met Omp85. Door de genen te inactiveren werd bepaald welke functies de gecodeerde eiwitten in OMP assemblage hebben. Net als in *E. coli* bleek ComL/BamD essentieel te zijn voor de levensvatbaarheid en voor OMP assemblage in *N. meningitidis*. BamE is niet essentieel, maar bleek bij te dragen aan een efficiëne OMP assemblage en aan de instandhouding van de integriteit van de buitenmembraan. Geen duidelijke OMP assemblage functies werden gevonden voor BamC en Mlp. Semi-natieve gelelektroforese experimenten identificeerden het RmpM eiwit als een extra onderdeel van het Bam complex. RmpM is niet vereist voor OMP biogenese maar stabiliseert OMP complexen. In *N. meningitidis* vormt Omp85 dus een complex met BamC, ComL, BamE en RmpM. Naast Omp85 lijken ComL en BamE het meest belangrijk te zijn voor OMP assemblage.

De periplasmatische chaperones Skp en SurA zijn betrokken bij de biogenese van OMPs in *E. coli*. In **hoofdstuk 3** werd onderzocht of deze chaperones soortgelijke functies uitoefenen in *N. meningitidis*. Daartoe werden *skp* en *surA* mutanten gemaakt en gekarakteriseerd. De *skp* mutant bleek minder porines (dat zijn de meest voorkomende OMPs) te bevatten dan wild-type cellen. Dit wijst erop dat, net zoals in *E. coli*, Skp betrokken is bij OMP biogenese in *N. meningitidis*. Een soortgelijk fenotype werd daarentegen niet gevonden voor de *surA* mutant. Onze resultaten duiden dus op een belangrijke rol voor Skp, maar niet voor SurA in OMP biogenese in *N. meningitidis*. Bovendien bleek in *N. meningitidis*, in tegenstelling tot *E. coli*, een *skp surA* dubbelmutant levensvatbaar te zijn. Dat betekent dat deze twee chaperones niet noodzakelijk zijn voor OMP biogenese in *N. meningitidis*, en/of dat hun functie overgenomen kan worden door andere, nog onbekende OMP biogenese component.

Wanneer OMPs uit andere Gram-negatieve bacteriën in *E. coli* worden geproduceerd, worden ze vaak niet op efficiënte wijze geassembleerd. Bovendien was eerder aangetoond dat Omp85 OMP substraten *in vitro* herkent in een soortspecifieke wijze. In **hoofdstuk 4** werd daarom uitgezocht of Omp85 homologen van *N. meningitidis*, *Neisseria gonorrhoeae*, *Bordetella pertussis*, *Burkholderia mallei* en *E. coli* Omp85 in *E. coli* en in *N. meningitidis* kunnen vervangen. Geen van de onderzochte Omp85 homologen functioneerde in een andere bacteriesoort, met uitzondering van *N. gonorrhoeae* Omp85, dat Omp85 van *N. meningitidis* volledig kon vervangen. Het *N. meningitidis* Omp85 eiwit werd wel geassembleerd in de

buitenmembraan van *E. coli;* bovendien was het ook geassocieerd met BamD, een essentiële component van het Bam complex in *E. coli*. Dus, onvoldoende substraat herkenning lijkt de belangrijkste reden te zijn voor het niet-functioneren van heterologe Omp85 eiwitten in *E. coli*. Omp85 wordt gedacht te bestaan uit twee domeinen: een N-terminaal periplasmatisch deel en een C-terminale β-barrel. Chimeren werden gemaakt door het uitwisselen van domeinen tussen *N. meningitidis* en *E. coli* Omp85 eiwitten. Echter, in geen van deze bacteriesoorten waren deze chimeren functioneel. Blijkbaar moeten beide Omp85 domeinen compatibel zijn om een functioneel eiwit te vormen.

Voor verdere karakterisering werden methoden ontwikkeld om grote hoeveelheden Omp85 van *N. meningitidis* en van *E. coli*, alsmede van subdomeinen daarvan, te produceren, zoals in **hoofdstuk 5** is beschreven. Eerder was beschreven dat de *E. coli* homoloog *in vitro* oligomeren kan vormen. Deze oligomeren werden verder bestudeerd met behulp van elektronenmicroscopie en ze bleken ringvormige structuren met een schijnbare centrale holte te vormen. Ook *N. meningitidis* Omp85 bleek *in vitro* oligomeren te vormen. Verder werden experimenten uitgevoerd om het eerder gepostuleerde twee-domein model van Omp85 te verifiëren. De β-barrels van OMPs zijn door hun compacte vouwing meestal ongevoelig voor proteases. Protease digestie experimenten leverden een proteaseresistent C-terminaal fragment van Omp85 op met eigenschappen, zoals een hoog β-sheet gehalte, die in overeenstemming zijn met de verwachting dat dit deel van het eiwit integraal in de buitenmembraan verankerd is. Dit C-terminale fragment van *E. coli* Omp85 werd gezuiverd. De mogelijk periplasmatische N-terminale fragmenten van beide Omp85 eiwitten werden geproduceerd in *E. coli*, en ze bleken onderling verschillende eigenschappen te hebben. Het *N. meningitidis* Omp85 fragment was veel minder oplosbaar in water dan dat van *E. coli* Omp85.

Hoofdstuk 6 beschrijft de karakterisering van de opgezuiverde Omp85 eiwitten en hun fragmenten in functionele assays *in vitro*. Eerder werd aangetoond dat *E. coli* Omp85 poriën in lipidenbilagen kan vormen; nu werd aangetoond dat deze poriën gevormd worden door het C-terminale β-barrel fragment van *E. coli* Omp85. Dit is in overeenstemming met ons topologie model. Verder bleek dat ook *N. meningitidis* Omp85 poriën kan vormen, echter met andere electrofysiologische eigenschappen dan *E. coli* Omp85. Met name bleken deze poriën aanzienlijk wijder te zijn, hetgeen erop kan duiden dat de poriën van verschillende Omp85 eiwitten op diverse manieren geheel of gedeeltelijk geblokkeerd kunnen worden. Eerdere studies hebben aangetoond dat Omp85 van *E. coli* substraten *in vitro* kan herkennen. Nu werd het minimale substraatfragment dat nodig is voor herkenning bepaald op acht aminozuren. Tryptofaanfluorescentie experimenten met het N-terminale fragment van *N. meningitidis* Omp85 toonden aan dat dit deel alleen voldoende is voor substraatherkenning. Dit water-onoplosbare N-terminale fragment bleek bovendien te inserteren in lipidenmonolagen, in tegenstelling tot het water-oplosbare N-terminale fragment van *E. coli* Omp85. Dit verschil in eigenschappen kan duiden op verschillen tussen Omp85 functies in *N. meningitidis* en *E. coli* in OMP assemblage.

Acknowledgements

In this part of the book I would like to thank everybody, who in one way or another, contributed profoundly to the successful completion of this thesis. First of all, Jan and Piet, thank you for choosing me to work on this project. I am grateful to Jan and Martine for everything I learned from them, and for their help and advice. My special thanks to Frank for all the countless purifications that he performed for this project. I would also like to thank Erika and Susanne, students who worked under my supervision, for their effort. Patrick, thank you for your help and assistance during my stay in Brussels. Fabrice, thanks for letting me use your set up and for your enthusiasm and inspiring discussions. Viviane, it has been a privilege to work on the same project with you. Piet and Lucy, thanks for your supervision and always finding time for me, I learned a lot on the eighth floor.

Greetings to everybody who I worked with during my years as a Ph.D student, in my hart I will remember every one of you.

Special thanks to all my friends for their support, without you the process would have been much more difficult. Finally, I would like to thank my family, and my husband Iouri, for always believing in me and for their never-ending patience.

Елена

Curriculum vitae

Elena Volokhina werd geboren op 23 februari 1979 te Novosibirsk, Rusland. In 1997 heeft zij haar diploma behaald aan de algemene middelbare school No. 130 en is zij begonnen aan de opleiding Biologie aan de Staatsuniversiteit te Novosibirsk. In 2000 heeft ze de opleiding Biologie voortgezet aan de Universiteit van Amsterdam en studeerde af in 2003. Tijdens deze studieperiode heeft zij twee stages gelopen: één aan de Technische Universiteit Twente bij de Biofysische Techniek groep van Prof. dr. J. Greve onder begeleiding van dr. A. G. J. Tibbe en één bij het Medisch Spectrum Twente onder begeleiding van Prof. dr. I. Vermes. Van januari 2004 tot juli 2008 is zij als assistent-in-opleiding werkzaam geweest bij de afdeling Moleculaire Microbiologie van de Universiteit Utrecht. Tijdens deze periode werkte zij aan het in dit proefschrift beschreven onderzoek onder begeleiding van Dr. M. P. Bos en Prof. dr. J. P. M. Tommassen. Sinds maart 2009 is zij als post-doctoraal onderzoeker werkzaam bij de afdeling Kindernefrologie in het Universitair Medisch Centrum St. Radboud te Nijmegen.

Publicaties

Volokhina, E. B., F. Beckers, J. Tommassen, and M. P. Bos. 2009. The β-barrel outer membrane protein assembly complex of *Neisseria meningitidis*. Submitted.

Robert, V., E. B. Volokhina, F. Senf, M. P. Bos, P. Van Gelder, and J. Tommassen. 2006. Assembly factor Omp85 recognizes its outer membrane protein substrates by a species-specific C-terminal motif. PLoS Biol. **4:**e377.

Volokhina, E. B., R. Hulshof, C. Haanen, and I. Vermes. 2003. Tissue transglutaminase mRNA expression in apoptotic cell death. Apoptosis **8:**673-679.

Uzunbajakava, N., A. Lenferink, Y. Kraan, E. Volokhina, G. Vrensen, J. Greve, and C. Otto. 2003. Nonresonant confocal Raman imaging of DNA and protein distribution in apoptotic cells. Biophys. J. **84:**3968-3981.